

# **Development of intelligent, robust, and non-linear Models in Dynamic Equivalencing for Interconnected Power Systems**

Zur Erlangung des akademischen Grades

**DOKTORINGENIEUR (Dr.-Ing.)**

der Fakultät der Elektrotechnik, Informatik und Mathematik

der Universität Paderborn

genehmigte Dissertation

von

Dipl.-Ing. **Oscar Clovis YUCRA LINO**

aus Oruro, Bolivien

Referent: PD. Dr.-Ing. habil. Michael Fette

Korreferent: Prof. Dr.-Ing. Jürgen Voß

Tag der mündlichen Prüfung: 04. Juli 2006

Paderborn 2006



# Acknowledgments

This research work in context of a doctoral dissertation was realized in the Department of Electrical Engineering of CINVESTAV Mexico (Centre of Research and Advances Studies), Consulting System & Dynamic, and the University of Paderborn since Juni 2002.

First of all, I would like to express my sincere gratitude and appreciation to my supervisor PD. Dr.-Ing. habil. Michael Fette (Consulting System & Dynamic, Germany), Prof. Dr. Zhao Dong (Department of Electrical Engineering, Queensland University, Australia), Prof. Dr. Juan Manuel Ramirez (CINVESTAV, Unity Guadalajara-Mexico) for discussions on power systems dynamics, the skilled guidance, valuable comments, constructive suggestions, collaboration, and encouragement that they give me over the years of research work on this doctoral project as well as to my co-advisor Prof. Dr. Jürgen Voß and Prof. Dr. Felix Gausch for the critical reading and discussion and also the useful suggestions.

Finally, I wish to express my utmost gratitude to my dear soul sister, Melvy for her care and support, love and friendship. She has stimulated me to begin the doctorate study and she has contributed to its completion through her encouragement. You have harmonized and enriched my life in the way I could never dream of; yet.

I will always be grateful heartily to God, the most Beneficent for standing by my side throughout all the sorrow and happiness, storm, tide, and sunshine days.

To my mother Desideria and father Santiago in eternal gratitude dedicated.

Essen, July 2006

Oscar Clovis Yucra Lino



---

# Contents

<b>Contents</b> .....	<b>i</b>
<b>List of Figures</b> .....	<b>v</b>
<b>List of Tables</b> .....	<b>ix</b>
<b>Nomenclature</b> .....	<b>xi</b>
<b>Acronyms</b> .....	<b>xvi</b>
<b>Chapter 1 Introduction</b> .....	<b>1</b>
1.1 Motivation .....	1
1.2 Objectives .....	3
1.3 Outlines of the dissertation .....	5
<b>Chapter 2 Background</b> .....	<b>6</b>
2.1 Dynamic equivalencing .....	6
2.1.1 Coherency identification and grouping of generators .....	8
2.1.2 Network aggregation .....	9
2.1.3 Static network reduction .....	10
2.1.4 Aggregation of control devices .....	11
2.2 Existing approaches .....	12
2.3 Power system simulation program .....	13
2.4 Summary .....	14
<b>Chapter 3 Electromechanical-based Identity Recognition in Dynamic Equivalencing</b> .....	<b>15</b>
3.1 Introduction .....	16

---

3.2	Coherency-based dynamic equivalencing.....	16
3.3	Identity recognition approach.....	20
3.3.1	Conditions.....	20
3.3.2	Procedure.....	26
3.3.3	Identity recognition algorithms.....	28
3.3.4	Comparative application.....	29
3.4	Electromechanical-based identity recognition.....	31
3.4.1	Inertia coefficient and electrical power.....	31
3.4.2	Electromechanical distance.....	37
3.5	Case studies.....	38
3.5.1	16 Multi-machine system.....	39
3.5.2	Simulation results and discussion.....	40
3.5.3	Interconnected European Network UCTE/CENTREL.....	47
3.5.4	Simulation results and discussion.....	49
3.6	Summary.....	56
<b>Chapter 4</b>	<b>Splitting Aggregation-based Dynamic Equivalencing.....</b>	<b>58</b>
4.1	Introduction.....	59
4.2	Conventional aggregation in dynamic equivalencing.....	59
4.2.1	Inertial Aggregation.....	60
4.2.2	Slow coherency aggregation.....	64
4.2.3	Power invariance aggregation.....	67
4.2.4	Berg and Ghafurian's aggregation.....	69
4.3	Splitting-based aggregation approach.....	70
4.3.1	Conditions.....	70
4.3.2	Aggregated electrical parameters.....	72
4.3.3	Splitting factors of generators.....	76
4.4	Case study.....	80
4.5	Simulation results and discussion.....	81

---

4.6 Summary .....	87
<b>Chapter 5 Dynamic Artificial Neural Network-based Dynamic Equivalencing ....</b>	<b>89</b>
5.1 Introduction.....	90
5.2 Conventional dynamic equivalencing.....	91
5.3 Dynamic ANN-based dynamic equivalencing .....	92
5.3.1 Artificial neural networks (ANN) for modeling.....	93
5.3.2 Modeling of dynamic system.....	96
5.3.3 Mathematical description .....	97
5.3.4 Power system model .....	100
5.3.5 Dynamic ANN model as external area .....	104
5.3.6 Robustness.....	113
5.4 Case studies.....	118
5.4.1 16 Multi-machine system with 2 boundary nodes.....	118
5.4.2 12 Multi-machine system with 3 to 8 boundary nodes.....	119
5.5 Simulation results and discussion.....	120
5.5.1 16 Multi-machine system with 2 boundary nodes.....	120
5.5.2 12 Multi-machine system with 3 to 8 boundary nodes.....	130
5.6 Summary.....	137
<b>Chapter 6 Closure.....</b>	<b>139</b>
6.1 Conclusions.....	139
6.2 Selection criteria.....	143
6.3 Suggestions for future work .....	145
6.4 List of publications .....	146
<b>Bibliography .....</b>	<b>147</b>
<b>APPENDIX A Classical dynamic equivalencing approaches.....</b>	<b>156</b>
A.1. Ward equivalent .....	156
A.2. Modal-based equivalencing .....	159

---

A.3. Coherency-based equivalencing.....	160
A.4. Hybrid modal procedures.....	162
A.5. Linear model reduction .....	163
A.6. Model identification methods .....	165
A.7. Flow chart of the power system simulation tool PSD.....	166
A.8. Flow chart of the coupling of the machine model to the analysis algorithm PSD.....	167
<b>APPENDIX B Identity recognition algorithms.....</b>	<b>168</b>
B.1. Hierarchical clustering .....	168
B.2. Partitioning clustering: K-means .....	169
B.3. Fuzzy clustering.....	170
B.4. Relationship between K-means (hard clustering) and Fuzzy clustering .....	174
B.5. Self organizing features maps (SOFM).....	175
B.6. Clustering quality .....	176
B.7. Practical comparison of identity recognition algorithms.....	177
<b>APPENDIX C DANN-based dynamic equivalencing .....</b>	<b>178</b>
C.1. ANN preliminaries.....	178
C.2. Learning strategies .....	179
C.3. Modeling.....	179
C.4. Non-linear models .....	180
C.5. Power system model .....	180
<b>APPENDIX D Data sets of 16 Multi-machine system.....</b>	<b>183</b>
<b>APPENDIX E Data sets of 12 Multi-machine system .....</b>	<b>188</b>
<b>APPENDIX F Data sets of the interconnected European power system UCTE / CENTREL .....</b>	<b>196</b>

# List of Figures

<b>Fig. 2.1.-</b> Classical dynamic equivalencing in power systems .....	7
<b>Fig. 3.1.-</b> Swing oscillating curve of the rotor angular speed representing the conditions for the identity recognition instead of the classical coherency.....	21
<b>Fig. 3.2.-</b> Classical Aggregation .....	22
<b>Fig. 3.3.-</b> Schematic representation of iterative assignment and construction of centroids or reference generators within a clustering procedure .....	27
<b>Fig. 3.4.-</b> Schematic representation of similar generators belonging to a cluster group taking into account its identical properties in phase and amplitude. ....	27
<b>Fig. 3.5.-</b> Flow chart of applied identity recognition algorithms.....	29
<b>Fig. 3.6.-</b> One-machine power system for sensitivity analysis .....	32
<b>Fig. 3.7.-</b> Graphical comparison of the normalized square mean values of the sensitivities of rotor angle $\delta_L$ with reference to the synchronous machine parameters.....	32
<b>Fig. 3.8.-</b> Graphical comparison of the normalized square mean values of the sensitivities of rotor angle, rotor current and angle with reference to the parameters of the synchronous machines .....	33
<b>Fig. 3.9.-</b> 16 Multi-machine system .....	39
<b>Fig. 3.10.-</b> Schematic representation of the grouped 16-machine System following disturbances at the boundary nodes C1 on 380kV and C8 on 220kV at the same time. ....	41
<b>Fig. 3.11.-</b> Assignment and grouping of identical external machines according to the identity recognition algorithms in conjunction to Fig. 3.10. ....	42
<b>Fig. 3.12.a, b.-</b> Comparison of time responses of C12 internal machine calculated with 3 cluster groups according to the electromechanical Fuzzy and K-means.....	43
<b>Fig. 3.13.-</b> Comparison of time responses of the internal machine <b>C14</b> depending on the reduction degree with 1, 3, 6 electromechanical Fuzzy algorithm-based equivalents. ....	44
<b>Fig. 3.14.-</b> Time responses of the <b>C2</b> internal machine calculated with 3 equivalent machines by different identity recognition-based algorithms. ....	45
<b>Fig. 3.15.-</b> Time responses of the <b>C2</b> internal machine following the disturbance (electrically and geographically closest) applied on C3 node of internal area.....	45
<b>Fig. 3.16.-</b> Time responses of the <b>C2</b> internal machine following the disturbance (electrically and geographically far away) applied on C9 node of internal area. ....	46
<b>Fig. 3.17.-</b> Interconnected European power system UCTE/CENTREL [142]. ....	48

<b>Fig. 3.18.a, b, c.-</b> Comparison of time responses of the <b>KIEL1</b> German machine calculated with 90 equivalent machines by different identity recognition algorithms and considering their electromechanical weighting (weighted K-means, weighted Fuzzy and Kohonen-SOFM). .....	50
<b>Fig. 3.19.a, b.-</b> Comparison of time responses of the <b>STDE1</b> German machine calculated with 65 equivalent machines by different identity algorithms with electromechanical distances (weighted K-means, weighted Fuzzy). .....	52
<b>Fig. 3.20.-</b> Behavior of the <b>BWKUESS</b> German machine using 65 equivalents considering their electromechanical-based algorithms and following a disturbance at <b>VEHANNSA (VEW)</b> .....	53
<b>Fig. 3.21.-</b> Behavior of the <b>BWKUESS</b> German machine using 65 equivalents considering their electromechanical-based algorithms and following a disturbance at <b>EVDELSSAD (EnBW)</b> . ..	53
<b>Fig. 3.22.-</b> Comparison of identity recognition algorithms considering electromechanical weighted distances by the mean value of <b>J</b> of the 67 German intern machines for a fault located at the boundary node <b>VEGROUSB(VEW)</b> with different number of external equivalents. ....	55
<b>Fig. 4.1.-</b> Synchronous machine models: L1-L2-L3 transformed in dq-system.....	61
<b>Fig.4.2.-</b> Slow coherency aggregation.....	65
<b>Fig. 4.3.-</b> Power invariance aggregation.....	68
<b>Fig. 4.4.a.-</b> Classical aggregation .....	71
<b>Fig. 4.4.b.-</b> Proposed splitting based-aggregation .....	71
<b>Fig. 4.5.-</b> Machine-splitting with reference to their nominal power according to the derived splitting factors $a_1$ and $a_2$ .....	72
<b>Fig. 4.6.-</b> Splitting-based aggregation .....	73
<b>Fig. 4.7.-</b> Interconnected 16 Multi-machine System.....	80
<b>Fig. 4.8.-</b> Comparison of time responses of an internal machine calculated with the original external system and with 3 equivalent machines using the classical aggregation. ....	82
<b>Fig. 4.9.-</b> Comparison of time responses of an internal machine calculated with the original external system and with 3 equivalent machines using the splitting based-aggregation. ....	82
<b>Fig. 4.10.-</b> Comparison of time domain behavior of an internal machine calculated with the original external system and with 3 equivalent machines using the splitting based-aggregation. ....	83
<b>Fig. 4.11.-</b> Behavior of any internal machine following a sequence of disturbances applied on different nodes electrically and geographically distinct from the equivalent disturbance. It is simulated with the original external area and with 3 splitting equivalents with Fuzzy factors....	84
<b>Fig. 4.12.-</b> Comparison of aggregation algorithms considering the classical inertial aggregation and the proposed splitting-based aggregation by the mean value of <b>J</b> of the intern machines for a fault located at the internal node with different number of external equivalents.....	86
<b>Fig. 5.1.-</b> Division of complex power networks in areas .....	92
<b>Fig. 5.2.-</b> Neural network structure .....	93
<b>Fig. 5.3.-</b> Basic structure of generalized neuron model.....	94
<b>Fig. 5.4.-</b> ANNs applied to the modeling of non-linear systems. Internal and external recurrent ANN can be used to develop the DANN-based dynamic equivalencing .....	95
<b>Fig. 5.5.-</b> Modeling structures. The system modeling used in this approach is emphasized as a hybrid procedure in black-box form with assumptions about the system .....	96

<b>Fig. 5.6.-</b> Generator equivalent circuit as voltage and current source .....	103
<b>Fig. 5.7.-</b> Internal and external area of a interconnected power system.....	104
<b>Fig. 5.8.-</b> Equivalent external area of a power system.....	104
<b>Fig. 5.9.-</b> External area as dynamic equivalent.....	106
<b>Fig. 5.10.-</b> Network structure for approximation of non-linear systems .....	108
<b>Fig. 5.11.-</b> Series-parallel configuration coupling back the observed system output.....	109
<b>Fig. 5.12.-</b> Parallel configuration with an internal recurrent link to the networks.....	110
<b>Fig. 5.13.-</b> System modeling for dynamic equivalencing.....	111
<b>Fig. 5.14.-</b> DANN representing the dynamic equivalent for disturbances applied in the internal area .....	114
<b>Fig. 5.15.-</b> Global dynamic ANN forming the dynamic of the external area.....	116
<b>Fig. 5.16 .-</b> Dynamic ANN forming the external dynamic with distributed operating points according to heterogeneous power levels of the internal area.....	117
<b>Fig.5.17.-</b> Procedure to developing ANN models as dynamic equivalents .....	117
<b>Fig. 5.18.-</b> 16 Multi-machine system with 2 interfaces and three areas.....	118
<b>Fig. 5.19.-</b> 12 Multi-machine system with multiple number of boundary nodes .....	119
<b>Fig. 5.20.i .-</b> Real part of the injected current at the second boundary node following a non-trained disturbance in area A.....	121
<b>Fig. 5.20.ii .-</b> Imaginary part of the injected current at the second boundary node following a non- trained disturbance in area A.....	121
<b>Fig. 5.21.i .-</b> Real part of the injected current at the first boundary node following a disturbance (100 ms) at node 7 in area A under changed operating point .....	122
<b>Fig. 5.21.ii .-</b> Imaginary part of the injected current at the first boundary node following a disturbance (100 ms) at node 7 in area A under changed operating point .....	122
<b>Fig. 5.22.i .-</b> Real part of the injected current at the first boundary node following a disturbance (100 ms) on node 6 in area B.....	123
<b>Fig. 5.22.ii .-</b> Imaginary part of the injected current at the first boundary node following a disturbance (100 ms) on node 6 in area B.....	123
<b>Fig. 5.23.i .-</b> Active power flow interconnection between nodes 5 in B and 8 in C boundary line of area B and C according to the currents of Fig. 5.21 .....	124
<b>Fig. 5.23.ii .-</b> Reactive power flow interconnection between nodes 5 in B and 8 in C boundary line of area B and C according to the currents of Fig. 5.21 .....	124
<b>Fig. 5.24.i .-</b> Real part of the injected current at the second boundary node following a disturbance on node 15 in 220 kV of area C .....	125
<b>Fig. 5.24.ii .-</b> Imaginary part of the injected current at the second boundary node following a disturbance on node 15 in 220 kV of area C .....	125
<b>Fig. 5.25.i .-</b> Active power flow interconnection between area C and B following a fault on node 5 in 110 kV of C by changed operation point.....	126
<b>Fig. 5.25.ii .-</b> Reactive power flow interconnection between area C and B following a fault on node 5 in 110 kV of C by changed operation point.....	126

<b>Fig. 5.26.i, ii.-</b> Power flow interconnection between area A and C following a sequence of nontrained faults on C by changed operation point and network topology .....	127
<b>Fig. 5.27.-</b> Evaluation of the prediction capability of ANN considering different non-trained disturbances and non-trained operating conditions .....	129
<b>Fig. 5.28.i .-</b> Active power flow interconnection at the 8 <sup>th</sup> boundary node or between node 39 and 40 following a fault on the node 20 within the internal area .....	131
<b>Fig. 5.28.ii .-</b> Reactive power flow interconnection at the 8 <sup>th</sup> boundary node or between node 39 and 40 following a fault on the node 20 within the internal area .....	131
<b>Fig. 5.29.i .-</b> Real part of the injected current at the 8th boundary node following a disturbance on the node 20 in internal area under non-trained operating point of case 4 in table 5.2 .....	132
<b>Fig. 5.29.ii .-</b> Imaginary part of the injected current at the 8th boundary node following a disturbance on the node 20 in internal area under non-trained operating point of case 4 in table 5.2 .....	132
<b>Fig. 5.30.-</b> Evaluation of the standardized prediction error $\bar{E}_S$ of recurrent ANN considering different disturbance duration ( $t_{\min}=100$ ms, $t_{\max}=150$ ms) and two sequential disturbances ( $t_1=100$ ms after 1s, $t_2=120$ ms after 2s) .....	133
<b>Fig. 5.31.-</b> $\bar{E}_S$ evaluation of the robustness of the recurrent ANN depending on the cases of table 5.2 and in the 12 multi-machine system with different boundary nodes .....	135
<b>Fig. A.1.-</b> Ward static equivalent by eliminating {L} load and {G} generators nodes. ....	156
<b>Fig. A.2.-</b> Reduction of the Ward-PV equivalent with n number of equivalent generator nodes.....	157
<b>Fig.A.4.-</b> Recognition of coherent generators based on generators electromechanical eigenvector .....	161
<b>Fig. A.3.-</b> Frequency response for input m.....	162
<b>Fig. A.5.-</b> Input Signals u, Output Signals y, and Disturbances e .....	165
<b>Fig. B.1.-</b> Flow chart of the concept of K-means for a set of clusters .....	169
<b>Fig. B.2.-</b> Flow chart of the concept of fuzzy c-means clustering.....	174
<b>Fig. B.3.-</b> Schematic representation of SOFM .....	175
<b>Fig. B.4.-</b> Schematic representation of the clustering quality .....	176
<b>Fig. C.1.-</b> Interconnections among subsystems .....	182
<b>Fig. E.1.-</b> 12-machine system with three boundary nodes .....	193
<b>Fig. E.2.-</b> 12-machine system with four boundary nodes .....	193
<b>Fig. E.3.-</b> 12 multi-machine system with five boundary nodes .....	194
<b>Fig. E.4.-</b> 12 multi-machine system with six boundary nodes .....	194
<b>Fig. E.5.-</b> 12 multi-machine system with eight boundary nodes.....	195
<b>Fig. F.1.-</b> As consequence of the fusion of traditional network operators : BAG, BEWAG, EnBW, PE, RWE, VEAG and VEW the number of the current operators has been considerably reduced. ....	200

# List of Tables

<b>Table 3.1.-</b> Disturbance specifications for the 16 multi-machine system.....	40
<b>Table 3.2.-</b> Subsystems in the European Interconnected Power System UCTE/CENTREL.....	47
<b>Table 3.3.-</b> Disturbance specifications for the European power system UCTE/CENTREL (the boundary nodes correspond to NL=Netherlands, CH=Switzerland, OEVG=Austria).....	49
<b>Table 5.1.-</b> Studied cases in the 16 multi-machine system.....	120
<b>Table 5.2.-</b> Scenarios to power-flow changes considering Fig.5.19 .....	130
<b>Table 6.1.-</b> Comparison of the proposed approaches to applicability considering power system relevant aspects .....	143
<b>Table B.1.-</b> Computation of distances [101].....	168
<b>Table D.1.-</b> Data sets of investigated multi-machine systems .....	183
<b>Table D.2.-</b> Generator data set of 16 multi-machine system .....	183
<b>Table D.3.-</b> Transmission line data set of 16- machine system .....	184
<b>Table D.4.-</b> Comparison of aggregation algorithms considering the classical inertial aggregation and the proposed splitting-based aggregation by the mean value of $\mathbf{J}$ of the internal machines for a fault located at the internal node with different number of external equivalents.....	185
<b>Table D.5.-</b> Evaluation of the prediction capability of ANN considering different operating conditions and points calculating $\overline{E}_s(j)$ .....	185
<b>Table D.6.-</b> Sum squared distance error and average error of the predicted boundary behavior following disturbances at all non-trained nodes of internal area A considering different operating points .....	186
<b>Table D.7.-</b> Sum squared distance error and average error of the predicted boundary behaviour following disturbances at all non-trained nodes of internal area B considering different operating points .....	186
<b>Table D.8.-</b> Sum squared distance error and average error of the predicted boundary behaviour following disturbances at all non-trained nodes of internal area C considering different operating points .....	187
<b>Table E.1.-</b> Generator data set of 12-machine system .....	188
<b>Table E.2.-</b> Transmission line data set of the 12-machine system .....	188
<b>Table E.3.-</b> Evaluation of the standardized prediction error of recurrent ANN considering different disturbance duration ( $t_{min}=100$ ms, $t_{max}=150$ ms) and two sequential disturbances ( $t_1=100$ ms after 1s, $t_2=120$ ms after 2s).....	190

---

<b>Table E.4.-</b> Evaluation of the robustness of the recurrent ANN depending on the cases explained in table 5.2 and networks based on the 12-multi-machine system with different boundary nodes .....	190
<b>Table E.5.-</b> Scenarios to power-flow changes and losses considering 12-machine system with 3 boundary nodes after Fig.B.1 .....	190
<b>Table E.6.-</b> Scenarios to power-flow changes and losses considering 12-machine system with 4 boundary nodes after Fig.B.2.....	191
<b>Table E.7.-</b> Scenarios to power-flow changes and losses considering 12-machine system with 6 boundary nodes after Fig.E.4.....	191
<b>Table E.8.-</b> Scenarios to power-flow changes and losses considering 12-machine system with 7 boundary nodes after Fig. E.5.....	192
<b>Table E.9.-</b> Scenarios to power-flow changes and losses considering 12-machine system with 8 boundary nodes after Fig. 5.18 .....	192
<b>Table F.1.-</b> Part of the generator data set of the European Interconnected Power System [142] ...	196
<b>Table F.2.-</b> Part of the transmission line data set of the European Interconnected Power System.	198
<b>Table F.3.-</b> Comparison of identity recognition algorithms considering electromechanical weighted distances by the mean value of $J$ of the 67 German intern machines for a fault located at the boundary node <b>VEGROUSB(VEW)</b> with different number of external equivalents.....	200

# Nomenclature

## Latin symbols

$\mathbf{A}, \mathbf{B}, \mathbf{C}, \mathbf{D}$	State, input and outputs matrices of a system.
$\mathbf{A}_R, \mathbf{B}_{R1}, \mathbf{B}_{R2}$	Rotor electrical matrices corresponding to the electrical state system.
$\mathbf{A}_M, \mathbf{B}_M$	Mechanical matrices corresponding to the mechanical state system.
$\mathbf{A}_E, \mathbf{B}_E$	Excitation matrices corresponding to the excitation state system.
$\mathbf{A}_T, \mathbf{B}_{T1}, \mathbf{B}_{T2}$	Turbine-governor state matrices.
$\mathbf{B}_1, \mathbf{B}_2$	The bias of the hidden and output layer of the ANN, respectively.
$a_{ij}$	Participation share or splitting factor of external generator $j$ according to the number of generated equivalents $i$ .
$\mathbf{C}_x$	Covariance matrix denoted by $c_{ij}$ , representing the covariances between components $x_i$ and $x_j$ .
$D_i$	Damping coefficient of the $i$ th generator.
$d_{ij}$	Minkowski distance between two $M$ -dimensional objects (data points) $i$ and $j$ .
$d_{ij}$	Distance between a generator and the reference generator.
$E$	Voltage at generator internal buses.
$\underline{E}_a$	Complex internal voltage of generator A.
$\underline{E}_b$	Complex internal voltage of generator B.
$E_d', E_q'$	Transient EMF's of the generator in the $d$ - and $q$ -axes.
$\underline{E}_E$	Internal voltage of the equivalent generator E.
$\underline{E}_j(0)$	Initial driving voltage of external fictive generator $j$ .
$E_p$	Terminal common voltage calculated by the splitted internal voltages.
$E_N(j)$	Error function. This measure is realized over the sampling points $N$ of the whole behavior and for the disturbance $j$ .
$\overline{E}_s$	Mean standardized error function.
$\mathbf{e}_i$	Eigenvector defining the axes of the components of the generator data matrix.

---

$e_{pi}^y(t)$	Sensitivity of a determined machine's behavior $y(t)$ with reference to generator parameters $P$ .
$f, g$	The state and output function, respectively.
$\mathbf{f}, \mathbf{g}, \mathbf{h}$	Non-linear vector functions, which can be modeled.
$\mathbf{h}_N$	Functional relationship approximates the real properties of the external area with a dynamic ANN.
$h$	Non-linear function, which must be modeled.
$\mathbf{l}_G$	Unit vector with cardinality of $\{G\}$ .
$\mathbf{I}$	Identity matrix.
$i$	subscript for $i$ th generator.
$i$	Index for generator being grouped.
$i_d, i_q$	Stator currents in d- and q-axes, respectively.
$\underline{\mathbf{i}}_e, \underline{\mathbf{i}}_b, \underline{\mathbf{i}}_i$	Injected currents of the external, the boundary and the internal buses, respectively.
$\mathbf{i}(t)$	Injected current is the output vector, and it is a function of all state variables.
$\underline{l}(t)$	Real-time complex current value.
$\underline{l}_o$	Initial complex injected current value at a static operating point.
$i_j(t)$	Injected current following disturbance $j$ considering the original external area.
$i'_j(t)$	Injected current following disturbance $j$ predicted by the ANN.
$J_m$	Objective function according to the $m$ fuzziness index.
$M$	Inertia constant in p.u.
$M_i$	Inertia coefficient of the $i$ th generator.
$M$	Number of cluster groups representing the dynamic equivalents.
$m$	Fuzziness index and influences the "fuzziness" of the obtained grouping.
$m_m$	Turbine mechanical torque.
$N$	Number of generators or features.
$N_D$	Number of non-trained disturbances with the same duration applied to the nodes, which are not considered in the training database.
$N_s$	Number of generators in the internal area.
$N_p$	Number of sampling points of the time behavior.
$NG$	Number of coherent or identical machines in a corresponding group.
$n_y, n_u$	Maximum integer lags in the output and input signal of a system.
$P$	Number of variables or patterns of the time data series.
$P_G, Q_G$	Real and reactive power injections at internal generator buses in p.u.
$P_L, Q_L$	Real and reactive power residual at load buses in p.u.
$P_{el}$	Generator electric power obtained from a load flow solution.
$P_m$	Mechanical power.

$P_m^{ref}$	Reference power set by LFC (Load Frequency Control).
R	Index for the reference generator for the group under consideration.
$r_E, X_E$	Resistances and inductances of the equivalent generator in p.u.
$\mathbf{S}(t)$	Search direction matrix, which contains the gradient search for the minimum of the performance function.
$S_j$	Nominal power of the $j$ th generator.
$S_{ri}$	Rated power of the $i$ th single generator.
$S_{rE}$	Resulting nominal power of the equivalent generator.
$S_E, P_E, Q_E$	Nominal power, active and reactive power, respectively.
$\mathbf{T}$	$N \times N$ matrix including the eigenvectors of the covariance matrix $\mathbf{C}$ .
$T'_{do}, T'_{qo}$	Transient time constants of the open circuit and damper winding in the $q$ -axis.
$T_m$	Mechanical torque applied to the shaft of the generator.
$T_{mE}$	Mechanical torque (inertial constant) of the equivalent generator.
$\mathbf{T}_q$	$N \times q$ matrix including $q$ significant eigenvectors of $\mathbf{C}$ corresponding to the $q$ largest eigenvalues of $\mathbf{C}$ .
$\underline{U}(t)$	Real-time complex voltage.
$\underline{U}_o$	Initial complex voltage at a static operating point of the studied power system.
$u_d, u_q, u_{fd}$	Stator voltage in $q$ and $d$ -axes and the field voltage, respectively.
$u_s, i_s$	Stator (terminal) voltage and current, respectively.
$u_{pss}$	Voltage input signal to the PSS (Power System Stabilizer).
$\mathbf{u}(t)$	Input vector, i.e. voltage signal, that consists of state and field voltages, and mechanical power input of each generator in the system at time $t$ .
$\underline{u}_e, \underline{u}_b, \underline{u}_i$	Voltages of the external, the boundary and the internal buses, respectively.
U	Voltage at load buses.
$U_a, U_b$	Load bus voltage magnitude to bus $a$ and $b$ .
$u''$	Driving voltage.
$\mathbf{v}(t)$	Random noise signal.
$W_j$	Weighting factor for the $j$ th generator.
$\mathbf{W}_1$	Neural network weights of the first hidden layer into the matrix.
$\mathbf{W}_2$	Neural network weights of the output layer into the matrix.
$w_j$	Weighting electromechanical factor to form the electromechanical distance.
$\mathbf{X}(N,M)$	Time response matrix of oscillating swing curves, exhibiting $N$ the number of generators and $M$ the number of sampling points of the time data set.
$\bar{\mathbf{X}}$	ist the mean of that population of $\mathbf{X}$ .
$X'_{dEi}$	Transient reactance connecting the equivalent generator to the $i$ th bus.
$x'_d$	Transient reactance.

---

$X_{os}$	Rotor reactance.
$X_{hd}, X_{hq}, X_{\sigma Dq}, X_{\sigma Dd}, X_{\sigma fd}, X_{\sigma fd}, X''_d, X''_q$	Synchronous reactance and subtransient synchronous reactances in d- and q-axes system.
$X_i$	This represents resistances, main-field and linkage inductance of all circuits.
$\mathbf{x}$	State variable vector.
$X_q, X_d, X'_d, X'_q$	Synchronous reactance and transient synchronous reactance of the machine.
$\mathbf{x}_R$	Rotor electrical state vector containing the state variables: $E'_d, E'_q$ .
$\mathbf{x}_M$	Generator mechanical state vector containing the state variables: $\delta, S_m$ .
$\mathbf{x}_E$	Excitation state vector.
$\mathbf{x}_T$	Turbine-governor state vector.
$\mathbf{x}(t)$	Vector of system states variables, it may contain variables associated with synchronous generators and their controllers and possible network dynamics.
$\mathbf{Y}$	Network admittances in matrix form.
$y(t)$	Machine's behavior.
$\mathbf{y}, \varphi$	Output and input vector of the neural network, respectively.
$\mathbf{y}(t)$	Output vector of the system.
$\mathbf{Z}$	Matrix, which contains the system output and the regressor.
$\mathbf{z}$	Algebraic variable vector.

## Greek symbols

$\alpha_a$	Relationship factor between $\underline{E}_E$ and $\underline{E}_a$ .
$\alpha_b$	Relationship factor between $\underline{E}_E$ and $\underline{E}_b$ .
$\alpha(t)$	It determines the length of the step in the search direction.
$\underline{\alpha}$	Complex constant.
$\delta$	Angle at generator internal buses (rotor shaft angle of the generator).
$\varepsilon$	User specified tolerance degree.
$\varphi(t)$	Time dependent regressor vector.
$\kappa$	Neural network activation function.
$\lambda_j$	Eigenvalues, which are equal to the variance of each generator behavior.
$\mu_{ij}$	Fuzzy membership degree of generator $x_j$ to cluster $c_i$ .
$\Delta$	Deviation from a specified steady state operating point.
$\Delta_j(t)$	Change of the injected current following disturbance $j$ .

---

$\Delta i'_j(t)$	Change of the injected current following disturbance $j$ predicted by the ANN.
$\bar{\Delta I}$	Current injection variable as phasor form.
$\Delta I_a, \Delta I_b$	Incrementals for the currents: $I_a$ and $I_b$ .
$\Delta P_{mi}$	Change in mechanical input power in p.u.
$\Delta P_{gi}$	Change in electrical output power in p.u.
$\Delta P(i)^{Original}$	Time domain behavior of the $i$ th internal generator calculated with the original external area.
$\Delta P(i)^{Dyn. Equi.}$	Time domain behavior of the $i$ th internal generator calculated with the the equivalent external area.
$\Delta \delta_a, \Delta \delta_b$	Incremental variables for $\delta_a$ and $\delta_b$ .
$\Delta \theta_i$	Incremental rotor phase angle of the $i$ th generator.
$\Delta \theta_R$	Incremental rotor phase angle of the reference generator.
$\Delta p_i(t)$	Active power variation.
$\Delta \delta_i(t)$	Generator angle deviation.
$\Delta \omega_i(t)$	Generator angular velocity deviation.
$\Delta \omega_i$	Speed deviation in p.u.
$\Delta \delta_i$	Rotor angle deviation in radians.
$\theta$	Angle at load buses.
$\theta$	denotes the collection of involved neural network parameters: $W_1, W_2, B_1, B_2$ .
$\theta_a, \theta_b$	Bus voltage angle a and b.
$\theta$	Bus angle at the generator terminals obtained from the network solution.
$\omega_o$	Network frequency referenced to p.u.
$\omega_L, \delta_L$	Rotor angular velocity and rotor angle, respectively.
$\omega, \omega_o$	Rotor angular velocity of the generator (synchronous speed of the system).
$\psi_L, \psi_S$	Rotor and stator flux linkage, respectively.
$\nabla E(\theta(t))$	Gradient of the error matrix with respect to the ANN parameters.
$\Sigma^2$	Diagonal variance matrix.

# Acronyms

AGC	Automatic Generation Control
AMS	Associative Memory Systems
ANN	Artificial Neural Network
BAG	Bayernwerk AG
BEWAG	Berliner Staedtische Elektrizitaetswerke AG
CENTREL	Central European Power System
COI	Center Of Inertia
DANN	Dynamic Artificial Neural Network
EnBW	Energie Baden Wuerttemberg
FACTS	Flexible AC Transmission Systems
FC	Fuzzy Clustering
HC	Hierarchical Clustering
LFC	Load Frequency Control
MIMO	Multi Input Multi Output
NARX	Non-linear AutoRegressive models with eXogenous inputs
NARMAX	Non-linear AutoRegressive Moving Average terms with eXogenous inputs
NH	Non-Hierarchical Clustering
NOE	Non-linear Output Error
OP	Operation Point
PCA	Principal Component Analysis
PE	Preussen Elektra
PSD	Power System Dynamic
PSS	Power System Stabilizer
RWE	Rheinisch-Westfaelisches Elektriizitaetswerk
SOFM	Self-Organizing Feature Maps
UCTE	Union for the Coordination of Transmission of Electricity
VEAG	Vereinigte Energiewerke AG
VEW	Vereinigte Elektrizitaetswerke Westfalen

*“The idea is to try to give all the information to help others to judge the value of your contribution; not just the information that leads to judgment in one particular direction or another.” -Richard P. Feynman-*

# Chapter 1

## Introduction

### 1.1 Motivation

The old electricity supply services were characterized by monopolistic and local market structures of the electricity industry. In the last two decades, this principle has been undergoing a radical reform by taking into consideration technical, economical, and political reasons and replacing those vertical structures with a deregulated electricity market open to the competition.

Due to the separation of energy producer and network operator and principally through the competition between the energy producers, a significant increase of energy transport costs in a complex interconnected power system operation has to be taken into account. This effect plays an important role considering the fact that plant locations are selected in the future no longer primarily in the neighborhood of consumer centers, but rather in priority after cost factors of the production.

With the increased market liberalization, the network operators must perform the minimization of the generation costs and transmission costs. Thus, significant changes of the network structures to the increased transmission lines are not plausible. But, it is more appropriate, that the network operators will operate their transmission lines more closely to the allowable transmission capability, especially to the stability limit.

In order to guarantee the reliability, the accuracy of stability analysis must be satisfied. Therefore, the energy providers should be able to estimate the dynamic behavior of their own power system exactly. In large power systems, it is difficult to perform the dynamic stability

analysis accurately because of the large number of transmission lines, system components, and the network boundaries. Also, the significant influences of the neighborhood networks to their own area have to be taken into consideration.

Nowadays, a detailed calculation of neighborhood networks is always not possible due to the complexity of interconnected power systems. Moreover, the hard competition between network operators due to the deregulated and liberalized electricity market leads to limited cooperation and restricted internal data availability between operators.

These aspects are clearly presented in the west European power system, which is coordinated by the UCTE (Union for the Coordination of transmission of Electricity). The energy market liberalization and the east expansion of the UCTE can be considered as the most essential change in the European energy economic of the last years. Additional to *UCTE*, the central European power system (*CENTREL*) includes the eastern European countries.

At present, the expansion of the UCTE network to east is in full swing. In planning consolidation and extension of the European interconnected power system, new problems concerning to the power flow and the stability aspects have to be solved.

The calculation of the complete European network would lead to an enormous technical expense due to its complexity. At the same time, it is not necessary for a national internal network operator to analyze other networks.

In spite of all, it is impossible to obtain all required data of the complete European network in detail. Moreover, the global data availability is limited by other local operators, since they do not want to reveal their own network specific data sets, i.e. the capability of their own power plants or the load performance, etc. Considering these reasons, it is suitable to represent the neighbor networks as equivalent networks, which are connected to the local internal area.

In order to determine such equivalent networks, various conventional procedures in frame of dynamic equivalencing were developed, which reduce a complex power system to a small and simplified one. Thus, these simplified power supply models that can be utilized in network reliability, management and planning to overcome blackouts situations and to affront new technical circumstances of the deregulated electricity market.

The classical dynamic equivalencing consists principally of the following main steps:

- Coherency Identification for grouping of coherent machines
- Aggregation of these machines
- Static network reduction
- Aggregation of control devices

Such equivalent systems are useful both for the planning and operation of interconnected large power systems. This simplifies the load flow calculations, transient stability calculations, and general investigations concerning protection and safety aspects. However, the classical well known procedures to form equivalent systems are mainly based upon linearized system models around a specific operating point with theoretical constraints validating. Consequently, they are restricted in its validity on practical non-linear, offline- and online-applications.

## 1.2 Objectives

Non-linear-based and innovative approaches for the equivalencing of complex large power systems have been developed in this dissertation. These new techniques satisfy the needs and requirements of all involved electricity market participants, especially for the network operators. In this context, the availability of a robust and consistent dynamic equivalencing using artificial intelligent systems plays an important role.

The objectives are to introduce new dynamic equivalencing concepts, where the *linear* and *non-linear characteristics* and *behavior* of the power system are essentially considered. Principally, the following approaches are proposed within the scope of this dissertation:

### i. Identity recognition instead of the classical coherency identification

This innovative approach replaces the classical coherency identification in dynamic equivalencing. It is based on the recognition of real identical machines using their linear and non-linear properties. The identical machines that swing together in the sense of new defined criteria are classified into cluster groups. Applying standard pattern recognition methods to dynamic equivalencing can satisfy the criteria.

## **ii. Electromechanical-based identity recognition**

The electromechanical influence of the generator is taken into consideration in the identity recognition procedure by means of the new proposed electromechanical distance to obtain '*electrically real identical generators in cluster groups*'.

The new defined electromechanical distance is based upon suitable machine model parameters. In this way, the electromechanical relationship between generators in the identity process will be considered. This method improves essentially the assignment of identical generators and the accuracy of dynamic equivalents.

The applicability and consistency of this new approach and its ability to grouping of real identical machines will be tested both in the 16-generators system and in the large-scale model of the interconnected European power system with 464 generators.

## **iii. Splitting-based aggregation instead of the classical aggregation**

This research focuses on the splitting of generators, which belong to different groups at the same time but with different membership degrees. Thus, the generators will be divided into representative parts, which will be aggregated to virtual equivalent generators.

This innovative approach forms "virtual" generator models. It is based on the application of principal component analysis (PCA) and the Fuzzy theory for generating a dynamic splitting of generators. These new aggregated equivalent generators are modeled upon the basis of the splitted parameters of all original external generators.

## **iv. DANN-based dynamic equivalencing**

By means of the identification of the non-linear behaviors of a power system, a knowledge- and signal-based robust dynamic artificial neural network (DANN) is developed. The artificial neural network can be considered as global external non-parametric dynamic equivalent to represent a non-linear Multi Input Multi Output (MIMO) system model, which replaces and identifies the static and dynamic behaviors of all elements of an interconnected power system, i.e. generators, transmission lines, converters, voltage and turbine controllers, amongst others, as global system.

This approach replaces successfully the stages of the classical dynamic equivalencing, such as coherency identification, aggregation, and network static reduction. It is proved to be an effective method for the online dynamic equivalencing of interconnected large power systems.

This approach is applied in a 12- and 16-machine system with many boundary nodes. The robustness considering different power flow conditions with the ANN-based stability analysis are examined.

### 1.3 Outlines of the dissertation

This dissertation is organized consisting of the following chapters:

In **CHAPTER 1**, an introduction about generic topics of this dissertation is presented. Following in **CHAPTER 2**, a general overview of the background and actual state of development of dynamic equivalencing is given.

The main focus of **CHAPTER 3** describes the identity recognition concept as alternative to the classical coherency identification. The electromechanical distance as an improvement factor in the procedure will be proposed generating electromechanical-based equivalents.

As an important contribution to aggregation of generators, **CHAPTER 4** describes the splitting-based aggregation instead of the classical aggregation forming virtual equivalent generators. Their theoretical background and the corresponding algorithm are explained.

An investigation about the system modeling of non-linear MIMO systems that comprise complex interconnected power systems is introduced in **CHAPTER 5** describing the replacement of external power systems with a dynamic artificial neural network (DANN).

Finally, **CHAPTER 6** includes a comparison, conclusion, and summary about the proposed innovative approaches, their applicability in practical situations of dynamic equivalencing. Suggestions on future research directions on this topic area are summarized.

*“Analysis of stability, equivalencing of network, ..., are greatly facilitated by classification of them into appropriate categories. Classification therefore is essential for meaningful practical analysis and resolution of a complex system problem”-A quotation from [3]-*

## Chapter 2

# Background

**Objective—** *This chapter briefly presents the key definitions and traditional concepts in power system dynamic equivalencing, which will be used as basis to develop innovative approaches throughout this thesis.*

**Index Terms—** *Clustering, Coherency Identification, Dynamic Equivalencing, Electromechanical Distance, Network Reduction, Modal Analysis, System Identification, Linear Model Reduction, Slow and Inertial Aggregation, Stability Analysis, Ward Reduction.*

**Organization—** *Section 2.1 describes the classical dynamic equivalencing. In section 2.2, the existing approaches are treated in detail and finally, in section 2.3, a brief summary is presented.*

### 2.1 Dynamic equivalencing

The dynamic equivalencing consists of forming equivalent machines, which represent the electrical and mechanical characteristics of the original machines. To this end, a complex large power system network may be divided into the following areas:

- **The internal area** has to be retained intact and unreduced in detail containing the internal machines for stability studies. The dynamic behavior of this area is simulated using dynamic equivalents of the neighborhood area.
- **The external area**, containing the external generators, transformers, transmission lines, additional devices, amongst others, will be simplified to a reduced system. The generators will be classified, grouped, and aggregated to a dynamic equivalent.

In order to realize the transient stability analysis, it is important to consider the impact of the external area to the internal area during the disturbance period. Following aspects between internal and external area should be considered:

- The detailed description of the external area is not important for stability studies. Therefore, the detailed equivalencing of the external area is not necessary [1-5].
- The external area is not of direct interest in stability studies and is of consequence only in so far as it influences the response of the internal area to disturbances within it.
- In general, the grouping of generators in the external area is mainly affected by disturbances coming from the internal area through the boundary nodes and lines.
- The impact of the external generators on the internal area depends generally on the electrical and geographical distance between the two areas and their boundary nodes.
- In dynamic equivalencing, the influence of particular disturbances in particular locations of the internal area should be considered.
- This equivalent external area coupled to the detailed model of the internal area must consistently form the same amplitude and frequency behavior of oscillations in the boundary buses. Consequently, the reduced system has the same dynamic behavior as the original interconnected power system.

The following diagram shows schematically the dynamic equivalencing.

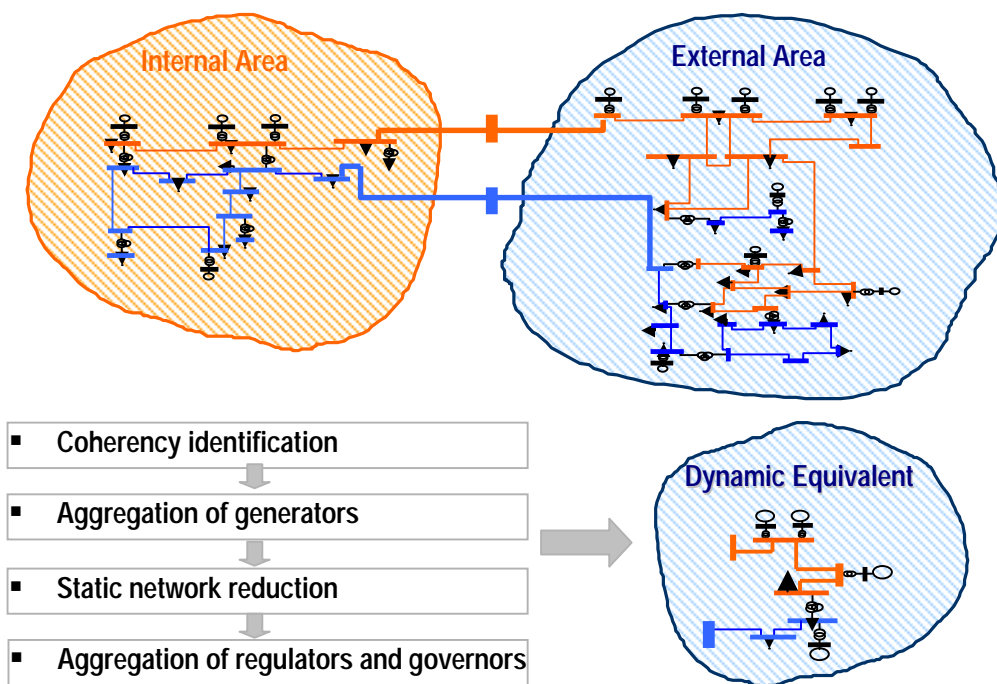


**Fig. 2.1.-** Classical dynamic equivalencing in power systems

The classic dynamic equivalencing consists of the basic steps [6, 7, and 8] mentioned in Fig. 2.1, which will be described in the following sections:

### 2.1.1 Coherency identification and grouping of generators

In this step, coherent generators are identified and grouped together. These aspects are evaluated in appendix A.3. This identification procedure can be significantly simplified by using the following assumptions:

- Non-generator dynamics may be ignored or simplified.
- Classical generator models can be used.
- The linearized system model preserves well the properties of coherency.

The following methods are available for determination of the coherent groups of generators:

- **Weak links coupling** [9].- In this method, the coherency is determined by analyzing the coupling of generators in the state matrix. A group of generators are identified as coherent if the coupling coefficients among them are high.
- **Two-time scale** [10].- This method is based on the concept that a slow oscillation is caused by two groups of strongly coherent generators interconnected through weak ties. In this case, the two oscillating generator groups can be easily identified by means of the eigenvector associated with the mode of oscillation. With this method, the system can be partitioned into an arbitrary number of coherent external generator groups by analyzing the same number of the slowest modes of oscillations. This method is extended not only for generators [11, 12] but also for generators and weak tie lines [13].
- **Slow coherency** [14] **and tolerance-based slow coherency** [15].- These contributions describe an algorithm for fault independent area grouping. However, they don't indicate how more complicated generating unit models can be handled. The slow coherent-decomposition is defined with respect to a select subset of modes of a linearized model, in which only the lowest electromechanical modes of the system are selected. The tolerance-based coherency procedure relaxes slow-coherency in the direction of slow-synchrony, although the dynamical implications are not exactly explored.
- **Linear time simulation** [17, 18].- This is the classical method to identify coherent generators. The time domain response of the system is solved for a specified fault in the power system, and the rotor angles of generators are compared. *Those generators with*

*rotor angles swinging together with respect to the phase angle are identified as coherent* (Podmore condition)<sup>1</sup>. This will be in detail explained in chapter 3.

#### Remarks:

- The *'tolerance-based slow coherency'* is similar to the previous 'two-time scale for generators only' method, but includes additional constraints to ensure that widely-separated generators are not aggregated.
- The *'two-time scale'* and *'slow coherency'* methods require the calculation of selected eigenvalues and eigenvectors of the full system and complicate its practical application. The modified Arnoldi eigenvalue solver used in [16] can be utilized to simulate large interconnected power systems.
- There are different possibilities to group coherent generators, which can be realized through the analytical method, such as *'the two-time scale method'* and *'the weak-link method'*. But the analytical method often produces incorrect results. To overcome the problem, heuristic methods are carried out in parallel with the analytical method [25].
- The method of Lee and Schweppe in [20] offers several methods [19, 21-24, 27-29] with reference to heuristic approaches based on the Podmore condition [17-18].
- An important technique in this step is the building of standard equivalents according to *'a pre-reduction of dynamic states identifying similar dynamic models'* or control devices to the corresponding generators at the same bus.
- To this aim, weighted average and least squares frequency domain algorithms to calculate the parameters of the aggregated generators and their control models are used. After this pre-procedure, the classical coherency methods are applied. However, the results are not promising [26].

### 2.1.2 Network aggregation

In this step, an aggregated network is constructed on the basis of the equivalent generator parameters for each coherent group of generators.

This obtained dynamic equivalent is a single unit that exhibits the same voltage, speed, and total mechanical and electrical power as grouping generators during any disturbances, where those generators show coherent properties.

---

<sup>1</sup> This method is developed on the basis of a simplified and linearized power system model representing the mechanical equations for the motion of synchronous generators. The swing curve simulation has been realized faster by using a linear model and solving it in many cases by means of trapezoidal integration algorithm.

Retaining the original steady state, power flows, and voltages in the network, only the network equations are modified, which is replaced by several coherent generators.

In the literature, the following classical aggregations which are given in detail in chapter 4, are presented:

- ***Inertial and slow aggregation*** [15, 30-33].- The generators in a coherent group are represented by an equivalent classical generator model. In its simplest form, the equivalent inertia is the sum of the inertia of all coherent generators in the group, and the equivalent transient reactance is obtained by paralleling the transient reactance of all generators in the group.
- ***Detailed aggregation*** [34].- In this method, if some or all generators in a coherent group have similar control systems, they can be aggregated to a detailed generator model with an equivalent exciter, stabilizer, and governor. The parameters of the equivalent models are obtained using a combination of two approaches: a least square fit of the frequency responses to determine the linear characteristics, and an evaluation of the time domain constraints to set the non-linear characteristics.
- ***Power invariance principle*** [35].- This method summarizes the equivalent generator representation and the network reduction retaining the terminal buses of each of the coherent generators. Hence, it preserves the basic physical structure of the original system. For each coherent group, a fictitious point is constructed such it connects all the internal voltage sources of the generators with one end of the transient reactance.
- ***Berg and Ghafurian method*** [36, 37].- In this method, the coherent group of generators can be replaced by an equivalent generator modifying the network by mathematical formulations according to complex ratios as weighting factors.

### 2.1.3 Static network reduction

Once equivalent generators are determined for the generators groups, a network reduction is performed<sup>2</sup>. This reduction is generally achieved in two steps:

- The equivalent generators are inserted into the system and the generators in the associated coherent groups are removed. The network is modified to maintain the balanced steady state power flow conditions.

---

<sup>2</sup> After the static network reduction procedure, the reduced network must have the exact electrical behavior as the original one.

- The network is reduced to restricted number of nodes. In this way, nodes are eliminated, and new transmission lines can be created or by using an adaptive reduction technique, similar to the one introduced in [40, 41]. The criterion for the nodes elimination is the network sparsity.

The network nodes can be eliminated mathematically. This is a simple network transfiguration. Equivalent lines and shunts as result can be obtained. Only if non-linear load are connected to the nodes, it is necessary to involve linearized load models into the transfiguration. The intention of transfiguration is the encoding of the real load flow properties rather than the reduction of computational efforts <sup>3</sup>.

### 2.1.4 Aggregation of control devices

Once equivalent generators are determined, and network reduction is performed, voltage regulators and governors will be aggregated in the dynamic behavior of power plants <sup>4</sup>.

In order to obtain accurate results, it is necessary to model these devices on the basis of their real structure and operating mode. This aspect leads to different types of control models. To meet the requirements in the practice, different modeling techniques are implemented into the stability analysis. However, this generates a large number of different controller models enclosed in data sets of real electric power systems. However, techniques for controller aggregation are not explored satisfactory yet.

In the corresponding literature, the following methods are presented:

- Splitting of coherent generator group in subgroups with similar controllers [26, 37].
- A controller with the best similarities to all controllers in the coherent group is chosen. The parameters fitting is realized by simulating disturbances in the frequency range. Usually, it is carried out in a network, where group members and the equivalent one are connected to the same bus [34, 38, and 39].
- A suitable fact is to choose the optimal equivalent controller using the controller of the largest subgroup. This optimal equivalent controller is used for the equivalent of the whole group [39].

---

<sup>3</sup> Actually, if too much nodes are eliminated, due to the large number of created equivalent lines, the effort can be increased significantly. It should emphasize, that for the simulation it is not necessary to reduce the network.

<sup>4</sup> If within a coherent group the controllers don't have the same structure and parameter settings, it is suitable to create an equivalent controller, which will be assigned to the equivalent generator.

- Another alternative is to select the controller of the greatest generator of the coherent group to build a standard controller.

The influence of controllers on the dynamic behavior of power systems is commonly significant. Consequently, it neither in the coherency identification nor in the aggregation of power plants can be neglected.

## 2.2 Existing approaches

In the past, the equivalencing procedure was realized on the basis of performing a static reduction of the equivalent area by essentially '*Gaussian elimination techniques*' [42]. According to this method small generators less than 50 MW were simply netted as negative load. Larger generators were retained and equivalenced by classical approaches [25].

Various approaches are proposed for dynamic equivalencing, in particular by exploiting modal and coherency properties of the machines. A detailed explanation of these approaches will be explained in appendix A. Subsequent developments led to the following classical types of dynamic equivalents:

- **Ward Types.-** In a preliminary way, the dynamic equivalencing was developed on the basis of Ward type equivalents, which are based on distribution factors used in power flow studies [48]. An interesting approach was proposed in [56] as dynamic Ward equivalent. Here, a transient energy function for a reduced system is built after the elimination of load buses provided with constant current and constant power loads <sup>5</sup>.
- **Modal equivalents.-** It involves two steps:
  - Construction of matrices, which represent equivalents of the external system.
  - Interfacing these matrices with the transient stability simulation of the internal area to simulate the complete system.

State changes in the external area are captured by a linearized model. The dynamic characteristics of this area are then expressed by using voltages and injected currents at the interconnected nodes as inputs and outputs, and they are linearized at the operating point as base case specified by a power flow <sup>6</sup>.

<sup>5</sup> This reduction employs a Ward equivalencing method in which the equivalent current injections are updated at each integration step of the path-dependent term of the energy function. Each step involves a single iteration of the Newton-Raphson procedure on the unreduced system.

<sup>6</sup> In the modal equation of the state space equation of the selected group of the generators, *the exact coherency is equivalent to the situation where only one mode is excited by any disturbance and all other modes are equal to zero*. The excited mode represents oscillations between the given group of generators and the rest of the system.

- **Coherency-based equivalents.-** An alternative approach to modal analysis is the coherency identification. Some previous attempts at the problem of identifying coherency have been heuristically-based and have utilized the concept of electrical distance [20-24]. A common limitation of the heuristic methods is the lack of accuracy and consistency demanded for using in routine planning applications.
- **Model reduction and identification methods.-** The need to use low-order dynamic models of a complex power system, especially for its stability analysis considering damping inter-area and local oscillations, is an important reason for a model reduction. Identification methods can be used in dynamic equivalencing. System identification deals with building dynamic models in form of a state-space system structure [84-86]. Identified models describe linear difference relationships between input and output signals.

## 2.3 Power system simulation program

In this research, the power system simulation program PSD (Power System Dynamic) is employed for dynamic studies. The appendix part A.7 shows the implementation of the PSD flow chart. The PSD is a program for modeling and simulating power systems including steady state analysis and online transient simulation. The applications and results of the program are reported in [87, 88]. PSD is based upon *the principles of electromechanical-transient computations in electrical networks*. The program has a *strong library providing accurate dynamic models for most known elements in power systems*, such as synchronous machine, two and three winding transformers, and transmission lines, among others. Thus, the user can choose a suitable model for the synchronous machine among the second-, fifth- and sixth-order models and define the parameters. It is also possible to build special units like FACTS, fuel cell devices, among others in a so-called “regulator files” depending on their block diagram models. These models are integrated into the network through connecting nodes, which helps the operator to build his own models for the regularly variant components like the voltage and speed governor regulators. The interaction between the built units and the network is accomplished through selected variables, which are exchangeable during the simulation process. The model structures of the regulator devices are implemented using a special standard code in the PSD simulation package. The interface of these units with the network is accomplished through the output active and reactive power at each time interval.

The program was carried out using FORTRAN and contains the coherency, aggregation and static network module as well the proposed approaches presented in chapter 3, 4 and 5, which have been implemented in frame of this research on the PSD platform [141].

Each power system studied is first being simulated by PSD in its original state using the standard models found in the library of the PSD validated in [87]. Following that, the new-

implemented modules in PSD will perform the dynamic simulation of the power system using the identity recognition, the splitting aggregation and the ANN-based equivalencing in interaction with additional special programs developed in some cases in MATLAB and FORTRAN [141].

Hence, after simulating the whole power system in the PSD simulation package, the dynamic performance of the one is studied taking into consideration the dynamic equivalencing. Firstly, a power flow calculation is carried out to define the initial operating condition of the power system. Different disturbances are then simulated in different areas of the system. The results of the simulations will show how close enough the proposed model's responses are to the original system's responses in the event when disturbance is applied.

## 2.4 Summary

- In above, the *basic steps of the classical dynamic equivalencing*, such as: (i) coherency identification, (ii) generator aggregation, (iii) network reduction and (iv) control aggregation, and their corresponding methods are summarized.
- The definition of coherency identification can be defined as: *closely those of the similarity rotor angle behavior of machines. All coherency-based approaches are based on this condition applied to linearized models of the power system.*
- *The modal-based approaches* are based on the inspection of *the eigenvalues of the linearized state matrix. However, it provides limited information about the mode behavior of generators for a given operating point.*
- The determination of *parametric properties of the multi-machine power system requires the use of linear model reduction approaches and linear parametric identification methods.*

The next chapters will present innovative non-linear dynamic equivalencing approaches using modern and non-conventional techniques.

*“The problem becomes highly complex when dealing with real disturbances, since linearization is totally ruled out. For these cases solution techniques using non-conventional methods should be discussed beginning with the statement of the problem under physical insight aspects” - M. A. Pai [135] -*

## Chapter 3

# Electromechanical-based Identity Recognition in Dynamic Equivalencing

**Objective—** *Aim of this chapter is to present a new electromechanical-based approach in transient stability of power systems for recognition of identical behaviors of machines. The approach reformulates the classical coherency condition on the basis of the identity recognition. Those conditions are used as a basis for generating dynamic equivalents incorporating physical and model system parameters of the external generators with high accuracy in the results. Hereby, it consists of the introduction of an electromechanical distance additional to the geometrical distance that it significantly improves the accuracy and efficiency of identity-based dynamic equivalents.*

*Test of this approach have been performed and evaluated on a 16 multi-machine system and on large-scale model of the interconnected European power system (UCTE/CENTREL).*

**Index Terms—** *Clustering, Coherency Identification, Dynamic Equivalent, Electromechanical Distance, Electromechanical Parameters, Identity Recognition, Network Reduction, Stability Analysis in Power System.*

**Organization—** *Section 3.1 and 3.2 of this chapter describe the introduction and the classical coherency identification, respectively. In section 3.3 the proposed identity recognition is presented, and mainly, the electromechanical-based identity recognition*

*approach is treated in section 3.4, followed in section 3.5 by the application in interconnected power systems. In section 3.6 the simulation results are evaluated and the summary in section 3.7.*

### **3.1 Introduction**

This chapter addresses *a new alternative to coherency identification*. It is the *identity recognition* as an efficient approach for recognizing the identical behavior of external generators forming cluster groups of identical generators and to show that once the identical behavior was known, significantly reduced dynamic equivalents could be obtained.

The approach presented is based upon necessary conditions to process the swing oscillating curves in time domain of the external machines. Those reformulated conditions may be realized using standard pattern recognition algorithms (clustering algorithms). In order to generate more accurate dynamic equivalents, the definition of an *electromechanical distance* considering the physical characteristics and model properties of the external generators in the identity recognition procedure will be proposed.

### **3.2 Coherency-based dynamic equivalencing**

*A coherent group of generators is defined as a group of generators oscillating with the same rotor angular speed. For this purpose, two generators buses are defined as coherent if their angular difference is constant within a certain tolerance over a certain time interval [17].*

The classical coherency identification of Podmore [17] is based upon the *determining the difference of the voltage angles of the terminal generator nodes, which is extended to the rotor phase angle behavior*. The coherency of both generator internal and terminal buses is of interest.

Therefore, the generator time responses are evaluated only regarding the rotor angular phase. This condition is necessary to form dynamic equivalents [17, 18]. This aspect represents a significant limitation of the equivalencing, because only linear processes and behaviors of the power system are considered without taking into consideration important factors of the real generator system, such as non-linear characteristics of governor-, turbine devices, real modeling parameters, among others.

### Disadvantages:

The formation of a simplified linear model of the power system is realized and solved using a fast trapezoidal integration algorithm. Considering this linearized simplified system model, the following disadvantages should be taken into account:

- Coherent groups forming the corresponding equivalents are not exact enough, since the performance of an equivalent system tends to depend on the applied disturbance.
- The coherent groups are independent of the amount of detail in the machine model, i.e. in the coherency procedure the real parameters and properties of the machines and governors in form of *non-linear behavior* are not considered in spite of all enhancements in the coherency strategy [19-25].
- A classical synchronous generator model is considered and the excitation and turbine-governor systems are ignored. This aspect is based upon the observation that the amount of detail in the generator unit models has a significant effect upon the swing oscillation curves, particularly the damping [17].

### Linearized system

The dynamic equation of the  $i$ th generator in a power system with the damping coefficient included can be formulated as linearized in the following form<sup>7</sup>:

$$M_i \Delta \ddot{\delta}_i = \Delta P_{m_i} - \Delta P_{G_i} - D_i \Delta \omega_i \quad i=1, \dots, n \quad (3.1)$$

where

- $i$  is a subscript for  $i$ th generator.
- $\Delta$  indicates that this variable represents a deviation from a specified steady state operating point.
- $M_i$  is the inertia constant in p.u.
- $\Delta \omega_i$  is the speed deviation in p.u.
- $\Delta \delta_i$  is the rotor angle deviation in radians.
- $D_i$  is the damping constant in p.u.
- $\Delta P_{m_i}$  is the change in mechanical input power in p.u.
- $\Delta P_{G_i}$  is the change in electrical output power in p.u.<sup>8</sup>

The changes in the complex voltages and power injections at the generator and load buses may be expressed using the Jacobian matrix in (3.2) and in simplified form in (3.3):

$$\begin{bmatrix} \Delta P_G \\ \Delta P_L \\ \Delta Q_G \\ \Delta Q_L \end{bmatrix} = \begin{bmatrix} \frac{\partial P_G}{\partial \delta} & \frac{\partial P_G}{\partial \theta} & \frac{\partial P_G}{\partial E} & \frac{\partial P_G}{\partial U} \\ \frac{\partial P_L}{\partial \delta} & \frac{\partial P_L}{\partial \theta} & \frac{\partial P_L}{\partial E} & \frac{\partial P_L}{\partial U} \\ \frac{\partial Q_G}{\partial \delta} & \frac{\partial Q_G}{\partial \theta} & \frac{\partial Q_G}{\partial E} & \frac{\partial Q_G}{\partial U} \\ \frac{\partial Q_L}{\partial \delta} & \frac{\partial Q_L}{\partial \theta} & \frac{\partial Q_L}{\partial E} & \frac{\partial Q_L}{\partial U} \end{bmatrix} \begin{bmatrix} \Delta \delta \\ \Delta \theta \\ \Delta E \\ \Delta U \end{bmatrix} \quad (3.2)$$

The variables used in the Jacobian matrix are defined as [17]:

- $P_G, Q_G$  are real and reactive power injections at internal generator buses in p.u.
- $P_L, Q_L$  are real and reactive power residual at load buses in p.u.
- $E, \delta$  are voltages and angles at generator internal buses.
- $U, \theta$  are voltages and angles at load buses.

The voltage dependence of the load powers is included in the  $\frac{\partial P_L}{\partial U}$  and  $\frac{\partial Q_L}{\partial U}$  terms and the changes in the power residuals  $\Delta P_L$  and  $\Delta Q_L$  are normally zero but may be assigned certain values in order to model a disturbance such as bus load shedding. Equation (3.2) can be simplified by accounting for the decoupling, which exists between the real and reactive power flows for a transmission system with high impedance ratios. The real power flows are largely dependent upon the voltage angles and as a first order approximation; the effect of variations in load bus voltage magnitude may be neglected by setting the terms  $\frac{\partial P_G}{\partial U}$  and  $\frac{\partial P_L}{\partial U}$  to zero. The voltage behind the generator transient reactance is constant thus,  $\Delta E = 0$ . According to these assumptions the incremental decoupled active power flow equation may be derived to:

$$\begin{bmatrix} \Delta P_G \\ \Delta P_L \end{bmatrix} = \begin{bmatrix} \frac{\partial P_G}{\partial \delta} & \frac{\partial P_G}{\partial \theta} \\ \frac{\partial P_L}{\partial \delta} & \frac{\partial P_L}{\partial \theta} \end{bmatrix} \begin{bmatrix} \Delta \delta \\ \Delta \theta \end{bmatrix} \quad (3.3)$$

<sup>7</sup> Equation (3.1) merely states that the accelerating power for each machine is balanced by the increase in kinetic energy of the rotor and the power absorbed by the damping forces with respect to a synchronous rotating reference frame.

<sup>8</sup>  $\Delta P_G$  in (3.1), in general is a very complicated expression calculated from the non-linear differential equations of the electrical part of the machine and the algebraic equations of the transmission network and the synchronous machine.

This equation may be arranged for notation convenience to the following form:

$$\begin{bmatrix} \Delta P_G \\ \Delta P_L \end{bmatrix} = \begin{bmatrix} H_{GG} & H_{GL} \\ H_{LG} & H_{LL} \end{bmatrix} \begin{bmatrix} \Delta \delta \\ \Delta \theta \end{bmatrix} \quad (3.4)$$

Hereby, the partial derivatives in (3.3) are most precisely calculated using the voltages and angles at the pre-fault steady state operating point.

The electrical power output of the generating units during a fault is calculated by solving the faulted network equations with the generator transient voltages fixed at the pre-fault values.

In (3.4) the bus load-dropping disturbance can be modeled by introducing step changes in the  $\Delta P_L$  and  $\Delta Q_L$  variables for the selected bus at the appropriate time.

### Coherency identification condition

The coherency algorithm minimizes the number of data curve comparisons by recognizing. Thus, the coherency of generators is a *transitive process*. A reference generator is defined in each group and other generators are always compared against this reference in order to determine whether they should fall in the same group.

The remainder of the generating units are evaluated in turn with two alternative consequences, either the unit is combined with an existing group or the unit does not combine with any existing group and a new group is generated.

*The Podmore's coherency criterion*, which is based on the examination of the phase behavior of the rotor angle oscillation and indirect of the generator voltage angle, is used for determining whether a generator should be added according to its behavior to an existing group as follows:

$$|\Delta \theta_i(t) - \Delta \theta_R(t)| < \varepsilon \quad (3.5)$$

For all the samples of time, where:

- $\varepsilon$  is a specified tolerance degree.
- $i$  is the index for generator being grouped.
- $R$  is the index for the reference generator for the group under consideration.

### 3.3 Identity recognition approach

The identity recognition leads to determining of grouping of identical generators, which are replaced by accurate equivalents one without changing the power flow relationships<sup>9</sup>. These generators, which are grouped together, have practically a strong coupling with reference to their

- *physical, mechanical and electrical properties and*
- *linear and non-linear characteristics.*

In order to consider these aspects, the classical coherency-based condition has to be reformulated. This fact implies the consideration of an additional and important condition for the grouping criterion, whose performance can identify identical linear and non-linear properties of external machines satisfactorily.

The main advantage of this approach is the possibility to consider the model parameters of machines within the identity recognition process.

#### Remarks:

- Usually, the analysis of identity recognition may be realized based on the time responses of generators to selected faults.
- The faults influence properly on the dynamic equivalencing. Location, kind, and duration of the faults influences on the form and quality of the dynamic equivalents.
- Time responses of machines to each fault can correspond to the active power variation  $\Delta p_i(t)$ . Further quantities and behaviors, e.g. the angular velocity  $\Delta \omega_i(t)$  or the angle deviation  $\Delta \delta_i(t)$  to the center of inertia (COI), can be used properly in the identity recognition procedure too.
- One of the advantages of using active power as time responses to be identical recognized, is its independence from reference frames.

#### 3.3.1 Conditions

The following figure illustrates the difference between the classical coherency identification and the proposed identity recognition:

---

<sup>9</sup> The resulted dynamic equivalents are single generators that exhibit the same voltage, speed, total mechanical and electrical power as grouping generators during the studied disturbance, where those generators show identical properties.

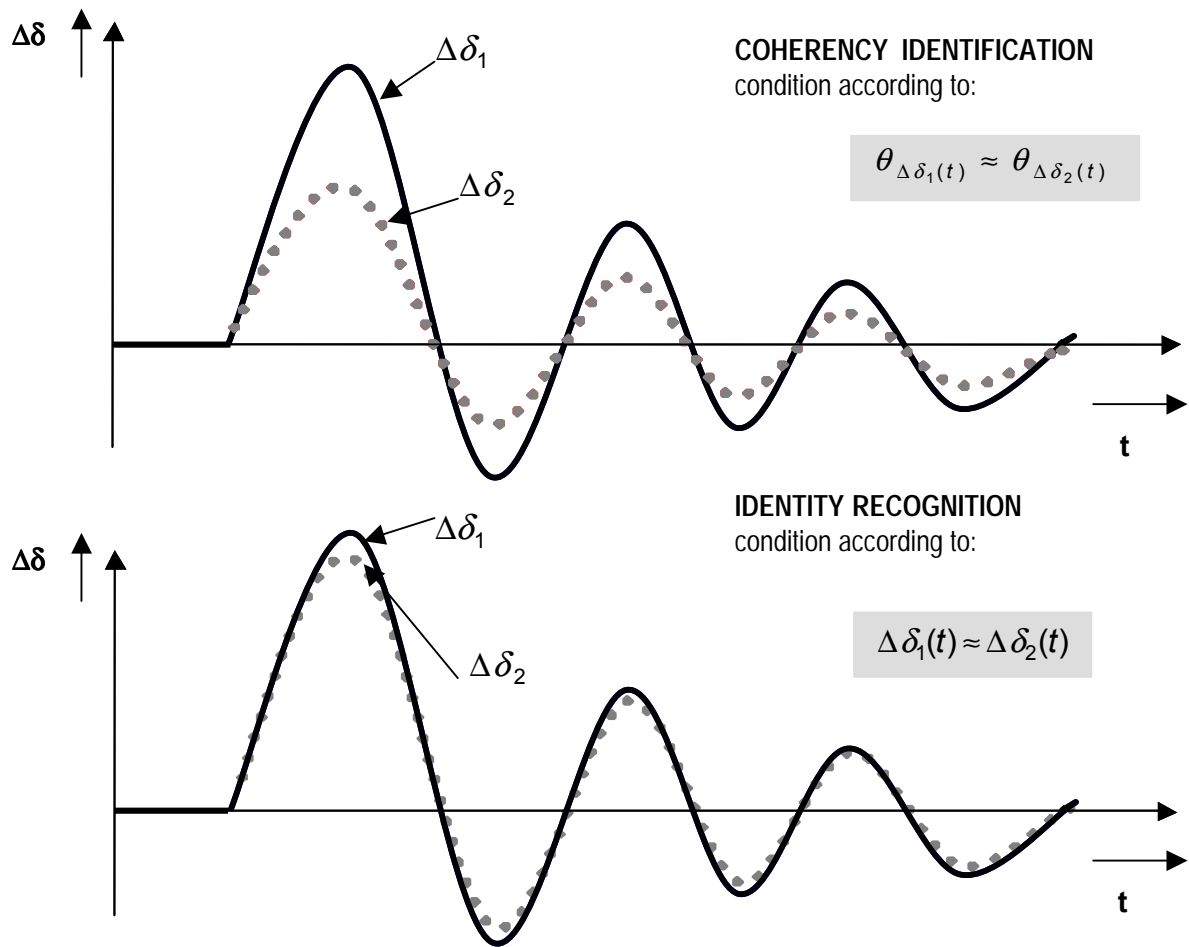


**Fig. 3.1.-** Swing oscillating curve of the rotor angular speed representing the conditions for the identity recognition instead of the classical coherency.

The first illustration shows the necessary condition for forming the coherency identification. This consists principally in the evaluation of the phase identity of the rotor angle to identify similar machines in terms of coherency. As it can be seen in the second illustration, *an additional and imperative condition is the evaluation of the amplitude and phase identity of the rotor angle of together oscillating machines.*

Therefore, the proposed identity recognition is based upon:

- *both the identity of amplitude size and*
- *the identity of phase angle or frequency of the rotor angle behavior.*

For the recognition and grouping of identical oscillating generators, *an analysis of the behavior of the generators has to be realized regarding these two important identities. Both indispensable conditions are criteria for the grouping of identical oscillating generators.*

### Verification of the identity recognition condition for two machines

These identity recognition conditions can be derived on the basis of the inertial aggregation [30, 34] considering that equivalent generator should represent the individual behavior of the single generators both in the initial state and in the whole time period. To this aim, it is more appropriate to perform aggregation at the machines internal nodes and not at the machine terminal buses, because the machine rotor angle is the phase angle of the internal node voltage phasor.

#### Aggregated model of Gen. a and Gen. b

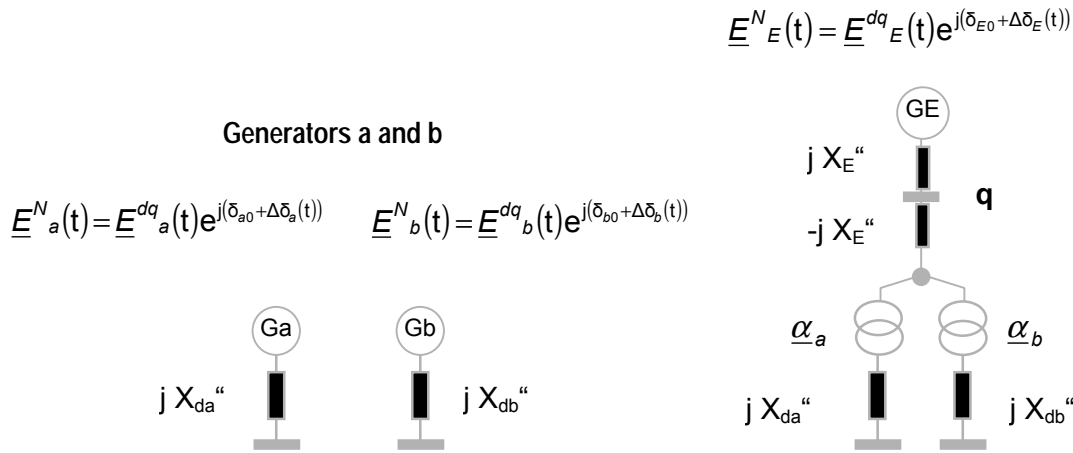


**Fig. 3.2.-** Classical Aggregation

The machine internal node voltages are tied to a common bus with appropriate transformers and phase shifters to preserve the power flow.

Defining the voltage transformation ratios from the internal voltages  $\underline{E}_a$  and  $\underline{E}_b$  to the common bus voltage  $\underline{E}_E$  and the corresponding reference frame 'dq' to 'N' from the steady state by :

$$\underline{\alpha}_i = \frac{\underline{E}_E^{dq}(0) e^{j\delta_{E0}}}{\underline{E}_i^{dq}(0) e^{j\delta_{i0}}} \quad i=a,b \quad (3.6)$$

and considering for the whole time period that the changes in the voltages are derived from the rotor flux linkages and caused by the rotor torsion  $\Delta\delta(t)$ :

$$\underline{\alpha}_i = \frac{\underline{E}_E^N(t)}{\underline{E}_i^N(t)} = \frac{\underline{E}_E^{dq}(t) e^{j\delta_{E0}}}{\underline{E}_i^{dq}(t) e^{j\delta_{i0}}} e^{j(\Delta\delta_E(t) - \Delta\delta_i(t))} \quad i=a,b \quad (3.7)$$

the following relationship may be supposed:

$$\frac{\underline{E}_E^{dq}(t)e^{j\delta_{E0}}}{\underline{E}_i^{dq}(t)e^{j\delta_{i0}}} \approx \frac{\underline{E}_E^{dq}(0)e^{j\delta_{E0}}}{\underline{E}_i^{dq}(0)e^{j\delta_{i0}}} = \alpha_i \quad i=a,b \quad (3.8)$$

Considering this relationship, the expression (3.7) can be satisfied by:

$$\Delta\delta_E(t) - \Delta\delta_i(t) = 0 \quad i=a,b \quad (3.9)$$

$$\Rightarrow \Delta\delta_a(t) = \Delta\delta_b(t) \quad (3.10)$$

*This condition implies, that two generators are defined as identical, if both amplitude and phase difference of their rotor angles are constants and minimal within a specified tolerance over a certain time interval.*

### Verification of the identity recognition condition for n-machines

The verification of the identity condition extending to a  $n$ -machine power system is based upon *the coupled active power flow equation of the external power system*. It is expressed on the equation (3.4) in the decomposed form as:

$$\Delta\mathbf{P}_G = \mathbf{H}_{GG} \Delta\boldsymbol{\delta}_G + \mathbf{H}_{GL} \Delta\boldsymbol{\theta}_L \quad (3.11)$$

$$\Delta\mathbf{P}_L = \mathbf{H}_{LG} \Delta\boldsymbol{\delta}_G + \mathbf{H}_{LL} \Delta\boldsymbol{\theta}_L \quad (3.12)$$

where index 'G' denotes the set of selected internal generator nodes assumed to be identical for any changes in form of disturbances on the internal area and index 'L' is the set of the remaining nodes in form of load buses of the external area.

Taking into account the square matrix  $\mathbf{H}_{LL}$  is regular and hence, it is invertible the following expression may be obtained from (3.12):

$$\Delta\boldsymbol{\theta}_L = \mathbf{H}_{LL}^{-1} \Delta\mathbf{P}_L - \mathbf{H}_{LL}^{-1} \mathbf{H}_{LG} \Delta\boldsymbol{\delta}_G \quad (3.13)$$

Replacing the voltage angles at the load buses in (3.11) the following transformed equation may be derived:

$$\Delta\mathbf{P}_G = [\mathbf{H}_{GG} - \mathbf{H}_{GL} \mathbf{H}_{LL}^{-1} \mathbf{H}_{LG}] \Delta\boldsymbol{\delta}_G + \mathbf{H}_{GL} \mathbf{H}_{LL}^{-1} \Delta\mathbf{P}_L = \mathbf{H}_G \Delta\boldsymbol{\delta}_G + \mathbf{R}_G \Delta\mathbf{P}_L \quad (3.14)$$

where

$$\mathbf{H}_G = \mathbf{H}_{GG} - \mathbf{H}_{GL} \mathbf{H}_{LL}^{-1} \mathbf{H}_{LG} \quad (3.15)$$

$$\mathbf{R}_G = \mathbf{H}_{GL} \mathbf{H}_{LL}^{-1} \quad (3.16)$$

The above derivation for  $\Delta P_G$  can be considered in the generator rotor movement. It is expressed as follows:

$$M_i \ddot{\Delta \delta}_i + D_i \dot{\Delta \delta}_i = \Delta P_{m_i} - \Delta P_{G_i} \quad i=1, \dots, n \quad (3.17)$$

In this case, the mechanical power is assumed as constant for a short duration of the fault period:

$$\Delta P_m = 0 \quad (3.18)$$

According to  $\Delta P_G$  (3.14) in (3.17) the following matrix notation can be obtained<sup>10</sup>:

$$\Delta \ddot{\delta}_G + \mathbf{D}_M \Delta \dot{\delta}_G = \mathbf{H}_M \Delta \delta_G + \mathbf{R}_M \Delta \mathbf{P}_L \quad (3.19)$$

with

$$\mathbf{H}_M = -\mathbf{M}_G^{-1} \mathbf{H}_G = h \mathbf{I}_G, \quad \frac{H_i}{M_i} = h, \quad \mathbf{H}_G = \text{diag}(H_i) \quad i=1, \dots, n \quad (3.20)$$

$$\mathbf{R}_M = -\mathbf{M}_G^{-1} \mathbf{R}_G = r \mathbf{I}_G, \quad \frac{R_i}{M_i} = r, \quad \mathbf{R}_G = \text{diag}(R_i) \quad i=1, \dots, n \quad (3.21)$$

$$\mathbf{D}_M = \mathbf{M}_G^{-1} \mathbf{D}_G = d \mathbf{I}_G, \quad \frac{D_i}{M_i} = d, \quad \mathbf{D}_G = \text{diag}(D_i) \quad i=1, \dots, n \quad (3.22)$$

$$\mathbf{M}_G = \text{diag}(M_i) \quad i=1, \dots, n \quad (3.23)$$

where  $M_i$  is the inertia coefficient of the  $i$ th generator. In this case, equation (3.19) is the second order state-space equation describing a selected identical group of generators, which can be solved in a similar form for the non-uniform damping case, for the uniform damping case and the zero damping case.

<sup>10</sup> Increments  $\Delta P_L$  of the active power of the remaining nodes modeled as bus load-dropping changes can be treated as the effect disturbance at a certain internal node on the external area.

The generators of group  $\{G\}$  are said to be exactly identical if increments  $\Delta\delta_i(t)$  of all grouping generators resulting from equation (3.19) are identical for all  $i \in \{G\}$ .

This may be expressed in matrix notation in the following way:

$$\Delta\delta_G(t) = \Delta\delta(t) \mathbf{I}_G \quad (3.24)$$

where  $\Delta\delta(t)$  is the scalar value and  $\mathbf{I}_G$  the unit vector with cardinality of  $\{G\}$ , i.e. of all identical components of the group. In this expression should be denoted that the magnitudes and phase angles of the rotor movement of the identical generators should be identical in sense of the identity recognition.

Relevant in this case is that the solution of the second order state-space equation system (3.19) must satisfy and fulfill above equation (3.24) for any disturbances expressed as step changes in  $\Delta P_L$  if all rows of certain sub matrix, describing the external area, are identical considering phase and amplitude.

Therefore, this identity criterion is specified by the property that following any disturbance the difference of the rotor angle behaviors of identical generators with reference to their phase and amplitude remains time-dependent and significant small. Thus, the following relationship<sup>11</sup> in terms of  $\Delta\delta_G(t)$  can be derived for two identical generators  $i$  and  $j$  as:

$$\begin{aligned} |\Delta\delta_i(t) - \Delta\delta_j(t)| &= |\Delta\delta_\varepsilon(t)| \leq \varepsilon \\ \Delta\delta_i(t) &\approx \Delta\delta_j(t) \end{aligned} \quad (3.25)$$

where  $\Delta\delta_\varepsilon(t)$  is the behavior difference during and after the fault and  $\varepsilon$  the specific tolerance. Taking into consideration this identity, the following additional identities may be obtained by differentiating:

$$\Delta\dot{\delta}_i(t) \approx \Delta\dot{\delta}_j(t) \quad (3.26)$$

$$\Delta\ddot{\delta}_i(t) \approx \Delta\ddot{\delta}_j(t) \quad (3.27)$$

<sup>11</sup> If (3.25) in (3.19) is fulfilled approximately for the linearized state space model then the external grouped generators are approximately in the same manner identical in the non-linearized model.

It means, if two generators are identical, they will have similar velocity and acceleration behaviors considering amplitude and phase.

### 3.3.2 Procedure

In a time period, the behavior of the machines as a time series matrix  $\mathbf{X}$  is established. This time data set can include voltage, current, power or rotor angle behavior of the generators considering the non-linear characteristics of governor and excite control devices.

The procedure to detect the identity consists of the following aspects:

**(i) Generate a time domain matrix** that reveals the behavior of the machines following simulated disturbances on a particular node of the system, like a three-phase fault at a particular node of the internal area.

The generator matrix may be characterized by following attribute vectors:

$$\begin{array}{ll}
 \text{Generator 1} & \rightarrow \mathbf{X}_1 = [x_{11}, x_{12}, x_{13} \dots x_{1M}] \\
 \text{Generator 2} & \rightarrow \mathbf{X}_2 = [x_{21}, x_{22}, x_{23} \dots x_{2M}] \\
 & \cdot \\
 & \cdot \\
 \text{Generator N} & \rightarrow \mathbf{X}_N = [x_{N1}, x_{N2}, x_{N3} \dots x_{NM}]
 \end{array} \tag{3.28}$$

Where the time data set matrix  $\mathbf{X}$  (N,M) includes the time responses in form of oscillating swing curves, exhibiting  $N$  the number of generators or features and  $M$  the number of variables or patterns or sampling points of the time data set.

**(ii) Initial cluster centers**, this procedure starts with a predefined number of cluster groups and corresponding cluster centers that can be considered as initial reference generators.

**(iii) Identity recognition according to clustering algorithm.** All generators are compared against the reference generators as cluster centers to determine whether they should fall in the cluster groups. All clustering algorithms are based on the minimizing of the within cluster squared distances by means of an iterative way or an optimization procedure.

This aspect can be illustrated iteratively in the following figure:

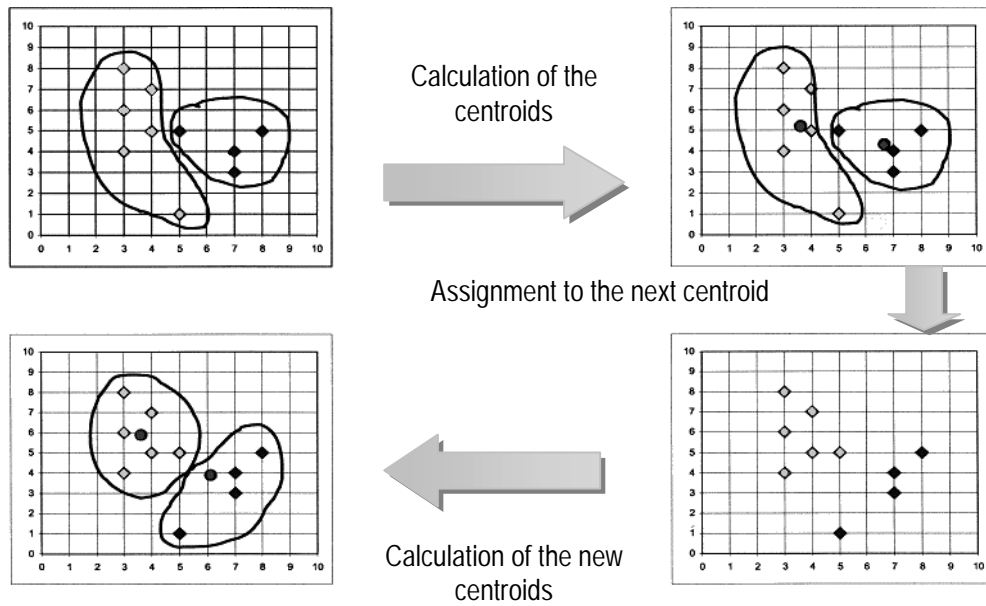


**Fig. 3.3.-** Schematic representation of iterative assignment and construction of centroids or reference generators within a clustering procedure

The assignment of generators to the cluster groups regarding their time behavior characteristics can be realized by means of the evaluation of a distance criterion between the grouping generator and the reference generator. In this case the following illustration can be sketched:

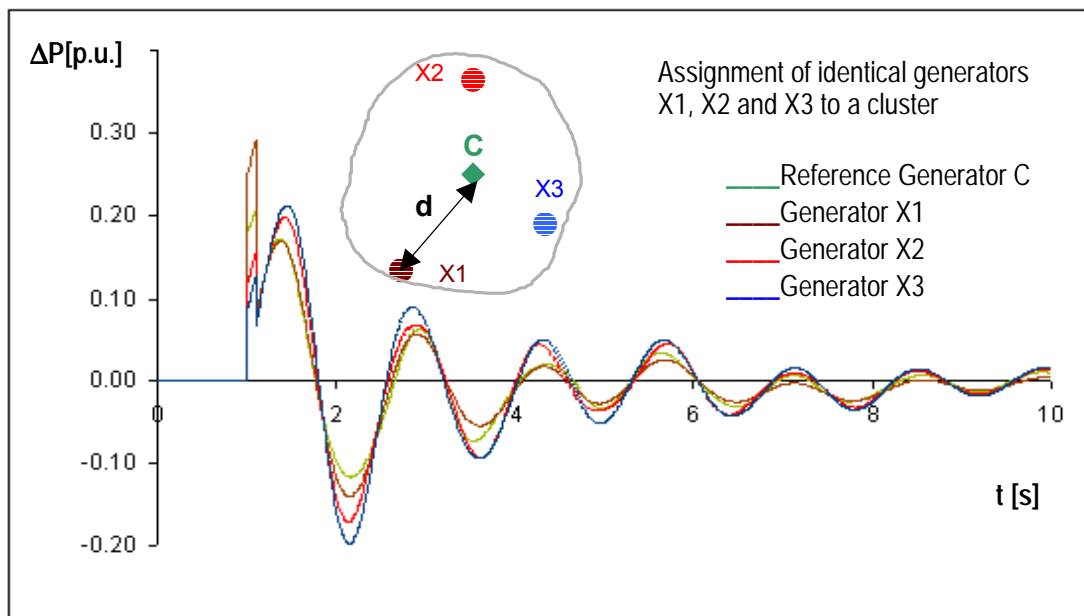


**Fig. 3.4.-** Schematic representation of similar generators belonging to a cluster group taking into account its identical properties in phase and amplitude.

### 3.3.3 Identity recognition algorithms

The identity recognition algorithms as clustering process consist of procedures, which divide the multidimensional data space of the features into a number of separated groups called clusters, whose features have identical patterns in a multidimensional space [91-98] and *the profiles of objects in the same groups are relatively homogenous* whereas the profiles of objects in different groups are relatively heterogeneous.

*This assignment in groups is based on the minimizing of the within cluster squared distances directly in an iterative way (partitioning), in a transitive process (hierarchical) or indirectly in an optimization procedure (Fuzzy and SOFM) and thus, the machines can be assigned to the corresponding most nearby clusters.*

In detail, the distance criterion can be described as follows:

- *The identity between objects can be recognized by means of distance measurement criteria between the data vectors in the multidimensional space in different ways.*
- For an extensive review of measures can be implemented the  $L_p$ -Metric or Minkowski distance. The Minkowski distance  $d_{ij}$  between two  $M$ -dimensional objects (data points)  $i$  and  $j$  is defined by the following expression:

$$d(x, y) = \left( \sum_{l=1}^M |x_{il} - y_{jl}|^p \right)^{\frac{1}{p}} \quad (3.29)$$

where  $x_{il}$  and  $y_{jl}$  are objects with  $M$  sampling points, whose distance has to be calculated.  $M$  corresponds to the number of variables.

- By these distance definition may be diverted other distance functions by means of new definition of  $p$ . An important distance measure is *the Euclidean distance metric*, which is defined by  $p=2$ .

The wide variety of existing clustering can be divided into four main groups, such as:

- **Hierarchical** [92-95],
- **Partition** [94-101] in form of K-means,
- **Fuzzy C-means** [102-105] and

- **Unsupervised neural networks** [106-109] in form of self-organizing feature maps (SOFM) or competitive networks, although other techniques are possible.

Facts of these standard algorithms are explained in detail in appendix B.

### 3.3.4 Comparative application

To compare the standard identity recognition algorithms, their properties and advantages should be discussed. In fact, each method works in a different way and very often yields results different from the others.

The identity recognition algorithms may be showed schematically in the following flowchart. Bold lines indicate the more successful methods with significant accuracy.

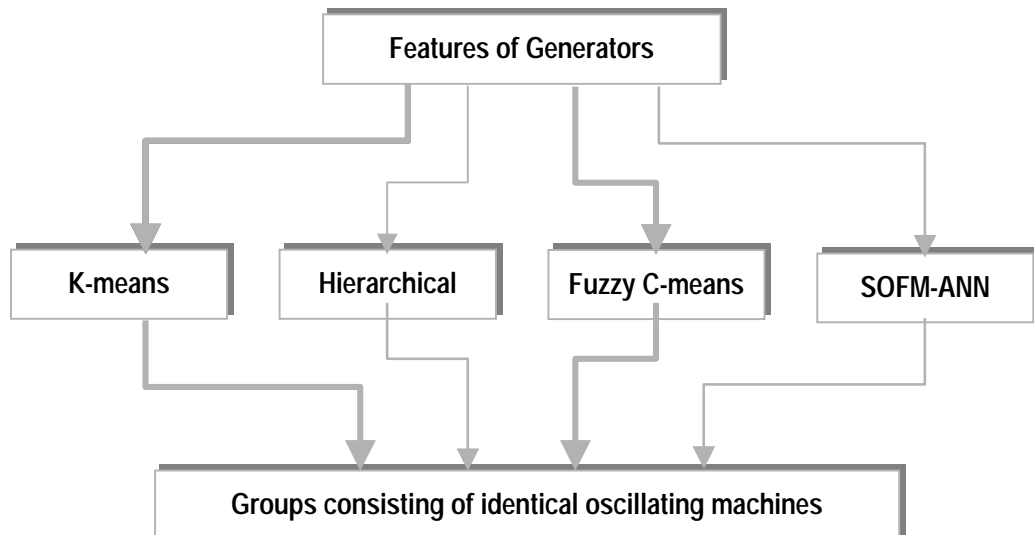


Fig. 3.5.- Flow chart of applied identity recognition algorithms.

#### ***Hierarchical clustering (HC)***

- It is the most widely used algorithm due to the computational simplicity, sometimes it is stated that this technique is no longer valid if applied to large data sets [92].
- Its main purpose is to provide the user with suitable *initial cluster* centers, and thus it is able to identify the initial seed points.
- The main disadvantage lies in the fact that, according to the logic of hierarchical clustering, a kind of hierarchical structure is imposed into the data, even if the data do not possess such structure. This can lead to a misclassification of the data structure [93].

***Partitioning or non-hierarchical clustering (NH) as K-means***

- It is free from the hierarchical disadvantage.
- Its main properties are its computational simplicity, the *re-determination*, and *adjustment* of the composition and population of clusters with *non-hierarchical clustering*.
- This clustering technique is referred to as 'hard clustering' schemes, where each object is assigned to one and only one cluster.
- In the case of touching or overlapped clusters this assumption is apparently invalid, leading consequently to misclassification.

***Fuzzy clustering (FC)***

- The procedure of dividing the  $N$  objects into  $k$  clusters is replaced by a procedure of determining the membership degree of each object belonging to each cluster group. From this point of view, 'hard clustering' can be considered as a particular case of Fuzzy clustering, i.e. when all membership coefficients, except one, of a single machine are equal to zero.
- Although this is yet another mathematical model that does not necessarily describe the real data structure, it seems that such an approach should lead to appropriate results.
- Fuzzy provides a clustering classification by using of membership degree coefficients between 0 and 1, which can contribute to divide an object in shares. The shares number corresponds to the number of defined cluster groups.
- The internal structure of clusters and their interrelationships can be determined with *Fuzzy-c means*. Moreover, the '*dispersion level*' or '*splitting*' of the grouped objects can be defined with help of the membership degrees.

***Kohonen self organizing features maps (SOFM)***

- Their application is restricted due to the large computation time with large number of objects, by which the network can be trained.
- A limitation of this method is that the number of groups not always corresponds to the defined number of output neurons, and thus the Kohonen network can fail.
- The procedure of Fuzzy c-means and K-means clustering has not this difficulty, because the cluster center forming is forced by the input of the number of objects. Nevertheless Kohonen maps can be considered as a complementary method to verify the results of previous clustering methods.

### 3.4 Electromechanical-based identity recognition

In spite of all identity recognition technique's properties, an important improvement in identity recognition can be reached by using electromechanical weighted distances to obtain '*electrically real identical generators grouped in clusters*'. In this context, following aspects should be considered:

- Factors, such as *the model parameter properties, physical characteristics and the particular influences of single generators on the power system*, must be considered to develop a *real electrical assignment preserving the singularity* of each machine.
- Thus, it is indispensable to *introduce characteristic sizes of generators*, which characterize the particular behavior and the proper impact of the machines on the external power system.
- The *electromechanical distance is introduced in the identity recognition process additionally to the geometrical distance*.
- Thus, it is not appropriate to apply the same distance criteria to generators located far from the area of interest as the nearest one.
- Electromechanical small machines with small characteristics have less influence on the whole system dynamic than larger machines.

#### 3.4.1 Inertia coefficient and electrical power

According to the following sensitivity analysis, model parameters, as pre- and during-fault relevant electromechanical factors may be selected, to improve the assignment to groups of machines according to their physical and model properties.

##### Sensitivity analysis

The sensitivity of a determined machine's behavior  $y(t)$  with reference to the parameters  $P$  may be defined mathematically as:

$$e_{pi}^y(t) = P_i \frac{\partial y(t)}{\partial P_i} \Big|_{P_i=P_{io}} \quad (3.30)$$

The sensitivity is a time function, which expresses the influence of parameter  $P_i$  on the investigated behavior  $y(t)$ , such as rotor speed, electrical power, rotor current, rotor voltage, etc. and a certain time during this behavior.

The rotor speed behavior is an important electromechanical behavior to be evaluated according to the sensitivity. For the sensitivity analysis the following one-machine system was evaluated:

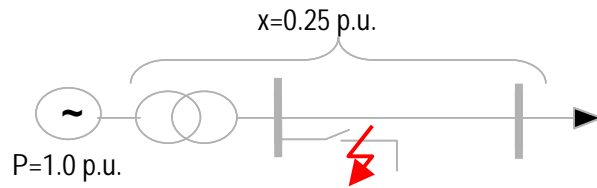


Fig. 3.6.- One-machine power system for sensitivity analysis

On the basis of this evaluation, the influence of the parameters on the electromechanical behavior of the machines may be quantitatively detected. In order to derive a quantity evaluation for sensitivity the square mean value is formed and afterwards normalization to unit is defined.

The following illustration shows a summarized comparison of the normalized square mean values of the sensitivities of rotor angle  $\delta_L$  with reference to important synchronous machine parameters.

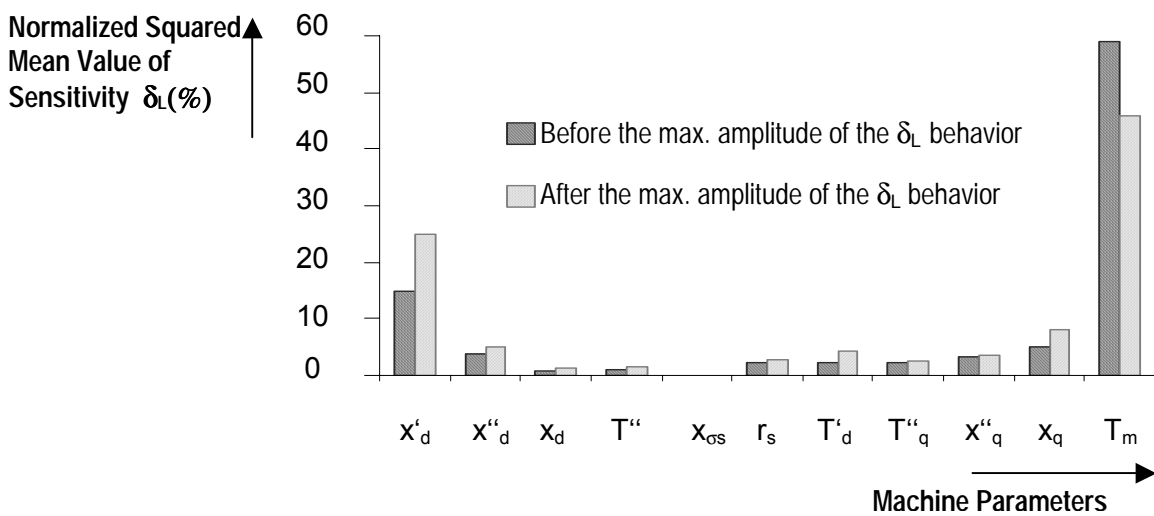
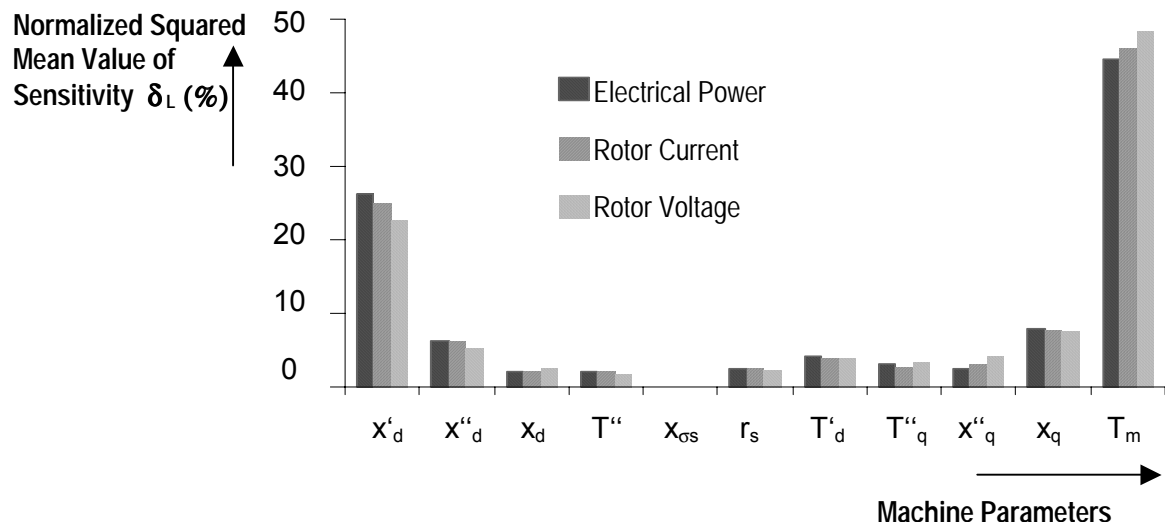


Fig. 3.7.- Graphical comparison of the normalized square mean values of the sensitivities of rotor angle  $\delta_L$  with reference to the synchronous machine parameters

This illustration shows the sensitivity of the rotor angle with reference to different machine parameters considering the time setting behavior before and after the maximum amplitude, which is generated following a three-phase short circuit on the one-machine system. On the basis of this illustration following aspects can be detected:

- The large influence of the inertial coefficient parameter  $T_m$  as well the small effect of other parameters on the behavior of  $\delta_L$  can be depicted.
- However,  $T_m$  decreases its influence after the maximum amplitude. On the other hand, the sensitivity influence of the other parameters, such as the transient reactance  $x'_d$  is increased in this case, but the sensitivity of  $T_m$  cannot be reached.
- The sensitivity has been evaluated taking into account the parameters defined in Fig. 3.6. With this wide range of model parameters the synchronous machine may be described completely.

Instead of the  $\delta_L$  other machine behaviors are considered, which can be showed in the following figure. It shows the squared mean values of the sensitivities.



**Fig. 3.8.-** Graphical comparison of the normalized square mean values of the sensitivities of rotor angle, rotor current and angle with reference to the parameters of the synchronous machines

In this illustration, the sensitivity of different behaviors, i.e. electrical power, rotor current and voltage is described. In this case, a similar tendency as in the previous figure can be detected.

*In summary,  $T_m$  and  $x'_d$  are relevant machine model parameters with significant influence on the behavior of the machine.*

According to the sensitivity analysis, following main conclusions can be summarized:

- The inertial constant  $T_m$  determines significantly the behavior of the generator during short circuit period. Under all machine model parameters, this constant has the largest influence on the system dynamics during the total stability analysis.
- Additional to this factor, the transient reactance  $x'_d$  plays an important role, but in a substantially lower grade than the inertial constant  $T_m$ .
- The sensitivity of the rotor angle speed, rotor current, and voltage with reference to the rotor reactance  $x_{os}$  is insignificantly low.

### Analytical verification to determine the relevance of the inertial coefficient $T_m$

In the following, an analytical verification will be realized to determine the influence of the inertial coefficient on the identity recognition. By differentiating the equation of identity (3.26), two machines will have equal velocity and acceleration according to (3.27) and (3.28). Since the proposed identity of generators does not depend on the disturbance, the linearized equation (3.17) can be simplified according to the following assumptions:

#### Assumptions:

- The electric power using the classical generator model may be found taking into account the admittance matrix denoted by  $Y_{ij}$ <sup>12</sup>.

$$P_G = \operatorname{Re} [E_i I_i^*] = \operatorname{Re} [E_i \sum_{j=1}^n Y_{ij}^* E_j^*] = \operatorname{Re} [ \sum_{j=1}^n |E_i| |Y_{ij}| |E_j| e^{-j(\theta_{ij} + \delta_j - \delta_i)} ] \quad (3.31)$$

Let

$$E_i = |E_i| e^{j\delta_i} \quad Y_{ij} = G_{ij} + jB_{ij} = |Y_{ij}| e^{j\theta_{ij}} \quad (3.32)$$

Then

$$P_G = |E_i|^2 G_{ii} + \sum_{\substack{j=1 \\ j \neq i}}^n |E_i| |E_j| |Y_{ij}| [\cos(\theta_{ij} - (\delta_i - \delta_j))] \quad (3.33)$$

- The mechanical power is considered as constant value for the fault period.

$$\Delta P_m = 0 \quad (3.34)$$

- Internal voltages of the generators  $E_i, E_j$  are nearly equal to 1.0 p.u.
- The network is considered as highly reactive.
- The angular differences ( $\delta_i - \delta_j$ ) are within  $30^\circ$ .

In consequence, the change in electrical power in (3.33) can be expressed as:

$$\Delta P_G = \sum_{j=1}^n Y_{ij} (\Delta \delta_i - \Delta \delta_j) \quad (3.35)$$

Substituting expressions (3.34) and (3.35) in (3.17), it becomes:

$$M_i \ddot{\Delta \delta}_i = \sum_{j=1}^n Y_{ij} (\Delta \delta_j - \Delta \delta_i) - D_i \dot{\Delta \delta}_i \quad (3.36)$$

The linearized power variation-based swing equation of the generators for the  $i$ th and  $j$ th generator can be expressed according to (3.36) as follows:

Terms relating other generators as the  $j$ th with  $i$ th generator

$$\ddot{\Delta \delta}_i = M_i^{-1} \left[ Y_{ij} (\Delta \delta_j - \Delta \delta_i) + \{ Y_{i1} (\Delta \delta_1 - \Delta \delta_i) + \dots + Y_{in} (\Delta \delta_n - \Delta \delta_i) \} \right] - M_i^{-1} D_i \dot{\Delta \delta}_i \quad (3.37)$$

Terms relating other generators as the  $i$ th with  $j$ th generator

$$\ddot{\Delta \delta}_j = M_j^{-1} \left[ Y_{ji} (\Delta \delta_i - \Delta \delta_j) + \{ Y_{j1} (\Delta \delta_1 - \Delta \delta_j) + \dots + Y_{jn} (\Delta \delta_n - \Delta \delta_j) \} \right] - M_j^{-1} D_j \dot{\Delta \delta}_j \quad (3.38)$$

The sign of the first term of the above two expressions are opposite to each other. Therefore, for any disturbance in power system an increase in acceleration of the  $i$ th generator causes an increase in  $\Delta \delta_i$  and  $\Delta \omega_i$ . The increase in  $\Delta \delta_i$  and  $\Delta \omega_i$  will tend to cause a decrease in the acceleration of the  $i$ th generator based on (3.37) and at the same time to increase the acceleration of the  $j$ th generator in (3.38). As the acceleration of the  $j$ th generator starts increasing, it causes to increase  $\Delta \delta_j$  and  $\Delta \omega_j$ .

<sup>12</sup> On the basis of the linearized model of the dynamic equation of the  $i$ th generator expressed in (3.1),  $P_e$  is the generator electric power obtained from a load flow solution.

Thus, the generators will try to swing together in terms of the synchronism through the mutual change effect defined by the first term. Therefore, the coefficient terms of expressions (3.37) and (3.38):

$$\left| \frac{Y_{ij} - Y_{ji}}{M_i - M_j} \right|, \quad \left| \frac{D_i - D_j}{M_i - M_j} \right|$$

together give an estimate of the relative variation between the acceleration  $\ddot{\Delta\delta}_i$  and  $\ddot{\Delta\delta}_j$ <sup>13</sup>.

Due to that  $M$  is considered as the per-unit value and proportional to  $T_m$ , those value can be found in the machine data set the following expression conveniently may be obtained:

$$M = \frac{T_m}{\pi f_o} = \frac{2 T_m}{\omega_o} \quad (3.39)$$

$$\Rightarrow M \sim T_m \quad (3.40)$$

From this viewpoint and *the previous sensitivity analysis*, the relevant role of *the inertia constant*  $T_m$  is determined with respect to identical recognition of together oscillating machines, which give an estimate of the electromechanical effect of the generators.

Following aspects are relevant to select the weighting factors:

- *The **inertial constant**  $T_m$  determines significantly under all machine model parameters the behavior of the generator during short circuit period, which has been demonstrated by the sensitivity analysis and in expressions (3.37-3.39).*
- *This widely used parameter informs about the machine's **ability to 'absorb'** and is used to quantify abrupt changes of their mechanical torque. In consequence, this constant characterizes the disturbed rotor angle trajectory.*
- *A significantly larger impact of this constant can be observed in nominal power, current, voltage or rotor angle behaviors of the machines according to Fig. 3.7 and Fig. 3.8.*
- *Because of this influencing factor, it is possible, to **treat differently in electromechanical terms all the generators in the identity recognition procedure.***

<sup>13</sup> Since  $Y_{ij}=Y_{ji}$ , the difference in the values of the coefficients of  $\Delta\delta$  in terms to find an equilibrium point, synchronism effect between together oscillating machines and minimal difference of the rotor angle behavior, is only due to the difference in  $M_i$  and  $M_j$ .

- *Another characteristic size of machines is **the nominal power**  $S_j$ , which characterizes the power balance experienced by each generator and its participation in the total power balance of the power system. Thus, it is a proper machine characteristic behavior.*
- *The nominal power  $S_j$  are particular size and characteristic of each machine that inform about the ‘degree of participation and effect’ of each machine in the during- and post-fault periods.*
- *Therefore, large generators with large nominal power and large inertial constants have more electromechanical influence on the system dynamic than smaller generators.*

In consequence, according to *the sensitivity analysis and the above verification*, the following weighting factor may be defined:

$$W_j = T_{mj} * S_j, \quad 1 < j < N \quad (3.41)$$

where  $T_{mj}$  is the inertial constant and  $S_j$  the nominal power of the corresponding generator.

### 3.4.2 Electromechanical distance

*The specific physical effect and electromechanical influence of the generators with regard to their properties and structure derived previously have to be considered into the clustering of the machines.* To this end, it is indispensable to include the weighting factors in the calculations of minimizing the cluster square distances to a centroid within each cluster resulting the so-called “*electromechanical distance*”.

This situation contributes to a *more accurate equivalencing* that forms clusters to *represent groups of entities with real electrical and physical identical properties*.

Hence, the grouping procedure can be adjusted by a weighted distance. These weights can be implemented in hierarchical, K-means and Fuzzy algorithms as distance criterion resulting the *electromechanical distance*. As can be obtained in the following way:

$$d_{\text{electromechanical}} = \sum_{j=1}^N \sum_{i=1}^K \sum_{l=1}^M W_j |x_{j,l} - c_{i,l}| = \sum_{j=1}^N \sum_{i=1}^K \sum_{l=1}^M T_{mj} S_j |x_{j,l} - c_{i,l}| \rightarrow \min \quad (3.42)$$

where  $W_j$  is the weighting expression consisting of the inertia constant and the nominal power according to the expression (3.41).

The expression in (3.42) has to be introduced into the algorithms, such as K-means and hierarchical to be minimized.

In Fuzzy clustering the electromechanical distance has to be integrated both in the distance calculation and in the objective function  $J_m$  (B.6), which is optimized iteratively according to the expression:

$$J_m(X;W,U,C) = \sum_{j=1}^N \sum_{i=1}^K \mu_{i,j}^m w_j d_{i,j}^2 \quad (3.43)$$

where

- $d_{ij}$  is the distance between the generator and cluster centers,
- $w_j$  is the weighting electromechanical factor to form the electromechanical distance,
- the membership degree of generator  $x_j$  to cluster  $c_i$  is denoted by  $\mu_{ij}$  and
- the parameter  $m > 1$  is called fuzziness index and influences the “fuzziness” of the obtained grouping.

*Accurate model parameter-based dynamic equivalents may be obtained by the electromechanical neighborhood relationships using the electromechanical distance between generators into the identity recognition.*

### 3.5 Case studies

In order to verify the effectiveness, accuracy, and applicability of the electromechanical-based identity recognition using K-means, hierarchical, Fuzzy and Kohonen-SOFM, a small-scaled and large sized interconnected power system are examined.

The investigated systems are:

1. 16 Multi-machine system consisting of 16 generators.
2. Interconnected European power system, known as UCTE/CENTREL consisting of the western European *Union for the Coordination of transmission of Electricity* (UCTE) and the *central European power system* (CENTREL) [142].

### 3.5.1 16 Multi-machine system

This system consists of three strongly meshed areas with different voltage levels (380kV, 220kV and 110kV) characterized by the area **A**, **B** and **C**. Each area has 5 or 6 generators. This system comprises hydro, nuclear, and thermal generators with ratings of 220MW, 247MW, and 259MW respectively. It can be seen in Fig. 3.9.

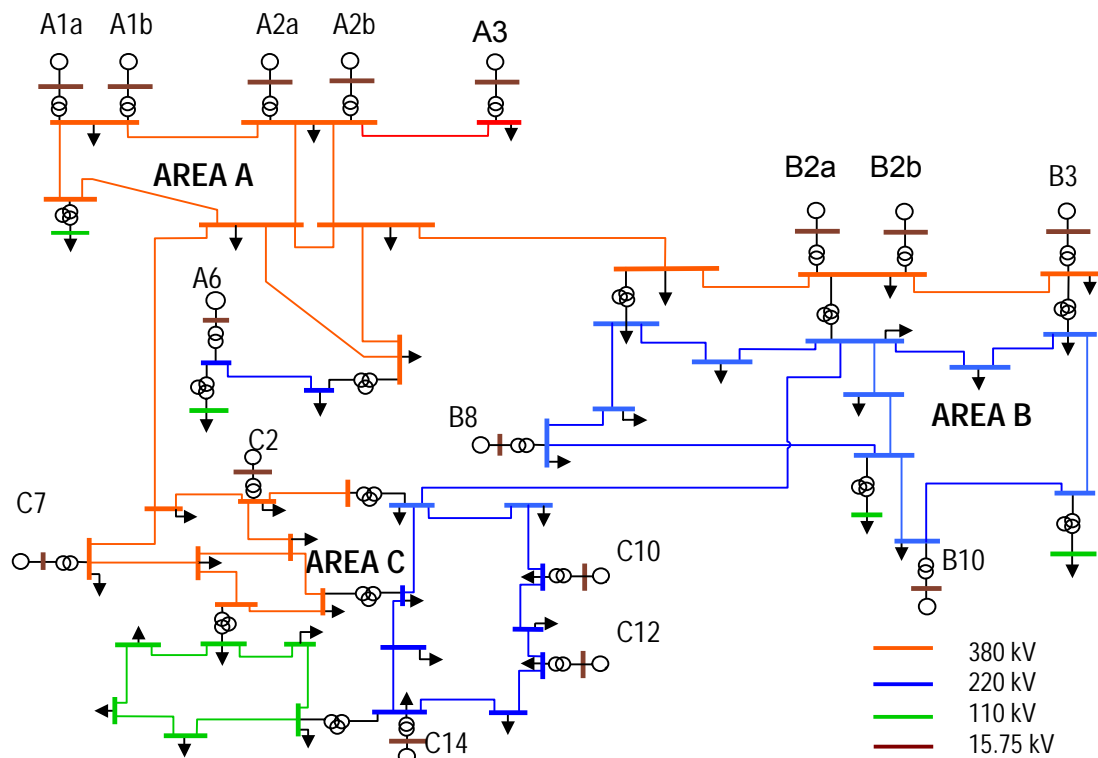


Fig. 3.9.- 16 Multi-machine system

Following system characteristics are important:

- In general, the system comprises 16 generators with their corresponding excitation and governor systems, 66 nodes, 16 two-winding transformation units, 12 three-winding transformation units and 54 transmission lines.
- The machines are described by *5th*, exciters by *2nd* and in some cases by *3rd* order models. IEEE standard controller parameters are used for the governors and the excitation systems. Thus, a state vector of large dimension characterizes the models.
- Area **A** contains mostly hydro power plants and it is structured to be a power exporting area and **B** and **C** as demanding distribution systems.
- Areas **A**, **B** and **C** are considered as *internal areas* separately and retained individually in detail. *The rest machines located outside* of this corresponding area, assumed as

*external area*, have to be replaced by dynamic equivalents *involving the electromechanical-based identity recognition and the classical inertial aggregation procedure*.

- Using the equivalent models of the external area, the dynamic behavior of the time response of an internal machine following a certain disturbance is simulated.
- The behavior of the internal area machines calculated with help of the dynamic equivalents is compared with them calculated on the basis of the original external area.
- In order to realize an adequate testing of the proposed electromechanical identity recognition, various stability scenarios was investigated taking into consideration as study areas, **A**, **B**, and **C** respectively. Different disturbances as three-phase short circuit with duration between 80 to 200 ms were selected on the specifications, as described in the following table.

**Table 3.1.-** Disturbance specifications for the 16 multi-machine system

Internal Area	Fault duration (ms)	Fault location (node)
<b>Area C</b>	100	C5 on 380kV
	100	C1 on 380kV
	100	C8 on 220kV and C1 on 380kV
<b>Area B</b>	150	B1 on 380kV
	150	B10 on 220kV
	150	B2 on 220kV
<b>Area A</b>	200	A5a on 380kV
	200	A5b on 380kV
	200	A2 on 380kV

These disturbances were applied to the boundary nodes between the areas. The boundary node location is a suitable choice for the application of a disturbance because electrically and geographically the disturbance is strongly coupled to all areas.

### 3.5.2 Simulation results and discussion

All results, considering the disturbances of table 3.1, are accurate enough. However, a representative scenario may be described. In this case, the internal area consisting of 5 internal machines of area **C**, which dynamics are of interest, is retained in detail, and the external area, consisting of 11 machines of areas **A** and **B**, is performed on basis of 3 equivalent machines applying the proposed identity recognition algorithms.

The disturbance is a three-phase short circuit during 100ms at the nodes **C01** on **380kV** and **C08** on **220kV** applied at the same time. This fault creates a major system-wide disturbance and is applied after 1 sec., the transient stability simulation duration is 10 sec.

Considering this disturbance, following aspects has been examined:

- i. *Clustering or grouping of external machines* according to the identity recognition.
- ii. *Internal machine behavior* using the identity recognition-based dynamic equivalents.
- iii. *Internal machine behavior* depending on different number of dynamic equivalents.
- iv. *Identity recognition accuracy* depending geographically on the disturbance location.

### i. Clustering

According to the above scenario, the following external machine grouping assignment can be obtained independent on the used identity recognition algorithm.

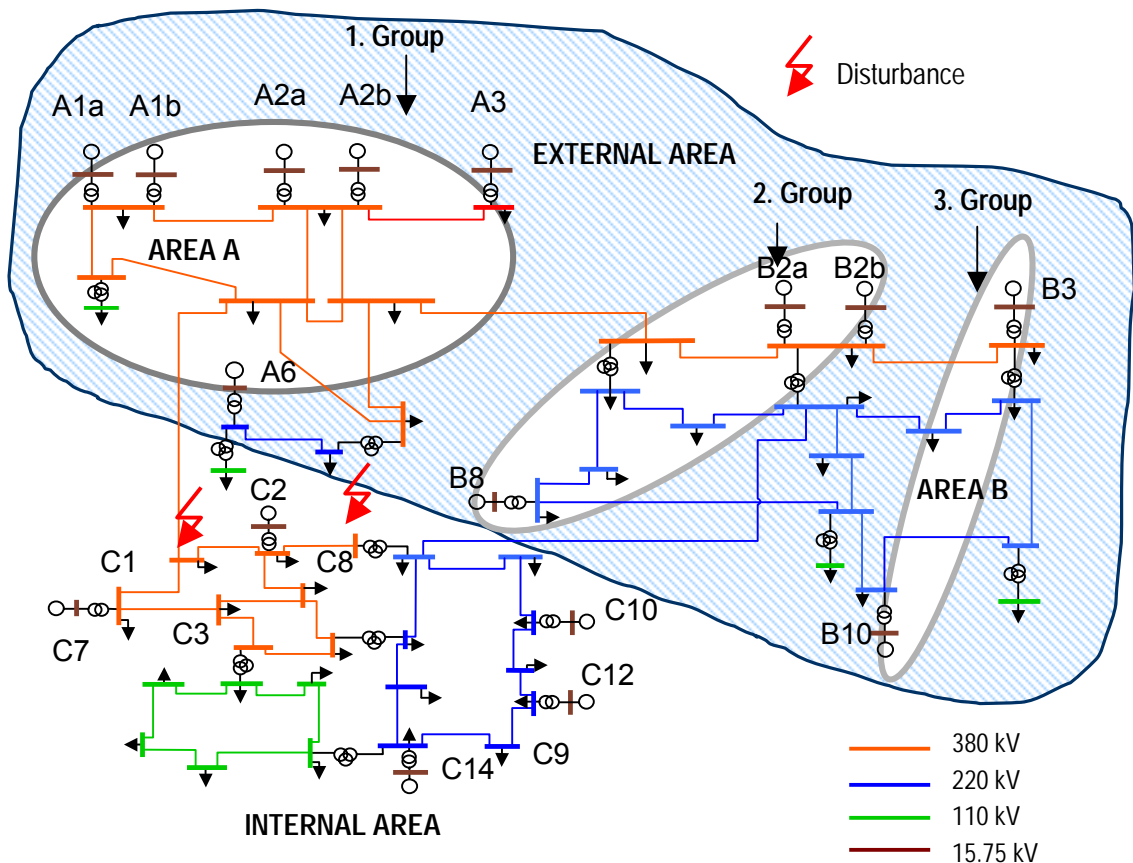


**Fig. 3.10.-** Schematic representation of the grouped 16-machine System following disturbances at the boundary nodes C1 on 380kV and C8 on 220kV at the same time.

This grouping, showed in Fig. 3.10, corresponds to the grouping of time responses represented in Fig. 3.11. These generator responses are simulated with PSD. Same machine assignment to the cluster groups and consequently similar dynamic equivalents are obtained using K-means, Hierarchical, Fuzzy, and SOFM.

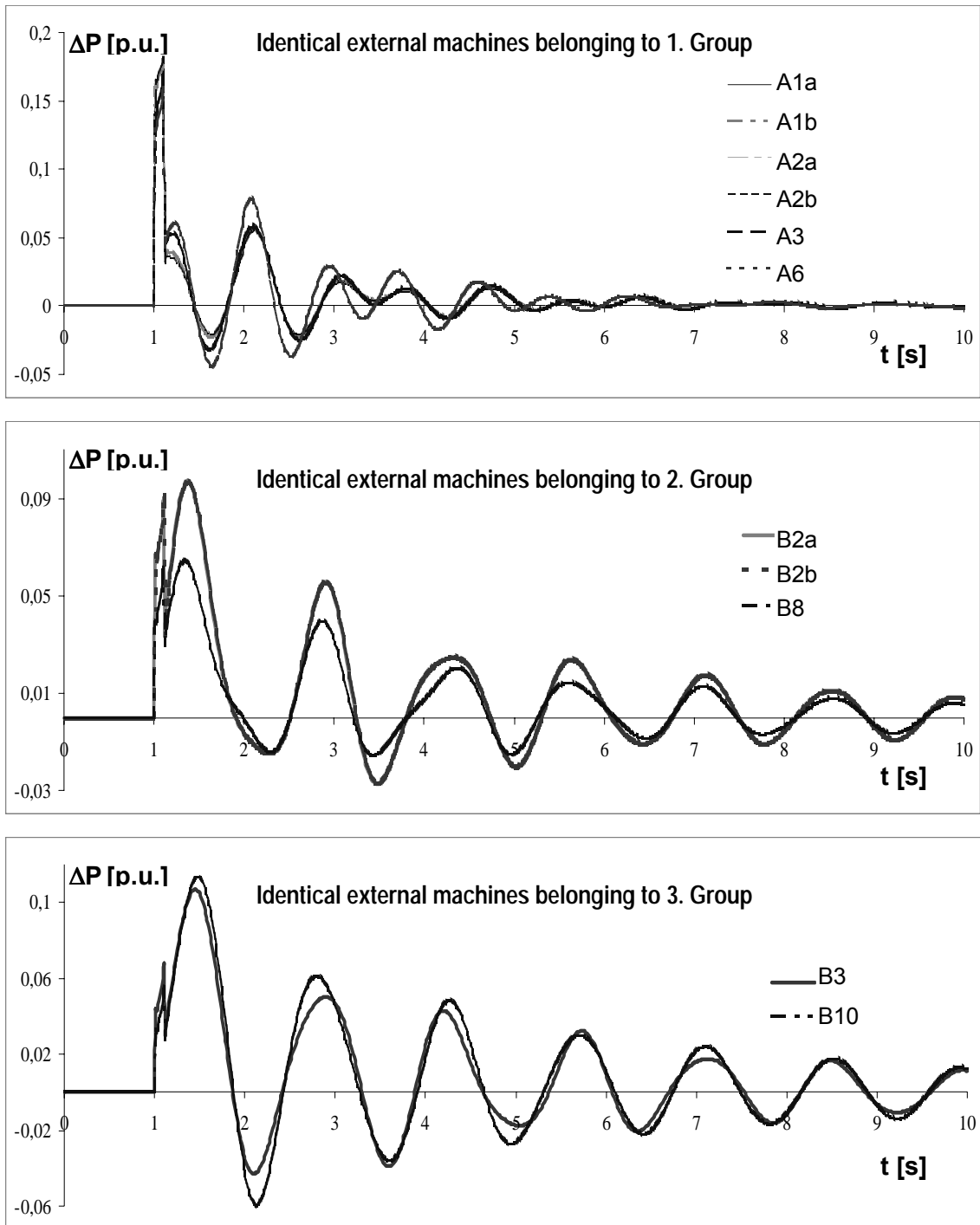


**Fig. 3.11.-** Assignment and grouping of identical external machines according to the identity recognition algorithms in conjunction to Fig. 3.10.

However, another cluster assignment can be obtained using the electromechanical-based recognition algorithms.

To compare the algorithms, the internal machines will be simulated using the equivalents and their behaviors evaluated taking into account their phase and amplitude.

## ii. Internal machine behavior with identity-based dynamic equivalents

The internal machine **C12** will be simulated in the stability analysis one hand with help of the dynamic equivalent of the external area on the basis of the identity recognition methods, and another hand with help of the original external area using PSD. For more details on the validity of PSD, the reader can refer to section 2.3.

All internal machine behaviors show the same accuracy independent of the used identity recognition algorithm, as can be seen in the following Fig. 3.12; the behavior of the internal generator **C12** is represented using the electromechanical-based Fuzzy and K-means.

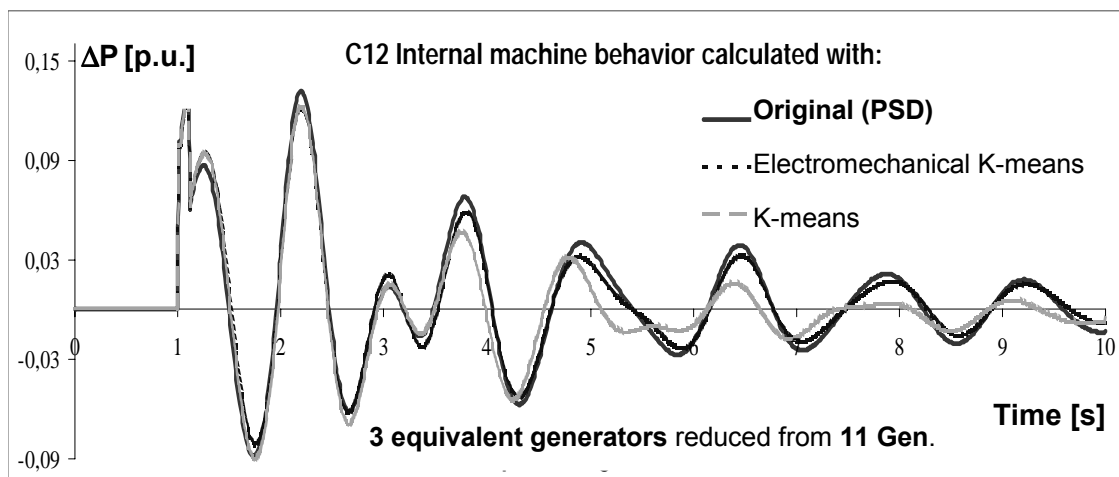
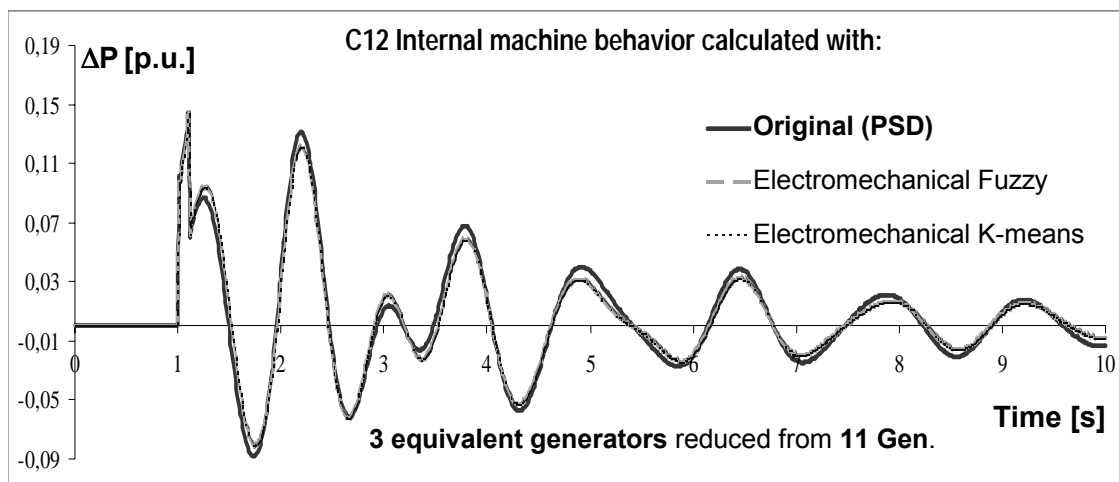


**Fig. 3.12.a, b.-** Comparison of time responses of C12 internal machine calculated with 3 cluster groups according to the electromechanical Fuzzy and K-means

As it can be seen in Fig. 3.12.b, an improvement in accuracy and agreement can be obtained using the electromechanical-based equivalents. Although, Fuzzy, hierarchical, K-

means, and SOFM generate similar grouping assignments, the electromechanical-based algorithms of Fuzzy, K-means and hierarchical generate other groups.

### iii. Internal machine behaviors with different number of dynamic equivalents

The following figure examines the internal machine **C14** using different numbers of identity recognition-based equivalents reduced from 11 machines.

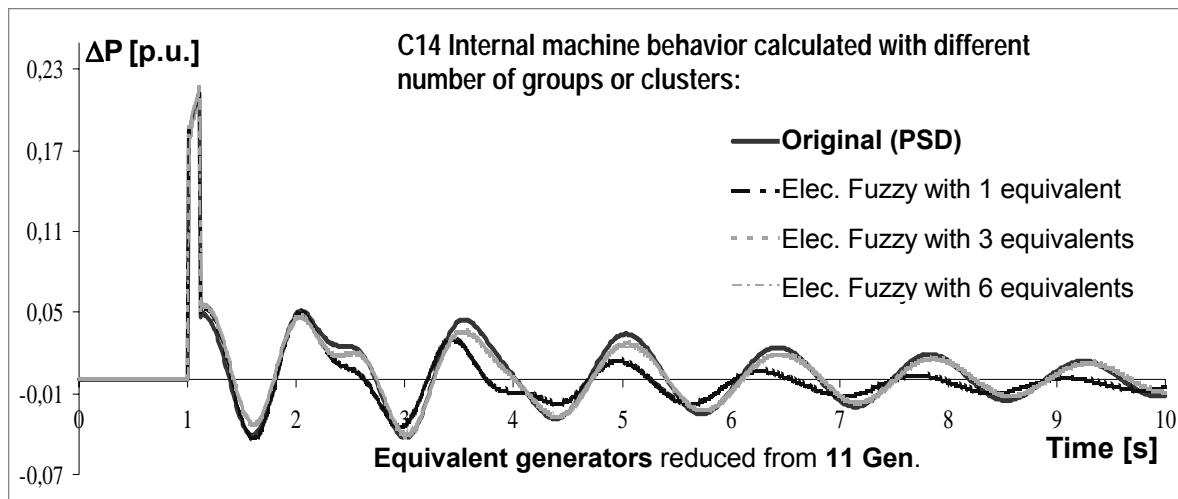


**Fig. 3.13.-** Comparison of time responses of the internal machine **C14** depending on the reduction degree with 1, 3, 6 electromechanical Fuzzy algorithm-based equivalents.

It can be detected that the oscillating swing curve for **C14** calculated with different number of equivalents is very close to that of the original behavior. However, a degradation in accuracy with one equivalent can be determined.

### iv. Internal machine behaviors depending on the disturbance location

A detectable degradation of agreement and accuracy can be discerned in the internal machines depending on the disturbance location.

- The internal machines, i.e. the **C10**, **C12** and **C14**, located far away from the disturbance, with which the identity recognition was realized, are less accurate (see Fig. 3.12 and Fig. 3.13).
- In contrast with this, the **C2** and **C7** machine behaviors are high accurate, as can be seen in the Fig. 3.14. These machines are closest to the disturbances of the equivalents derived (disturbances on node C1 and C8 of area C, see Fig. 3.10).

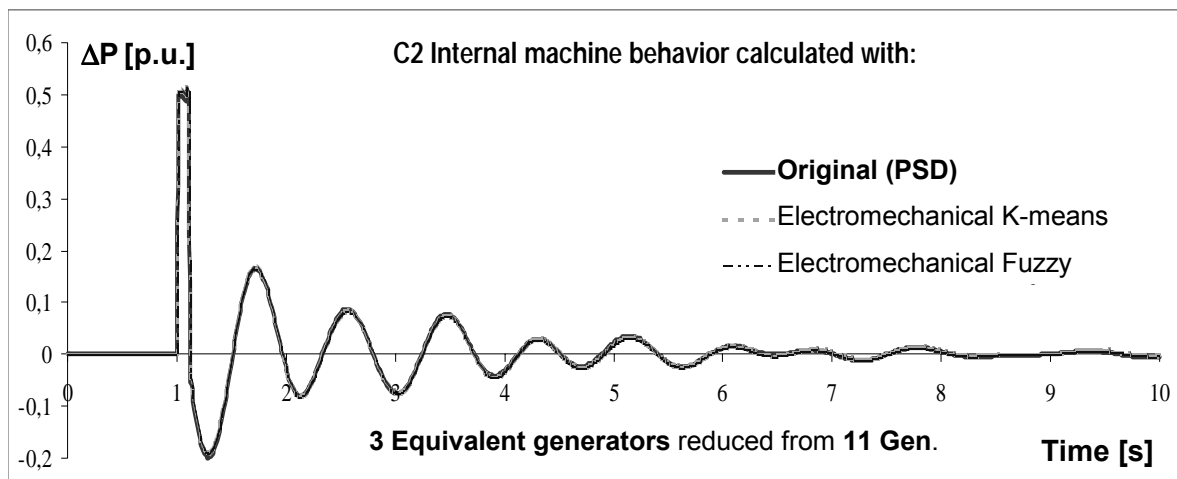


**Fig. 3.14.-** Time responses of the **C2** internal machine calculated with 3 equivalent machines by different identity recognition-based algorithms.

The same identity recognition-based equivalents can be used to simulate other disturbances, which have to be coupled electrically and geographically to the one. The following cases can be simulated:

- In Fig. 3.15, the behavior of the C2 generator following the disturbance on the node C3 in 380kV area is represented. This disturbance is electrically and geographically in close to the disturbance of the equivalents derived.
- In Fig. 3.16, the behavior of the C2 generator following the disturbance on the node C9 in 220kV area is represented. This disturbance is electrically and geographically far away from the disturbance of the equivalents derived.

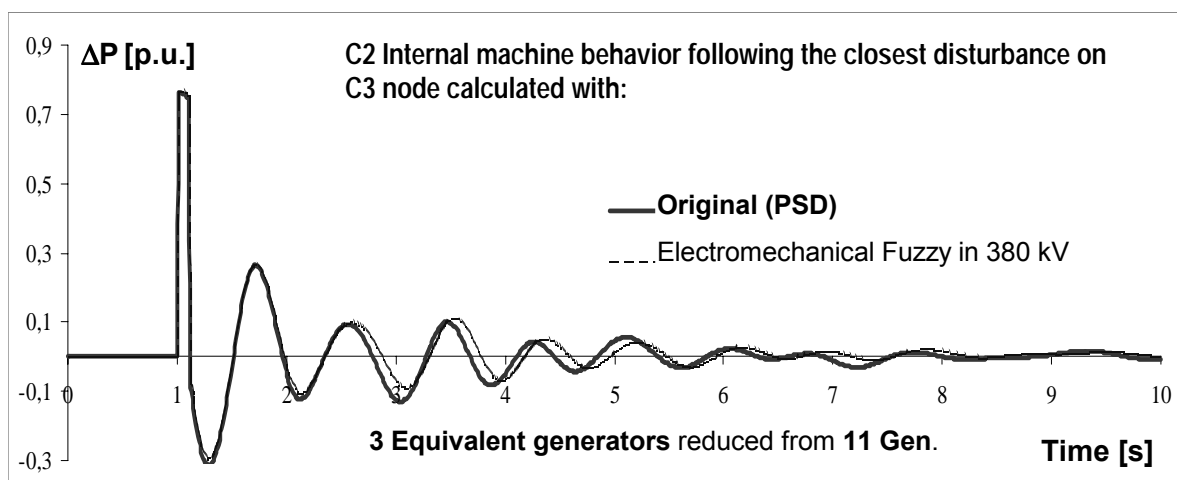


**Fig. 3.15.-** Time responses of the **C2** internal machine following the disturbance (electrically and geographically closest) applied on C3 node of internal area.

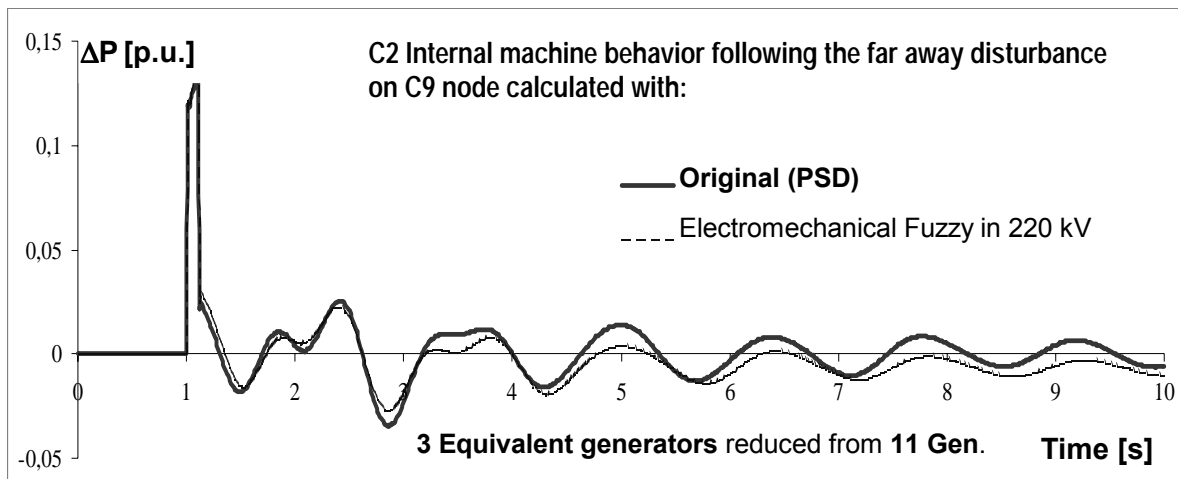


**Fig. 3.16.-** Time responses of the **C2** internal machine following the disturbance (electrically and geographically far away) applied on C9 node of internal area.

The oscillation behavior of Fig. 3.15 shows a higher degree of agreement than the one of Fig. 3.16. Thus, the electromechanically derived equivalents are also valid for other disturbances limitedly, that are electrically and geographically in close distance to the fault of the equivalents derived, i.e. the closer these disturbances, higher the accuracy of the equivalents.

Following aspects can be briefly summarized:

- All identity recognition algorithms provide the same machine assignment and grouping of external machines for this 16 multi-machine system. Consequently, they generate identical dynamic equivalents.
- Improved dynamic equivalents are obtained using electromechanical-based identity recognition algorithms.
- The accuracy of the identity recognition depends upon important aspects, such as:
  - *the identity recognition capability of the algorithms.*
  - *number of dynamic equivalents.*
  - *the geographical and electrical distance between internal machines and disturbances.*

A discernible accuracy improvement by means of the electromechanical distances can be detected at the stability analysis in a large interconnected power system, as it can be presented in the following case study.

### 3.5.3 Interconnected European Network UCTE/CENTREL

The electromechanical identity recognition was applied to *the Interconnected European power system UCTE/CENTREL*, consisting of 464 machines, 2016 nodes and 2098 transmission lines with their excitation and governor control models [142].

Additional to *the western European Union for the Coordination of Transmission of Electricity (UCTE)*, *the central European power system (CENTREL)* includes the eastern European countries. The following table shows different European network subsystems.

**Table 3.2.-** Subsystems in the European Interconnected Power System UCTE/CENTREL

Power Subsystem	Country	Power Subsystem	Country
ALB	Albania	MAZ	Macedonia
B	Belgium	NL	The Netherlands
BAG	Germany	OEVG	Austria
BEWAG	Germany	PE	Germany
BG	Bulgaria	PL	Poland
BiH	Bosnia/Herzegovina	Po	Portugal
CEZ	Czech Republic	ROM	Romania
CH	Switzerland	RWE	Germany
ELSAM	Denmark	SEP	Slovakia
EnBW	Germany	SL_HR	Slovenia/Croatia
FR	France	Sp	Spain
GR	Greece	VEAG	Germany
HU	Hungary	VEW	Germany
IT	Italy	YU	Yugoslavia
LVOV	Ukraine		

The integration of the systems UCTE and CENTREL leads to a complex stability behavior and reciprocal dynamic impact between strongly meshed subsystems. Taking into consideration the liberalization of electric market in Europe, the operators are forced to operate the subsystems near to the stability limits and outside their local area. Consequently, the operators due to safety reasons have to realize different stability assessment and analysis actions within their internal subsystems. To this end, information, and knowledge over the network structure and the actual operation situation of the external subsystems, i.e. outside of the internal subsystem, should be available limitedly involving dynamic equivalents.

In this study, the available data for the UCTE/CENTREL system include transformers, machines, loads, transmission lines, amongst others. The machine model is either described by 5<sup>th</sup> or 6<sup>th</sup> order models including governors and exciters by 2<sup>nd</sup> and 3<sup>rd</sup> order models.

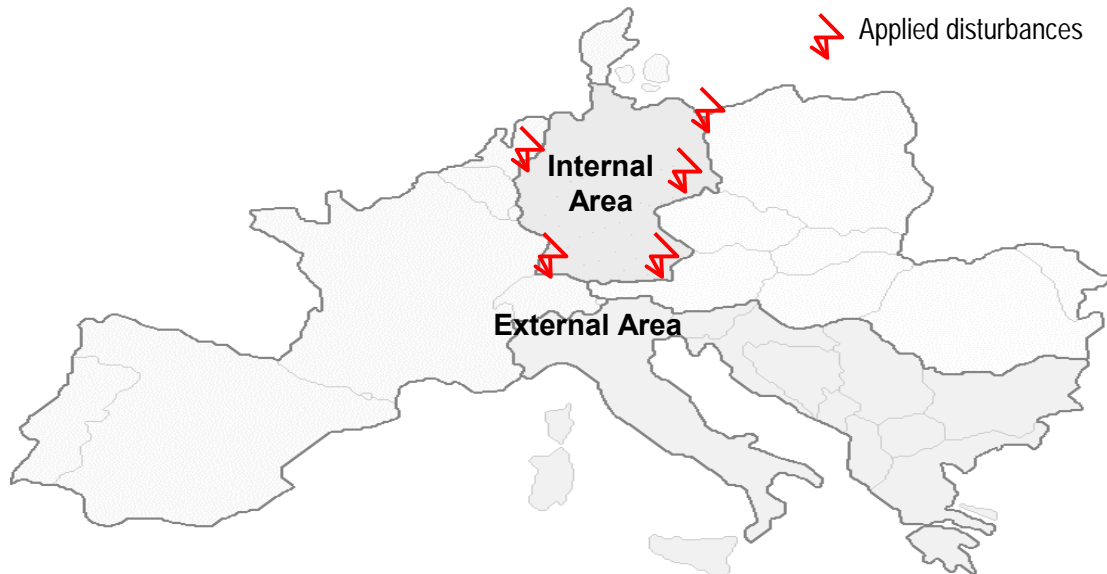


Fig. 3.17.-Interconnected European power system UCTE/CENTREL [142].

For the simulation following aspects are relevant:

- The power system is divided into *the German system consisting of the old operators: BAG, BEWAG, EnBW, HEW, PE, RWE, VEAG and VEW forming the internal area. It has to be preserved in the original form, consisting of 67 machines, which are available physically in the actuality in spite of all liberalized market operations (For details see appendix Fig. F.1). All these machines are retained individually.*
- The rest 397 machines located outside the German area, considered as external area, have to be replaced by dynamic equivalents involving the electromechanical identity recognition and the classical inertial aggregation procedure.
- The electromechanical identity recognition performance will be evaluated by comparing the oscillating swing curves of the internal area machines. They will be simulated using PSD in one hand with help of the full external area and another hand by the dynamic equivalent of the external area. (For more details on PSD see section 2.3)
- To this end, several disturbances as three-phase short circuit with a duration between 80 to 200 ms were selected, which are applied at the boundary between the German and external area. These disturbances are described in table 3.3.

**Table 3.3.-** Disturbance specifications for the European power system UCTE/CENTREL (the boundary nodes correspond to NL=Netherlands, CH=Swissland, OEVG=Austria)

Cases	Fault location (German network operator)	Neighborhood nodes
1	VEGROUSB (VEW)	NLHENGL4 (NL)
2	BWKUJESSA (EnBW)	CHLAC SA (CH) CHLAUBSB (CH) CHLAVOG4 (CH) CHGOEESA (CH) CHBASUSA (CH)
3	RWHERBG2 (RWE )	OBUERS2 (OEVG) CHWINKL2 (CH)
4	EVPULDSB (EnBW)	CHLAUBSB (CH)
5	RWLEULSA (RWE)	OWESTT1 (OEVG)

Considering these faults, all simulations are similar and show a high accuracy and agreement. A representative scenario is the disturbance, which is based on the case 1 during 100 ms at the boundary node **VEGROUSB (VEW)**. This node is located in the near to the Dutch node **NLHENGL4 (NL)**. The three-phase short circuit is applied to a 500kV bus, which connects the Dutch and the German system.

This fault creates a major system-wide disturbance and is applied after 2 sec., the transient stability simulation duration is 10 sec.

### 3.5.4 Simulation results and discussion

*This disturbance is simulated using the original external area and the reduced external models, which are based on different number of dynamic equivalents from 180 until 20. The proposed identical recognition algorithms will be applied.* Hence, the following representative cases are presented:

- Case 1 — 90 European dynamic equivalents reduced from 397 machines
- Case 2 — 65 European dynamic equivalents reduced from 397 machines
- Case 3 — Electrical and geographical coupled 65 European dynamic equivalents

#### Case 1 — 90 European dynamic equivalents reduced from 397 machines

In this case, the time behavior of the German machine **KIEL1** following the disturbance at the boundary node **VEGROUSB (VEW)** is calculated, in one hand, with the unreduced 397-machine external area and in the other hand with 90 equivalents. K-means, Fuzzy and

SOFM and their corresponding electromechanical algorithms have been applied, as can be shown in the following figures:

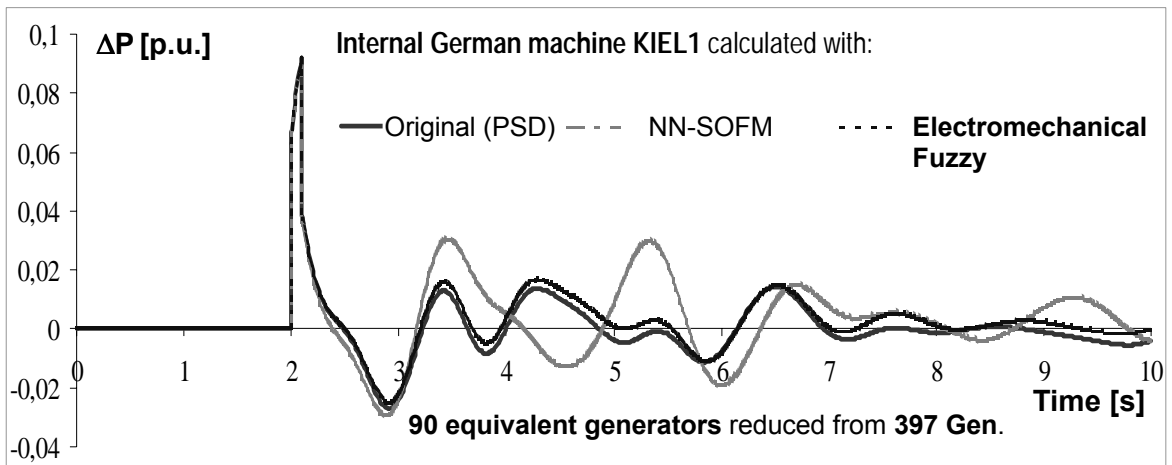
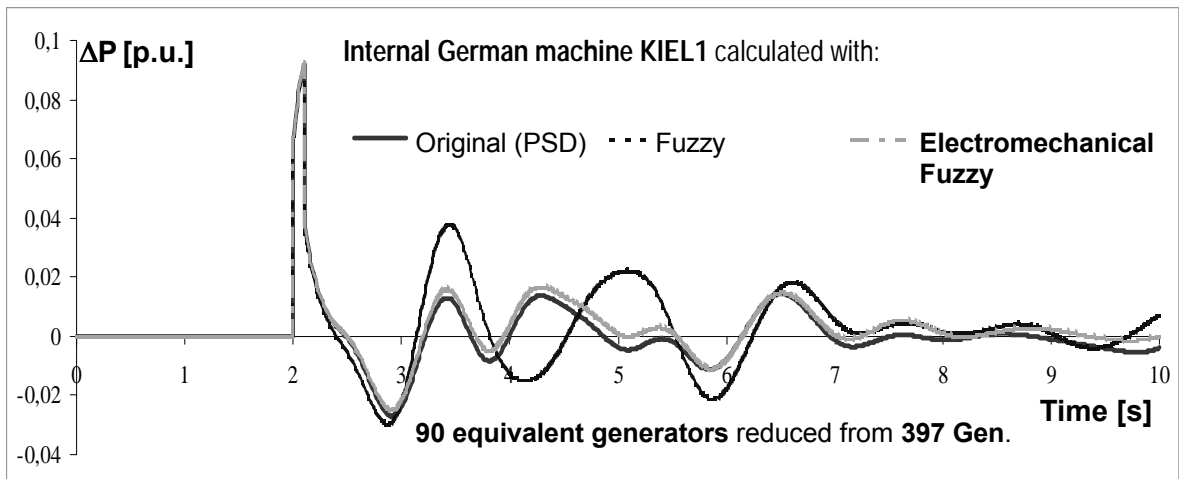
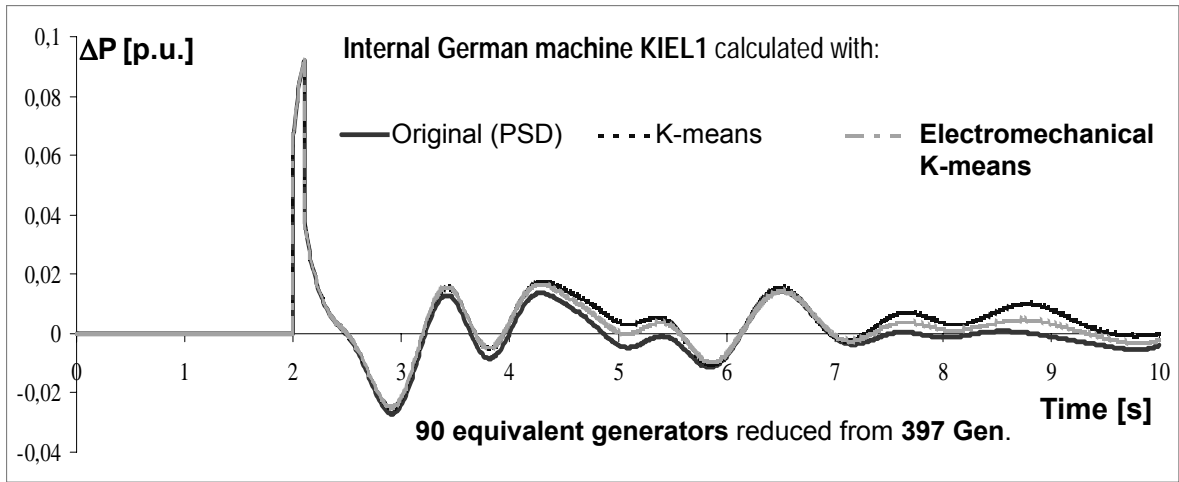


**Fig. 3.18.a, b, c.-** Comparison of time responses of the **KIEL1** German machine calculated with 90 equivalent machines by different identity recognition algorithms and considering their electromechanical weighting (weighted K-means, weighted Fuzzy and Kohonen-SOFM).

Upon the basis of Fig. 3.18 following aspects are detected:

- The *time responses of the internal machines with the dynamic equivalents considering the electromechanical distances in all identity recognition algorithms* (as K-means in Fig. 3.18.a, and Fuzzy in Fig. 3.18.b) *is very close to that of the unreduced system* for the whole time simulation.
- Considering only the algorithms without electromechanical distance, a notable accuracy of K-means in Fig. 3.18.a can be detected in comparison to Fuzzy in Fig. 3.18.b and SOFM in Fig. 3.18.c, which show a great deviation over 3 sec. to 6 sec. concerning phase and amplitude.
- However, it should be mentioned that same accuracy by Fuzzy and SOFM is achieved directly after the disturbance, i.e. during the first 3 seconds and over 6 seconds of the simulation.
- Therefore, *depending on the applied algorithm a detectable degradation in accuracy may be discerned in large-scaled power systems.*
- *K-means and relatively Fuzzy recognizes better identical groups of generators than SOFM, but through the electromechanical distance all algorithms recognizes electromechanically close identical groups* taking into consideration the physical parameters of the grouped generators and consequently they form more accurate dynamic equivalents.

## Case 2 — 65 European dynamic equivalents reduced from 397 machines

In this case, the Figs. 3.19.a and 3.19.b show the oscillation time responses of the **STDE1** German machine. They are simulated using the dynamic equivalent consisting of 65 equivalent machines and following the disturbance at node **VEGROUSB (VEW)**.

Remarks to Fig. 3.19.a and Fig. 3.19.b:

- The same degradation of accuracy in K-means and Fuzzy of oscillation of the **STDE1** German machine following the same disturbance in case 1 of table 3.3 can be observed in Fig. 3.19.a and Fig. 3.19.b, respectively. In this context, a considerable deviation of the time oscillation both in K-means and Fuzzy in amplitude and phase over 4 seconds until to 6 seconds during the simulation can be detected.
- However, a significant enhancement of the agreement can be discerned considering the electromechanical parameters as weighting distances in K-means (Fig. 3.19.a) and Fuzzy (Fig. 3.19.b), as well in the previous case.
- Both above aspects, such as the degradation of accuracy and *enhancement through the electromechanical distance* are observed in dynamic equivalencing procedures on the

European power system independent of the reduction degree of the external area, i.e. equivalents of 90, 65, and lower number of equivalent machines reduced from 397 external machines outside of the German area.

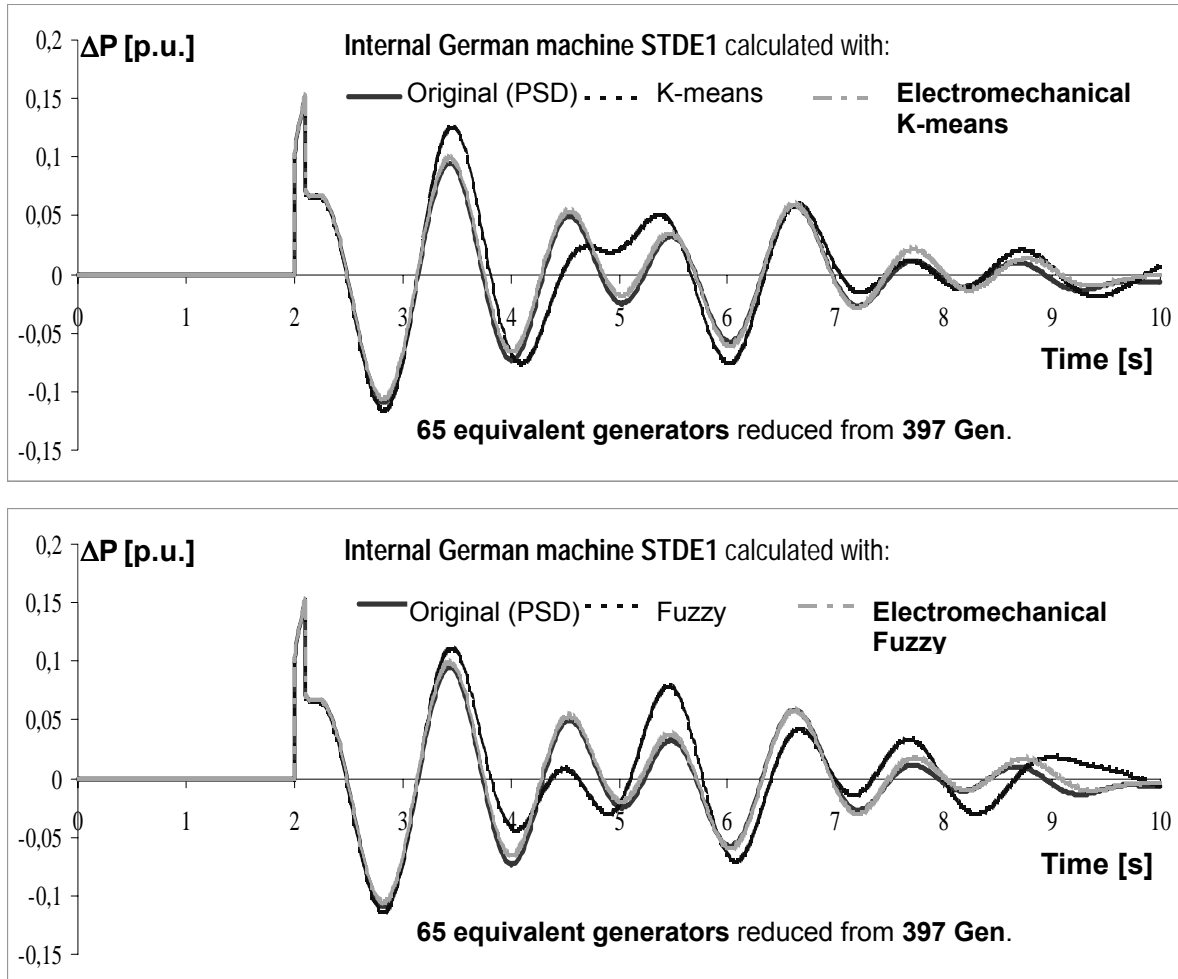


**Fig. 3.19.a, b.-** Comparison of time responses of the **STDE1** German machine calculated with 65 equivalent machines by different identity algorithms with electromechanical distances (weighted K-means, weighted Fuzzy).

The high accuracy through the electromechanical distance was determined for all machines in the German system.

### Case 3 — Electrical and geographical coupled 65 European dynamic equivalents

The derived equivalents calculated by the electromechanically identical groups following the disturbance at **VEGROUSB (VEW)** (equivalent disturbance) were valid in the same manner for disturbances too, whose locations are electrically and geographically in the near or close to this equivalent disturbance. The following cases can be simulated:

- In Fig. 3.20, the behavior of the **BWKU ESS** German machine following the disturbance on the node **VEHANNSA (VEW)** is represented. This disturbance is electrically and geographically in close to the disturbance of the equivalents derived.
- In Fig. 3.21, the behavior of the same German machine following the disturbance on the node **EVDELSSAD (EnBW)** is represented. This disturbance is electrically and geographically far away from the disturbance of the equivalents derived.

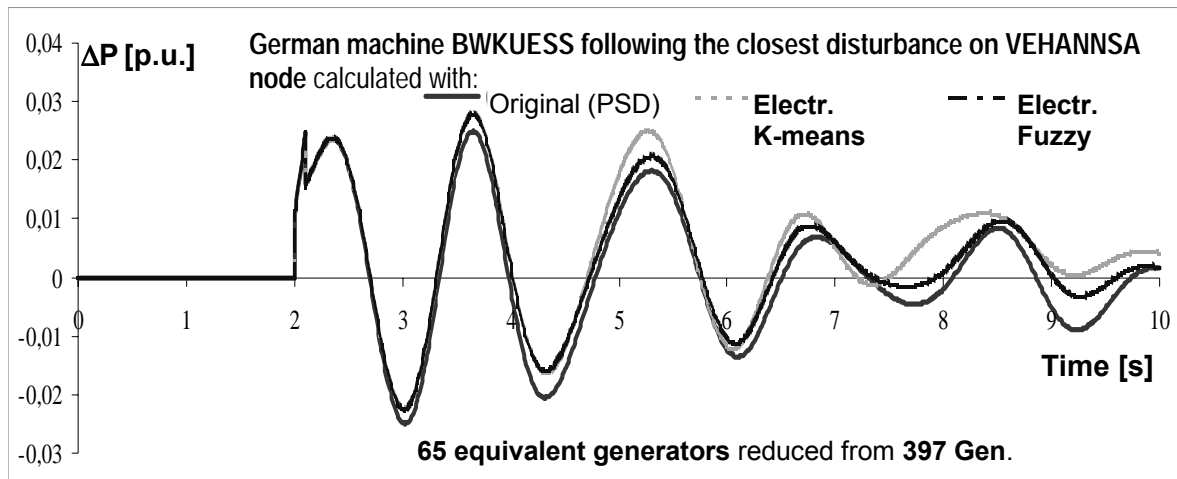


**Fig. 3.20.-** Behavior of the **BWKU ESS** German machine using 65 equivalents considering their electromechanical-based algorithms and following a disturbance at **VEHANNSA (VEW)**.

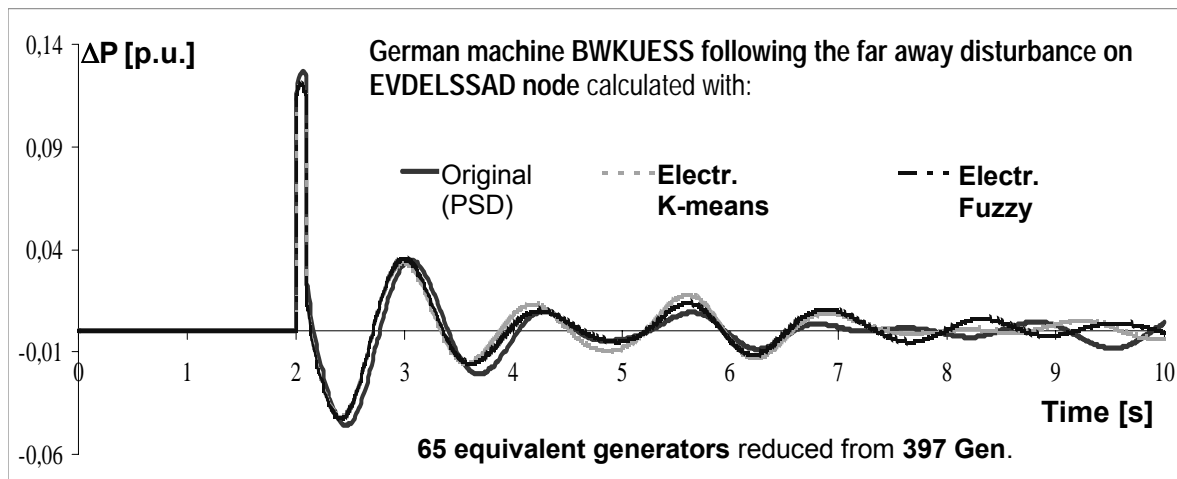


**Fig. 3.21.-** Behavior of the **BWKU ESS** German machine using 65 equivalents considering their electromechanical-based algorithms and following a disturbance at **EVDELSSAD (EnBW)**.

In Fig. 3.20, it can be seen a quite agreement of the time responses in the first 5 sec. following a degradation in accuracy over 7 sec. Thus, the electromechanical weighted algorithms show a detectable improvement.

Fig. 3.20 and Fig. 3.21 show that electromechanical identity recognition-based dynamic equivalents are valid for other disturbances, whose location have to be geographically and electrically coupled to the disturbance, for which the equivalent was developed.

*In both cases, the oscillation behavior shows a high degree of agreement. Although, the disturbance on **EnBW** subsystem (in Fig. 3.21) is far away geographically from the disturbance on **VEW** subsystem, a significant accuracy of the derived equivalents can be obtained. However, considering all German machines, the electromechanically derived equivalents are also valid for other disturbances that are independent electrically and geographically of close distance to the disturbance of the equivalents derived. Therefore, electromechanical-based identity recognition makes it possible that disturbance-independent dynamic equivalents can be generated.*

### Quality measurement of the identity recognition approach

In this section, the behavior of all German machines is investigated using the following proposed algorithms regarding their suitability and accuracy:

- Identity recognition algorithms, such as Fuzzy, K-means, Hierarchical, and SOFM.
- Electromechanical-based algorithms, such as electromechanical Fuzzy, K-means and Hierarchical.

The measure for evaluating the three methods is defined as follows:

$$J(i) = 1 - \frac{\sum_{l=1}^{N_p} (\Delta P_l(i)^{Original} - \Delta P_l(i)^{Dyn.Equi.})^2}{N_p} \quad \therefore i = 1, \dots, N_s \quad (3.44)$$

where

- $\Delta P(i)^{Original}$  and  $\Delta P(i)^{Dyn. Equi.}$  are the time domain behavior of the  $i$ th generator in the German system, which are calculated with the original European external area and the equivalented one.  $(\Delta P(i)^{Original} - \Delta P(i)^{Dyn. Equi.})^2$  is defined as squared distance error.
- $N_p$  is the number of sampling points and
- $N_s$  is the total number of generators in the internal area.

The “best” identity recognition algorithm is the one that gives the minimum squared distance error or maximizes  $J(i)$ . Taking into consideration all German machines, the following mean value  $\bar{J}$  may be defined as:

$$\bar{J} = \frac{\sum_{i=1}^{N_s} J(i)}{N_s} \quad (3.45)$$

This  $\bar{J}$  may be called the identity coefficient corresponding to a used algorithm.

Of course, by means of this value the quality, accuracy and grouping capability of a identity recognition algorithm can be characterized and compared depending on the reduction degree of 397 external machines from 20 to 180 dynamic equivalents, as it can be seen in the following figure:

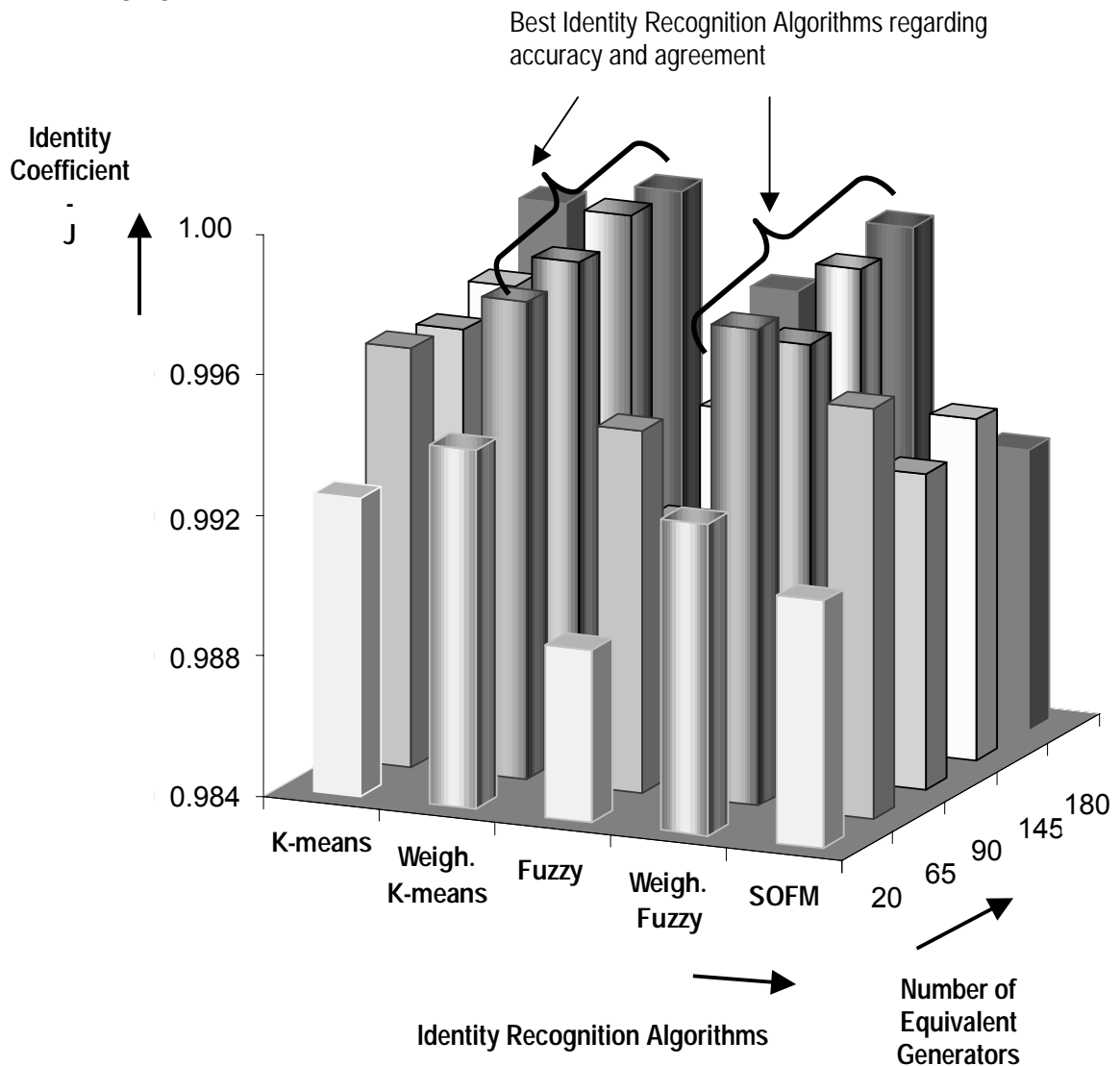


**Fig. 3.22.-** Comparison of identity recognition algorithms considering electromechanical weighted distances by the mean value of  $J$  of the 67 German intern machines for a fault located at the boundary node **VEGROUSB(VEW)** with different number of external equivalents.

As it can be seen in Fig. 3.22, the proposed electromechanical-based identity recognition with Fuzzy and K-means, i.e. weighted Fuzzy and weighted K-means, gives the best result and accuracy, as accentuated and highlighted beams illustrated, independent of the number of equivalents. The detailed values are given in the appendix table F.3.

#### Remarks to Fig. 3.22:

- Both SOFM and Fuzzy algorithms show a considerable degradation in agreement and accuracy in contrast to K-means.
- The identity recognition capability of the SOFM is limited due to the slow learning process and the unsupervised nature of the ANN learning.
- In Fig. 3.22, it is depicted that lower the number of equivalents, the less accurate are the algorithms, i.e.  $\bar{J}$  for 20 dynamic equivalents are lower  $\bar{J}$  for 180 dynamic equivalents. It is due to the nature of the clustering procedure.
- The best identity algorithms and consequently the small distance errors are the electromechanical-based algorithms independent of the number of equivalents.
- This aspect leads to electrically efficient and more accurate dynamic equivalents. Consequently, in the grouping process is taken into account the electromechanical properties of the interconnection among the external machines.

It should be noted that the electromechanical-based identity recognition is applicable without restriction to a power system independent of its structure, size and complexity. This is fairly demonstrated both on the 16 multi-machine system and the interconnected European system UCTE/CENTREL obtaining strongly accurate equivalents.

### 3.6 Summary

- A new approach in dynamic equivalencing of power systems, called *electromechanical-based identity recognition*, as alternative to the classical coherency identification is proposed to obtain *identity-based equivalent generators* of external large power systems.
- Through this approach, *the grouping of generators is considered as an identity analysis task*. Together oscillating machines have to be determined by evaluating *the amplitude and phase identity of the rotor angle behavior* of the generators, and not only *the phase of the rotor angle (coherency identification)*.
- *The phase and amplitude of the behavior have to be examined applying standard pattern recognition algorithms*, such as hierarchical, K-means, Fuzzy and SOFM.

- The proposed identity recognition can *incorporate machine system model parameters* in dynamic equivalencing process.
- Thus, specific physical effects and electromechanical influences of the generators with regard to their properties, modeling and structure can be considered to cluster the machines *according to the proposed electromechanical distance*. These parameters are defined using the sensitivity analysis. Thus, *large generators with large nominal power and large inertial constants have more electromechanical influence on the system dynamic than smaller generators*.
- Therefore, the obtained *electromechanical-based identity recognition* forms improved and high accurate dynamic equivalents.
- This approach is verified both *on the 16 multi-machine system and the interconnected European power system UCTE/CENTRAL without restriction*. It is applicable to all forms of power systems independent of their structure, size, and complexity.
- *In small power systems, all electromechanical identity recognition algorithms generate similar accurate dynamic equivalents with high agreement. But, in the Interconnected European power system UCTE/CENTREL, in which the German network as internal area is simulated, the results are significantly accurate.*
- Best *results with a high degree of accuracy* are achieved with help of the electromechanical distances *forming weighted K-means and weighted Fuzzy algorithms*. SOFM are not appropriate due to the ineffectiveness of its learning process and neural network topology for complex systems.
- Further, it has been determined, *that grouping process is partially independent of the fault location*. However, *more accurate dynamic equivalents can be achieved by disturbances, which are electrically and geographically strong connected to the one*.
- But, *the derived equivalents* calculated by the electromechanical identity recognition following a certain disturbance *are valid in the same manner for other disturbances too, whose locations are electrically and geographically in close to the equivalent disturbance or far away from the one*.

*“He was under the impression that a system description (by the system decomposition) is exactly the same as a system in a concrete physical sense.”-R. Kalman [138]-*

## Chapter 4

# Splitting Aggregation-based Dynamic Equivalencing

**Objective—** *The objective of this chapter is to develop an innovative aggregation approach to construct representative machines with improved accuracy and to consider essentially characteristics of the generators regarding their electromechanical parameters.*

*This chapter mainly describes the concept and strategy of an aggregation approach on the basis of the fictive splitting of external machines. This splitting strategy is used as a basis for implementing mathematical reduction techniques in dynamic equivalencing and thus obtaining a reduced electromechanical system of the area being equivalenced, which can be applied in transient stability studies.*

*The splitting factors may be derived by mathematical reduction techniques, such as the Fuzzy theory or principal component analysis. The relevant property of this approach consists of incorporating of new defined electromechanical splitting-based machine parameters that it significantly improves the accuracy and efficiency of dynamic equivalents and thereby enhances their effectiveness and application.*

*Simulations of this approach have been performed and evaluated in an interconnected 16 multi-machine power system.*

**Index Terms—** *Aggregation, Coherency Identification, Dynamic Equivalent, Electromechanical Parameters, Identity Recognition, Splitting-based Parameters.*

**Organization—** *Section 4.1 describes the introduction and section 4.2 of this chapter the classical methodologies concerning generator aggregation. The proposed splitting-based*

*aggregation approach is discussed in section 4.3, followed in section 4.4 by the application. In section 4.5 the simulation results are evaluated and in section 4.6 the summary is given.*

## 4.1 Introduction

Generally, a complex power system can be divided into two areas, the internal area that has to be retained for analysis, and the external area that is to be reduced to a simplified aggregated model of the external machines. The conventional aggregation in dynamic equivalencing generates aggregated equivalents on the external area on the basis of inertial and slow aggregation [30-32], which can be replaced by an innovative approach, i.e. the splitting-based aggregation. Using this concept, the classification and grouping of together oscillating machines are replaced by a virtual splitting of machines.

The developed approach is based upon the splitting strategy to process the swing oscillating curves in time domain of the external machines. This strategy generates splitting-based electromechanical parameters considering the physical characteristics of the whole number of external machines.

## 4.2 Conventional aggregation in dynamic equivalencing

The classical dynamic equivalencing involves mainly a three-stage procedure of:

- **Identification** of coherent generators in the external area forming groups [17, 18].
- **Conventional Aggregation** of the grouped external generators without changing the power flow relationships where these generators show coherent [17] properties.
- **Static network reduction**

A coherent group of generating units is defined as a group of generators oscillating with the same rotor angular speed. The representative machine parameters of this group can be calculated according to the classical aggregation approaches, such as the inertial and slow aggregation, which are zero and first order approximations of singularly perturbed two-time-scale power system models, respectively [30, 31, and 35].

The inertial aggregation does not involve linearization aspects, because its procedure operates only on the generator terminal buses of the grouped generators. However, these approaches require the determination and classification of coherent machines, which is not necessary according to the proposed splitting based aggregation. It represents a significant change of the classical dynamic equivalencing procedure because non-linear processes and behaviors of the power system can be taken into account.

**Disadvantages:**

Considering the grouping-based simplified models, which are required by the classical aggregation, the following disadvantages may be determined:

- *The inertial and slow aggregation are performed only and limitedly on a per coherent area of external subsystem.*
- *The aggregation of the network in one coherent or identical area can affect electrically the network aggregation in other coherent areas. Consequently, the error in the aggregation approximation may result in a decrease of accuracy.*
- *On the coherent-based models of power systems, the aggregated area that includes generator and non-generator buses (PV and PQ nodes) is aggregated to the machine terminal node and non-generator buses are not considered in the aggregation procedure. As a result, the accuracy of aggregated network is reduced.*
- The aggregated groups are independent upon the detailed machine model, i.e. the physical parameters of the machines. Moreover, although many improvements in the classical aggregation strategies [30] and coherency [19] were made, the related non-linear behavior cannot be considered accurate enough for forming equivalent parameters.
- Due to the grouping procedure, the corresponding equivalents are not exact enough, since the whole aggregation structure of the external area can be lost.

## 4.2.1 Inertial Aggregation

### Modeling of synchronous machines

There are various types of models of synchronous machines for power system transient stability studies. In aggregation simulation using PSD [87, 141] (for details see section 2.3), the machine model can be coupled into the analysis program PSD according to the flow chart in appendix A.8. These machines are expressed by the direct- and quadrature axis having one damper circuit both in d- and q-axis, which can be transformed from the L1, L2 and L3 stator to dq0 system, as it can be graphically represented as follows:

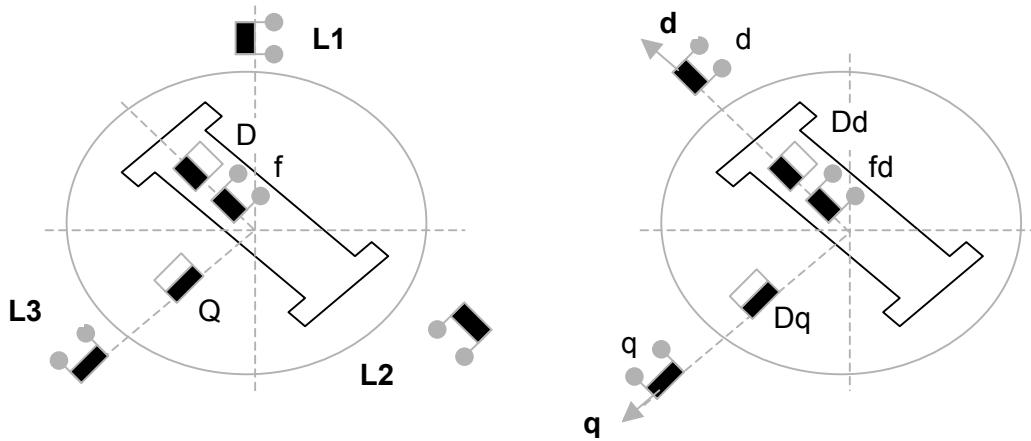


Fig. 4.1.- Synchronous machine models: L1-L2-L3 transformed in dq-system

In this model following aspects are important:

- The quasi-state synchronous machine model is based upon the voltage:

$$\begin{bmatrix} u_d \\ u_q \\ u_{fd} \\ 0 \\ 0 \end{bmatrix} = \begin{bmatrix} r_s & 0 & 0 & 0 & 0 \\ 0 & r_s & 0 & 0 & 0 \\ 0 & 0 & r_{fd} & 0 & 0 \\ 0 & 0 & 0 & r_{Dd} & 0 \\ 0 & 0 & 0 & 0 & r_{Dq} \end{bmatrix} \begin{bmatrix} i_d \\ i_q \\ i_{fd} \\ i_{Dd} \\ i_{Dq} \end{bmatrix} + \begin{bmatrix} 0 & -\omega_L & 0 & 0 & 0 \\ \omega_L & 0 & 0 & 0 & 0 \\ 0 & 0 & 0 & 0 & 0 \\ 0 & 0 & 0 & 0 & 0 \\ 0 & 0 & 0 & 0 & 0 \end{bmatrix} \begin{bmatrix} \psi_d \\ \psi_q \\ \psi_{fd} \\ \psi_{Dd} \\ \psi_{Dq} \end{bmatrix} + \begin{bmatrix} \dot{\psi}_d \\ \dot{\psi}_q \\ \dot{\psi}_{fd} \\ \dot{\psi}_{Dd} \\ \dot{\psi}_{Dq} \end{bmatrix} \quad (4.1a)$$

flux linkage:

$$\begin{bmatrix} \psi_d \\ \psi_q \\ \psi_{fd} \\ \psi_{Dd} \\ \psi_{Dq} \end{bmatrix} = - \begin{bmatrix} x_{hd} + x_{\sigma s} & 0 & x_{hd} & x_{hd} & 0 \\ 0 & x_{hq} + x_{\sigma s} & 0 & 0 & x_{hq} \\ x_{hd} & 0 & x_{hd} + x_{\sigma fd} + x_{\sigma fdD} & x_{hd} + x_{\sigma fdD} & 0 \\ x_{hd} & 0 & x_{hd} + x_{\sigma fdD} & x_{hd} + x_{\sigma Dd} + x_{\sigma fdD} & 0 \\ 0 & x_{hq} & 0 & 0 & x_{hq} + x_{\sigma Dq} \end{bmatrix} \begin{bmatrix} i_d \\ i_q \\ i_{fd} \\ i_{Dd} \\ i_{Dq} \end{bmatrix} \quad (4.1b)$$

and mechanical equations:

$$\frac{d\delta_L}{dt} = (\omega_L - \omega_o) \quad (4.1c)$$

$$\frac{d\omega_L}{dt} = \frac{1}{T_m} [(\psi_d i_q - \psi_q i_d) + m_m] \quad (4.1d)$$

- All state variables will be transformed into the rotor coordinate system with the aim that the stator flux linkage is not a state variable and thus, it follows changes of the stator voltage and rotor flux linkage. Hence, the stator flux linkage in the rest state space equations for rotor flux linkage and mechanical behavior may be eliminated [87]. For transient stability analysis a quasi-state model is sufficient.

- Thus,  $\dot{\psi}_d = 0$  and  $\dot{\psi}_q = 0$  lead to the following simplified state space form of synchronous machines:

$$\begin{bmatrix} \dot{\psi}_{fd} \\ \dot{\psi}_{Dd} \\ \dot{\psi}_{Dq} \\ \dot{\omega}_R \\ \dot{\delta}_R \end{bmatrix} = - \begin{bmatrix} T_{fd}^{-1} & T_{Dfd}^{-1} & 0 & 0 & 0 \\ T_{fDd}^{-1} & T_{Dd}^{-1} & 0 & 0 & 0 \\ 0 & 0 & T_{Dq}^{-1} & 0 & 0 \\ k_{fd} i_q & k_{Dd} i_q & k_{Dq} i_d & 0 & 0 \\ \frac{T_m}{0} & \frac{T_m}{0} & \frac{T_m}{0} & -1 & 0 \end{bmatrix} \begin{bmatrix} \psi_{fd} \\ \psi_{Dd} \\ \psi_{Dq} \\ \omega_R \\ \delta_R \end{bmatrix} + \begin{bmatrix} r_{fd} k_{fd} i_d + u_{fd} \\ r_{Dd} k_{fd} i_d \\ r_{Dq} k_{Dq} i_q \\ (X_d'' - X_q'') i_d i_q + m_m \\ \frac{T_m}{\omega_b} \end{bmatrix} \quad (4.2)$$

where the time constants are:

$$\begin{aligned} T_{fd} &= \frac{Det}{r_{fd}(X_{hd} + X_{\sigma Dd} + X_{\sigma fd})} & T_{fDd} &= \frac{-Det}{r_{fd}(X_{hd} + X_{\sigma fd})} & T_{Dq} &= \frac{(X_{hd} + X_{\sigma Dq})}{r_{Dq}} \\ T_{Dfd} &= \frac{-Det}{r_{Dd}(X_{hd} + X_{\sigma fd})} & T_{Dd} &= \frac{Det}{r_{Dd}(X_{hd} + X_{\sigma fd} + X_{\sigma Dd})} \end{aligned} \quad (4.3)$$

Hereby are:

$$Det = (X_{hd} + X_{\sigma fd})(X_{\sigma fd} + X_{\sigma Dd}) + X_{\sigma fd} X_{\sigma Dd}$$

$$K = \begin{bmatrix} k_{Dd} & k_{fd} & 0 \\ 0 & 0 & k_{Dq} \end{bmatrix}$$

$$k_{Dd} = \frac{X_{\sigma fd} X_{hd}}{Det} \quad k_{fd} = \frac{X_{\sigma Dd} X_{hd}}{Det} \quad k_{Dq} = \frac{X_{hq}}{X_{\sigma Dq} + X_{hq}} \quad (4.4)$$

where

- $X_{hd}$ ,  $X_{hq}$ ,  $X_{\sigma Dq}$ ,  $X_{\sigma Dd}$ ,  $X_{\sigma fd}$ ,  $X_{\sigma fd}$ ,  $X_d''$ ,  $X_q''$  are the synchronous reactance and subtransient synchronous reactance, respectively.
- $u_d$ ,  $u_q$ ,  $u_{fd}$  are the stator voltage in q and d-axes and the exciter voltage respectively.
- $u_s$ ,  $i_s$  are the stator (terminal) voltage and current, respectively.
- $m_m$  is the turbine mechanical torque.
- $i_d$ ,  $i_q$ , are the stator currents in q and d-axes, respectively.
- $T_m$  is the shaft inertia constant.
- $\omega_b$  is the network frequency referenced to p.u.
- $\psi_L$ ,  $\psi_S$  are the rotor and stator flux linkage, respectively.
- $\omega_L$ ,  $\delta_L$  are the rotor angular velocity and rotor angle, respectively.

- The state space equation of the machine may be coupled to the power system through the following complex algebraic equation and according to the appendix A.8:

$$\underline{u}_s = (r_s + jx_q'')i_s'' + \underline{u}'' \quad (4.5)$$

where the driving voltage  $u''$  is a function of the state variables flux linkages, rotor position angle and partly of the stator current, as follows:

$$\underline{u}'' = \underline{u}''_o + \Delta \underline{u}'' = (u''_{d0} + ju''_{q0})e^{j\delta_L} + j(x_q'' - x_d'')i_d'' e^{j\delta_L} \quad (4.6)$$

$$\underline{u}'' = \left\{ \omega_0 (-k_{Dq}\psi_{Dq} + j(k_{fd}\psi_{fd} + k_{Dd}\psi_{Dd})) + j(x_q'' - x_d'')i_d'' \right\} e^{j\delta_L} \quad (4.7)$$

- By means of  $e^{j\delta_L}$ , a transformation from the rotor to the network coordinate system is realized. The quasi-state space equation (4.2) is solved by numerical integration in PSD, when  $i_d, i_q$  are known [87]. This model is used within classical aggregation [15, 30-33].

Following aspects are relevant to the **machine equivalent**:

- This model of the classical aggregation creates a new terminal bus and connects it to the internal busses of each individual generator via pseudo transformer. The transformation ratios are chosen so that the driving voltages of generators will be transformed to the aggregated driving voltage of the equivalent generator to a uniform one, according to the relationships (3.6) and (3.7).
- The circuit must be completed by a branch with the negative transient reactance of the equivalent generator to get the new terminal bus according to Fig. 3.2. The transient reactances combined with the transformers, allow the elimination of the internal nodes of original generators.

Aspects of the **machine parameters** are summarized as follows:

- The machine parameters are calculated from the weighted mean values of generators inductances and resistances as reciprocal values in p.u., as follows:

$$r_E = \frac{1}{\sum_i^{NG} \frac{1}{r_i}} \quad x_E = \frac{1}{\sum_i^{NG} \frac{1}{x_i}} \quad (4.8)$$

where

- $x_i$  represents resistances, main-field and linkage inductance of all circuits.

- $NG$  is the number of coherent or identical machines in the corresponding group.
- Equation (4.8) means that the parameters will be connected parallel and it is one of the possible solutions. Another way would be the calculation of aggregated parameters for the transient, subtransient reactance, time constants system parameters directly.
- The sum of active and reactive power at the internal nodes behind transient reactances must be supplied by equivalent generator, too. The resulting nominal power of the equivalent machine is the sum of all generator powers given by:

$$S_{rE} = \sum_i^{NG} S_{ri} \quad (4.9)$$

- The nominal voltage of the machine is not a relevant variable, but it has to be considered in the tape ratio of pseudo transformers.
- The resulting inertial constant of the equivalent machine is given by:

$$T_{mE} = \sum_i^{NG} T_{mi} \quad (4.10)$$

- When all parameters are given, the driving voltage of the equivalent behind of the resulting transient reactance can be calculated.
- After then the equalizer transformers are included into the network. These transformers don't have inner impedance. Therefore the individual generator reactance can be interpreted as transformer impedance, so that the transformers are placed between the individual terminal buses and the joined aggregated point.

*The advantage is its simplicity. In dynamic behavior, it shows a sufficient accuracy.*

## 4.2.2 Slow coherency aggregation

The classical slow coherency aggregation [15, 30-33] is based upon an impedance modification to the inertial aggregation.

This slow aggregation starts with a linearization at the generator terminal buses. Then, the fast inter-machine variables, defined by the singular perturbations theory, are eliminated, and a power network is reconstructed from the reduced linearized model.

A schematic illustration of the slow coherency aggregation is shown in the following figure.

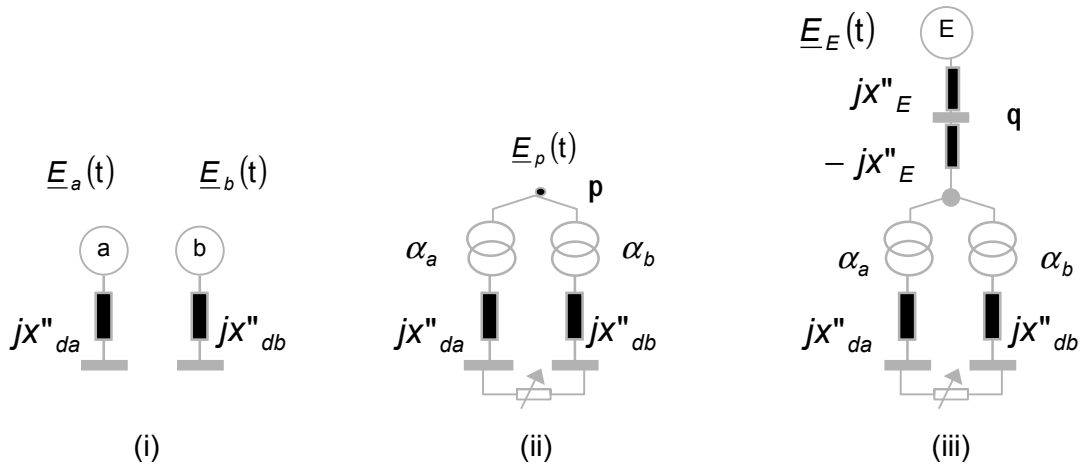


Fig.4.2.- Slow coherency aggregation

### Linearized model of the slow and fast subsystem

The slow coherency aggregation is characterized by the linearizing about the generator buses and internal nodes. These linearized swing equations for the generators at the operating power flow equilibrium:

$$E_i = E_{i0}, \quad \delta_i = \delta_{i0}, \quad U_i = U_{i0}, \quad \theta_i = \theta_{i0} \quad i = a, b \quad (4.11)$$

are

$$2M_i \Delta \ddot{\delta}_i = -\frac{E_{i0} U_{i0} \cos(\delta_{i0} - \theta_{i0})}{x_{di}} \Delta \delta_i - \frac{E_{i0} \sin(\delta_{i0} - \theta_{i0})}{x_{di}} \Delta U_i + \frac{E_{i0} U_{i0} \cos(\delta_{i0} - \theta_{i0})}{x_{di}} \Delta \theta_i \quad (4.12)$$

$$\Delta \bar{I}_i = -\frac{\bar{E}_{i0}}{x_{di}} \Delta \delta_i + \frac{e^{j\theta_{i0}}}{jx_{di}} \Delta U_i + \frac{\bar{U}_{i0}}{x_{di}} \Delta \theta_i \quad i = a, b \quad (4.13)$$

where

- $\Delta \delta_a$  and  $\Delta \delta_b$  are the incremental variables for  $\delta_a$  and  $\delta_b$ .
- $\Delta I_a$  and  $\Delta I_b$  the incremental for  $I_a$  and  $I_b$ .
- $U_a, U_b$  are the bus voltage magnitude to bus a and b.
- $\theta_a$  and  $\theta_b$  are the bus voltage angle a and b.
- $E_a, E_b$  are the individual generator internal voltage of generator a and b.
- $M_i$  is the inertia constant of the  $i$ th generator.

Defining the state variable vector  $\mathbf{x}$ , the algebraic variable vector  $\mathbf{z}$  and the current injection variable  $\Delta \bar{I}$  as phasor form with:

$$\mathbf{x} = \begin{bmatrix} \Delta \delta_a \\ \Delta \delta_b \end{bmatrix} \quad \mathbf{z} = \begin{bmatrix} \Delta V_a \\ \Delta V_b \\ \Delta \theta_a \\ \Delta \theta_b \end{bmatrix} \quad \Delta \bar{I} = \begin{bmatrix} \Delta \bar{I}_a \\ \Delta \bar{I}_b \end{bmatrix} \quad (4.14)$$

the matrix form of the state system can be obtained as:

$$\dot{\mathbf{x}} = K_1 \mathbf{x} + K_2 \mathbf{z} \quad (4.15a)$$

$$\Delta \bar{I} = K_3 \mathbf{x} + K_4 \mathbf{z} \quad (4.15b)$$

Another important step in slow aggregation is the transforming to slow and fast variables. In this case, when the machines form a slow coherent group, their center of angle is considered as the slow variable and the inter-machine oscillations as the fast variables.

In order to perform the slow aggregation, the original machine angles have to be transformed to these new slow and fast variables. These transformation and aggregation can be realized on a per coherent area, sequentially in any order of the coherent areas.

The slow aggregate variable  $\delta_s$  and the fast local variable  $\delta_f$  are defined as:

$$\delta_s = \frac{T_{ma} \delta_a + T_{mb} \delta_b}{T_{ma} + T_{mb}} \quad (4.16)$$

$$\delta_f = \delta_b - \delta_a \quad (4.17)$$

Applying the transformation (4.16) and (4.17) to the linearized model (4.15), in matrix form the linearized system in two time-scales can be obtained:

$$\begin{bmatrix} \ddot{\Delta \delta_s} \\ \ddot{\Delta \delta_f} \end{bmatrix} = \begin{bmatrix} K_{11} & K_{12} \\ K_{13} & K_{14} \end{bmatrix} \begin{bmatrix} \Delta \delta_s \\ \Delta \delta_f \end{bmatrix} + \begin{bmatrix} K_{21} \\ K_{22} \end{bmatrix} \mathbf{z} \quad (4.18)$$

$$\Delta \bar{I} = \begin{bmatrix} K_{31} & K_{32} \end{bmatrix} \begin{bmatrix} \Delta \delta_s \\ \Delta \delta_f \end{bmatrix} + K_4 \mathbf{z} \quad (4.19)$$

Assuming that the fast dynamics in  $\Delta \delta_f$  have decayed, i.e.  $\ddot{\Delta \delta_f} = 0$ , the quasi-steady of  $\Delta \delta_f$  is:

$$\Delta\delta_f = -K_{14}^{-1} (K_{13} \Delta\delta_s + K_{22} \mathbf{z}) \quad (4.20)$$

Eliminating  $\Delta\delta_f$  from other variables, the following expressions can be obtained:

$$\Delta\ddot{\delta}_s = K_{1s} \Delta\delta_s + K_{2s} \mathbf{z} \quad (4.21)$$

$$\Delta\dot{\mathbf{i}} = K_{3s} \Delta\delta_s + K_{4s} \mathbf{z} \quad (4.22)$$

Hereby

$$K_{1s} = K_{11} - K_{12} K_{14}^{-1} K_{13} \quad K_{2s} = K_{21} - K_{12} K_{14}^{-1} K_{22} \quad (4.23)$$

$$K_{3s} = K_{31} - K_{32} K_{14}^{-1} K_{13} \quad K_{4s} = K_{41} - K_{32} K_{14}^{-1} K_{22} \quad (4.24)$$

System (4.21) represents the linearized model of the slow subsystem. A power network must be reconstructed whose linearization would yield (4.21).

The **machine equivalent** parameters are defined as follows:

- The terms  $K_{1s}$ ,  $K_{2s}$  and  $K_{3s}$  are needed to construct lines connecting bus 'p' to the original generator terminal buses 'a' and 'b', and the term  $K_{4s}$  is needed for the lines interconnecting buses 'a' and 'b' according to Fig. 4.2 ii.
- In addition, the reconstruction from  $K_{4s}$  will not satisfy the network flow condition. Therefore, after the line reconstruction for buses 'a' and 'b' is completed, the balance of the power flow by adding loads to these buses has to be realized.
- The creation of bus 'q' and adjusting generation on buses 'a', 'b' and 'q' are similar to the procedure on inertial aggregation, as can be seen in Fig. 4.2 iii.

*This analytical aggregation approach is suitable to be used, when linearized modes only are considered.*

### 4.2.3 Power invariance aggregation

This method is based on the concept of the power invariance [35] at the generator internal buses and at the terminal buses, in which the generators of a coherent group are connected.

Since a generator is represented by a voltage source behind transient reactance in series with its transient reactance and connected to the terminal bus, *a fictitious point can be assumed in between the internal voltage source and the transient reactance* (see Fig. 4.3).

Following aspects to the **machine equivalent** are important:

- For a group containing  $NG$  generators (see Fig. 4.3 i), *fictitious points are connected together such that it connects all the internal voltage sources of that group and one end of the transient reactances in a common point*, as it can be shown in Fig. 4.3 ii.
- The paralleled internal voltage sources of the group are now replaced by an equivalent voltage source considering in terms of the generator current injection into corresponding buses, which may be observed in Fig. 4.3 iii:

$$E_E = \left( \frac{\sum_{i=1}^{NG} E_i^* I_i}{\sum_{i=1}^{NG} I_i} \right)^* \quad i = a, \dots, NG \quad (4.25)$$

- It will be capable of supplying the active and reactive power equal to the sum of the active and reactive powers delivered by all the generators of the group.
- This changing structure can be showed schematically as follows:

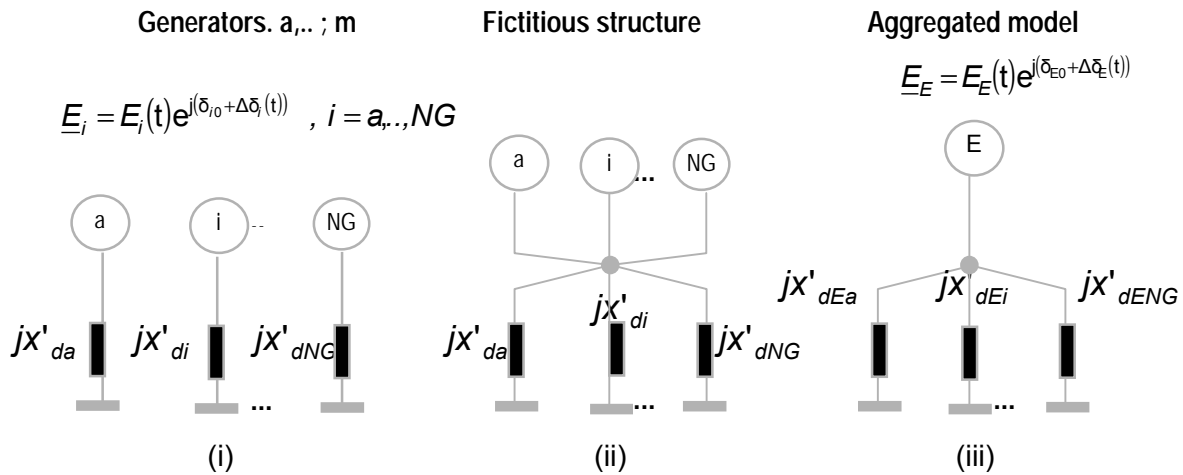


**Fig. 4.3.-** Power invariance aggregation

Aspects to the **machine parameters** are summarized as follows:

- The transient reactance of the individual machine of coherent group is modified to retain the original power division from the equivalent voltage source to the points of the connection in the network as:

$$X'_{dEi} = \left( \frac{E_E - U_i}{E_i - U_i} \right) X'_{di} \quad i = a, \dots, NG \quad (4.26)$$

where,  $X'_{dEi}$  is the transient reactance connecting the equivalent generator to the  $i$ th bus.

- After modifying the reactances of all the coherent generators, all the load buses and the generator terminal buses are eliminated retaining only the generator internal buses.
- The loads are converted to constant admittance to ground.
- Thus, the reduced order system admittance matrix obtained from the bus admittance is used in the dynamic equation for transient stability analysis.
- The inertia constant, damping coefficient, electrical and mechanical power of the equivalent machine are obtained respectively as:

$$M_E = \sum_{i=1}^{NG} M_i \quad ; \quad D_E = \sum_{i=1}^{NG} D_i \quad ; \quad P_{mE} = \sum_{i=1}^{NG} P_{mi} \quad (4.27)$$

- This method is suitable in case of equivalent generator representation and in network reduction retaining the terminal bus of each of the coherent generators. Hence, it preserves the basic structure of the original system.

#### 4.2.4 Berg and Ghafurian's aggregation

In this method an equivalent generator can replace the coherent group of generators and the following mathematical steps modify the network [36, 37]:

$$E_E = \left( \frac{X'_{dNG}}{X'_{dNG-1}} + \underline{\alpha}^* \underline{\alpha} \right)^{-1} \left( \frac{X'_{dNG}}{X'_{dNG-1}} E_{NG-1} + \underline{\alpha}^* E_{NG} \right) \quad (4.28)$$

$$X'_{dE} = X'_{dNG} \left( \frac{X'_{dNG}}{X'_{dNG-1}} + \underline{\alpha}^* \underline{\alpha} \right)^{-1} \quad (4.29)$$

where  $NG$ th and  $(NG-1)$ th generators are coherent,

$$\frac{E_{NG}}{E_{NG-1}} = \underline{\alpha} \quad \alpha \text{ is a complex constant.} \quad (4.30)$$

A coherent group of *NG* generators can be reduced to an equivalent generator *by a sequential procedure of elimination of one generator at a time*. The inertia, damping and mechanical power of the equivalent are obtained in terms of the power invariance equations.

### 4.3 Splitting-based aggregation approach

According to the classical aggregation, external generators [17, 18] can be replaced by means of an equivalent generator using the concept of ‘direct assignment’ (see Fig. 4.4.a).

The proposed approach presents an innovative concept based *on the splitting of the complete number of external generators into fictive shares in terms of virtual generators*.

*The impact of power generation of the generators on the dynamic behavior of power systems is splitted into significant parts*, which represent the influences of the original generators on the dynamic equivalents according to a ‘share assignment’ or effect degree, as shown in Fig. 4.4.b. In this context, following aspects are important:

- Completely, all external generators will be considered in the calculation of the aggregated electrical splitting based-parameters shown in Fig. 4.4.b.
- *Instead of the classical coherency identification and grouping, by means of this share assignment, new methods of consistent dynamic equivalencing can be explored satisfactory according to mathematical approaches and reduction techniques.*
- Of course, this splitting based-aggregation provides a new viewpoint and theoretical founding in dynamic equivalencing.

This procedure implies the reformulation of the classical aggregation criterion.

#### 4.3.1 Conditions

Fig. 4.4 illustrates schematically important aspects and the differences between the classical aggregation and the proposed splitting technique:

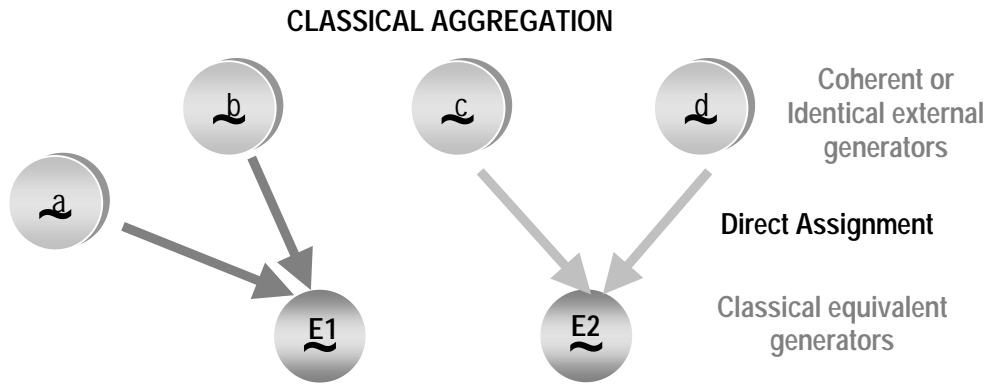


**Fig. 4.4.a.-** Classical aggregation

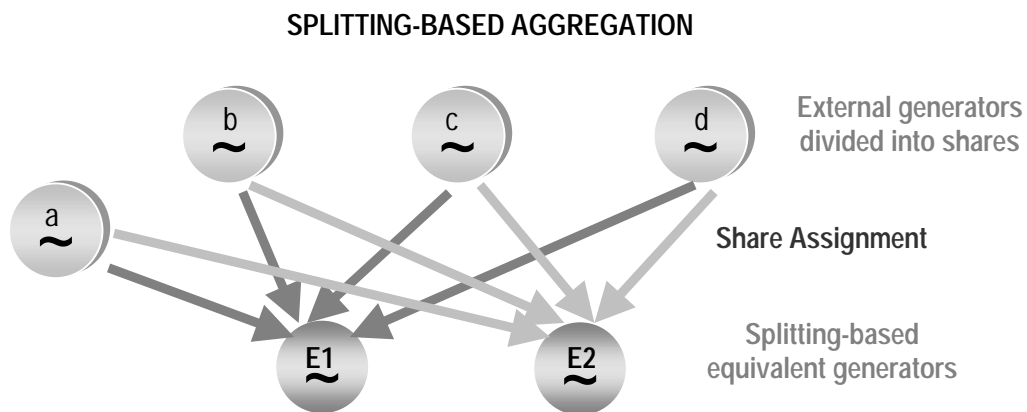


**Fig. 4.4.b.-** Proposed splitting based-aggregation

**Remarks to Fig. 4.4:**

- Fig. 4.4.a shows schematically the necessary condition for forming classical aggregated dynamic equivalents. This consists of forming of similar generator grouping of the external area to generate equivalents in terms of a direct assignment.
- As can be seen in Fig. 4.4.b, all external generators have a participation assignment to form equivalent aggregated generators. The participation assignment is evaluated by means of a splitting power factor.

This novel splitting method is simulated in the following two-machine power system, as given in Fig. 4.5. Here an external machine in Fig 4.5 i, can be divided fictively considering the participation assignment to form virtual generators, as shown in Fig.4.5 ii. On the basis of these virtual generators, the equivalents can be calculated, as can be seen in Fig.4.5 iii:

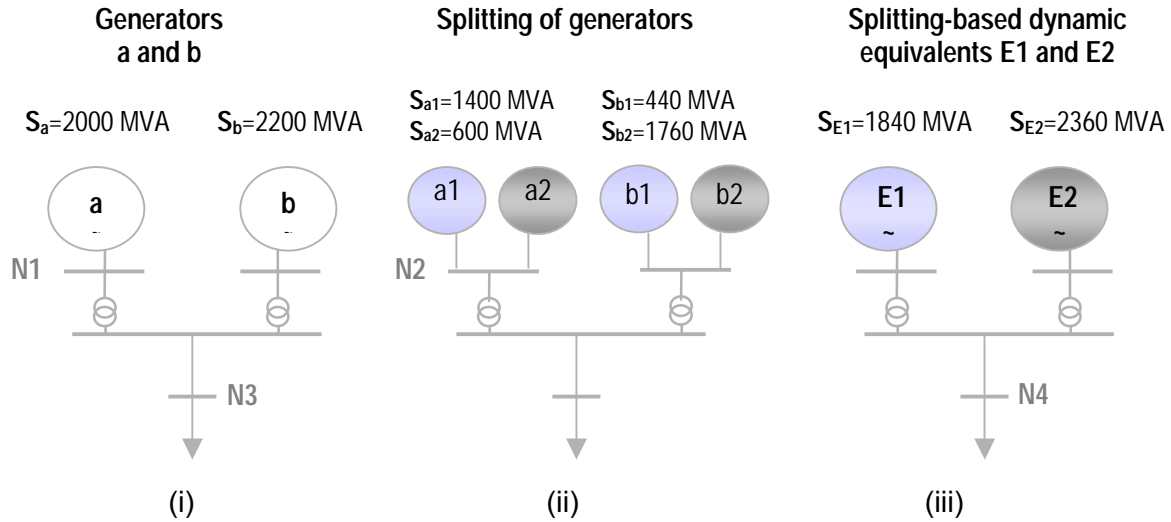


**Fig. 4.5.-** Machine-splitting with reference to their nominal power according to the derived splitting factors  $a_1$  and  $a_2$ .

Following aspects can be detected on basis of Fig. 4.5:

- The generator 'a' is splitted into 70% and 30% of its rated power and generator 'b' into 80% and 20%. Under following conditions, the splitting can be defined.
- A necessary condition is the invariance of the dynamic behavior: i.e. after a disturbance, the dynamic generator output in node **N1** must be similar to the behavior in node **N2** considering the splitting factors.
- After the splitting of the external generators, the corresponding shares, for example parts **1** of generators 'a' and 'b', have to be aggregated to generate the equivalent generator 'E1' and the **2** shares of 'a' and 'b' to 'E2' as well.
- Another essential condition is that the dynamic behavior at the original node **N3** must be relatively equal to the behavior at aggregated node **N4**.
- Considering the above aspects, the splitting-based electromechanical parameters of the equivalent generator can be determined.

### 4.3.2 Aggregated electrical parameters

These generator parameters can be derived on the basis of the proposed splitting approach that the aggregated equivalent should have the same behavior of all the external generators in the whole time period. This aggregation is more appropriate to be performed at the internal nodes and not at the generator terminal buses. The proposed splitting approach is shown schematically in Fig.4.6 as follows:

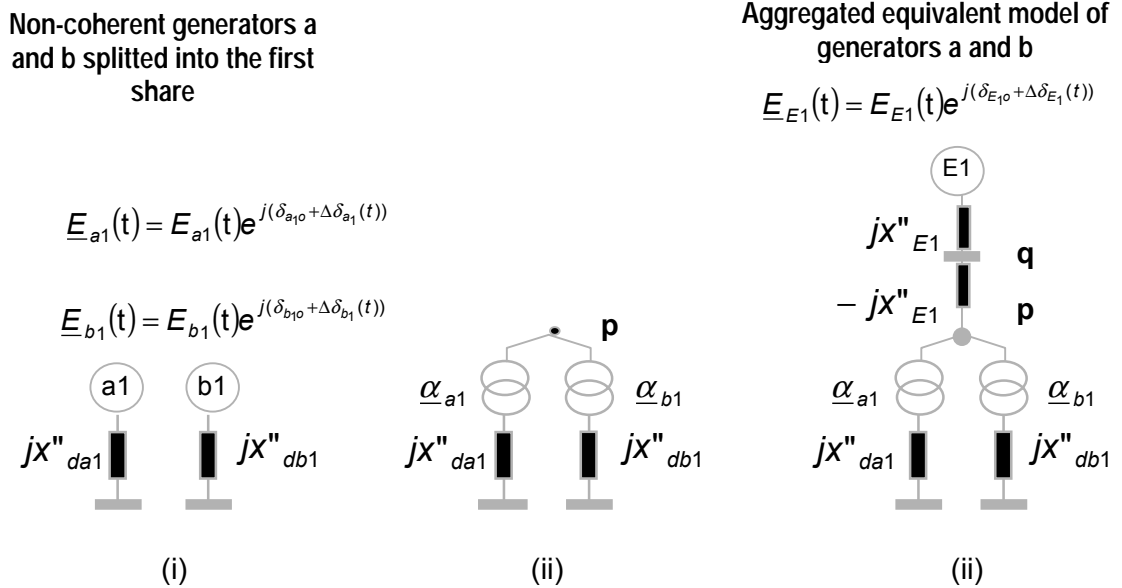


Fig. 4.6.- Splitting-based aggregation

The machine equivalent can be generated as follows:

- From the splitted bus injection  $P_{i,j} + jQ_{i,j}$  ( $i$ =number of external machines,  $j$ =number of splitting factors or equivalents) and the generator current injection, the corresponding internal voltage  $\underline{E}_{i,j}$  of the splitted generators can be computed, as shown in Fig. 4.6 i.
- The internal nodes of the individual non-coherent external virtual generators in Fig. 4.5 ii, i.e. generators 'a1' and 'b1' are connected to a common bus with appropriate pseudo transformers and phase shifters to preserve the power flow relationships (see Fig. 4.6 ii).
- Defining the ratio of the pseudo transformers from the internal voltages  $\underline{E}_{a1}$ ,  $\underline{E}_{b1}$  ( $\underline{E}_{i,j}$ ) of the virtual splitted generators and the common bus voltage  $\underline{E}_{E1}$  (see Fig. 4.6 iii).  $\underline{E}_{E1}$  is defined as the aggregated driving voltage of the equivalent generator 'E1'. The circuit must be implemented with the negative subtransient reactance of the equivalent generator to create a single generator internal node and new terminal bus  $\underline{E}_q$ .
- The pseudo transformers are needed for transforming the different driving voltages of the virtual generators to an uniform one.
- The subtransient reactances combined with the transformers, allow the elimination of the internal nodes of the original fictive generator in terms of the static network reduction.
- The nominal voltage of the internal node and of the connected equivalent generator must be defined properly. However, it can affect the transformer ratio.
- Equivalent generators must supply the sum of the splitted active and reactive power.

- The subtransient reactance  $jx'_d$  is used instead of the transient reactance  $jx_d$  because it is the small possible reactance that the machine can take within a disturbance.

Taking into consideration the splitting factors in this procedure, the following matrix can be represented. It can be used to calculate the machine parameters.

$$\begin{array}{c}
 \text{Number of external generators } j=1\dots N \\
 \left. \begin{array}{c}
 \mathbf{A} = \begin{bmatrix}
 a_{1,1} & a_{1,2} & \dots & a_{1,N} \\
 a_{2,1} & a_{2,2} & \dots & a_{2,N} \\
 \dots & & & \\
 a_{M,1} & a_{M,2} & \dots & a_{M,N}
 \end{bmatrix} \\
 \end{array} \right\} \begin{array}{l}
 \text{Number of dynamic} \\
 \text{equivalents } i=1\dots M
 \end{array} \quad (4.31)
 \end{array}$$

**Machine parameters** can be determined as follows:

- The voltage of the common bus 'p' is calculated using a splitting-based nominal power as weighted average of the individual virtual generator internal voltage.
- The common driving voltage can be calculated using the splitting internal voltages:

$$\underline{E}_{E_i}(0) = \frac{\sum_j^N S_j a_{i,j} \underline{E}_j(0)}{\sum_j^N S_j a_{i,j}} \quad i=1\dots M \quad (4.32)$$

and the nominal power, active and reactive power by

$$S_{E_i} = \sum_j^N S_j a_{i,j} \quad P_{E_i} = \sum_j^N P_j a_{i,j} \quad Q_{E_i} = \sum_j^N Q_j a_{i,j} \quad i=1\dots M \quad (4.33)$$

where

- $\underline{E}_j(0)$  is initial driving voltage of external fictive generator  $j$  in p.u.,
  - $S_j$  is the rated unit power and
  - $a_{i,j}$  the participation share or splitting factor of external generator  $j$  according to the number of generated equivalents  $i$ .
- Pseudo transformation ratios from the internal voltages of the virtual generators to the common bus voltage  $\underline{E}_{E_i}$  are defined by:

$$\frac{\underline{E}_{E_i}(t)}{\underline{E}_{i,j}(t)} = \frac{E_{E_i}(t)e^{j\delta_{E_i,0}}}{E_{i,j}(t)e^{j\delta_{i,j,0}}} e^{j(\Delta\delta_{E_i}(t) - \Delta\delta_{i,j}(t))} \quad i=1..M; j=1..N \quad (4.34)$$

- Though there are pseudo transformers, pseudo transmission lines and transient reactances, the power flow relationships result of Fig.4.6 iii remains the same as which in Fig.4.6 i.
- Considering the splitting factors of (4.31), the parameters of the equivalent generator can be calculated from the mean values of the splitted generator inductances and resistances as reciprocal values:

$$r_{E_i} = \frac{\sum_j^N S_j a_{i,j}}{\sum_j^N \frac{1}{r_j} S_j a_{i,j}} \quad x_{E_i} = \frac{\sum_j^N S_j a_{i,j}}{\sum_j^N \frac{1}{x_j} S_j a_{i,j}} \quad i=1..M \quad (4.35)$$

Where the relationship in (4.35) means that the splitting-based parameters are connected in parallel. The time constants can be calculated based on these parameters.

- Thus, the resulting inertial constant of the equivalent generator is given by:

$$T_{mE_i} = \frac{\sum_j^N T_{mj} S_j a_{i,j}}{\sum_j^N S_j a_{i,j}} \quad i=1..M \quad (4.36)$$

- In order to create an internal node 'E' for the equivalent generator, bus 'p' should be extended to an additional bus 'q' with the impedance  $-jx''_{dE_i}$ , and then to the bus 'E' with impedance  $jx''_{dE_i}$ . Therefore, the bus 'E' has the same voltage as bus 'p' according to Fig. 4.6 iii.
- Bus 'q' can be considered as the terminal bus and bus 'E' as the internal bus of the equivalent.
- Consequently, the voltage at bus 'q' is set by  $\underline{E}_{p_i}(t)$  and it is connected to the individual buses a and b. Therefore, the voltage of the equivalent can be calculated starting from the internal voltage, which is given in (4.32) as:

$$\underline{E}_{E_i}(t) = E_{E_i}(t) e^{j(\delta_{E_i,0} + \Delta\delta_{E_i}(t))} \quad i=1..M \quad (4.37)$$

- Because the individual buses a and b are no longer generator terminal buses and the system size is already reduced, it is possible to eliminate these buses, nodes, and transmission lines by the classical static network reduction. It is suitable to couple this step with the factorization of the admittance matrix.

### 4.3.3 Splitting factors of generators

The aggregated parameters in equations (4.32-4.36) imply that non-linear reduction techniques may be applied to generate accurate and representative equivalent generators.

This aspect can be realized by mathematical approaches, such as Fuzzy theory or the principal component analysis.

#### i. Fuzzy clustering

The splitting or virtual division of machines using the splitting factors can be described by means of their Fuzzy membership degrees. Hereby, the similarity of one generator to the other generators can be expressed quantitatively by partitioning the generator using the membership degree.

#### Remarks:

- This algorithm extends the identity analysis to an optimization problem [102-105]. *With Fuzzy clustering, each generator belongs to all classification cluster groups simultaneously. However, it has different degrees according to its identity with other generators.*
- Fuzzy logic is a generalization of yes and-no Boolean logic. Assigning 0 to false values and 1 to true ones. *Fuzzy logic also allows in-between values.* Assuming that  $\mu$  is asset of values of *member degrees*, Fuzzy logic defines a mapping from  $\mu$  to the unit interval through a membership function.
- This *Fuzzy similarity should be understood as mathematical similarity*, measured in some well-defined sense, for example by using a distance norm.
- The Fuzzy clustering is based on the within groups sum of squared errors objective function  $J_m$ . The set of solutions that satisfy the minimum  $J_m$  is simplified by the weighting factor  $\mu_{ij}$ , as can be seen in the following equation:

$$J_m(X, U, C) = \sum_{j=1}^N \sum_{i=1}^M \mu_{i,j}^m d_{i,j}^2 = \sum_{j=1}^N \sum_{i=1}^M \mu_{i,j}^m \|x_j - c_i\|^2 \rightarrow \min \quad (4.38)$$

where

- $N$  corresponds to the number of external generators,
  - $M$  the number of cluster groups representing the dynamic equivalents and
  - $d_{i,j}$  is the distance between the machine and the reference generators.
  - $\mu_{i,j}$  denotes the membership degree of generator  $x_j$  to cluster group  $c_i$ .
  - $m > 1$  is the fuzziness index and influences the “fuzziness” of the obtained partition.
- This Fuzzy clustering is subjected by the following constraints [105]:

$$\forall 1 < i \leq M: \sum_{j=1}^N \mu_{i,j} > 0 \quad (4.39)$$

$$\forall 1 < j \leq N: \sum_{i=1}^M \mu_{i,j} = 1 \quad (4.40)$$

- Because of the optimal nature of the problem (4.38), methods of calculus of variations are used to derive the necessary conditions, such as the membership degree condition:

$$\mu_{i,j} = \frac{1}{\sum_{r=1}^M \left( \frac{d_{i,j}^2}{d_{i,r}^2} \right)^{\frac{1}{m-1}}} = \left( \sum_{r=1}^M \left( \frac{d_{i,j}^2}{d_{i,r}^2} \right)^{\frac{2}{m-1}} \right)^{-1} \quad i=1..M; j=1..N \quad (4.41)$$

- For the initial values of the membership degree can be derived the following formulation:

$$\mu_{i,j} = \frac{d_{i,j}^{-1}}{\sum_{i=1}^M d_{i,j}^{-1}} \quad (4.42)$$

- According with the solution for local extreme, the cluster centers as reference generators can be reached as other important condition:

$$c_i = \frac{\sum_{j=1}^N \mu_{i,j}^m x_j}{\sum_{j=1}^N \mu_{i,j}^m} \quad 1 \leq i \leq M \quad (4.43)$$

- Conditions (4.41) and (4.43) are first-order necessary conditions for local extreme of  $J_m$ . All procedures used to solve (4.38) should satisfy both (4.41) and (4.43). These conditions are derived in appendix B.3.

*The relevant result of Fuzzy clustering are the membership coefficients expressing the identity degree that a machine is similar to other generators with identical properties belonging to a cluster, i.e. the membership factor expresses the weakness or strength of the assignment of the generators to all groups with identical properties in time domain. This aspect will be applied to the virtual splitting of generators, which belong to all clusters simultaneously but with different ‘weakness or strength degree’.*

## ii. Principal component analysis

The principal component analysis, known as eigenvalue analysis, is a *mathematical way of determining that linear transformation of a sample of time behaviors in N dimensional space along the coordinate axes, whose sample variances are extremes and uncorrelated.*

According to the proposed generator aggregation, no significant and redundant generator behaviors can be neglected. The property of transforming the coordinates along the principal axes into physical meaningful parameters can be reached by this approach.

*The PCA is applied to the time behavior matrix of external generators by projection onto a smaller number of orthonormal axes. This leads to a coordinate system with the axes of largest spread. The property of the PCA is that the original features of the generators described by the time behavior will be transformed into new meaningful ones. These significant generator features represent the whole original system, which is reduced neglecting its redundancy.*

### Remarks:

- According to the machine matrix (3.28), the covariance matrix of the same data set is <sup>14</sup>:

$$\mathbf{C}_x = E\{(\mathbf{X} - \bar{\mathbf{X}})(\mathbf{X} - \bar{\mathbf{X}})^T\} \quad (4.44)$$

<sup>14</sup> The mean of that population is denoted by  $\bar{\mathbf{X}} = E\{\mathbf{X}\}$

- The covariance matrix of  $\mathbf{C}_x$ , denoted by  $c_{ij}$ , represents the covariances between components  $x_i$  and  $x_j$ . These generator behaviors should span the same subspace as the original vectors of original generators; however they are now characterized by a set of eigenvalues and eigenvectors.
- Consequently, from the symmetric matrix such as the covariance matrix, an orthogonal basis by findings its eigenvalues  $\lambda_i$  and eigenvector  $\mathbf{e}_i$  can be calculated by:

$$\mathbf{C}_x \mathbf{e}_i = \lambda_i \mathbf{e}_i \quad i=1 \dots N \quad (4.45)$$

- These values can be found by finding the solutions of the characteristic equation

$$|\mathbf{C}_x - \lambda \mathbf{I}| = 0 \quad (4.46)$$

- If  $\mathbf{T}$  is a  $N \times N$  matrix including the eigenvectors of the covariance matrix  $\mathbf{C}$ , the diagonal variance matrix  $\mathbf{\Sigma}^2$  is given by:

$$\mathbf{\Sigma}^2 = \mathbf{T}^T \cdot \mathbf{C} \cdot \mathbf{T} \quad (4.47)$$

- The eigenvalues  $\lambda_i$  of the covariance matrix  $\mathbf{C}$  are equal to the elements of the variance matrix  $\mathbf{\Sigma}^2$ , which includes the variances  $\sigma^2_i$ .
- By ordering the eigenvectors in the order of descending eigenvalues  $\lambda_1 \geq \lambda_2 \geq \dots \geq \lambda_N$ , one can create an orthogonal basis with the first eigenvector having the direction of largest variance of the data set of generators. In this way, directions can be found, in which the data set has the most significant amounts of energy.
- *The time behavior of generators represented as multi space matrix could be well reduced by approximation with a reduced dimensional representation concentrated along particular and significant eigenvectors.*
- In comparison to  $\mathbf{T}$  as  $N$  dimensional matrix,  $\mathbf{T}_q$  is a  $N \times q$  matrix including  $q$  significant eigenvectors of  $\mathbf{C}$  corresponding to the  $q$  largest eigenvalues of  $\mathbf{C}$ . The value of  $q$  determines the size of the new dimension and is smaller than  $N$ .
- Let  $\mathbf{T}_q$  be a matrix consisting of eigenvectors of the covariance matrix as the row vectors. By transforming a data vector  $\mathbf{X}$ , the orthogonal space representation as reduced generator time behavior can be obtained as:

$$\mathbf{Y}_q = \mathbf{T}_q (\mathbf{X} - \bar{\mathbf{X}}) \quad (4.48)$$

which is a reduced generator data matrix in the orthogonal coordinate system defined by the eigenvectors <sup>15</sup>.

Splitting of the oscillating curves of the external generators in orthogonal part oscillating can be obtained *according to the eigenvectors as splitting factors, which provide the share of the principal components in the complete oscillating.*

## 4.4 Case study

The accuracy of the proposed splitting-based dynamic equivalencing are evaluated in a 16 multi-machine system. This power system is described in chapter section 3.5.1. Thus, the order of the dynamic model of the test system is relatively high. The following illustration shows the topology of the 16 multi-machine system.

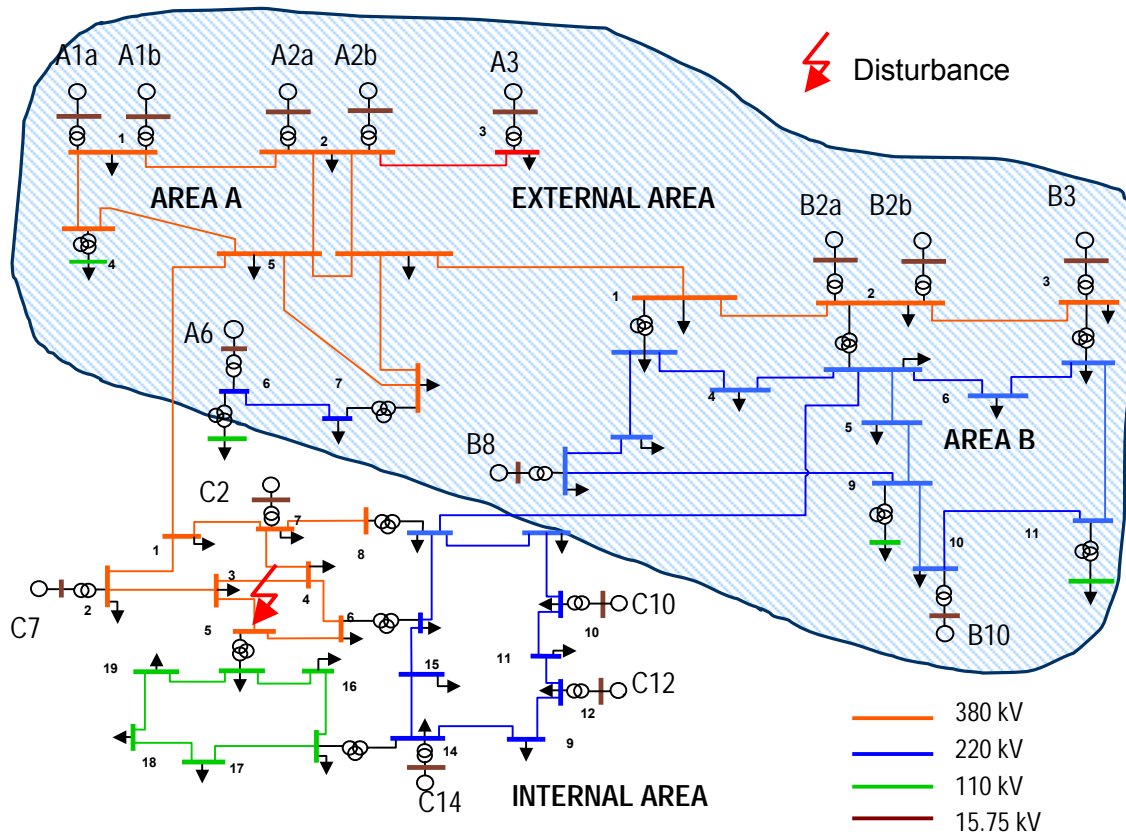


Fig. 4.7.- Interconnected 16 Multi-machine System.

<sup>15</sup> Components of  $Y_q$  can be seen as coordinates in the orthogonal base and vectors of the reduced behavior matrix of the external generators.

This power system was divided into two areas, where the area C as internal area, will be preserved in the original form. This area consists of 5 machines. The rest 11 machines located outside this area, as external area, will be replaced by dynamic equivalents. For the simulation following aspects are relevant:

- Following disturbances, the dynamic performance of the internal area will be simulated in two steps: First, the original whole external area is simulated. Then, based on the aggregated equivalent external area, new simulation will also be preceded.
- This external area will be aggregated based on both the splitting based aggregation and classic aggregation approach. Thus, the comparison between these two approaches can be realized.

## 4.5 Simulation results and discussion

After simulating the whole power system and aggregating the external area with the abovementioned configuration, the dynamic performance of the internal area is studied. Firstly, a power flow calculation is carried out to define the initial operating condition of the power system.

The accuracy of the splitting-aggregated equivalents can be evaluated by comparing the oscillating swing curves of the internal area machines with the original power system. The simulation is realized using PSD. For more details on the validity of PSD see section 2.3.

A representative scenario was simulated, where the fault is located at the node 5 of internal area C with duration of 100 ms as shown in Fig. 4.7. This disturbance begins at 1.0 second and it has great impact on the whole system. It is simulated for 10 seconds.

In Fig. 4.8 and Fig. 4.9, the time domain behavior of an internal machine in area C is illustrated on the abovementioned conditions. In Fig. 4.8, 3 dynamic equivalent generators of the external area are employed using the classical inertial aggregation and the enhanced electromechanical identity recognition with K-means as grouping technique. The oscillating swing curves of the internal machines are then compared with the original power system behavior.

It can be seen in the following figure, that the phase and amplitude for all generators in the internal area using the classical inertial aggregation are relatively accurate.

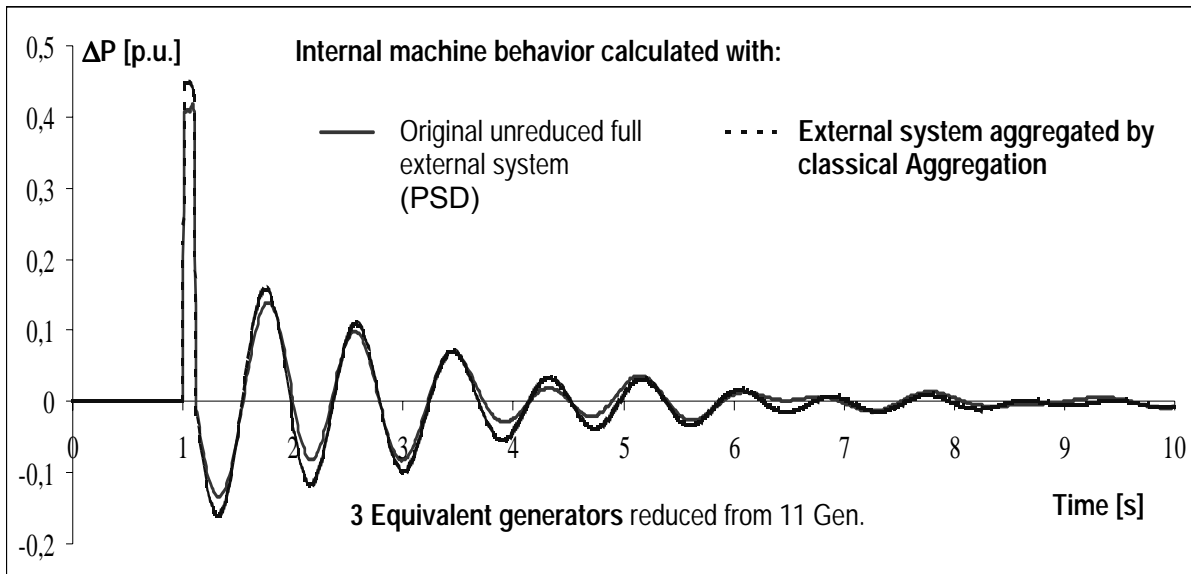


**Fig. 4.8.-** Comparison of time responses of an internal machine calculated with the original external system and with 3 equivalent machines using the classical aggregation.

In comparison to the behavior in Fig. 4.8, the time domain behavior of the same internal machine using the proposed splitting aggregation approach in the external area is presented in the following figure:

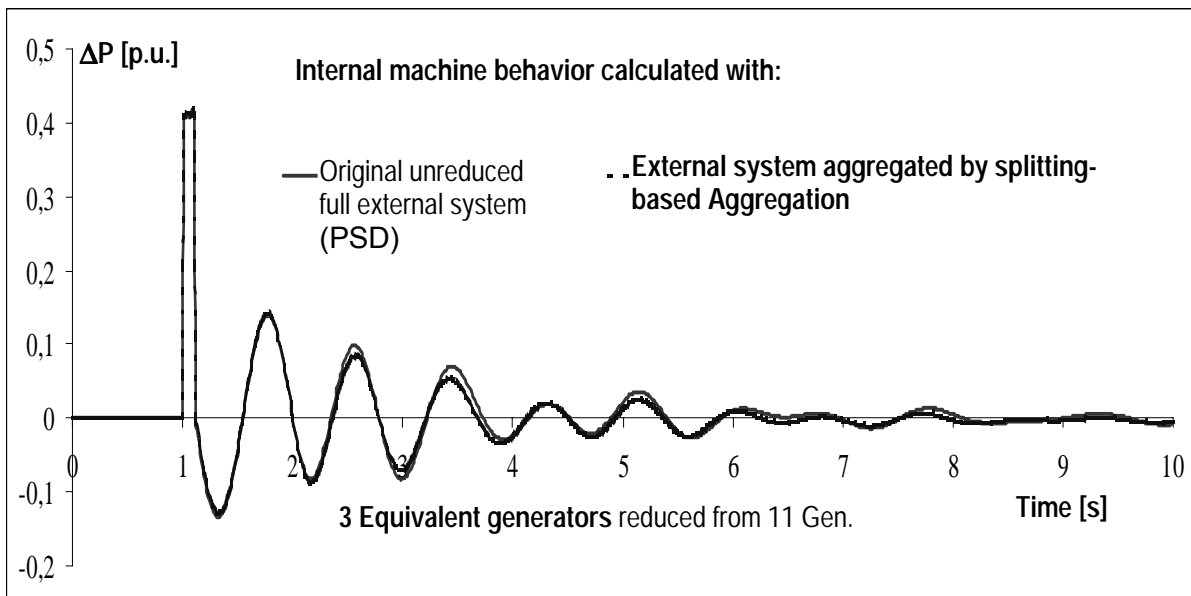


**Fig. 4.9.-** Comparison of time responses of an internal machine calculated with the original external system and with 3 equivalent machines using the splitting based-aggregation.

The oscillating swing curves of an internal machine are calculated with 3 dynamic equivalent machines, whose aggregation is based upon the splitting approach with Fuzzy membership degrees according to expression (4.41) as splitting factors. Following aspects in Fig. 4.9 can be detected:

- Hereby, the performance of the internal machines is accurate during the whole simulation, i.e. before and after the disturbance. These simulation results are much better than the results calculated by the classical inertial aggregation (see Fig. 4.8). Although only the simulation result of one internal machine is presented, the results of other internal machines in same manner are also accurate.
- Moreover, the behavior of all internal machines shows a notable accuracy and agreement with different number of dynamic equivalents aggregated using the splitting-based aggregation.

The time domain simulation results during the first 3 seconds of Fig. 4.8 and Fig. 4.9 are given in detail in Fig. 4.10.

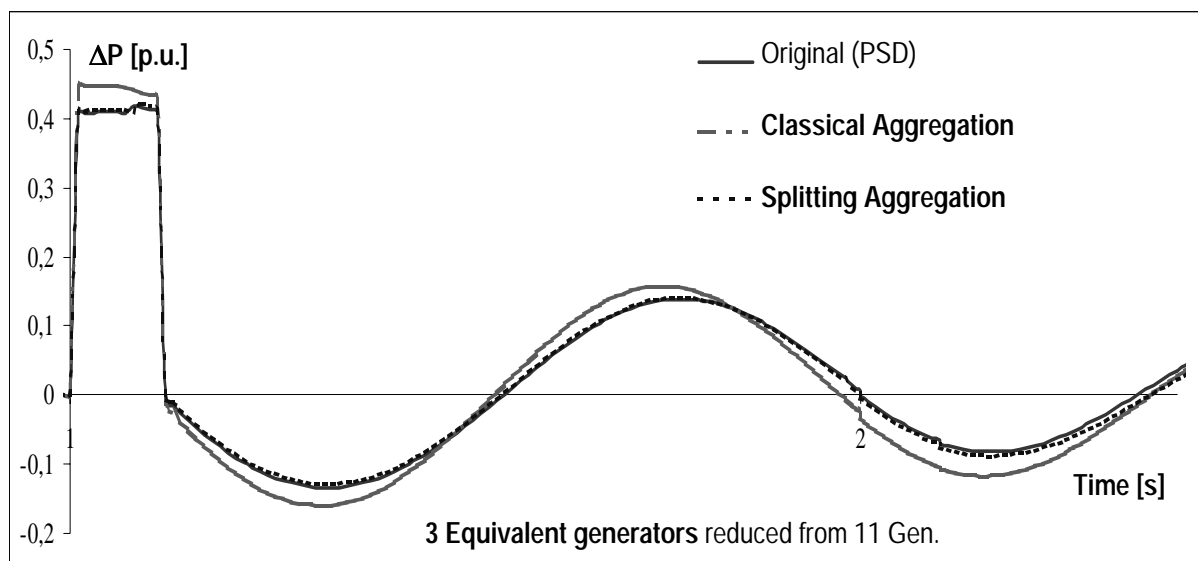


**Fig. 4.10.-** Comparison of time domain behavior of an internal machine calculated with the original external system and with 3 equivalent machines using the splitting based-aggregation.

In Fig. 4.10, it can be detected an enhanced agreement of the power oscillating curve applying the splitting aggregation both within the damping zone and during the disturbance.

The splitting equivalents are valid for disturbances too, which are electrically and geographically independent of the equivalent disturbance and too of the extent of severity (fault duration) and of the load generation balance prior the occurrence of the faults.

This equivalencing robustness can be demonstrated in the following figure, where the behavior of any internal machine using the splitting aggregation following a sequence of faults (The first fault after 1 sec. and the second fault after 2 sec. with a duration of 150 ms. and 200 ms., respectively) is simulated.

These faults are applied to node 3 (380kv area) and node 9 (220kv area) in area C, respectively, i.e., these disturbances are electrically and geographically closest and far away from the equivalent disturbance, with which the equivalents are derived.

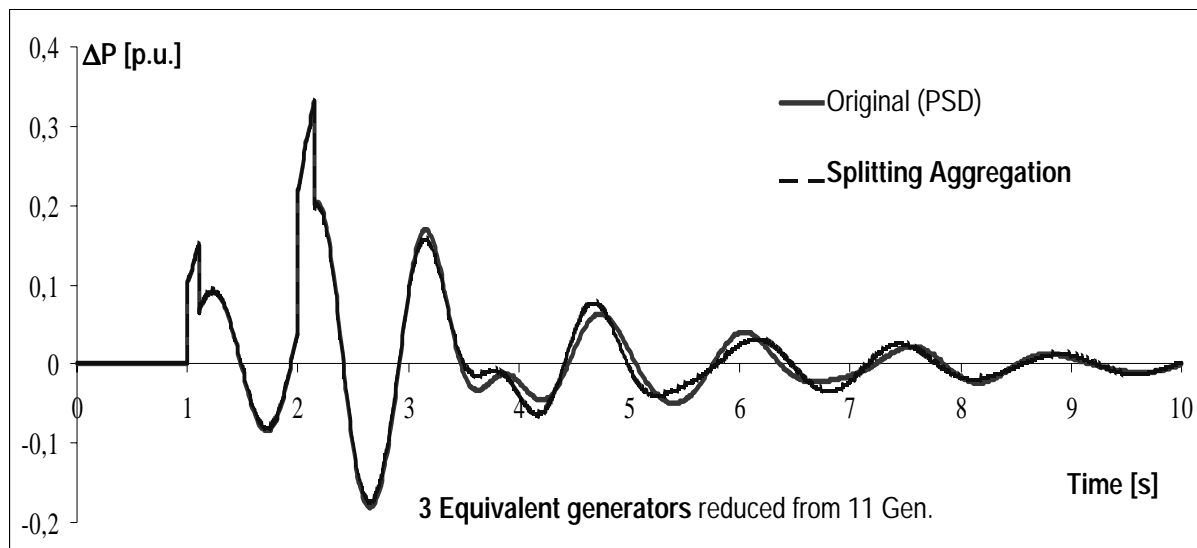


**Fig. 4.11.-** Behavior of any internal machine following a sequence of disturbances applied on different nodes electrically and geographically distinct from the equivalent disturbance. It is simulated with the original external area and with 3 splitting equivalents with Fuzzy factors.

Hereby a quite agreement of the internal machine responses over the whole time period can be detected. This notable accuracy in robustness can be determined for all generators in the internal area C using the splitting-based aggregation.

In contrast to this aggregation the classical inertial aggregation with coherency grouping is not able to obtain this robustness and approximation capability.

#### Quality measurement by standardized sum distance error

In this section, the behavior of all internal machines is investigated using the following three methods regarding their suitability and accuracy:

- Splitting based-aggregation method with the Fuzzy membership degrees as splitting factors
- The classical aggregation method with Fuzzy clustering
- The classical aggregation method with K-Means

The measure for evaluating the three methods is defined as follows:

$$J(i) = 1 - \frac{\sum_{l=1}^{N_p} (\Delta P_l(i)^{Original} - \Delta P_l(i)^{Dyn.Equi.})^2}{N_p}, \dots, i = 1, \dots, N_s \quad (4.49)$$

where

- $\Delta P(i)^{Original}$  and  $\Delta P(i)^{Dyn. Equi.}$  are the time domain behavior of the  $i$ th generator in the internal system, which are calculated with the full external system and the aggregated external system respectively. In this research,  $(\Delta P(i)^{Original} - \Delta P(i)^{Dyn. Equi.})^2$  is defined as squared distance error.
- $N_p$  is the number of sampling points and
- $N_s$  is the total number of generators in the internal area.

The “best” aggregation method is the one that gives the minimum squared distance error or maximizes  $J(i)$ . Taking into consideration all internal machines, the following mean value  $\bar{J}$  may be defined:

$$\bar{J} = \frac{\sum_{i=1}^{N_s} J(i)}{N_s} \quad (4.50)$$

Of course, by means of this value the quality, accuracy and reduction capability of the splitting aggregation approach in comparison to the classical inertial aggregation can be characterized and evaluated depending on the reduction degree of 11 external machines to 3 and 6 dynamic equivalents, as it can be seen in the following figure.

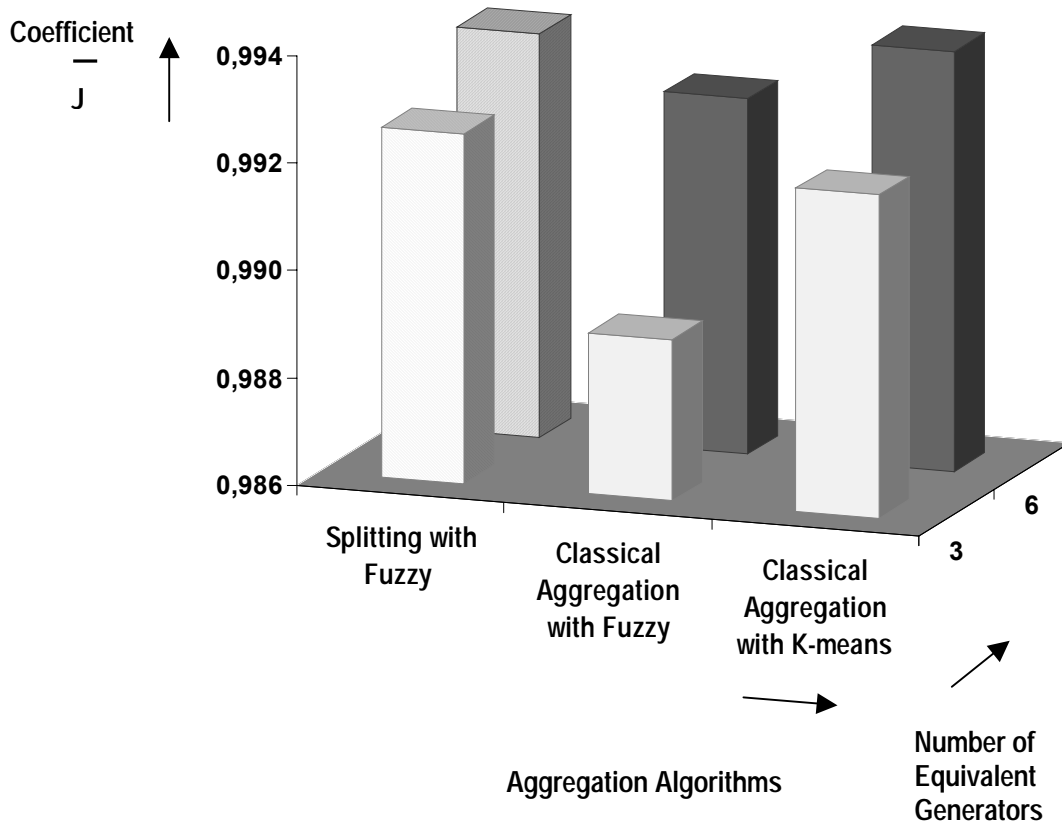


**Fig. 4.12.-** Comparison of aggregation algorithms considering the classical inertial aggregation and the proposed splitting-based aggregation by the mean value of  $\bar{J}$  of the intern machines for a fault located at the internal node with different number of external equivalents.

Fig. 4.12 can be interpreted as follows:

- The best results and accuracy, as shaded beams illustrated, are to be found in the cases for which the proposed splitting-based aggregation is used in dynamic equivalencing with Fuzzy membership degrees independent on the number of equivalents. The detailed values in Fig. 4.12 are given in the appendix table D.4.
- Comparable agreement and similar accuracy between the splitting-based equivalents and equivalents, which are calculated by the classical aggregation and electromechanical identity recognition (K-means algorithm), are provided.
- The splitting technique shows a significant enhancement in accuracy in comparison with the equivalents calculated by the classical aggregation with Fuzzy clustering as identity recognition.
- In Fig. 4.12, the accuracy is independent of the number of equivalent machines.
- The best aggregation and consequently the small distance errors defined in (4.49) are given by the splitting technique.

This approach has been applied to the interconnected European power system too, but the result is not satisfactory. Some restrictions arise when applying this approach to large-scaled power systems and also the number of external machines can cause some limitations in the splitting procedure. Thus, the splitting factors, which determine the splitting electrical parameters of the equivalent generator, can be dispersed. For instance, each of the 397 external machines of the European power system outside of the German system can be splitted into 40 share factors. Some of them can tend to an insignificant factor, and so its influence to build the equivalent, can disappear. This leads to an accumulation of error yielding inaccuracy in the results. Hence, all splitting parameters of the external machines are required to calculate the electrical parameters of equivalent according to equations (4.32) to (4.37). This new proposed aggregation approach leads, however, to electrically efficient, in terms of splitting-based machine parameters and more accurate dynamic equivalents.

## 4.6 Summary

- A new aggregation concept and strategy for the dynamic equivalencing, which is called *splitting-based aggregation*, as alternative to the classic inertial and slow aggregation, is proposed to obtain accurate, non-linear, splitting-based aggregated equivalent machines of external large power systems.
- The *fictional splitting of generators in virtual generators is based on the share factors, such as the Fuzzy membership degrees and eigenvectors*. They are considered in forming accurate dynamic equivalents on the basis of the time behaviors of the external machines. The share factors can be derived from *mathematical reduction techniques* according to the Fuzzy theory or principal components.
- The significant benefit of splitting-based aggregation is principally that *the resulting aggregated dynamic equivalent is composed of splitting electrical system parameters*.
- *The main advantages of this approach is that the splitting factors or participation shares of the machines are considered to define splitting-based electromechanical equivalent parameters incorporating significantly mathematical reduction techniques*, which generate highly accurate aggregated equivalents in terms of:
  - *Linear independent dynamic equivalents* with orthogonal oscillating swing curves by principal components or
  - *Representative non-linear equivalents* with oscillating swing curves by Fuzzy membership degrees.
- The splitting equivalents are valid for disturbances too, which are electrically and geographically independent of the equivalent disturbance and too of the extent of severity (fault duration).

- *Notable accuracy using splitting-aggregated dynamic equivalents can be reached in comparison to the equivalent machines calculated with the classical inertial aggregation in the 16 multi-machine power system.*
- This splitting-based aggregation approach is applied to a 16 machine interconnected power system, where the internal area is simulated regarding the transient stability. *The results are accurate independent of the number of dynamic equivalents.* Best results with a high degree of accuracy are achieved using splitting by Fuzzy membership factors.
- *In comparison with the classical aggregations which are performed only and limitedly on a per coherent area basis, the proposed splitting-based aggregation is extended to the complete external area.*
- In consequence, the aggregation approximation of the network in the complete external area may result in an increase in accuracy.
- In comparison with the electromechanical-based identity recognition, *this approach omits the first step of the classical dynamic equivalencing, i.e. the grouping or electromechanical clustering of similar generators on a coherent or identical area basis.*
- This approach *can be applied in small-scale power systems effectively obtaining significant accurate dynamic equivalents.* A similar accuracy is obtained by using the electromechanical-based identity recognition applied to small-scale power systems independent of the number of equivalents, too.
- However, its application in large-scale power systems, such as the European power system, *is limited because of the influence of other electromechanical factors of the power system on the splitting process of the external machines.* Therefore, in comparison with the electromechanical-based identity recognition, the results are not enough accurate. Thus, a drawback of this method is the accumulation of error when it is applied to large number of external machines.

*“All these constructions and the laws connecting them can be arrived at by the principle of looking for the mathematically simplest concepts and the link between them”-A. Einstein- “A basic rule in estimation is not estimate what you already know”-A quotation from [129]-*

## Chapter 5

# Dynamic Artificial Neural Network-based Dynamic Equivalencing

**Objective—** *The aim of this chapter is to present a novel approach to construct an intelligent system as interconnected external area. It considers and captures essentially non-linear characteristics and behavior of the power system components.*

*This intelligent system is developed using dynamic artificial neural networks (DANN) as dynamic models, which is proposed as alternative to the conventional dynamic equivalencing. The conventional steps to generate dynamic equivalents are replaced by the properly chosen recurrent artificial neural network taking into consideration a suitable off-line training process, in which the effect of the disturbance influence of the internal area on the external area has to be considered globally.*

*Thus, the proposed approach is based upon the modeling of non-linear systems using dynamic ANNs in form of dynamic equivalents, which can be applied to dynamic stability studies.*

*Simulation results demonstrate the effectiveness, high accuracy, and robustness of this approach in different large multi-machine power systems with 2 to 8 boundary nodes.*

**Index Terms—** *Dynamic Equivalents, Model Reduction, Recurrent Artificial Neural Network, Stability in Power Systems, System Modeling.*

**Organization—** *Section 5.1 describes the introduction and section 5.2 of this chapter the classical methods. The proposed recurrent ANN-based approach with mathematical*

*preliminaries is treated in section 5.3, followed in section 5.4 by the application. In section 5.5, the simulation results are discussed and the conclusion in section 5.6.*

## 5.1 Introduction

Interconnected power system can be simulated difficultly for stability analysis due to their large size, non-linear behavior of generators and components, such as voltage and turbine governors, exciters, loads, electronic converters, among others. In order to utilize limited technical resources and limited data exchange between energy utilities the dynamic equivalencing of power system is indispensable.

The conventional dynamic equivalencing [6, 7, 15, 17, and 30] consists mainly of the following steps:

- Coherency identification
- Aggregation of generators
- Static network reduction
- Aggregation of control devices

The nature of power system is essentially non-linear and consequently, the nature of equivalents should be non-linear, too. Mathematically speaking, non-linear systems are known to be very hard to manage. To overcome this problem, when studying the behavior of a power system in a neighborhood of an equilibrium point, it is a common assumption that the power system is a linear, time-invariant system [3, 133]. Thus, the initial non-linear system is approximated by linear one. In many cases of practical importance, this assumption works quite well yielding numerous advantages. However, when transient stability of the system is investigated, the use of a linear model cannot be justified. There are several reasons for questioning the validity of the linear model. The main reason is the dependence of the qualitative behavior of the power system model on the non-linear nature of its components. Therefore, it is important to find a dynamic non-linear model of an interconnected power system.

In this chapter, an innovative approach for forming dynamic equivalents of the external area on the basis of the dynamic ANN is proposed. The basic concept underlies the replacement of the non-linear external area by a robustly trained recurrent ANN, which is connected to the internal area through tie lines and busses. *Using this ANN-based approach the abovementioned classical steps of dynamic equivalencing will be omitted.*

## 5.2 Conventional dynamic equivalencing

Various dynamic equivalencing methods are proposed, in particular by exploiting modal, coherency, linear model reduction and model identification properties.

### Linearization

The most important dynamic equivalencing methods, which are described in appendix A, are based upon linearization of the mathematical description of the system. They have had a limited success, and their use is justified by the following facts:

- Linearization around the equilibrium yield mathematically tractable linear models.
- The output of system can be computed for any arbitrary input.
- Most non-linear systems could be approximated satisfactorily in their normal ranges of operation.

### Remarks to linearization:

- However, in many cases, systems are required to operate in regions in the state space where linear models do not give satisfactory results. In order to cope with this, research on developing input-output models (empirical approach), i.e., models that rely completely on the inputs and the outputs of the system, has increased [116-120].
- Several model structures are available for developing input-output models of complex systems. These include models based on spline functions, polynomial models, and threshold models. Their limitation is that they can only be used for interpolation.
- If the system behavior is understood, but not so well that the adequate mathematical model based on the fundamental laws could be developed, it can be reasonable to construct a model based on unconventional methods.
- An unified framework for developing a non-linear model is not available. The true modeling capability of any given system model depends on its structure and dynamic. Thus, search of an appropriate structure and global description using non-conventional or empirical methods can be incorporated in the modeling phenomenon.

### 5.3 Dynamic ANN-based dynamic equivalencing

The proposed approach is based on a robustly trained recurrent (dynamic) ANN that models the external area including the non-linear properties of all power system components. The behavior of the external area will be described *through the dynamic of a ANN* in contrast to the methods described in [116, 143], which are disturbance-dependent and non-robust. The power system can be divided in the following form:

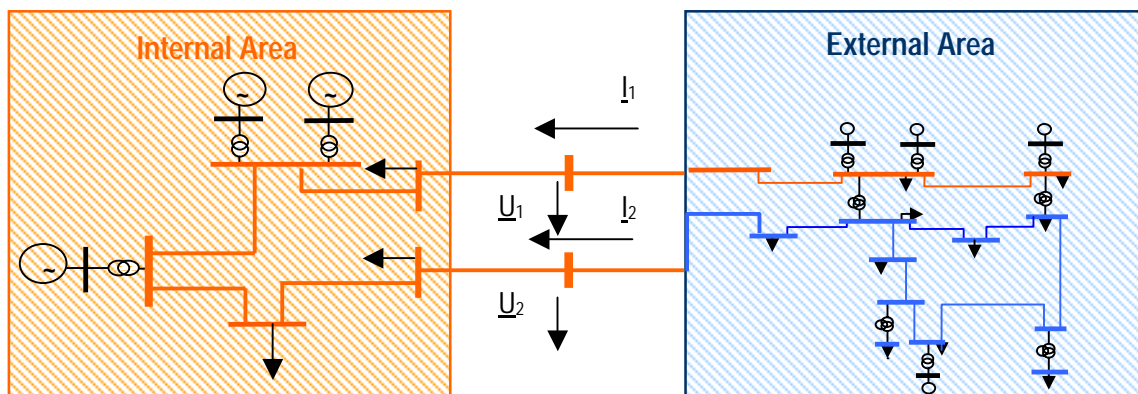


Fig. 5.1.- Division of complex power networks in areas

Essential aspects of this approach can be briefly summarized as:

- An *external area is replaced by a dynamic ANN* considering important aspects, such as:
  - The dynamic structure of the static ANN system is *preliminary determined on the estimated order of the external area after a linear modeling (knowledge-based)*. Through a tuning process, it can be adjusted gradually to the electromechanical order of the external area.
  - The DANN-based model requires simulation results or measurements only at the boundary buses *obtaining Multi Input Multi Output (MIMO) magnitudes that are defined using the Norton model of machines (signal-based)*.
- In consequence, *this approach may be defined as a knowledge- and signal-based system modeling*. The key issues of the ANN based system modeling are both the parameter determination, ANN-structure selection and the quality of selected input, output signals.
- In the training procedure of the ANN, in which the parameters are determined, *the external area has to be excited through efficiently generated disturbance sets located in the internal area*.

- The well-trained dynamic ANN must be able to approximate and describe globally the non-linear behavior of the external area following disturbance sets in the internal area. To obtain a robust, operating point-independent ANN, a normalized MIMO with reference to a certain operating point will be used.

In the following, key approach steps will be explained in detail.

### 5.3.1 Artificial neural networks (ANN) for modeling

To predict the behavior of an unknown system, ANN can learn and identify the system from experience. Its highly parallel distributed architecture and the ability to learn based on limited data makes ANN a powerful computing resource. Following ANN-aspects are important:

- A multi-layer neural network, consisting of one input layer, one output layer and an appropriate number of hidden layers, can be used either as a static or dynamic approximator, where information flows in one direction, as shown in Fig. 5.2.
- A desired accuracy in non-linear problems is achieved by suitable number of hidden layers and neurons. The multi-layer neural network of hyperbolic tangent units and the output layer of linear units are capable of approximating the non-linear dynamic of a complex system. A one multi-layer feedforward ANN can be represented, as follows:

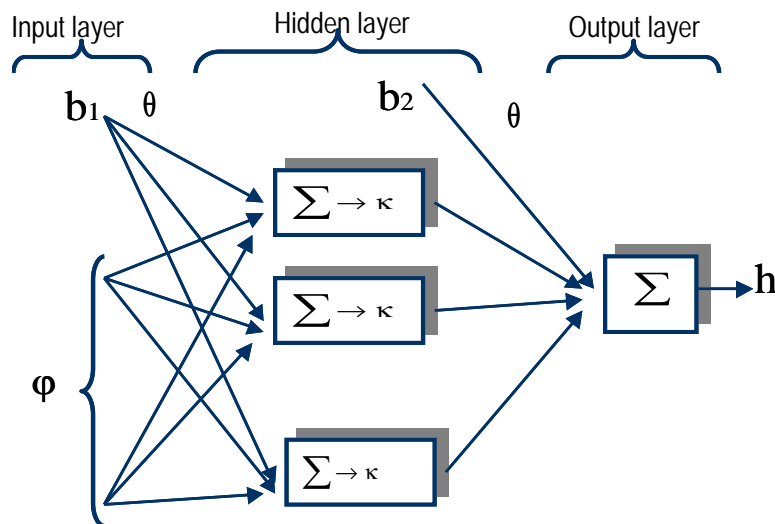


Fig. 5.2.- Neural network structure

- Its mathematical description is given by:

$$\begin{aligned}
 \mathbf{y} &= \mathbf{h}(\boldsymbol{\varphi}, \boldsymbol{\theta}) = \mathbf{W}_2 \boldsymbol{\kappa} (\boldsymbol{\varphi}^T \mathbf{W}_1 + \mathbf{B}_1) + \mathbf{B}_2 \\
 \boldsymbol{\theta} &= (\mathbf{W}_1 \quad \mathbf{B}_1 \quad \mathbf{W}_2 \quad \mathbf{B}_2)
 \end{aligned}
 \tag{5.1}$$

where  $\varphi$  is the input vector,  $\kappa$  the activation function,  $\theta$  parameter set,  $\mathbf{W}$  the weight matrix and  $\mathbf{B}$  denotes the bias that is considered, for simplicity, a weight associated with an unitary input.

- Neuron models have in common the structure according to three criteria: *Input operator*, *activity function*, and *learning rule* (These aspects are explained in appendix C.1 and C.2.) shown in the following diagram:

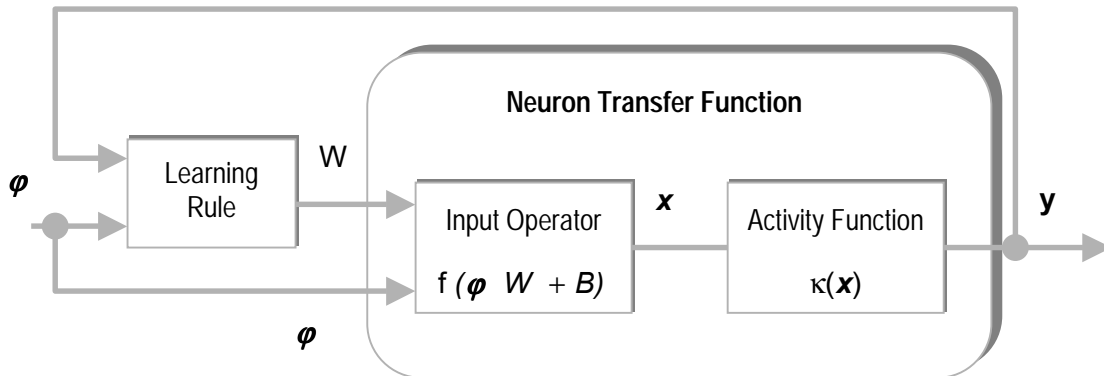


Fig. 5.3.- Basic structure of generalized neuron model

#### ANN advantages:

In neural networks, the relations are not explicitly given, but are coded in a network and its weights. Its main advantages are [120-132]:

- **Non-linearity:** The mathematical interconnection of the ANN structure provides non-linear characteristics to the complex system.
- **Input/Output Mapping:** The identification paradigm used is based on nonparametric statistical inference, where no assumptions have to be made about the model under study. Thus, the network learns from experience.
- **Adaptability:** An ANN adapts its synaptic weights to changes in the environment. An initial training is usually made to model the stationary state of the system providing the initial estimates for the ANN parameters. Real time adaptivity is required to model non-stationary environments where some characteristics are dynamic and time variant.

#### ANN systems:

ANNs can be employed in a wide spectrum of problems in technical aspects. Thus, four categories of ANN may be distinguished according to its applicability. From the viewpoint of non-linear modeling three dynamic structures of ANNs subdivided *into structures, such as*

the internal recurrent networks, external recurrent with lumped dynamics and distributed dynamics [119], can be determined, as it can be shown in the following diagram.

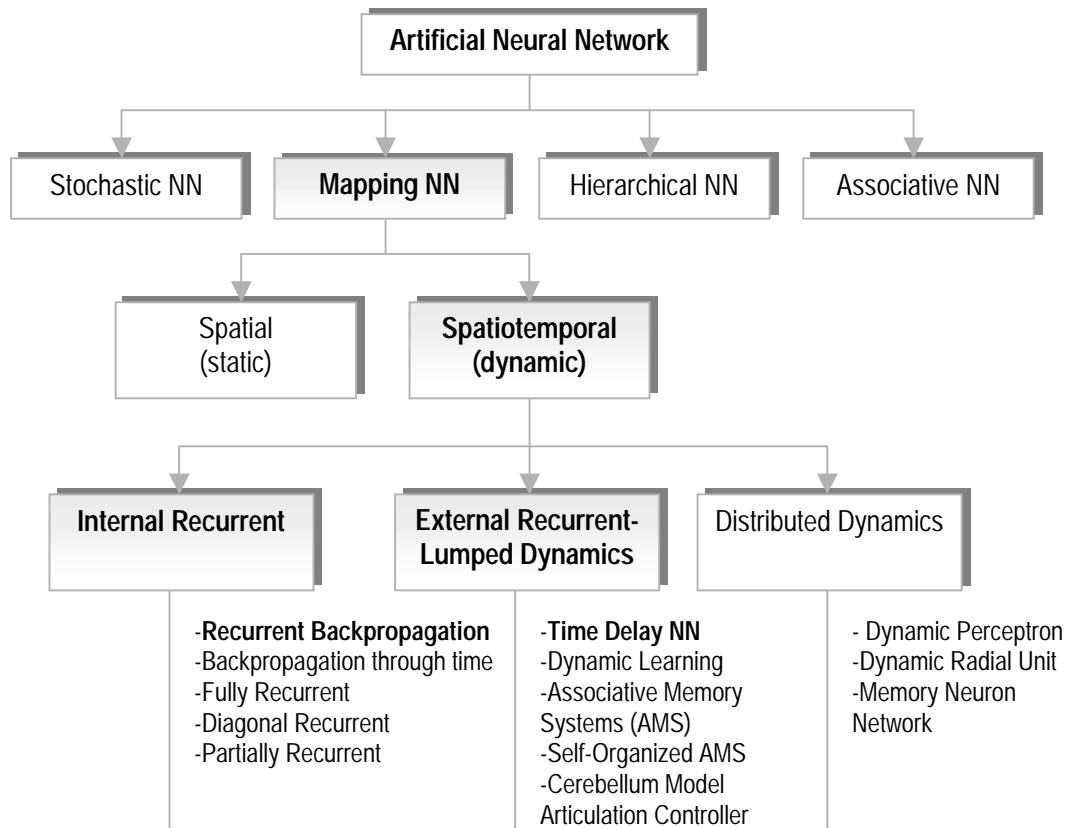


**Fig. 5.4.-** ANNs applied to the modeling of non-linear systems. Internal and external recurrent ANN can be used to develop the DANN-based dynamic equivalencing

#### Remarks to Fig. 5.4:

- *Mapping ANN* represents *non-linear parametric models* without requiring a specified a priori accurate assumption about the system structure. Thus, the learning procedure estimates the unknown network's weights, which represent the model's parameters.
- ANN, which belongs to the class of mapping neural networks, performs mathematically a mapping action from a domain of its input space to the output space [117-122].
- The mapping task is labeled in spatial if there is no time-dependency. In general, these ANNs can be applied to identify static non-linear systems.
- Another mapping task is the spatiotemporal mapping. In this case, the modeling and identification of dynamic non-linearities involved in subjects, such as behavior, response, and non-parametric modeling of complex systems, can be considered as an approximation of spatiotemporal rules.

In power systems, the dynamic external area can be approximated by means of dynamic ANNs. The dynamics are realized either using static ANN combined with an external

feedback connection (recurrent ANN) or using internal recurrent dynamic ANN, where feedback is introduced internally to the inputs of antecedent neurons.

*In this study, both options are examined and assessed, and the external recurrent ANN was found as the suitable resource to describe accurately the whole behavior of a complex power system. These options are emphasized in the Fig. 5.4.*

### 5.3.2 Modeling of dynamic system

Its main purpose is to identify a model of an unknown complex system in order to predict and gain insight into the behavior of the system [116]. The key problem in system modeling is to find a suitable model structure. To this end, prior knowledge and physical insight about the system should be utilized.

#### Types of models:

The system modeling based on physical and experimental aspects of non-linear systems can be summarized in the following diagram:

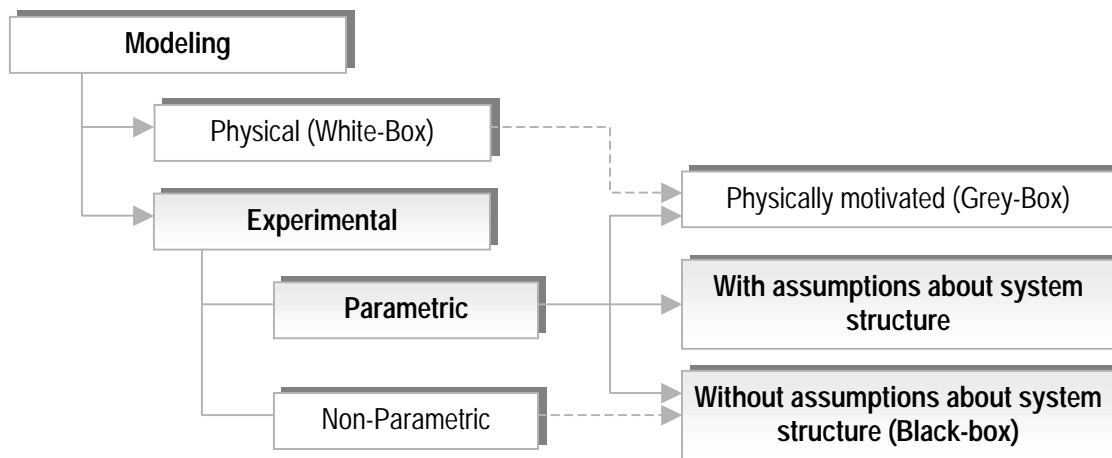


**Fig. 5.5.-** Modeling structures. The system modeling used in this approach is emphasized as a hybrid procedure in black-box form with assumptions about the system

Following aspects of Fig. 5.5 can be emphasized:

- In *white-box models*, some prior physical information is available (e.g. physical knowledge, linguistic rules, vague state-space model).
- But, in comparison in *grey-box models* this information is not complete. In order to get better model some parameters must be determined from the data.

- A *grey-box* approach is an approach to hybrid modeling. Another important alternative is an approach where an a priori mathematical model is used as a starting point and a radial basis function expansion compensates the mismatch between the mathematical model and the process data.
- The system modeling on experimental variables involves *parametric* and *non-parametric models*.
- Modeling of *parametric* models entails the estimation of unknown parameters of an appropriate model structure, which is chosen a priori (*black-box*) or partially motivated by physical analysis (*grey-box*).
- In *black-box* structure for a dynamical system, no prior information about the system is available. The modeling must be done relying on the observed data and describing the system in an input/output sense. The *non-linear black-box* is difficult, because nothing system behavior should be excluded and consequently a very rich spectrum of possible models descriptions must be taken into consideration.
- The main futures of *parametric* models are the explicit small set of used parameters and the model structure. In contrast, *non-parametric* models don't possess a given structure and, furthermore, use a large set of parameters.
- The system modeling used in this approach is realized as a hybrid procedure in black-box form with assumptions about the estimated linear system.
- There are different non-linear models, such as the **non-linear Output Error (NOE)**, **non-linear AutoRegressive models with eXogenous inputs (NARX)**, **non-linear AutoRegressive Moving Average terms with eXogenous inputs (NARMAX)**, etc. These models are treated in detail in appendix C.4.

### 5.3.3 Mathematical description

The modeling can be divided into two basic functions (explained in Appendix C.3 and C.4):

- Mapping from past observed data to a **regression vector** (by preprocessing of data).
- **Non-linear mapping** from regressor space to the output space, which is typically formed as a basis function expansion.

Dynamic systems can be described using the regressor vector. It starts from the state form:

$$\begin{aligned}\dot{\mathbf{x}}(t) &= \mathbf{f}(t, \mathbf{x}(t), \mathbf{u}(t)) \\ \mathbf{y}(t) &= \mathbf{g}(t, \mathbf{x}(t))\end{aligned}\tag{5.2a}$$

Discretizing (5.2a) yields to:

$$\begin{aligned}\mathbf{x}(t+1) &= \mathbf{f}(t, \mathbf{x}(t), \mathbf{u}(t)) \\ \mathbf{y}(t) &= \mathbf{g}(t, \mathbf{x}(t))\end{aligned}\quad (5.2b)$$

where  $\mathbf{x}(t)$  is the vector of system states at time  $t$ ,  $\mathbf{u}(t)$  is an input, i.e. control signal, and  $\mathbf{y}(t)$  is the output of the system. Linear models can be formed by linearizing (5.2):

$$\begin{aligned}\mathbf{x}(t+1) &= \mathbf{A}\mathbf{x}(t) + \mathbf{B}\mathbf{u}(t) \\ \mathbf{y}(t) &= \mathbf{C}\mathbf{x}(t)\end{aligned}\quad (5.3)$$

where

$$\mathbf{A} = \left. \frac{\partial \mathbf{f}}{\partial \mathbf{x}} \right|_0, \quad \mathbf{B} = \left. \frac{\partial \mathbf{f}}{\partial \mathbf{u}} \right|_0, \quad \mathbf{C} = \left. \frac{\partial \mathbf{g}}{\partial \mathbf{x}} \right|_0 \quad (5.4)$$

This non-linear time-discrete system (5.2b) can be described by the following equation:

$$\mathbf{y}(t) = \mathbf{g}(\mathbf{x}(t-1), \mathbf{u}(t-1), \mathbf{u}(t)) \quad (5.5)$$

Usually, (5.2b) can be reformulated too as a general discrete time dynamic system looking for a relationship between past observations and future outputs in terms of the regression vector as:

$$\mathbf{y}(t) = \mathbf{h}(\mathbf{y}(t-1), \mathbf{u}(t)) \quad (5.6)$$

Hereby, the goal is to model a dynamic system in discrete time with input and output using observations. The fact that the next output  $\mathbf{y}(t)$  will not be an exact function of past data is described by the additive term  $\mathbf{v}(t)$  which usually is described as a random noise signal. The goal is to find a model of 'h' which can be used to predict future  $\mathbf{y}(t)$  with a system mapping and a regressor vector as:

$$\begin{aligned}\mathbf{y}(t) &= [y(t), y(t-1), \dots, y(t-n_y)]^T \\ \mathbf{u}(t) &= [u(t), u(t-1), \dots, u(t-n_u)]^T\end{aligned}\quad (5.7)$$

where integers  $n_u$ ,  $n_y$  are the maximum lags in the input and output and they determine the system order. If their values are too large, the model is overparametrized and thus the generalization property of the model is affected. As a result of choosing too small values the model cannot model all the important dynamics of the system.

Thus, the general description in (5.6) is normally divided into two mappings. The first mapping gives a regressor from the data as:

$$\boldsymbol{\varphi}(t) = \boldsymbol{\varphi}(u(t), u(t-1), \dots, u(t-n_u), y(t-1), y(t-2), \dots, y(t-n_y) \dots) \quad (5.8)$$

where  $\boldsymbol{\varphi}(t)$  is the parameter vector of fixed dimension. The second transformation maps  $\boldsymbol{\varphi}(t)$  to the space of the outputs in the following form:

$$\hat{\mathbf{y}}(t) = \mathbf{h}(u(t), \dots, y(t-1), \dots, \boldsymbol{\theta}) = \mathbf{h}(\boldsymbol{\varphi}(t), \boldsymbol{\theta}) \quad (5.9)$$

where  $\hat{\mathbf{y}}(t)$  is the model estimate of  $y(t)$  and  $\boldsymbol{\theta}$  contains the parameter matrix of the model.

The regressor vector (5.8) can be parametrized as:

$$\boldsymbol{\varphi}(t) = \boldsymbol{\varphi}(u(t), u(t-1), \dots, u(t-n_u), y(t-1), y(t-2), \dots, y(t-n_y), \dots, \boldsymbol{\eta}) \quad (5.10)$$

which may be denoted as  $\boldsymbol{\varphi}(t, \boldsymbol{\eta})$ . Sometimes  $\boldsymbol{\eta} = \boldsymbol{\theta}$ , i.e. the regression vector depends on all the model parameters.

Following aspects of modeling are relevant:

- The data observation set  $y(n)$  and  $u(n)$  is a projection of the multivariate state space of the system onto the reduced dimensional space.
- In order to realize the prediction, it is needed to reconstruct as well as possible the state space of the system using the input output data information of the observation set.
- Recurrent ANN can also be described with the recurrence in the regressor combined with a static mapping ' $\mathbf{h}$ '.
- There are several advantages with describing the model as a concatenation of two mappings instead of using one single function to capture the entire model as is common in the neural network.
- First the mapping ' $\mathbf{h}$ ' is static and all the dynamics are described by  $\boldsymbol{\varphi}(t)$ .
- Second, as mentioned above, it is possible to introduce non-linear black-box models as generalizations of linear black-box models by keeping the same  $\boldsymbol{\varphi}(t)$  but changing ' $\mathbf{h}$ ' from linear to non-linear.

### 5.3.4 Power system model

The major component of the dynamics within a power system, which can be described by the recurrent ANN is generated by the generator and its controllers. Therefore, appreciating the importance of the generators, its description will be treated in the following section.

#### Modeling of synchronous machines

Depending on the nature of a study, several models of a synchronous generator, having different levels of complexity, can be utilized [3, 134, 135, and 136]. In the simplest case, a synchronous generator is represented by a second-order differential equation, while studying fast transients in the generator's windings would require the use of a more detailed model, e.g., 8th order or Krause model [135].

The dynamical characteristics of a generator, whose structure modeling are based upon a field coil on the d-axis and a damper coil on the q-axis, can be accurately represented by the following differential equations:

$$\frac{dE_q'}{dt} = \frac{1}{T_{do}} [-E_q' + (x_d - x_d')i_d + E_{fd}] \quad (5.11)$$

$$\frac{dE_d'}{dt} = \frac{1}{T_{qo}} [-E_d' - (x_q - x_q')i_q] \quad (5.12)$$

$$\frac{d\delta}{dt} = \omega - \omega_o \quad (5.13)$$

$$\frac{d\omega}{dt} = \frac{1}{M} [P_m - D(\omega - \omega_o) - P_G] \quad (5.14)$$

$$P_G = E_q' i_q + E_d' i_d + (x_d' - x_q') i_d i_q \quad (5.15)$$

In the equations above, the following symbols are used to denote:

- $E_q'$ ,  $E_d'$  denominate the transient EMF's of the machine in the  $q$ - and  $d$ -axes.
- $\delta$  is the rotor shaft angle of the generator.
- $\omega$  is the rotor angular velocity of the generator. The  $\omega_o$  is the synchronous speed of the system.
- $M$  is the shaft inertia constant of the generator.

- $P_m$  is the mechanical torque applied to the shaft of the generator.
- $P_G$  is the output electrical power of the generator.
- $i_q, i_d$  are the equivalent currents of the synchronous machine in the  $q$ - and  $d$ -axes.
- $D$  is the damping coefficient of the generator.
- $T_{do}, T_{qo}$  are transient time constants of the open circuit and a damper winding in the  $q$ -axis.
- $X_q, X_d, X'_d, X'_q$  stand for the synchronous reactance and transient synchronous reactance of the machine.

According to the equivalent circuit form of the two axes model [3] the voltage equations in d- and q-coordinate system may be simplified neglecting stator transients and as well the flux linkage equations may be simplified ignoring the damper winding. Defining the stator flux transient flux linkages and the corresponding speed voltages, the stator equations are:

$$E_q' + x_d' i_d - R_a i_q = u_q \quad (5.16)$$

$$E_d' - x_q' i_q - R_a i_d = u_d \quad (5.17)$$

From the above equations,  $i_d$  and  $i_q$  are solved as:

$$\begin{bmatrix} i_q \\ i_d \end{bmatrix} = \frac{1}{x_q' x_d' + R_a^2} \begin{bmatrix} R_a & x_d' \\ -x_q' & R_a \end{bmatrix} \begin{bmatrix} E_q' - u_q \\ E_d' - u_d \end{bmatrix} \quad (5.18)$$

These can be substituted in equations (5.11) and (5.12) and *the machine rotor electrical equations* can be expressed as state space representation:

$$\dot{\mathbf{x}}_R = \mathbf{A}_R \mathbf{x}_R + \mathbf{B}_{R1} E_{fd} + \mathbf{B}_{R2} \begin{bmatrix} u_q \\ u_d \end{bmatrix}, \quad \mathbf{x}_R = \begin{bmatrix} E_q' & E_d' \end{bmatrix}^T \quad (5.19)$$

*The mechanical equations* (5.13) to (5.15) may be expressed as:

$$\dot{\mathbf{x}}_M = \mathbf{A}_M \mathbf{x}_M + \mathbf{B}_M P_m + \mathbf{B}_M P_G, \quad \mathbf{x}_M = [\delta \quad \omega]^T \quad (5.20)$$

$$P_G = P_G(\mathbf{x}_R, v_q, v_d) \quad (5.21)$$

When equation (5.18) is substituted in (5.15)  $P_G$  becomes a non-linear function  $f_2$  of  $E_q'$ ,  $E_d'$  and  $v_d$ ,  $v_q$ , which is depicted in appendix Fig. C.1. In the same manner, the modeling of the excitation system, the turbine and governor system are explained in appendix C.5.

### Equivalent generator

In order to realize a steady state analysis, the generator stator can be incorporated in the network. Thus, the network may be represented on a single-phase basis using phasor quantities for slowly varying sinusoidal voltages and currents in the network. Therefore, the generator stator can also be represented on a single-phase basis.

Equation (5.18) can be expressed as a single equation in phasor quantities if transients saliency is neglected, that is,  $x'_d = x'_q = x'$  obtaining:

$$i_q + jj_d = \frac{1}{R_a + jX'} [(E_q' + jE_d') - (u_q + ju_d)] \quad (5.22)$$

Hereby,  $\bar{E}'$  is the phasor voltage behind the transient impedance of the machine known as the transient internal voltage and has two components  $\bar{E}_q'$  and  $\bar{E}_d'$ . According to this basis, the current phasor  $\bar{I}_a$  can also be represented on a synchronously rotating reference frame as:

$$\bar{I}_a = i_q + jj_d = (i_q + jj_d)e^{j\delta} = \frac{1}{R_a + jX'} [\bar{E}' - \bar{U}_t] \quad (5.23)$$

where

$$\begin{aligned} \bar{E}' &= E_q' + jE_d' = (E_q' + jE_d')e^{j\delta} \\ \bar{U}_t &= u_q + ju_d = (u_q + ju_d)e^{j\delta} = U_t e^{j\theta} \end{aligned} \quad (5.24)$$

On the basis of equation (5.23), *an equivalent circuit of the generator using the Norton model can be represented* as follows:

$$Y_G = \frac{1}{R_a + jX'} \quad (5.25)$$

$$\bar{I}_G = \bar{E}' Y_G = \frac{(E_q' + jE_d') e^{j\delta}}{R_a + jX'} \quad (5.26)$$

Therefore,  $\bar{I}_G$  is a function of all state variables ( $E'_q$ ,  $E'_d$  and  $\delta$ ). Hence, it does not change suddenly whenever there is a network switching. The equivalent circuit can be merged with the power network external to the generator.

This equivalent circuit can be represented schematically according to expressions (5.25-5.26) as follows:

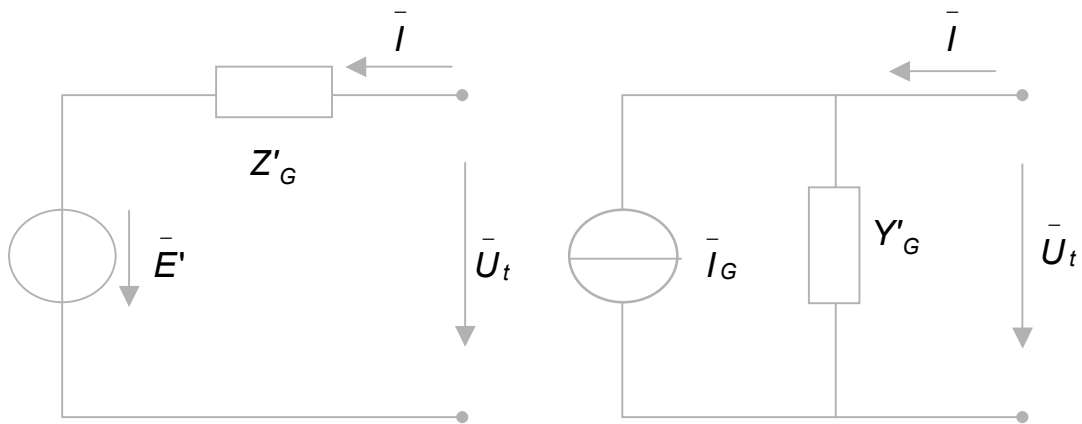


Fig. 5.6.- Generator equivalent circuit as voltage and current source

Considering this representation of generators *using the Norton model in the network equation for a interconnected power system*, the boundary voltages between the internal and external area may be used as the inputs to the model (independent variables), while the injected current as the outputs (dependent variables), described as follows:

$$\bar{I} = -\frac{U}{Z_G} \quad (5.27)$$

Thus, this injected current is a function of all state variables of the generator, including its control devices, such as voltage regulator and governor.

Thus, extending this model to complex systems the injected generator currents of the external network presented in Fig. 5.7 as currents  $\bar{i}_{G1}$ ,  $\bar{i}_{G2}$ ,  $\bar{i}_{G3}$  and  $\bar{i}_{G4}$  are functions of the state variables of the generators 1, 2, 3 and 4, respectively. As it may be seen in the following figure <sup>16</sup>:

<sup>16</sup> Extending the Norton model to a complex power system divided in external and internal area, which are connected over the boundary busses, the injected currents within the boundary busses (see Fig. 5.7) are in same manner functions of all generator state variables of the whole external area including all their components.

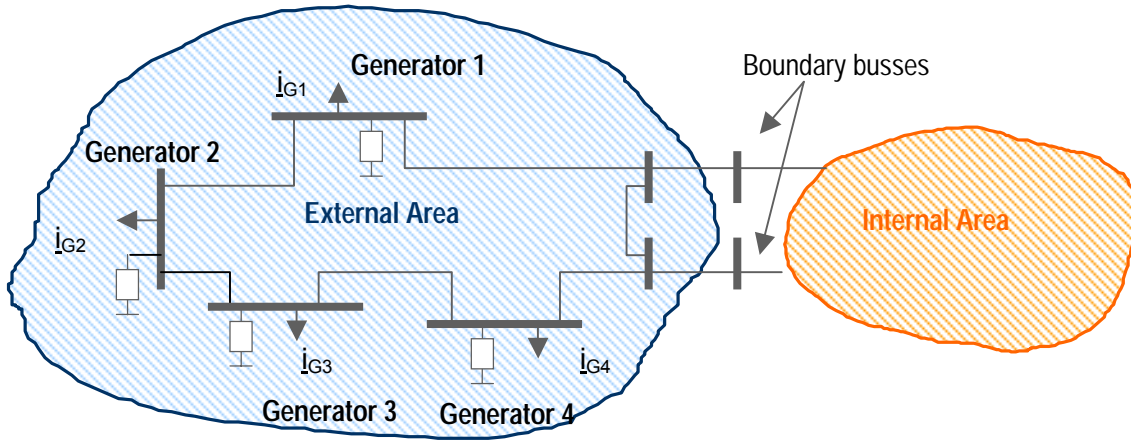


Fig. 5.7.- Internal and external area of a interconnected power system

As a result injected currents within the boundary busses appear according to Fig. 5.8. These currents ( $i_{E1}$  and  $i_{E2}$ ) are functions of all generator state variables of the external network on the basis of injected currents  $i_{G1}$ ,  $i_{G2}$ ,  $i_{G3}$  and  $i_{G4}$ . At the same time, the equivalent admittances at the boundary busses are a result of the passive network reduction as follows:

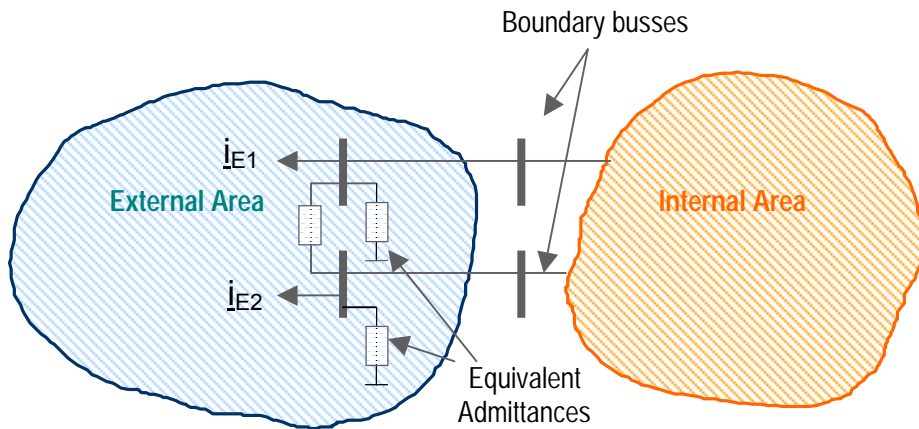


Fig. 5.8.- Equivalent external area of a power system

### 5.3.5 Dynamic ANN model as external area

The Norton model replaces a system with dependent and independent sources. It requires the voltage as independent input variable and the injected current as output of the system. Thus, the power system which may be replaced, can be described as follows:

$$\begin{bmatrix} i_e \\ i_b \\ i_i \end{bmatrix} = \begin{bmatrix} Y_{ee} & Y_{eb} & Y_{ei} \\ Y_{be} & Y_{bb} & Y_{bi} \\ Y_{ie} & Y_{ib} & Y_{ii} \end{bmatrix} \begin{bmatrix} u_e \\ u_b \\ u_i \end{bmatrix} \tag{5.28}$$

where

- $\underline{i}_e, \underline{i}_b, \underline{i}_i$  are injected currents of the external, the boundary and the internal buses, respectively.
- $\underline{u}_e, \underline{u}_b, \underline{u}_i$  are voltages of the external, the boundary and the internal buses, respectively.
- $\underline{Y}$  is the network admittance including external, internal and boundary areas.

In mathematical terms, this equation can be solved using step by step triangular factorization of the admittance matrix and transfiguration of the node currents. Given the partition of the network equations according to equation (5.28), the external nodes will be transformed first.

More specifically, the dynamic ANN model can replace an external area taking into consideration following fields:

#### i. The discrete-time input-output representation

The dynamic behavior of the external area in terms of a general continuous state space model is described as:

$$\begin{aligned} \dot{\mathbf{x}} &= \mathbf{Ax} + \mathbf{Bu} \\ \mathbf{y} &= \mathbf{Cx} + \mathbf{Du} \end{aligned} \quad (5.29)$$

It may be modeled identifying the corresponding matrices **A**, **B**, **C**, and **D** in parametric form. But, a non-linear model of a power system in system modeling is suitable to describe the real properties of a power system. It can be obtained using input and output information, which are defined on the injected current and voltage measurements on the boundary nodes, i.e. considering the Norton model. This system modeling allows the determination of the model structure as well as the description of the behavior of system in non-parametric form.

Thus, now the methods of transient stability analysis can be applied in conjunction with the system equivalent as non-linear model (see the Fig. 5.9). It can be illustratively shown as follows:

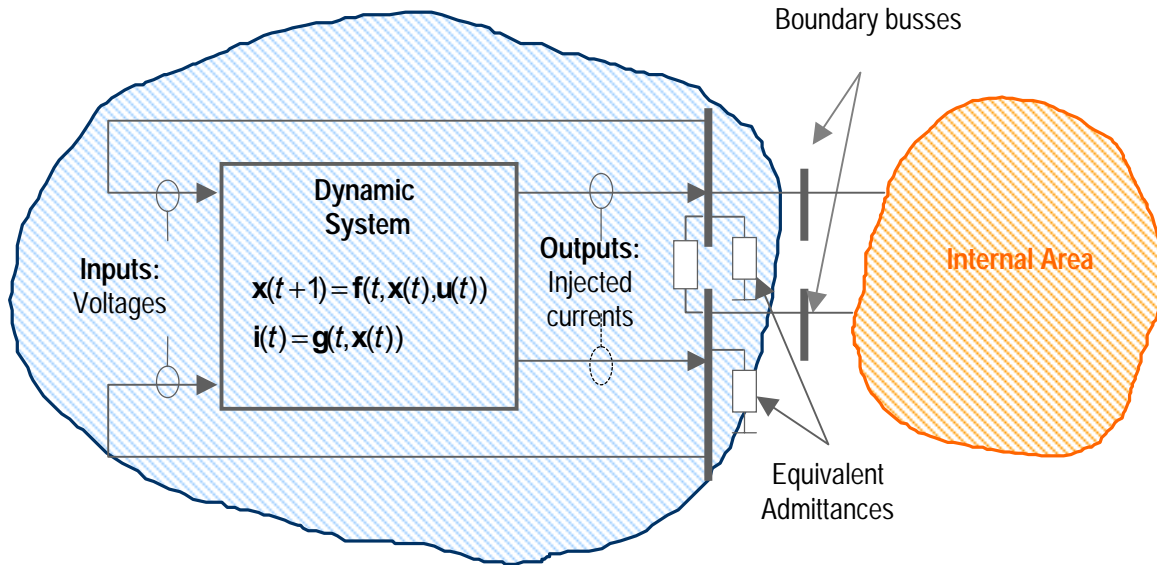


Fig. 5.9.- External area as dynamic equivalent

Thus, considering the input-output representation of a time-discrete approximation of a continuous time dynamic system with a recurrent ANN during a simulation transient period, the external area (according to Fig. 5.9) can be described by a set of differential and algebraic equations in discretized non-linear form as:

$$\mathbf{x}(t+1) = \mathbf{f}(t, \mathbf{x}(t), \mathbf{u}(t)) \quad (5.30)$$

$$\mathbf{i}(t) = \mathbf{g}(t, \mathbf{x}(t)) \quad (5.31)$$

In that case, the actual output vector  $\mathbf{i}(t)$  depends on the actual time dependency and also the actual value of the state variables  $\mathbf{x}(t)$ . Whereas the next value of the state vector  $\mathbf{x}(t+1)$  depends on the actual input  $\mathbf{u}(t)$  and the actual state value  $\mathbf{x}(t)$ .

In equations (5.30-5.31) above, the following symbols are used to denote:

- $\mathbf{u}(t)$  is an input vector, i.e. voltage signal, that generally consists of state and field voltages, and mechanical power input of each generator in the system at time  $t$ ,
- $\mathbf{x}(t)$  is the vector of system states variables, it may contain variables associated with synchronous generators and their excitation systems including turbines and governing systems, other controllers, and possible network dynamics.
- The injected current  $\mathbf{i}(t)$  is the output vector, and it is a function of all state variables.
- $\mathbf{f}$ ,  $\mathbf{g}$  are non-linear vector functions.

This way of representing a dynamic system will be called the **discrete-time state-space representation**<sup>17</sup>. Substituting (5.30) in (5.31) the output can be expressed as:

$$\mathbf{i}(t+1) = \mathbf{g}(t+1, \mathbf{f}(t, \mathbf{x}(t), \mathbf{u}(t)), \mathbf{u}(t+1)) \quad (5.32)$$

This equation can be expressed according to a new vector function 'h' as:

$$\mathbf{i}(t+1) = \mathbf{h}(t+1, t, \mathbf{x}(t), \mathbf{u}(t), \mathbf{u}(t+1)) \quad (5.33)$$

Usually, this expression can be reformulated as a general discrete time dynamic system as:

$$\mathbf{i}(t) = \mathbf{h}(\mathbf{i}(t-1), \mathbf{u}(t)) \quad (5.34)$$

This type of representation will be called the **discrete-time input-output representation**. This functional relationship 'h' of discrete-time dynamic systems can be identified with a system based upon the optimal mapping and a suitable regressor vector as:

$$\mathbf{i}(t) = [i(t-1), i(t-2), \dots, i(t-n_i)]^T \quad (5.35)$$

$$\mathbf{u}(t) = [u(t-1), u(t-2), \dots, u(t-n_u)]^T \quad (5.36)$$

In the input output representation following aspects can be emphasized:

- The state space system (5.30-5.31) in input-output form consists of a collection of finite sequences of input samples  $\mathbf{i}(t)$  and corresponding sequences of output samples  $\mathbf{u}(t)$  as follows:

$$\mathbf{i}(t) = \mathbf{h}(i(t-1), \dots, i(t-n_i), u(t), u(t-1), \dots, u(t-n_u)) \quad (5.37)$$

- $i(t)$  and  $u(t)$  are past output and input values, respectively. Integers  $n_i, n_u$  (maximum lags) reflex relatively the order of the system<sup>18</sup>. These values can be estimated initially based on the linear system modeling of the non-linear complex system.
- The suitable number of past inputs and outputs are collected into the *regressor vector*.

<sup>17</sup> Thus, in mathematical terms, the objective is to study the stability of the dynamic system by solving the system (5.30-5.31) with steady-state operating conditions or by describing the dynamic system using dynamic ANNs.

<sup>18</sup>  $n_i, n_u$  must be chosen properly. If their values are too large, the model is overparametrized and thus the generalization property of the model is affected. As a result of choosing too small values, the model cannot describe the whole system.

$$\boldsymbol{\varphi}(t) = \left[ i(t-1), \dots, i(t-n_i), u(t), u(t-1), \dots, u(t-n_u) \right]^T \quad (5.38)$$

- Then the problem is to map  $\boldsymbol{\varphi}(t)$  to the next output  $\mathbf{i}(t)$  with a non-linear function 'h':

$$\mathbf{i}(t) \rightarrow \mathbf{h}(\boldsymbol{\varphi}(t)) \quad (5.39)$$

- This mapping can be realized by the NARX model (Nonlinear Auto Regressive model with Exogenous inputs), which provides an unified representation for a wide class of discrete-time non-linear systems. In a NARX description, the system is modeled in terms of a non-linear functional expansion of past inputs and outputs:

$$\mathbf{i}'(t | \boldsymbol{\theta}) = \mathbf{h}_{\mathbf{N}}(\boldsymbol{\varphi}(t), \boldsymbol{\theta}) \quad (5.40)$$

- The functional relationship ' $\mathbf{h}_{\mathbf{N}}$ ' approximating the real-properties of the external area can be identified with a **DANN** as **external recurrent artificial neural network** (time delay ANN) with proper weighting parameters  $\boldsymbol{\theta}$  and a suitable regressor vector  $\boldsymbol{\varphi}(t)$ .

## ii. ANN Model structure

This dynamic ANN structure has to capture fitting function ' $\mathbf{h}_{\mathbf{N}}$ ' representing a global approximation of the dynamic non-linear function of the external area. A model based on estimated function ' $\mathbf{h}_{\mathbf{N}}$ ' in (5.40) can be constructed according to the following **time-delay neural network** structure:

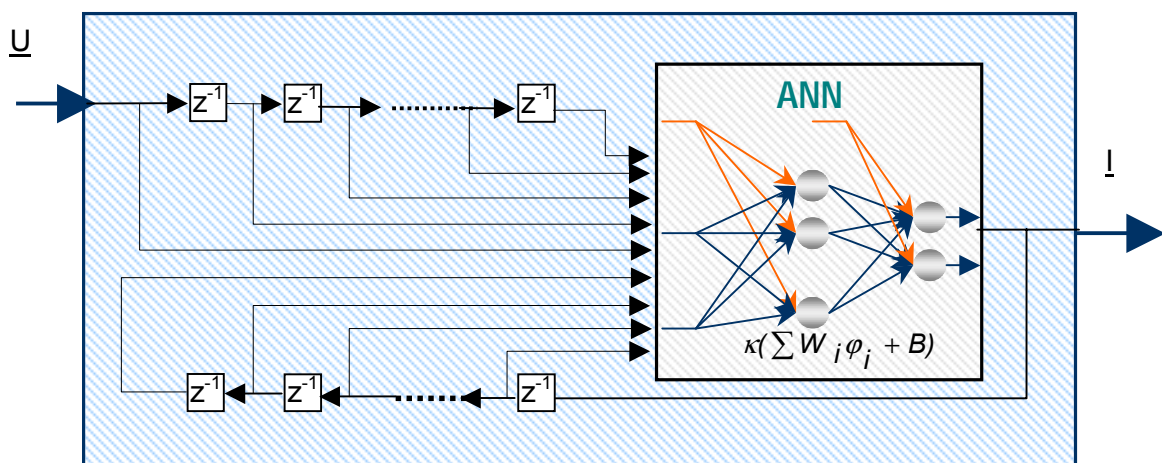
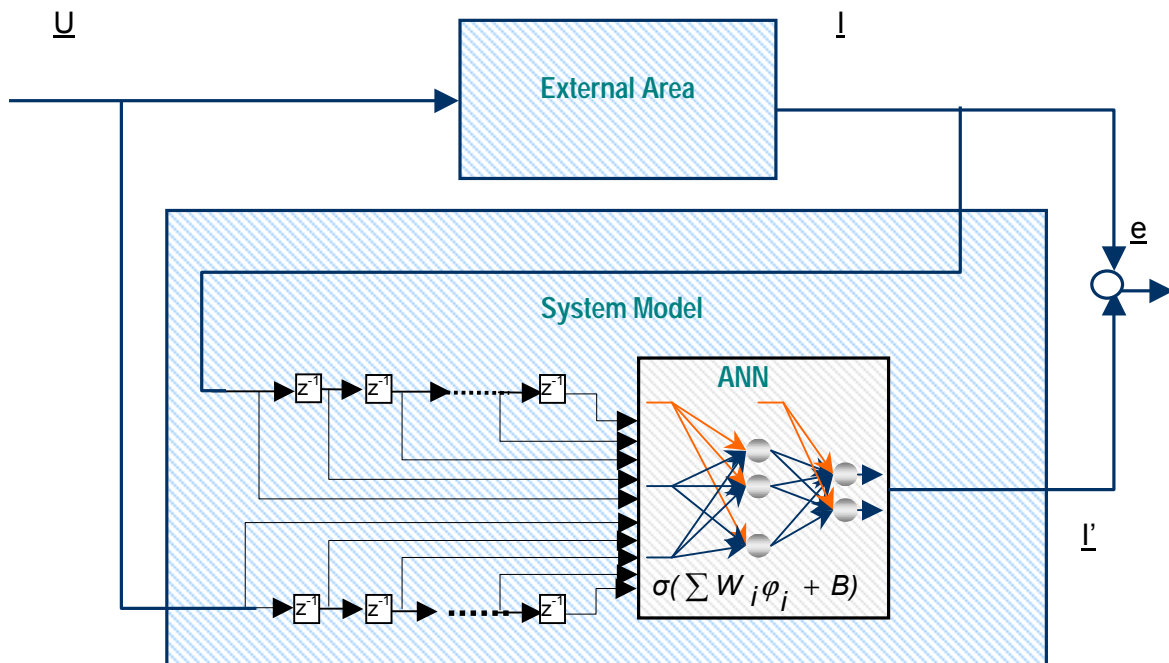


Fig. 5.10.- Network structure for approximation of non-linear systems

The ANN dynamics are realized either using static ANN combined with an external feedback connection (recurrent ANN) or using internal recurrent dynamic ANN, where feedback is introduced internally to the inputs of antecedent neurons. In this study both options are examined and evaluated. Thus, the external recurrent ANN is more enable to provide better and accurate results (For details see Fig. 5.4).

This static ANN depicted in Fig. 5.10 is provided with current and delayed values of the external area inputs and outputs magnitudes. According to equation (5.34) in Fig. 5.10, the implicit time dependence of the system mapping function is thus transformed to an explicit spatial representation by additional inputs to the network, i.e. the neural network learns to associate an output value  $i(t)$  depending on the trajectory determined by the input vector elements  $i(t-1), \dots, i(t-n_i), u(t), \dots, u(t-n_u)$  at the neural network's input.

According to the discrete-time input-output dynamic system representation in (5.37), there are principally two possibilities to implement the ANN structure of Fig. 5.10 in the procedure of the modeling of the complex external area. It can be realized either by means of a configuration presented in the following figure and termed as **series-parallel model** or by **the parallel configuration** represented in Fig. 5.12.



**Fig. 5.11.-** Series-parallel configuration coupling back the observed system output

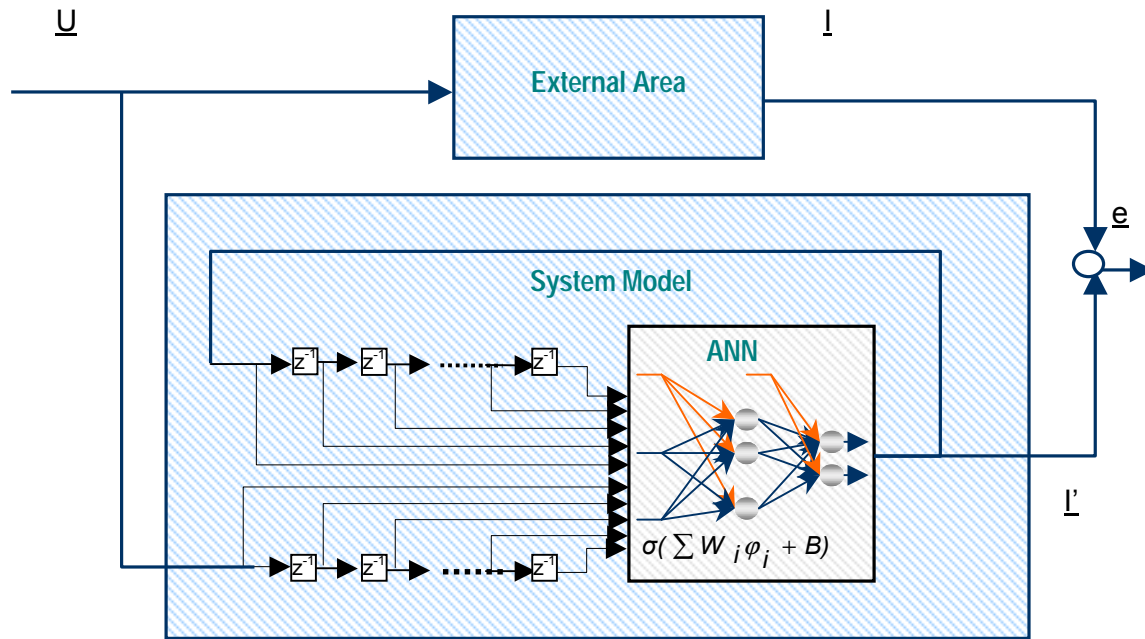


Fig. 5.12.- Parallel configuration with an internal recurrent link to the networks

**Remarks to Fig. 5.11 and Fig. 5.12:**

- The *series-parallel model* in Fig. 5.11 is connected to the external area in a parallel manner with respect to its input and in a serial manner to its output (observer).
- This configuration is advantageous for training purposes, where the desired external area output can be provided to the neural network. Once the ANN has been trained, the identified model can be used independent of the complexity of external area by feeding back the ANN output instead of the real external area output.
- In contrast to this configuration, the *parallel model* in Fig. 5.12 requires an input that is provided and estimated from the ANN self and not from the external area.
- Through this input sequence the error training and cost function evaluated over time intervals will increment significantly.
- However, the primary benefit of this parallel model refers to the very simple synthesis procedure of the ANN whose intern dynamic is implemented requiring the development of time-dependent estimation schemes.
- According to these evaluated factors, the series parallel model has the capability to identify the complex non-linear external area based on the linear system order, which can be implemented according to the number of delays of the external recurrent links of the ANN. The delays approximate the dynamic of the external area.

### iii. Recurrent ANN model as external area

The recurrent ANN is able to capture the dynamic of the external area in the following configuration and on this way it will be interfaced to the internal area for stability studies <sup>19</sup>.

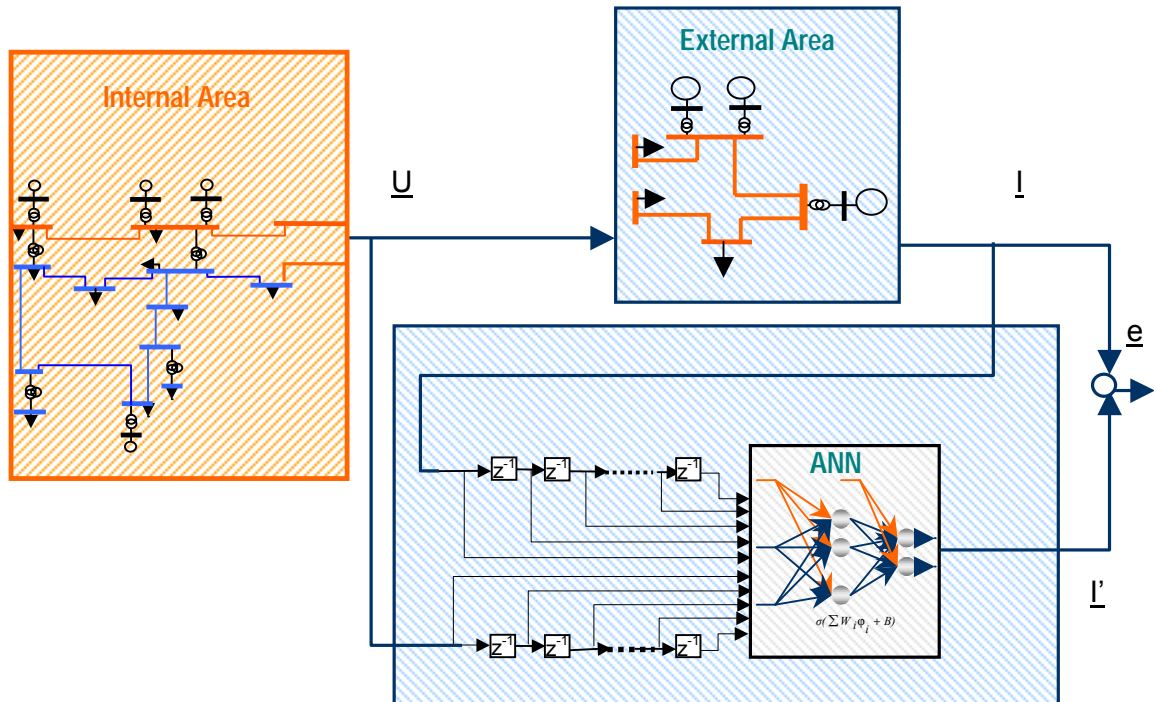


Fig. 5.13.- System modeling for dynamic equivalencing

In this figure the dynamic behavior of the external area can be modeled *using voltage at the boundary buses as input magnitudes and the injected currents into the boundary lines as output* (Norton model). All variables are complex quantities and thus they are treated separately. Therefore, the *selected parameter and structure* of the recurrent ANN must be able to describe a MIMO-system.

The multi-layer network, consisting of an *input layer, one output layer, and an appropriate number of hidden layers* (containing two to four hidden layers with 10 to 24 neurons) depending of the complexity of the system, *may be used as a dynamic approximator*. The multi-layer neural network of hyperbolic tangent units and the output layer of linear units are capable of approximating any non-linear dynamic of the external area and to obtain *optimal non-linear mappings*.

The *number of time delays* in terms of  $n_i$ ,  $n_u$  in (5.35-5.36) must be chosen properly to generate an *optimal regressor vector and estimated initially based on the linear system*

*modeling of the non-linear complex system*, i.e. according to the linear order model of the system and then, it may be adjusted gradually to reach the non-linear description.

It should be noted that the data set as inputs and outputs of the recurrent ANN is chosen taking into account *the variance of the sampling points of the observed data set*. In this case, the littler the distance between sampling points, more accurate will be the modeling of the state space of the complex system, but the mapping function may be too complicated to approximate the external area from the learning and estimation viewpoint and in consequence, the integration time interval between sampling points of the model must be suitably chosen.

#### iv. Estimation of the ANN-model parameters

The structure model of Fig. 5.13 represents the predictor. Its error is evaluated to select the best model using the equation (5.42). Thus, the predicted output  $\mathbf{i}'(t)$ ' of the model is:

$$\mathbf{i}'(t) = E[\mathbf{i}(t) | \varphi(t)] \quad (5.41)$$

The prediction errors  $e(t)$  are a white noise sequence whose variance is minimized. The variance of the prediction error is minimized with respect to the some performance function (5.43) using the minimization of a fit criterion, which is the sum of square errors:

$$E_N(\theta, \mathbf{Z}) = \frac{1}{N} \sum_{t=1}^N \|\mathbf{i}(t) - \mathbf{i}'(t | \theta)\|^2 \quad (5.42)$$

$$E_N(\theta, \mathbf{Z}) = \frac{1}{N} \sum_{t=1}^N \|\mathbf{i}(t) - h_N(\varphi(t), \theta)\|^2 = \frac{1}{N} \sum_{t=1}^N e^2(t, \theta) \quad (5.43)$$

where

- $N$  is the number of samples or the length of data set and
- $\mathbf{Z}$  is a matrix, which contains the system output, and the regressor matrix [128].

Minimization of (5.43) is realized by a parameter estimation algorithm, which iteratively adjusts model parameters  $\theta$  until they achieve optimal values  $\theta^*$  defined as:

$$\theta^* = \arg \min E(\theta, \mathbf{Z}) \quad (5.44)$$

<sup>19</sup> Thus, this *recurrent neural network structure* represented as a partial Finite-Impulse-Response system (causal filter), can replace the external area in terms of a series-parallel configuration as it may be seen in Fig. 5.13.

As can be seen in Fig. 5.13, when the recurrent ANN is used as a parametrized function ' $\mathbf{h}_N$ ', its weights are the model parameters that have to be adjusted as:

$$\boldsymbol{\theta} = [\theta_1, \dots, \theta_n]^T \quad (5.45)$$

Parameter estimation algorithms are those based on gradient numerical optimization, which adjust model parameters according to the following iterative expression:

$$\boldsymbol{\theta}(t+1) = \boldsymbol{\theta}(t) + \Delta\boldsymbol{\theta}(t) = \boldsymbol{\theta}(t) + \alpha(t) \mathbf{S}(t) \nabla E(\boldsymbol{\theta}(t)) \quad (5.46)$$

where:

- $\mathbf{S}(t)$  is the search direction matrix, which contains the gradient search for the minimum of the performance function. Alternative search directions are the gradient direction, Gauss Newton direction and the Lavenberg Marquardt direction.
- $\alpha(t)$  determines the length of the step in the search direction.
- $\nabla E(\boldsymbol{\theta}(t))$  is the gradient of (5.43) with respect to the ANN parameters.

### 5.3.6 Robustness

The approach robustness is characterized by the training, learning procedure and the local distributed dynamics of the recurrent ANN, which will be described as follows:

#### (i) Training procedure

The objective in the training phase is to *take into account extreme and representative disturbance situations* obtaining global MIMO data sets at the boundary nodes. *To generate a suitable set of disturbance, its form and magnitude in the internal area, extended to all disturbance variations, have to be considered.* Following training aspects are important:

- In order to generate global training data sets, *relevant disturbance scenarios in form of three phase short circuits must be carried out involving the whole external area* according to:
  - Faults with defined minimal and maximal duration till to reach the critical time. *A wide range of the fault is suitable.*

- Faults applied on different nodes of the internal area, which are *located principally in different areas* of the internal area.
- These aspects will avoid a redundancy and concentration of training data sets in any small sub area in the internal area.
- The factors that influence the transient stability, such as:
  - *nature, extent of severity, and location of faults,*
  - *load generation balance prior the occurrence of faults and*
  - *network configuration*

must be taken into account in the training range reflecting *the global performance of the replaced external area under various operating conditions.*

- The dynamic ANN-model can predict injected currents following a certain disturbance in the internal area, where *these faults are located in the trained area, i.e. for faults located in the training time range and inside the training location area of internal area.*
- The simulation of each fault is carried out for 10 s, which is enough to restore the dynamic behavior conditions after the disturbance.
- A 10 ms integration time step is used in the simulation generating the pattern variables.
- Complex injected currents and voltages at the boundary buses are stored during the stability simulation and subsequently used to prepare suitable patterns for training the ANN in off-line form.

### (i) Learning procedure

To generate a robust ANN, which is valid for different power flow conditions in the internal area, normalized deviations of the corresponding boundary currents and voltages are used to ANN-learning, as it can be seen in Fig. 5.14.

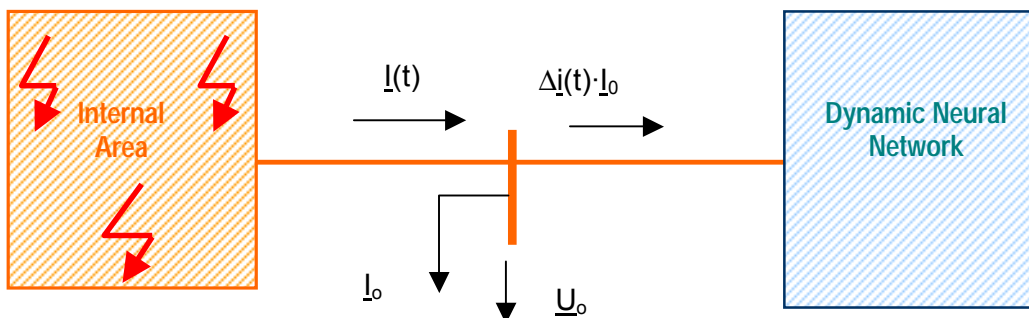


**Fig. 5.14.-** DANN representing the dynamic equivalent for disturbances applied in the internal area

These referenced boundary complex values can be expressed as follows:

$$\Delta \underline{u} = \frac{\Delta \underline{U}(t)}{\underline{U}_o} = \frac{\underline{U}(t) - \underline{U}_o}{\underline{U}_o} \quad (5.47)$$

$$\Delta \underline{i} = \frac{\Delta \underline{I}(t)}{\underline{I}_o} = \frac{\underline{I}(t) - \underline{I}_o}{\underline{I}_o} \quad (5.48)$$

where

- $\underline{U}(t)$ ,  $\underline{I}(t)$  correspond to the real-time complex voltage and current value, respectively
- $\underline{U}_o$ ,  $\underline{I}_o$  corresponds to the initial complex voltage and injected current value at a static operating point of the external area of power system.

Following aspects are important in the learning strategy:

- The use of normalized deviations according to (5.47) and (5.48) allows that the ANN learns during the training process only *the changes of the boundary input and output magnitudes at a certain operating point* with reference to the static operating point or base case specified by loads flow of the power system, characterizing the robustness of the dynamic ANN.
- In this case, this ANN represents a normalized “per unit” model scaled on initial conditions at the boundary buses. Thus, the robust ANN can be used with trained and changed power flow conditions outside the ANN.
- The data pre- and post-processing, i.e. normalization and back normalization, respectively have to be realized outside the ANN.
- The ANN itself acts as a Norton model, where the normalized deviations of voltages are used as main inputs and the normalized deviations of currents represent the outputs.
- Other magnitudes, such as the active and reactive power, or the absolute value and phase of the voltage and current as input and output for the ANN, respectively can be used. However, these measured data signals don't provide the physical and non-linear combination between input and output sets.
- Thus, the use of voltage and current gives better convergence in the training process in comparison with the use of power magnitudes due to the complete decoupling and independency between inputs and outputs of the ANN.
- It should be mentioned, that the results with ANN trained by power variables as input and output variables in one-boundary power systems are high accurate as well as with the ANN trained with injected currents and voltages. But, this aspect can be detected only in power systems with one boundary node between internal and external area.

### (iii) Dynamic ANN with locally distributed dynamic areas

In order to achieve a more accurate ANN-based system model, whose training procedure is less time consuming and offers limited computational requirements, *the learning operating point and dynamic of this ANN-based system model can be distributed according to the power levels of the retained or internal area.*

In comparison to the ANN with distributed dynamics, in the following figure, the global ANN captures the dynamic of the external area excited by internal area with heterogeneous power levels.

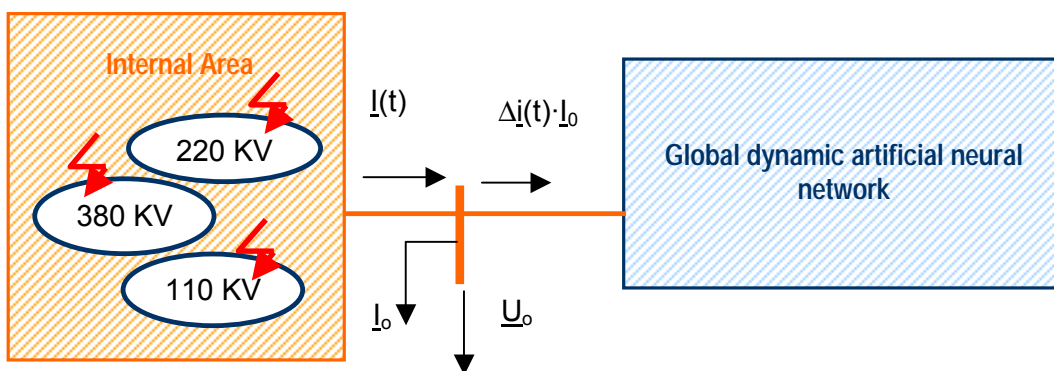


**Fig. 5.15.-** Global dynamic ANN forming the dynamic of the external area

*In order to predict accurate injected currents with less computational requirements, ANNs with locally distributed dynamics are proposed.* This ANN structure with distributed dynamics can interact with an internal area, which consists of heterogeneous power levels, according to its training operating point, i.e. for each power level of the internal area a corresponding ANN will be trained. Thus, following aspects are relevant to the ANN-dynamic distribution:

- The necessary input variables for the training procedure can be obtained by disturbance scenarios in the area of the corresponding power level to form an adequate ANN locally trained.
- The offline locally trained ANN structure will replace the external area dependent on the power level-located disturbance.

The ANN structure with distributed dynamics can be illustrated schematically in the following diagram:

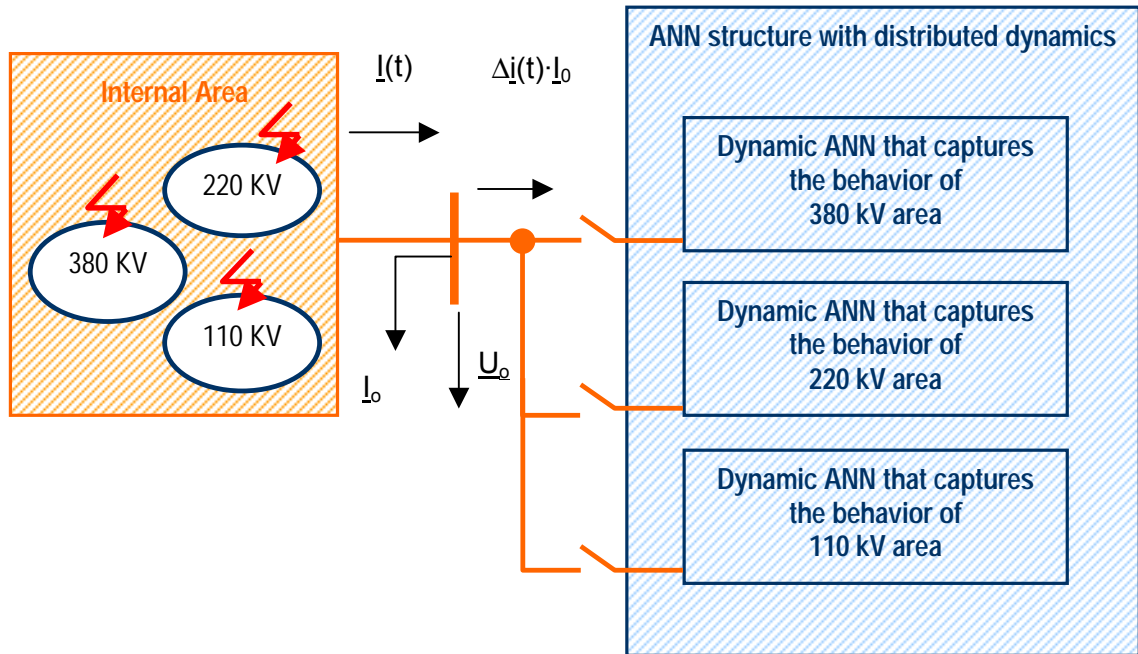


**Fig. 5.16 .-** Dynamic ANN forming the external dynamic with distributed operating points according to heterogeneous power levels of the internal area

**Remarks:**

Briefly, recurrent ANN-based dynamic equivalencing involves following aspects, which are discussed in a previous way extensively:

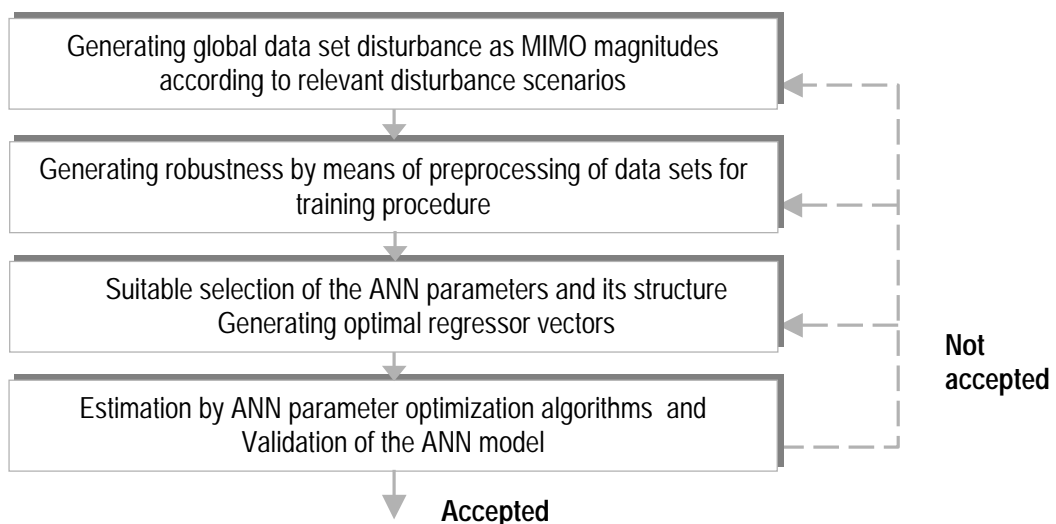


**Fig.5.17.-** Procedure to developing ANN models as dynamic equivalents

However, in order to develop accurate results considering computational aspects, ANN with locally distributed dynamics can be realized according to the previous procedure.

### 5.4 Case studies

The accuracy, effectiveness, and robustness of the recurrent-ANN as dynamic equivalent are evaluated on basis of two multi-machine systems. The following power systems are studied:

- 16 Multi-machine system with 2 boundary nodes and
- 12 Multi-machine system topologically adapted from 3 to 8 boundary nodes.

In both power systems, the synchronous machines are described by 5<sup>th</sup> order models, exciters by 2<sup>nd</sup> and in some cases by 3<sup>rd</sup> order models. A state vector of large dimension characterizes the models of the external areas in both cases.

#### 5.4.1 16 Multi-machine system with 2 boundary nodes

The 16 multi-machine system shown in Fig. 5.18 comprises 16 hydro, nuclear and thermal generators with their corresponding excitation systems.

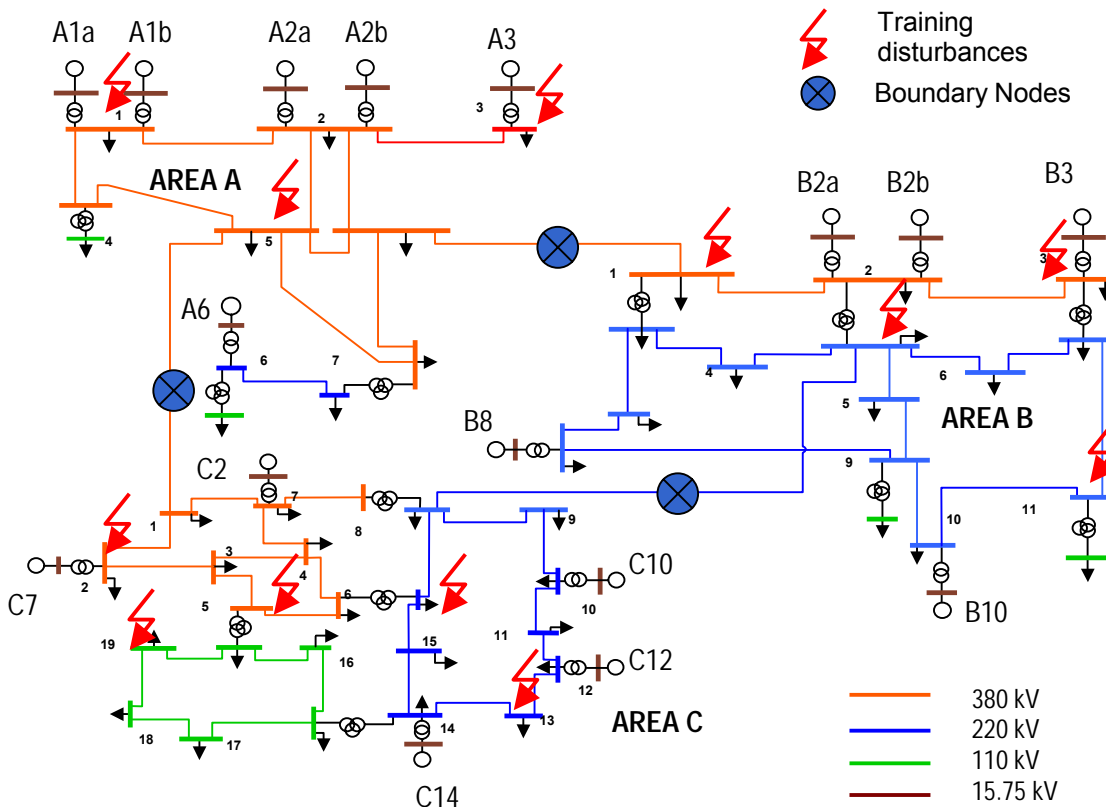


Fig. 5.18.- 16 Multi-machine system with 2 interfaces and three areas

This system consists of three strongly meshed areas A, B and C with different voltage levels, which are connected by boundary buses. Each area has 5 or 6 generators and it has been considered as internal area. Area A is structured to be a power exporting area.

### 5.4.2 12 Multi-machine system with 3 to 8 boundary nodes

This power system contains 12 generators as hydro power plants with their corresponding voltage regulators and governors. On the basis of this network topology, different power systems with different boundary nodes between 3 to 8 nodes may be derived, which may be seen in appendix in Fig. B.1 to Fig. B.5. All systems consist of a 380 kV network with the corresponding internal and external area.

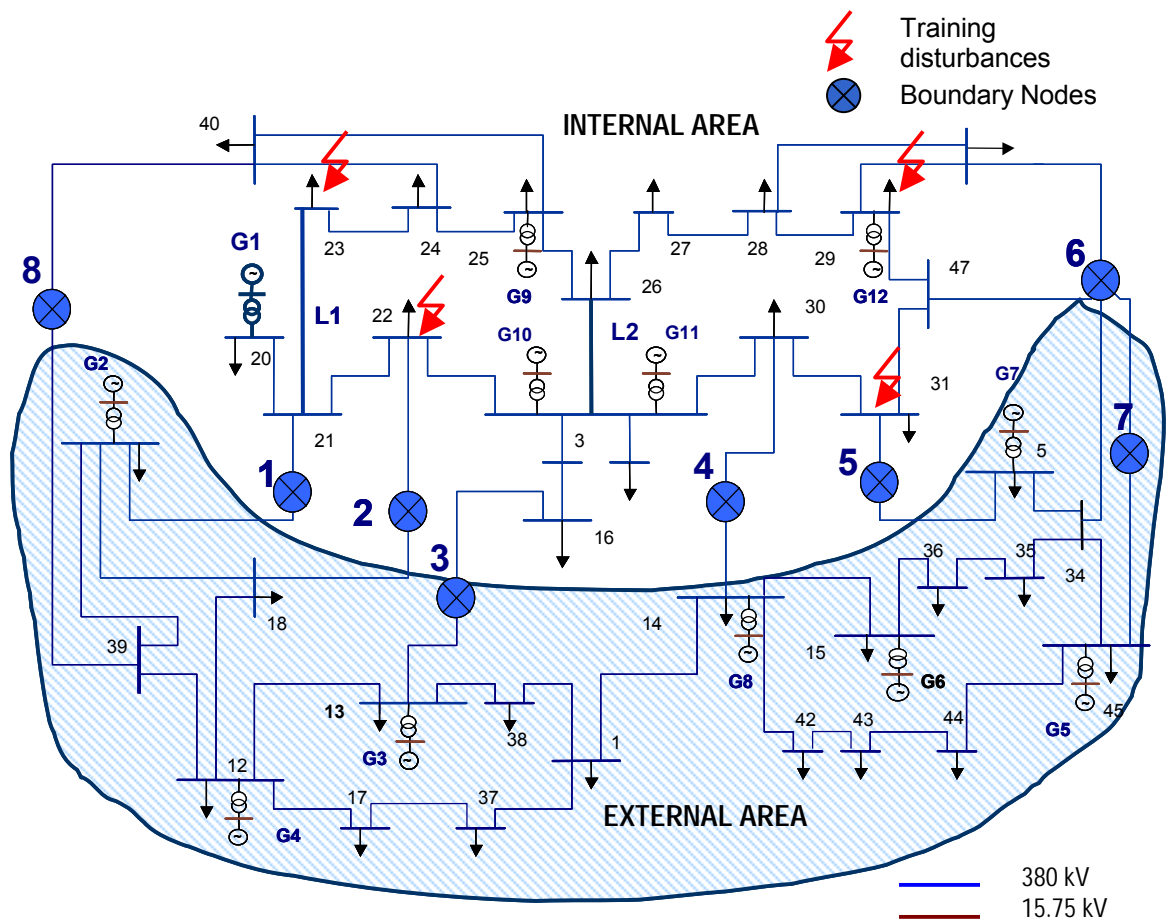


Fig. 5.19.- 12 Multi-machine system with multiple number of boundary nodes

The internal area contains 5 generators and it is a load demanding area. This system is designed in such a way that successively any desired number of boundary interconnections between 3 to 8 can be implemented (MIMO system). The accuracy and principally the robustness of this ANN-based equivalencing approach will be verified in this power system.

## 5.5 Simulation results and discussion

To verify the performance of the recurrent ANN as dynamic equivalent, the ANNs are trained with data sets generated by appropriate disturbance scenarios on various nodes in the internal areas. The location of the disturbances is shown in Fig. 5.18 and Fig. 5.19 and with duration from 100 ms to 150 ms. In case of using the ANN-based equivalent as external area, these disturbances (as three-phase short circuits) and nodes will not be considered within the transient stability simulation. This disturbance begins at 1.0 seconds. The whole system is simulated for 10 second.

The accuracy of the ANN-based dynamic equivalents can be evaluated by comparing the oscillating swing curves of the boundary injected currents and the boundary power flow interconnection with the original power system. The injected currents are calculated with respect to a synchronously rotating reference frame. The original boundary behavior is simulated with the unreduced external area using PSD. For details on PSD see section 2.3.

These simulations are realized in both power systems: i) 16 multi-machine system and ii) 12 multi-machine system.

### 5.5.1 16 Multi-machine system with 2 boundary nodes

This power system is investigated considering following internal and external areas:

**Table 5.1.- Studied cases in the 16 multi-machine system**

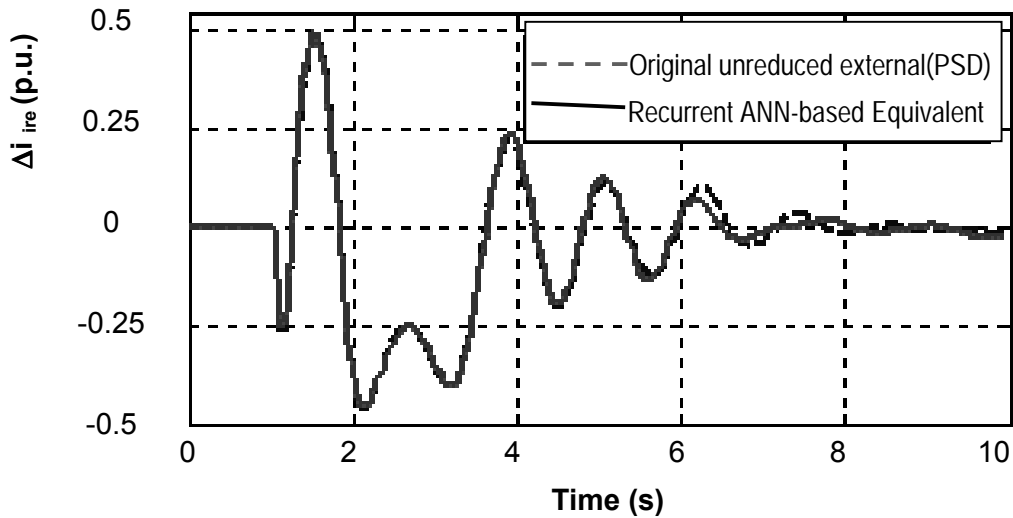
<b>Cases</b>	<b>Internal area</b>	<b>External area</b>
1	380 kV area <b>A</b>	<b>B and C</b>
2	380 kV and 220 kV area <b>B</b>	<b>A and C</b>
3	110 kV, 220 kV and 380 kV area <b>C</b>	<b>A and B</b>

Considering that areas A and B have an uniform voltage level and C incorporates varying voltage levels (see Fig. 5.19), the ANNs are capable to replace heterogeneous external areas from Table 5.1. Areas A, B and C are connected by two boundary lines.

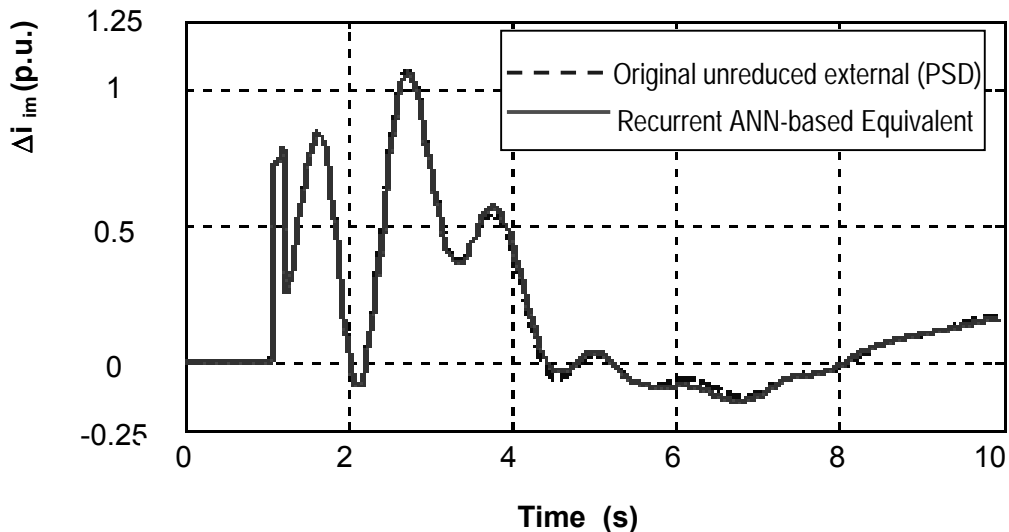
Interfacing the robust trained ANN with the transient stability simulation of the internal area, following cases from Table 5.1 can be evaluated.

**Case 1 — Area A is the internal area, external areas B and C are replaced by the ANN.**

The following figures demonstrate the boundary-injected currents following a non-trained disturbance with duration of 100 ms on the node 4 in area A.



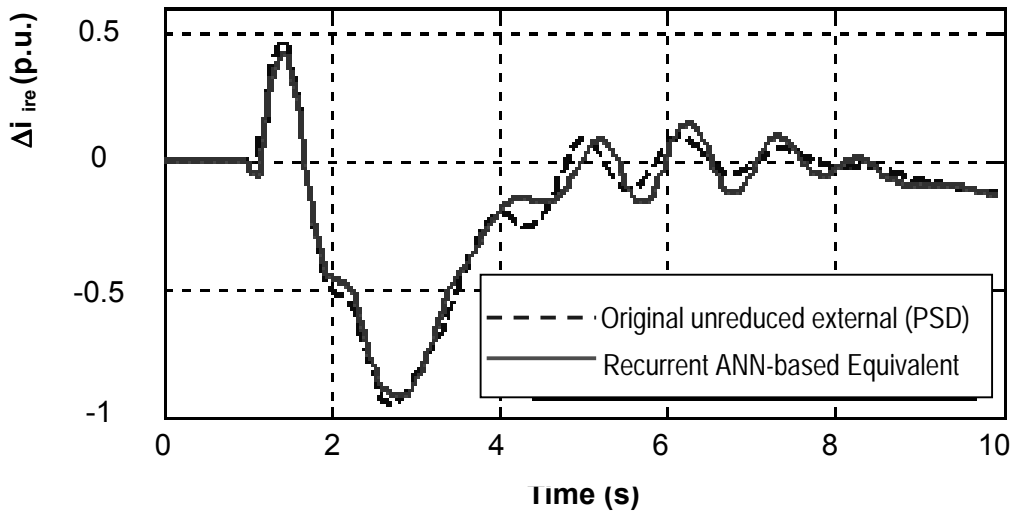
**Fig. 5.20.i** - Real part of the injected current at the second boundary node following a non-trained disturbance in area A



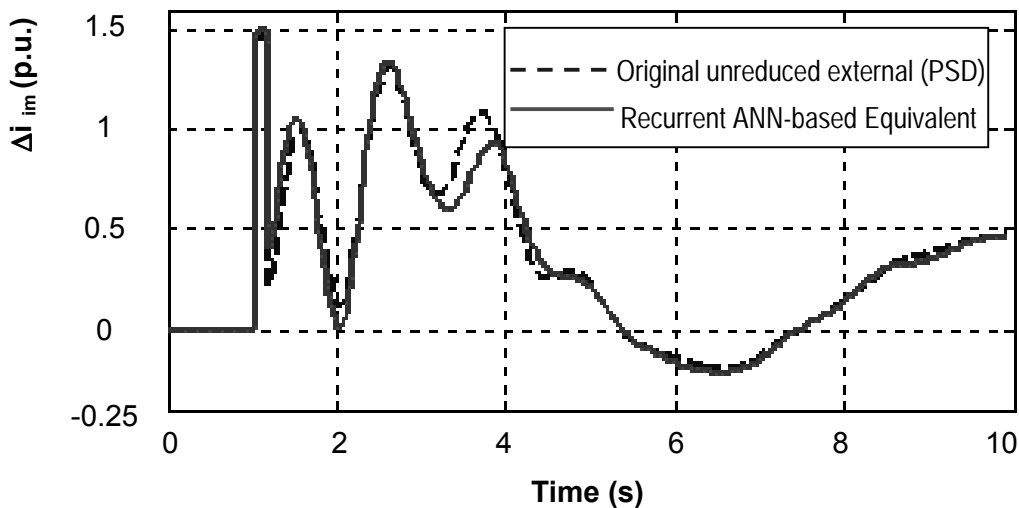
**Fig. 5.20.ii** - Imaginary part of the injected current at the second boundary node following a non-trained disturbance in area A

Fig. 5.20.i and Fig. 5.20.ii show a high degree of accuracy of the predicted current from the ANN with respect to them simulated with the original external area. Relatively, the same prediction quality is obtained at boundary nodes following other non-trained faults on the nodes 2, 6, 7 and 8 (see Fig. 5.18) in the internal area A.

Successfully, the robustly trained ANN captures the external area dynamics considering other load flow condition, i.e. the ANN can be interconnected to a changed internal area with other operating point, where the load in the internal area A was reduced to half of its previous value of the training. The simulation results are shown in Fig. 5.21:



**Fig. 5.21.i** .- Real part of the injected current at the first boundary node following a disturbance (100 ms) at node 7 in area A under changed operating point



**Fig. 5.21.ii** .- Imaginary part of the injected current at the first boundary node following a disturbance (100 ms) at node 7 in area A under changed operating point

It can be seen in Fig. 5.20 and Fig. 5.21 that the phase and amplitude of all predicted boundary injected currents shows a notable accuracy and agreement with respect to them simulated with the original area. The dynamic behavior of these currents under different operating points (trained and non-trained) is quite identical over the whole time period.

The sum squared distance error and average error of the predicted boundary behaviors following disturbances at all non-trained nodes of internal area A and considering different operating points (trained and non-trained) are summarized in appendix in table D.5 and D.6.

### Case 2 — Area B constitutes the internal area, areas A and C are replaced by ANN

In same manner, Fig. 5.22 shows a high degree of accuracy of the ANN-predicted injected current in comparison to the real time currents using the original external area. This stability simulation is realized following a non-trained disturbance of 100 ms at the node 6 in area B.

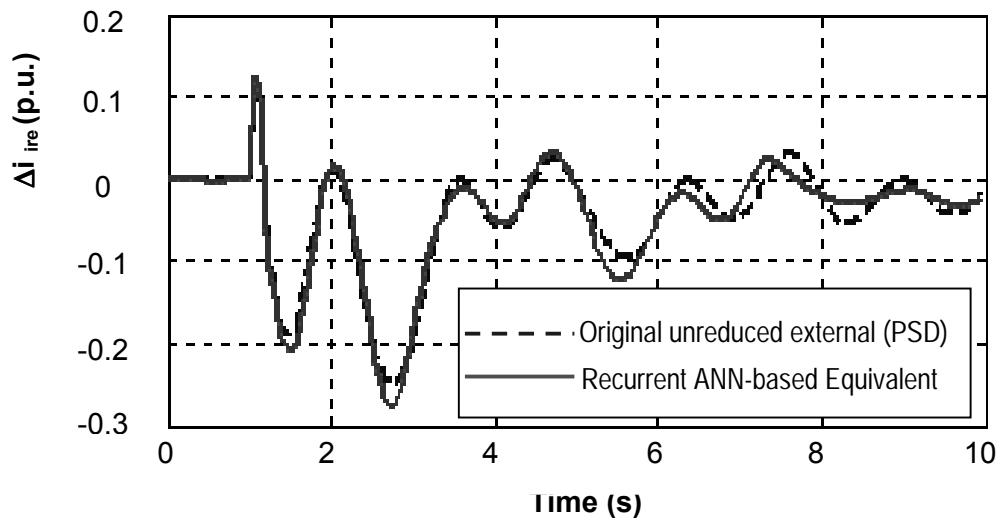


Fig. 5.22.i .- Real part of the injected current at the first boundary node following a disturbance (100 ms) on node 6 in area B

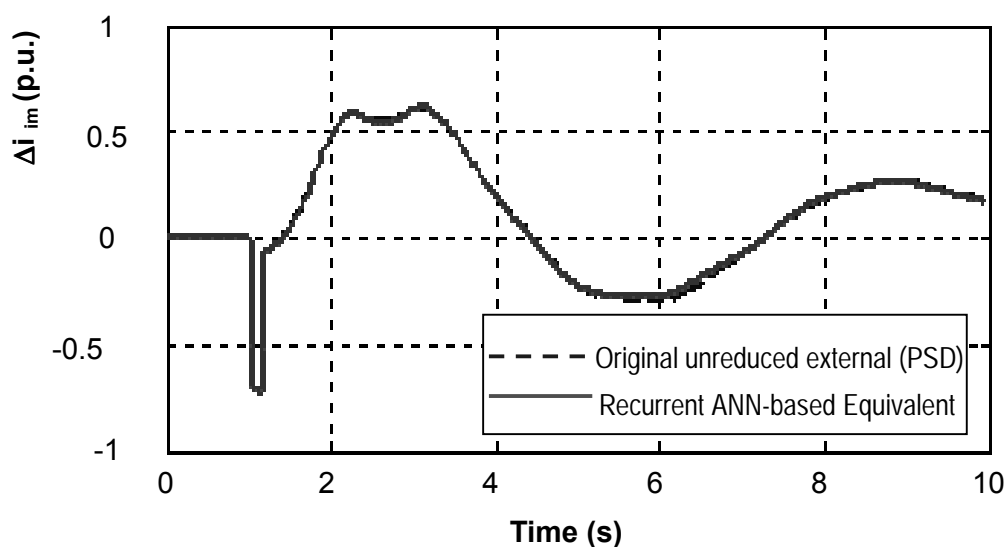
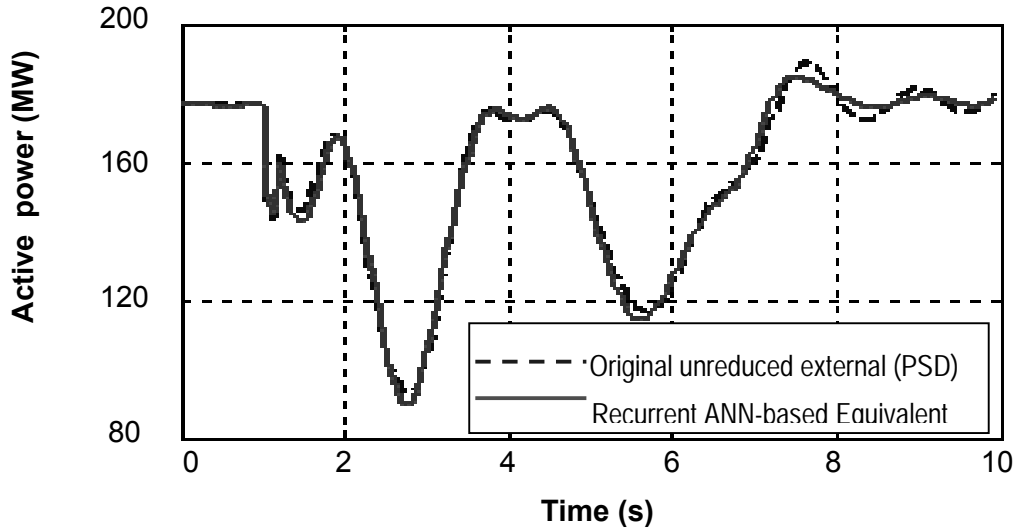
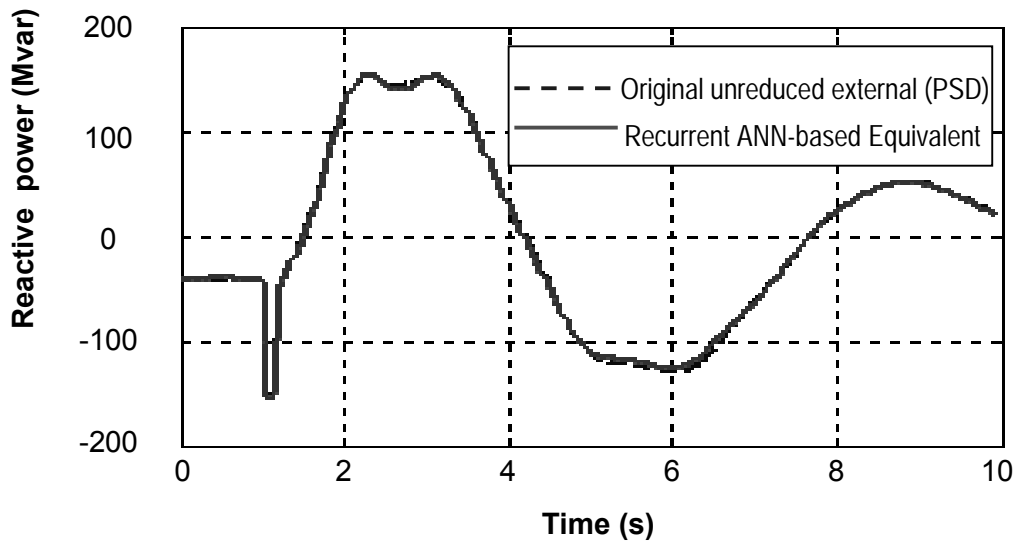


Fig. 5.22.ii .- Imaginary part of the injected current at the first boundary node following a disturbance (100 ms) on node 6 in area B

In Fig. 23.i and Fig. 23.ii, active and reactive power flows in interconnection between nodes 5 in B and 8 in C (boundary line of area B and C) are shown, together with waveforms obtained in the original system.



**Fig. 5.23.i** .- Active power flow interconnection between nodes 5 in B and 8 in C boundary line of area B and C according to the currents of Fig. 5.21



**Fig. 5.23.ii** .- Reactive power flow interconnection between nodes 5 in B and 8 in C boundary line of area B and C according to the currents of Fig. 5.21

This power transmission between area B and C suggest that the ANN-based equivalent successfully capture the external area dynamic with a high degree of accuracy after and before the disturbance and the overall response quality is satisfactory.

The sum squared distance error and average error of the ANN-predicted boundary behaviors following disturbances at all non-trained nodes of internal area B and considering different operating points are summarized in appendix part in table D.5 and D.7.

### Case 3 — C is the internal area, areas A and B are replaced by the ANN

The ANN-predicted current is quite accurate, compared with the current simulated with help of the original external area. This simulation is realized following a non-trained disturbance of 120 ms at node 15 in 220 kV of C, as shown in Fig. 5.24.

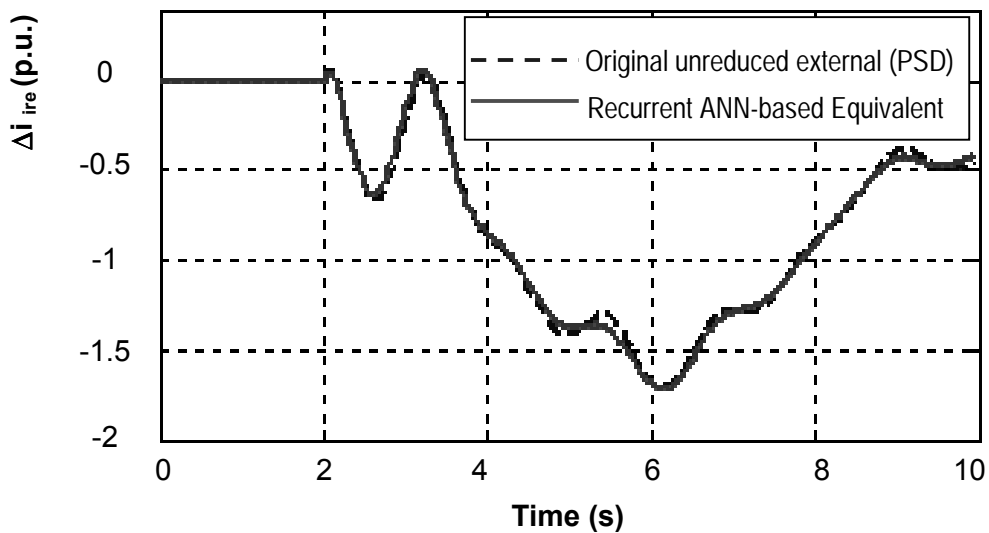


Fig. 5.24.i .- Real part of the injected current at the second boundary node following a disturbance on node 15 in 220 kV of area C

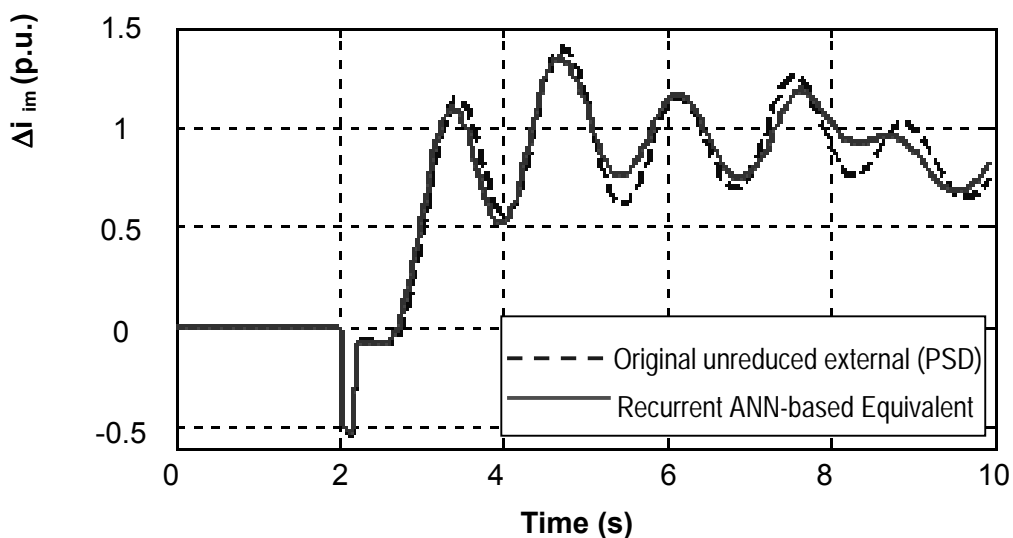


Fig. 5.24.ii .- Imaginary part of the injected current at the second boundary node following a disturbance on node 15 in 220 kV of area C

The robustness of the ANN equivalent can be evaluated under changed operating points, caused by load changes, generator disconnection and disconnection of the transmission line between node 3 and 4 in area C. From the ANN-predicted currents the following power flow interconnection between area C and B can be derived following a fault of 120 ms at node 5 in 110kV of area C.

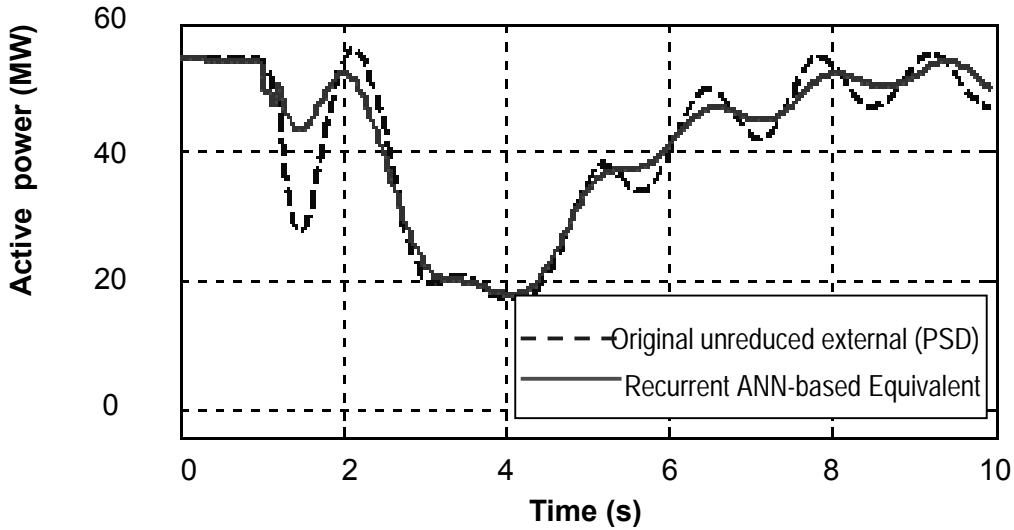


Fig. 5.25.i .- Active power flow interconnection between area C and B following a fault on node 5 in 110 kV of C by changed operation point

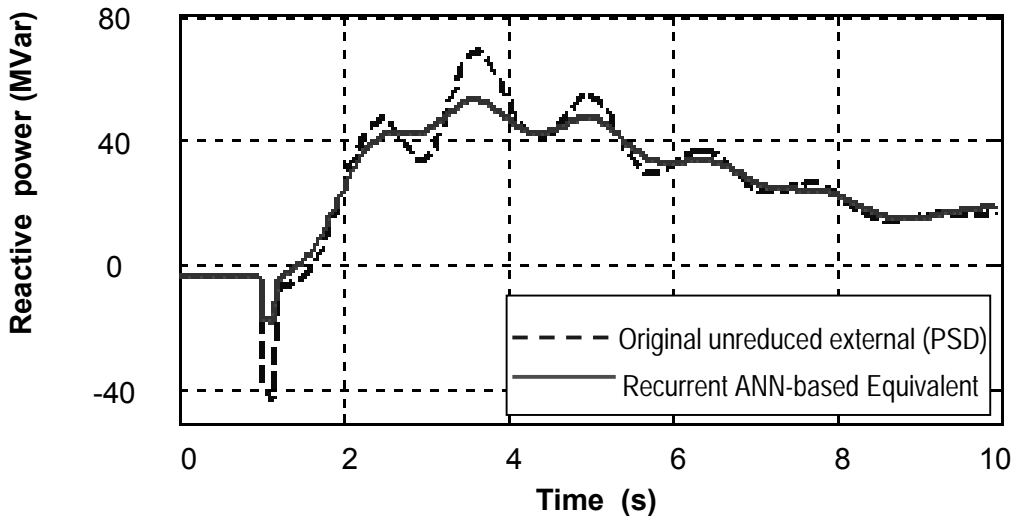
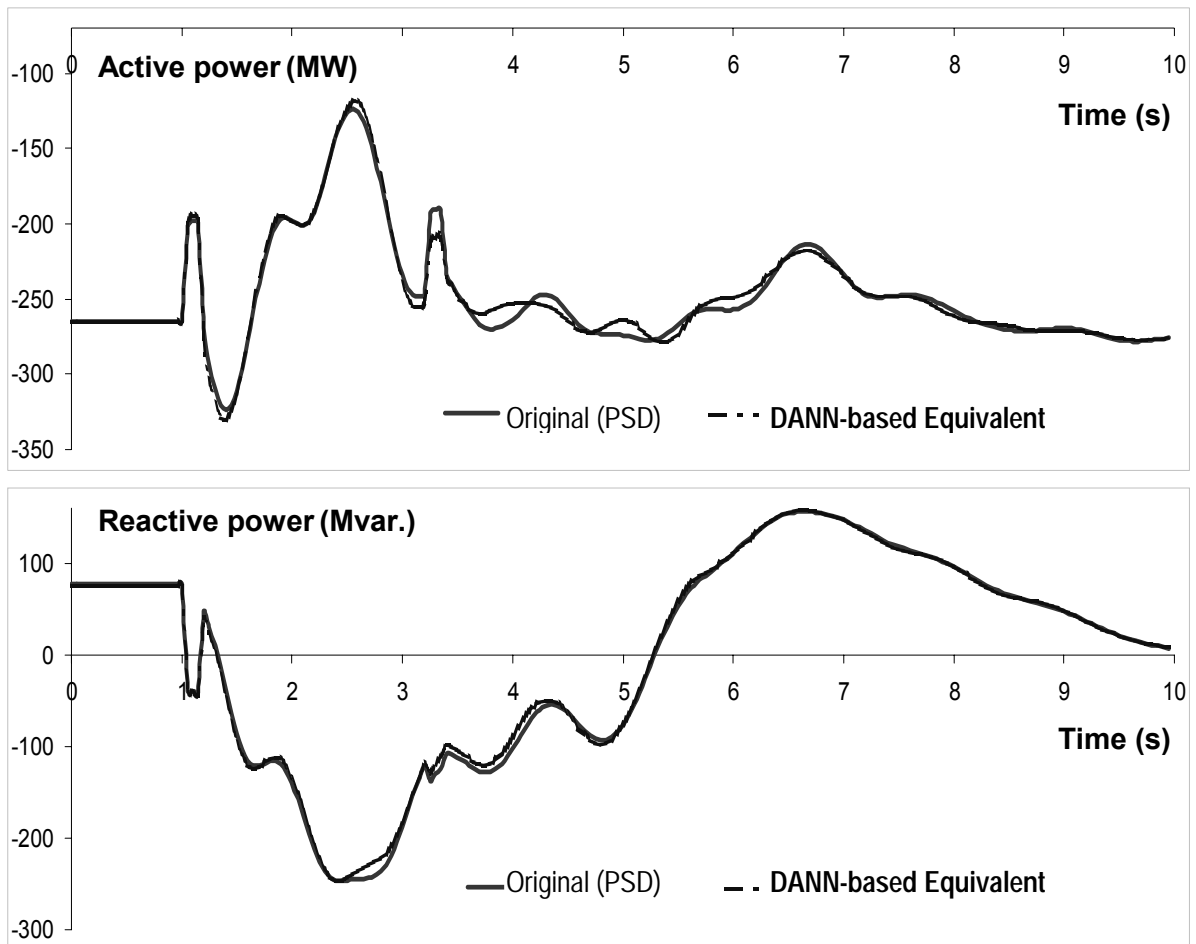


Fig. 5.25.ii .- Reactive power flow interconnection between area C and B following a fault on node 5 in 110 kV of C by changed operation point

In Fig. 5.25, the active and reactive power flow behaviors show a low loss of accuracy. This is not surprising, since the disturbance and operating point are not in the training database.

Moreover, this ANN captures the dynamic of the external area independent of the disturbance and under changed operating point, caused by generator disconnections, line disconnections and strong load reduction in the internal area, i.e. the ANN can be interconnected to the changed internal area with regard to the network topology, and power generating.

Thus, on the basis of the ANN-predicted injected current the power flow transmission between area A and C can be on-line simulated in conjunction with PSD. This simulation following a sequence of non-trained faults (after 1 sec. and 3 sec. with 150 ms and 200 ms duration, respectively) applied on non-trained nodes is shown in the following figures:



**Fig. 5.26.i, ii.-** Power flow interconnection between area A and C following a sequence of nontrained faults on C by changed operation point and network topology

This predicted power flow transmission in Fig 5.26 suggests that the ANN-based equivalent successfully capture the system dynamic of the interconnected external area with a high degree of accuracy considering the changed operating point condition. Through this aspect the robustness of this ANN-based approach is being extensively demonstrated.

The sum squared distance error and average error of the predicted boundary behaviors following disturbances at all non-trained nodes of internal area C and considering different non-trained operating points are summarized in appendix part in table D.5 and D.8.

### Quality measurement of the ANN-based dynamic equivalent

For a more precise evaluation of the approximation between the injected currents calculated with the original external area and the injected currents predicted by the ANN, the following sum of square error can be defined:

$$E_{N_p}(j) = \frac{1}{N_p} \sum_{t=1}^{N_p} [\Delta i_j(t) - \Delta i_j'(t)]^2 \quad (5.49)$$

where

- $\Delta i_j(t)$  the change of the injected current following disturbance  $j$  considering the original model of the external area,
- $\Delta i_j'(t)$  the change of the injected current following disturbance  $j$  predicted by the ANN as dynamic equivalent,
- $E_{N_p}(j)$  is the error function. This measure is realized over the sampling points  $N_p$  of the whole behavior and for the disturbance  $j$ .

The standardized form of this error function can be reformulated as:

$$E_s(j) = 1 - E_{N_p}(j) \quad (5.50)$$

$$\bar{E}_s = \frac{1}{N_D} \sum_{j=1}^{N_D} E_s(j) \quad (5.51)$$

The standardized error function of the injected current of all non-trained disturbances is summarized and averaged to form their mean value as expression (5.51). Where  $N_D$  is the number of non-trained disturbances with the same duration applied to the nodes, which are not considered in the training database.

By means of the standardized error function  $\bar{E}_s$ , the ANN-based dynamic equivalencing will be evaluated regarding the quality, accuracy, and modeling capability. The disturbances and the nodes (on which the disturbances are applied) are not trained.

The result simulations of the 16 multi-machine system which was investigated according to cases 1, 2, and 3 of table 5.1, are compared with reference to their accuracy considering separately area A, B and C as internal areas.

Considering the non-trained disturbances in the internal area A, B and C, and the non-trained operating points, such as load reduction on the corresponding internal area, the prediction capability and robustness of the ANN are evaluated using the beam representation of the  $\bar{E}_s$  value in the following illustration <sup>20</sup>:

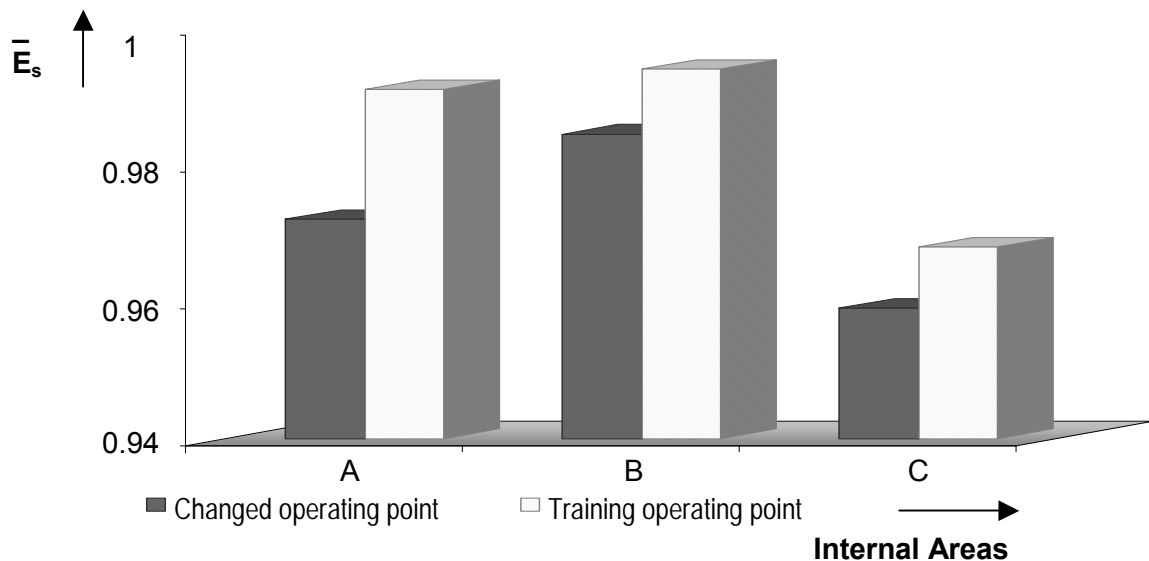


**Fig. 5.27.-** Evaluation of the prediction capability of ANN considering different non-trained disturbances and non-trained operating conditions

Following aspects in Fig. 5.27 can be detected:

- The ANN replacing the areas A and B as external area, i.e. C as internal area, shows results, which are less satisfactory considering both operating points. This behavior is because of the heterogeneous voltage levels of the internal area C and in consequence due to the different operating points of the dynamic ANN to capture the dynamic of the external area. This degradation in accuracy may be observed representatively in Fig. 5.24 and Fig. 5.25.
- In this case, an improvement in accuracy can be obtained using the ANN structure with locally distributed dynamics.

<sup>20</sup> The values are summarized in appendix part in table D.5, D.6, D.7 and D.8, in which the sum squared distance error and average error of the predicted boundary behavior are presented.

- Moreover, in case of considering area A and B as internal areas, a low mean error function or significant accuracy can be obtained. However, in the three cases, area A, B and C as internal area, best results are achieved under the training operating points.
- The mean error function under changed operating points (illustrated by dark bar) is low enough considering A, B and C as internal areas, which may be observed in Fig. 5.21 and Fig. 5.25 as extreme cases. With this evaluation the robustness of this approach is successfully verified.
- Its reduced accuracy with reference to the training operating point in the three cases can be accepted. As can be seen in Fig. 5.21 and Fig. 5.25, the injected currents and power flow interconnections are satisfactorily accurate.

### 5.5.2 12 Multi-machine system with 3 to 8 boundary nodes

In order to evaluate the robustness of the ANN-based equivalencing, the 12 multi-machine system, which is topologically adapted from 3 to 8 boundary nodes, i.e. to 6 different power systems with 12 machines, is evaluated according to different operating conditions <sup>21</sup>. These conditions are summarized in the following Table:

**Table 5.2.-** Scenarios to power-flow changes considering Fig.5.19

Cases	Load Conditions	Location in network
1	Initial Loading Condition (Training operating point)	
2	Generator Disconnection	G1
3	Transmission Line Disconnection	L1, L2
4	Generator, Line Disconnection and Load Reduction	G1, L1, L2 and load reduction on all nodes of internal area
5	Load Reduction to half	On almost all load nodes in internal area

In case 1, the ANN replaces the original external area under the same operating point, under which the training of the ANN was realized. Consequently, this case may be considered as an initial or reference operating point. In the subsequent cases, the global trained ANN will replace the external area under new non-trained operating conditions.

<sup>21</sup> The corresponding power flow changes and losses of the 12-machine system with different boundary nodes are summarized in appendix part in tables E.5 to E.9.

All results of the power systems with 3 to 8 boundary nodes are similar accurate. However, a representative scenario as worst case will be presented in Fig. 5.28. It is based on the 12 multi-machine system with 8 boundary nodes, where the non-trained fault of 120 ms is applied on the node 20 in the internal area under the trained operating point according to case 1 in table 5.2.

In Fig. 5.28, the power flow interconnection between node 39 and 40 on the 8<sup>th</sup> boundary line is demonstrated (see Fig. 5.19). Hereby, it may be detected that the performance of the ANN-predicted active and reactive power shows a quite agreement and accuracy during the whole simulation, i.e. before and after the disturbance.

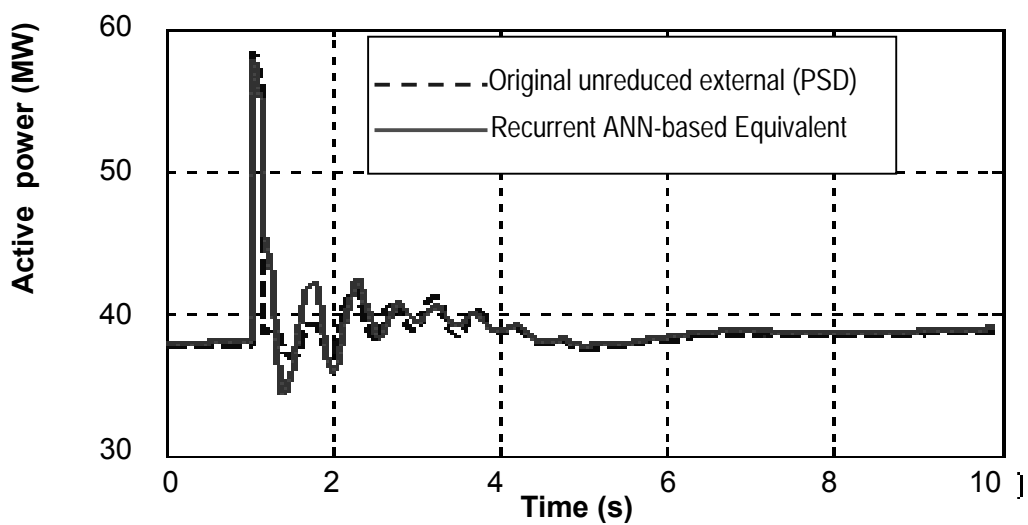


Fig. 5.28.i .- Active power flow interconnection at the 8<sup>th</sup> boundary node or between node 39 and 40 following a fault on the node 20 within the internal area

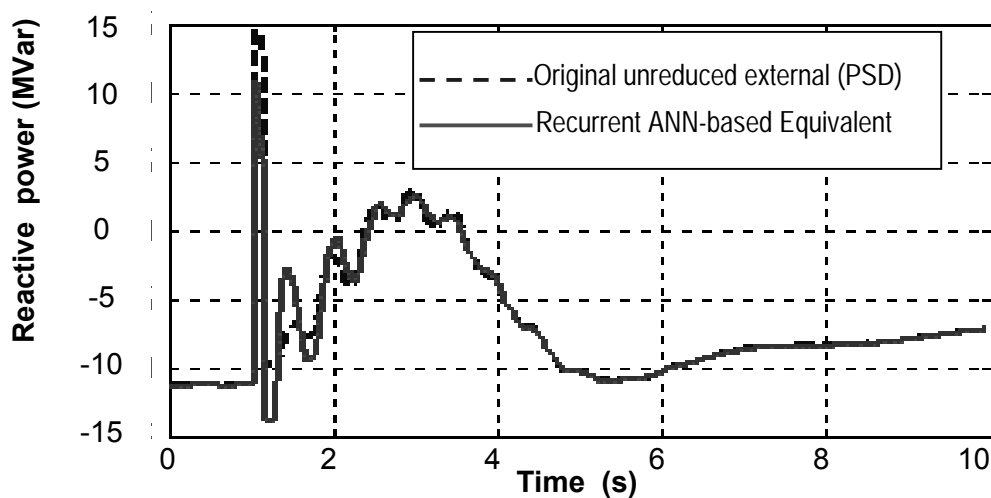
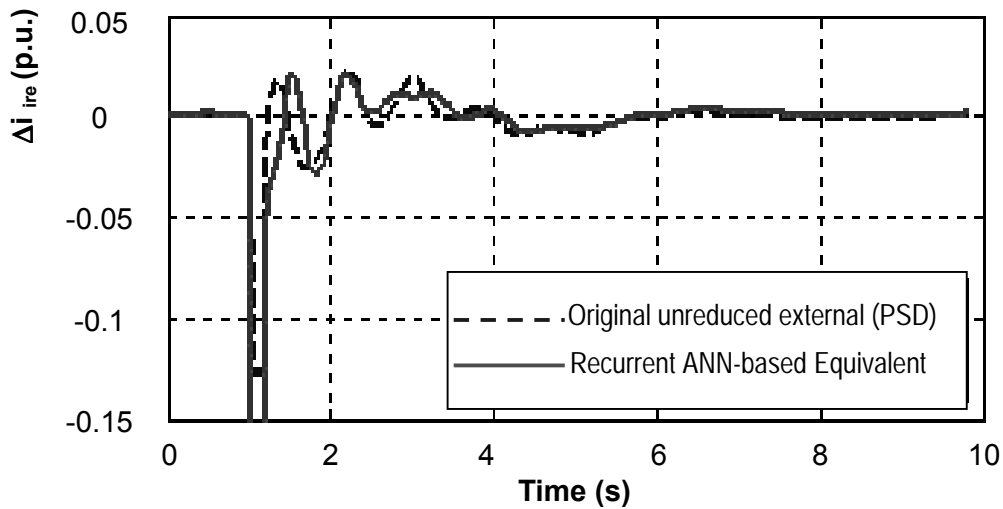


Fig. 5.28.ii .- Reactive power flow interconnection at the 8<sup>th</sup> boundary node or between node 39 and 40 following a fault on the node 20 within the internal area

This high accuracy has been determined too in the 12 machine systems whose internal and external area are connected by 3 until 8 boundaries and considering extremely changed operating points based upon cases 2 to 4 from table 5.2.

In Fig. 5.29, a representative scenario as the worse case is presented, where a non-trained disturbance of 100 ms is located on node 26 in internal area in the 12-machine power system with 8 boundary nodes under extremely changed operating conditions (case 4 from Table 5.2), i.e. considering at the same time generator disconnection G1, lines disconnections L1 and L2 and a considerable load reduction in the internal area.



**Fig. 5.29.i** .- Real part of the injected current at the 8th boundary node following a disturbance on the node 20 in internal area under non-trained operating point of case 4 in table 5.2

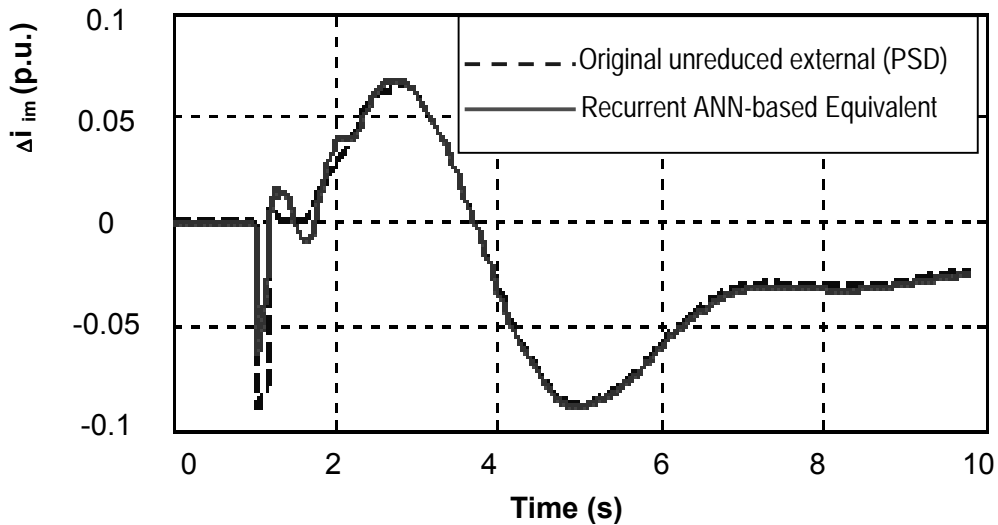


**Fig. 5.29.ii** .- Imaginary part of the injected current at the 8th boundary node following a disturbance on the node 20 in internal area under non-trained operating point of case 4 in table 5.2

The Fig. 5.29.i and Fig. 5.29.ii show an acceptable accuracy. However, this is not surprising, since both the disturbance and the operating point are not in the training database.

Both Fig. 5.28 and Fig. 5.29 as worse cases show a good agreement of the ANN-predicted active, reactive power and complex injected currents in its dynamic performance.

However, degradation in accuracy may be detected after the number of boundaries. The behavior waveforms are more accurate and agreement, the smaller the number of boundaries in the power system, as it can be showed illustratively in Fig. 5.31.

### Evaluation of the ANN-based equivalencing in the 12 multi-machine system

The mean square error function  $\bar{E}_s$  of the ANN-predicted injected currents according to (5.51) in power systems with 3 to 8 boundary nodes may be calculated considering:

- Different durations of non-trained disturbances and
- Different non-trained operating conditions according to table 5.2

#### a) Different duration of non-trained disturbances

In the Fig. 5.30, the abovementioned evaluation can be realized using the beam representation of the  $\bar{E}_s$  value for the 12-machine system with 3 to 8 boundary nodes.

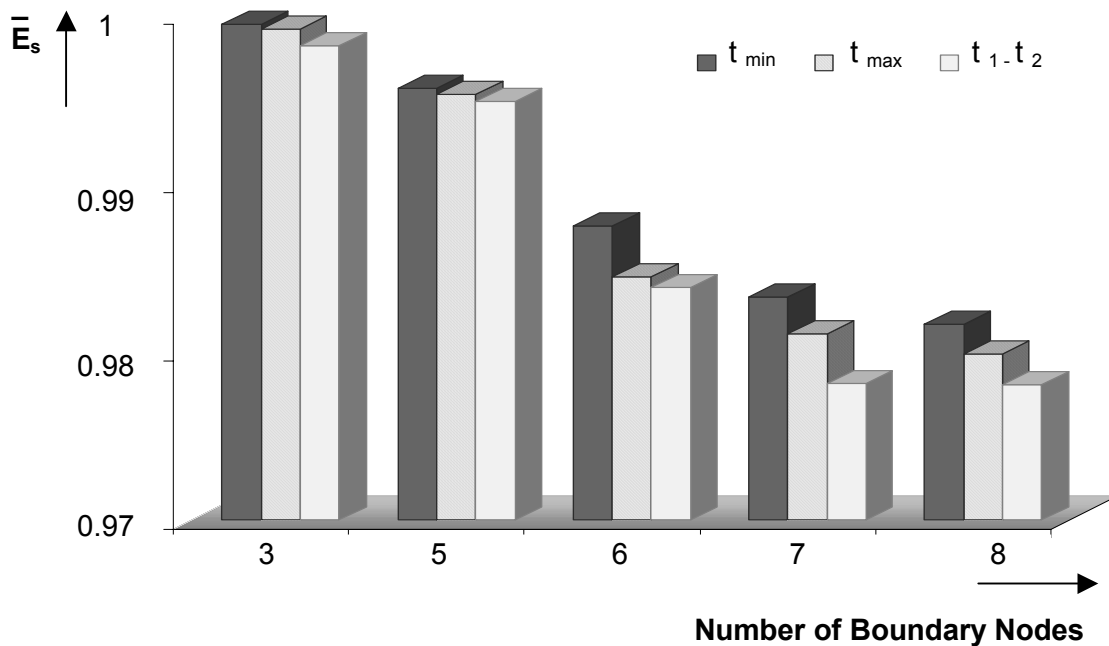


**Fig. 5.30.-** Evaluation of the standardized prediction error  $\bar{E}_s$  of recurrent ANN considering different disturbance duration ( $t_{min}=100$  ms,  $t_{max}=150$  ms) and two sequential disturbances ( $t_1=100$ ms after 1s,  $t_2=120$  ms after 2s)

The disturbance durations <sup>22</sup> correspond to:

- $t_{\min}=100\text{ms}$
- $t_{\max}=150\text{ms}$  and
- the sequence of 2 different disturbances with a duration of  $t_1=100\text{ms}$  applied after 1sec.,  $t_2=120\text{ms}$  after 2 sec. on different nodes.

Fig. 5.30 may be interpreted as follows:

- It shows a low mean prediction error in the 12 machine system with 3 and 5 boundary nodes for all disturbance durations and the sequence of disturbances.
- However, with the increase of the number of boundary nodes, this mean error function is also increased, but a satisfactory accuracy in the 12 machine system with 3 to 8 boundary nodes can be obtained, as can be observed in the presented worst cases in Fig. 5.28 and Fig. 5.29.
- From the Fig. 5.30 is depicted that following a sequence of disturbances, not enough accurate results are determined in the 12 machine system with 7 and 8 boundary nodes.
- However, these results for stability studies can be accepted, because a good agreement between original and ANN-predicted injected currents is obtained.

#### b) Different operating points

In order to evaluate the robustness of the ANN-based dynamic equivalent under different operating power flow conditions <sup>23</sup> expressed in cases 2 to 5 (i.e. non-trained operating points) in table 5.2, the mean standardized square error function  $\bar{E}_s$  of all injected currents following the non-trained faults applied on non-trained nodes in the 12 machine system with 3 to 8 boundary nodes are calculated. The power flow relationships of these power systems are summarized in the appendix table E.5 to table E.9.

Illustratively, these evaluation results are presented using the beam representation of the  $\bar{E}_s$  value in the following figure. Numerically, the results are summarized in the appendix in table E.4.

<sup>22</sup> These disturbance durations must be within the range, in which the training procedure was realized.

<sup>23</sup> The offline trained ANN can be used in a transient stability analysis under different operating points. Transmission line disconnection, loss of a large generator and load modulation are impacts, which create an imbalance between generation and load with respect to the initial training operating point.

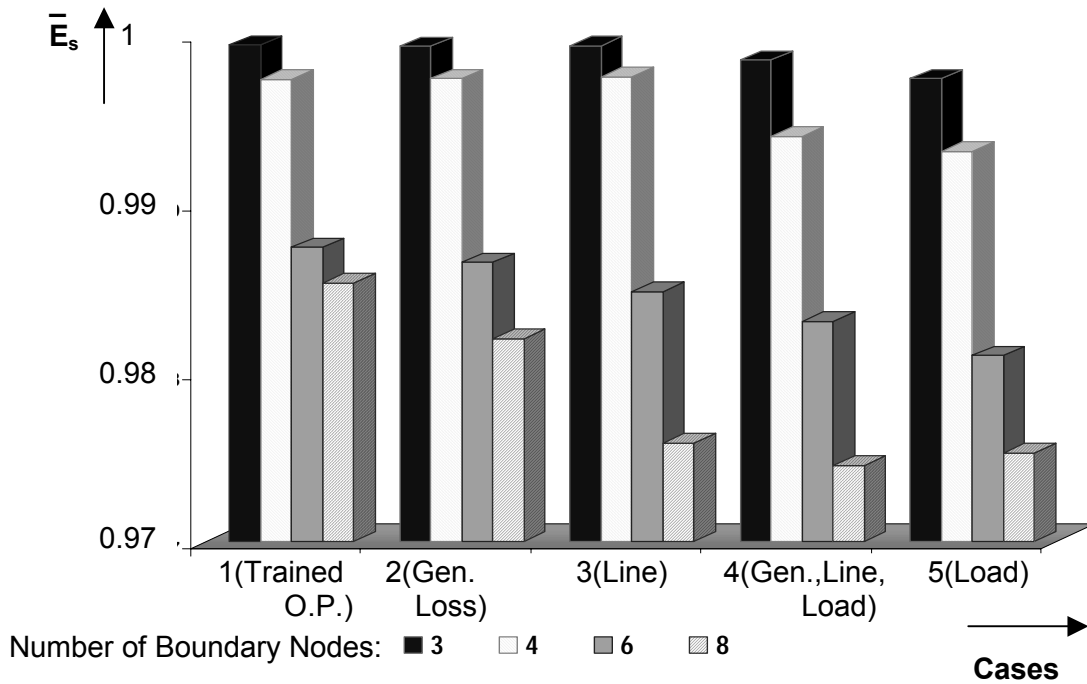


**Fig. 5.31.-**  $\bar{E}_s$  evaluation of the robustness of the recurrent ANN depending on the cases of table 5.2 and in the 12 multi-machine system with different boundary nodes<sup>24</sup>

Fig. 5.31 shows following characteristics:

- Case 1 shows the lowest mean standardized square errors  $\bar{E}_s$  considering the operating point, in which the ANN was off-line trained for all adapted networks of the 12 machine system with 3, 4, 6 and 8 boundary nodes. Therefore, in this case, the best agreement and accuracy of the ANN-predicted currents are obtained.
- In case 2 (in spite of a large generator disconnection, i.e. changed operating point), the mean error function is similar to them of case 1 (trained operating point) in all 12 machine systems with different number of boundary nodes.
- In cases 3 to 5 (extremely changed power flow conditions), the light bars (corresponding to systems with 6 and 8 boundary nodes) show a detectable increasing of the mean error function depending on the strong of the operating point change.
- In all cases, the mean errors corresponding to the 12 machine systems with 3 and 4 boundary nodes (1. and 2. hatched bars) are lower than one of systems with 6 and 8 boundary nodes and relatively constant.
- *Briefly, considering all cases, i.e. all examined changed operating points, with the increase of the number of boundary nodes, the mean error of the predicted currents will be increased or  $\bar{E}_s$  is decreased. This aspect is due to the limited MIMO modeling*

*capability of the recurrent ANN. Moreover, because of the limited computational resources.*

- *However, an accurate modeling capability of the ANN for power systems with small number of boundary nodes can be detected independent of the change of the operating point.*
- *In spite of the lowest mean standardized error of worst cases 4 and 5 (extremely changed power flow conditions) in the 12 multi-machine system with 8 boundary nodes, the ANN-based equivalent predicts accurate injected currents (whose response quality are satisfactory), which can be observed in Figure 5.29.*

This approach is very useful and applicable as dynamic equivalent of a power system independent of its size, complexity and number of boundary nodes. Because it does not require the full system parameters and the state variables of the external area. This aspect was fairly demonstrated in the 16 multi-machine system and 12 multi-machine system, with 2 and 8 boundary nodes, respectively.

In practical application following aspects can be determined:

- Some restrictions arise when applying this approach to large number of external machines, such as in the interconnected European power system and also the non-linear system dimension can cause some limitations in the computational procedures.
- However, this approach can be suitably applied to an analogous strongly meshed power system, such as the Western North American System (WSCC) [144]. This system comprises 46 nodes, 19 generators; the full model is characterized with a 123-dimensional state vector, which is analogue to the 16 multi-machine system.
- The problem of the interconnected European power system is the complex order of the state system of the external area, because higher is the dimension of the state vector, higher is the number of hidden units, too.
- Thus, the increase of hidden units influences the computational complexity of the DANN-based dynamic equivalencing. However, a suitable alternative can be to generate homogeneous local sub areas from the whole external area.
- For instance, in the European external area involving the 397 machines can be composed on the basis of the power subsystems given in table 3.2 and using the proposed DANN with locally distributed dynamics.

---

<sup>24</sup> In case 1, 2 3, 4 and 5, the 4 bars represent the mean error in the adapted 12 machine systems with 3, 4, 6, and 8 boundary nodes.

## 5.6 Summary

- With the limited data exchange and sporadic cooperation between energy utilities due to the economic interests in the increasingly liberalized and deregulated energy markets, this proposed novel approach is suitable to be used in transient analysis, because it needs only reduced boundary data sets between internal and external area operators.
- The proposed approach *replaces the classical steps of the dynamic equivalencing*, such as *grouping, generator aggregation, control aggregation, and static network reduction* by means of a robust recurrent ANN as dynamic equivalent.
- Its main advantage is that *it describes the non-linear dynamic behavior of the external area considering all power system components*, i.e. transmission lines, converters, generators with their additional devices such as governor, excitation systems, etc.
- This *global trained recurrent ANN-based dynamic equivalent is subject to a wide range of disturbances applied geographically and electrically in an extensive way in the internal area*. The so generated MIMO disturbance data sets are provided to the ANN.
- Through the wide range and the normalization of *the boundary MIMO magnitudes with respect to an initial static operating point*, a robust ANN equivalent is obtained.
- The ANN structure can be realized *either as global recurrent ANN or as ANN with locally distributed dynamics according to its operating points* in conjunction to a heterogeneous voltage level of the internal area.
- This novel *approach is tested in various power systems with 2 to 8 boundary nodes under different power flow conditions*.
  - Tests in the *16 multi-machine system have demonstrated that this ANN-based equivalent is applicable and enough accurate in power systems with heterogeneous voltage levels* subject to non-trained disturbances of different durations.
  - Tests in the *12 multi-machine system have verified that the ANN-based equivalent is extremely robust for stability analysis of internal areas with changed power flow conditions caused by disconnections of transmission lines, loss of generators and changes in the load-generation balance*.
- The stability analysis using *the ANN-based dynamic equivalent is highly efficient, because different non-trained disturbances on the internal area can be applied under non-trained operating conditions and the ANN captures adequately the external area dynamic. Although, the disturbance and the operating point differs extremely from the ANN training case*.

- In comparison with the conventional proposed approaches, such as the electromechanical-based identity recognition and splitting-based dynamic equivalencing, the ANN-based dynamic equivalents can be applied to complex interconnected power systems independent of the operating point and independent of the disturbance in terms of time duration and location applied on the corresponding internal area.
- This approach is based on an intelligent robust model of the external area allowing its complete replacement in comparison to the classical development of dynamic equivalents by identity recognition and splitting-based aggregation.
- The robust ANN-based dynamic equivalent can be integrated in transient stability analysis for all forms, extent, and locations of disturbances on the internal area. The dynamic equivalents by identity recognition and splitting-based aggregation are validated only for a specific disturbance and for other disturbances geographically and electrically in the near. Moreover, these dynamic equivalents may be applied only for a specific operating point of the internal area.
- This approach can be applied to the interconnected European system difficultly due to the increase of hidden units, which influences the computational complexity of the DANN-based dynamic equivalencing. However, a suitable alternative can be to generate homogeneous local sub areas derived from the whole external area.
- With reference to the accuracy and agreement, this ANN-based approach is more accurate than the dynamic equivalencing using the electromechanical-based identity recognition and splitting-based aggregation in a small-scale power system, such as the 16-machine-system. However, it can work in conjunction with these classical equivalents to reduce the effects of uncertainties.

*“In all human affairs there are efforts, and there are results, and the strength of the effort is the measure of the result.”-J. Allen [140]-*

## Chapter 6

### Closure

#### 6.1 Conclusions

The major focus of this work has been the development of models in dynamic equivalencing using intelligent systems generating innovative approaches as alternatives to the classical dynamic equivalencing in power systems. The growing importance of considering the properties of the components of power systems encourages the investigation of this research area.

The proposed approaches can be roughly categorized into three main groups:

- Grouping of generators,
- Aggregation procedure of generators, and
- Construction of robust and intelligent dynamic equivalents.

The main conclusions obtained in this research can be summarized as follows:

#### **1 Electromechanical-based identity recognition in dynamic equivalencing**

- In a preliminary way, an innovative approach in dynamic equivalencing, called identity recognition, as alternative to the classical coherency identification is proposed to obtain identity-based equivalents.
- Through this approach, the grouping of generators is considered as an identity analysis task according to the introduced conditions for together oscillating machines, i.e. evaluating the identical rotor angle behavior of the machines. The condition of the identity recognition is reformulated in a way, in which the identity of the phase and amplitude of the behavior of the machines has to be considered. By this rigorous identity evaluation,

together oscillating machines can be grouped. These conditions are satisfactorily verified on a theoretical way.

- The evaluation can be practically realized using standard pattern recognition algorithms, such as hierarchical, K-means, Fuzzy and static ANN-based SOFM.
- Due to its nature, the proposed identity recognition can incorporate machine model parameters in dynamic equivalencing establishing the proposed electromechanical-based identity recognition.
- Thus, specific physical effects and electromechanical influences of the generators can be considered to group identical generators.
- These effects are selected by realizing a sensitivity analysis on a one-machine system, suitable machine parameters, such as the inertial constant and nominal power, are determined. In conjunction with these parameters, the geometrical distance of the pattern recognition algorithms is reformulated in an electromechanical distance.
- By means of the obtained electromechanical-based identity recognition, improved and accurate dynamic equivalents are generated.
- In order to verify the effectiveness of the proposed approach, it was tested both in the 16 multi-machine system and the interconnected European power system UCTE/ CENTRAL. In the small-scaled power system, all algorithms generate similar grouping compositions and in consequence, same accurate dynamic equivalents with high agreement. But, in the interconnected European power system, in which the German network was simulated as internal area, dynamic equivalents with different degrees of accuracy can be obtained depending from the applied algorithm.
- Thus, the results with a high degree of accuracy are obtained using the electromechanical weighted K-means and electromechanical weighted Fuzzy algorithms. SOFM are not appropriate to this identity task in complex power systems due to the ineffectiveness of its learning process.
- Further, *the electromechanically derived equivalents following a disturbance are valid in the same manner for other disturbances too, whose locations are electrically and geographically in close to the one.* Thus, this approach makes it possible that disturbance-independent dynamic equivalents can be generated in limited terms.
- The accuracy of this approach depends upon important aspects, namely upon:
  - *The identity recognition capability of the algorithms.*
  - *Number of dynamic equivalents.*
  - *The geographical and electrical distance between internal machines and disturbances.*

## 2 Splitting aggregation-based dynamic equivalencing

- An innovative aggregation approach in dynamic equivalencing, called splitting-based aggregation, as an alternative to the classical aggregation, is proposed to obtain accurate splitting-based aggregated equivalent machines.
- *The fictional splitting of generators in virtual generators is based upon the share factors. They can be derived from mathematical reduction techniques.*
- *The main advantage of this approach is that it can incorporate mathematical reduction techniques in dynamic equivalencing, which can generate highly accurate aggregated equivalents in terms of:*
  - *Linear independent dynamic equivalents with orthogonal oscillating swing curves by principal components. The dynamic behavior of the external machines is splitted into orthogonal part oscillating swings involving principal components (eigenvectors).*
  - *Representative non-linear equivalents by Fuzzy membership degrees. The identity assignment of the external machines is realized by fuzziness membership degrees.*
- *The proposed splitting-based aggregation is extended to the complete external area. This is in contrast to the classical aggregations, which are performed only and restrictively on a per coherent area basis.*
- In comparison to the electromechanical-based identity recognition, *this approach omits the first step of the dynamic equivalencing, i.e. the electromechanical grouping of identical generators on the external area.*
- This splitting-based approach was tested in the 16 multi-machine system. *Notable accuracy of splitting-aggregated dynamic equivalents can be obtained independent of disturbance in terms of duration, location, and sequence faults, in comparison to the equivalent machines calculated with the classical inertial aggregation. Further, the accuracy is independent of the number of dynamic equivalents.* Best results with a high degree of accuracy are achieved using *splitting by Fuzzy membership factors.*
- Independent of the number of equivalents, a similar high accuracy is obtained using the electromechanical-based identity recognition applied to small-scale power systems, e.g. the 16 multi-machine system, too.
- However, its application in large-scale power systems, such as the interconnected European power system UCTE/CENTRAL, *is restricted. This is due to the influence of other electromechanical factors of the power system on the splitting process of the external machines.* Thus, the splitting factors, which determine the splitting electrical parameters of the equivalent generator, can be dispersed. Therefore, in contrast to the electromechanical-based identity recognition, the results are not sufficiently accurate.

### 3 DANN-based dynamic equivalencing

- This proposed approach *omits the classical steps of the dynamic equivalencing, such as grouping, generator aggregation, control aggregation, and static network reduction* by means of a robust recurrent ANN as dynamic equivalent. This intelligent robust model replaces completely the external area.
- The main advantage is that *it describes and captures properly the non-linear behavior of an external area considering all power system components, i.e. transmission lines, converters, generators with their governor, excitation systems, and amongst others.*
- This *recurrent ANN-based dynamic equivalent is globally trained with a wide range of disturbances. There are applied geographically and electrically in an extensive way in the internal area.* The generated MIMO disturbance data sets are provided to the ANN.
- A *robust ANN equivalent* is obtained through this wide range and the normalization of *the boundary MIMO magnitudes with respect to an initial static operating point.*
- The ANN structure can be realized *either as global recurrent ANN or as ANN with locally distributed dynamics according to the ANN operating points* in conjunction with the heterogeneous voltage levels of the internal area.
- This innovative ANN-based *approach was tested in various power systems with 2 to 8 boundary nodes under different power flow conditions.*
  - Tests in the *16 multi-machine system have demonstrated that this ANN-based equivalent is applicable and enough accurate in power systems with heterogeneous voltage levels* subject to non-trained disturbances of different durations.
  - Tests in the *12 multi-machine system have verified that the ANN-based equivalent is extremely robust for stability analysis of internal areas with changed power flow conditions caused by disconnections of transmission lines, loss of generators and changes in the load-generation balance.*
- The ANN-based dynamic equivalents can be applied to strongly meshed interconnected power systems with high accuracy independent of the operating point and the disturbance in terms of time duration, location, and fault sequence. However, this approach can be difficultly applied to the interconnected European system due to the increase of hidden units, which influences the computational complexity of the ANN-based dynamic equivalent. A suitable alternative can be to generate ANN models for small homogeneous local sub areas, which are splitted from the whole external area.
- The robust ANN-based dynamic equivalent is valid for all forms, extent, and locations of disturbances and operating points on the internal area. This is in contrast to the dynamic

equivalent using identity recognition and splitting-based aggregation, which are generated mainly for a specific operating point of the power system.

## 6.2 Selection criteria

In the following table, a summarized selection criteria schema is presented.

**Table 6.1.-** Comparison of the proposed approaches to applicability considering power system relevant aspects

Selection aspects	Electromechanical identity recognition-based equivalencing	Splitting-based equivalencing	Recurrent ANN-based equivalents
Small-scale power system	+++	+++	+++
Large-scale power system	+++	-	-
Disturbance independent	++	+++	+++
Operating point independent	---	---	+++
Number of equivalents	+	++	
Data availability of external area	-	-	+++
Physical structure	++	+++	--
Boundary magnitudes	-	-	++
Resources	Electromechanical distance	Mathematical reduction techniques	Intelligent model system

In the previous table according to the comparison technical aspects, the applicability of the approaches has been summarily evaluated involving different usages and practical factors.

According to the relevant aspects of the dynamic equivalencing, the most appropriate approaches are assigned by the symbols '+++', and the less appropriate by '---'. These symbols can be chosen as an indicator to assess and use suitably the approaches for forming dynamic equivalents in transient and dynamic stability studies according to the corresponding practical aspect.

As small-scale power system, the 16 multi-machine and 12 multi-machine systems are considered, and as large-scale power system the interconnected European power system, as well. However, these proposed approaches can work in conjunction to reduce the effects of uncertainties in dynamic equivalencing.

Under the following criteria aspects an appropriate approach could be selected in detail:

## Electromechanical-based identity recognition in dynamic equivalencing

- This electromechanical-based approach is suitable to develop dynamic equivalents both *in small-scaled power systems and in the interconnected European power system UCTE/CENTRAL without restriction independent of its size and complexity.*
- The accuracy of the dynamic equivalents depends upon the used algorithm, the number of equivalents and the electrical distance of internal machines to the disturbance.
- Further, the electromechanical derived equivalents are also valid with a degradation of accuracy for other disturbances that are electrically and geographically in close distance to the fault of the equivalents derived.
- These dynamic equivalents are operating point dependent. Moreover, this approach needs considerable data sets of the external area to generate the dynamic equivalents.

## Splitting-aggregation based dynamic equivalencing

- This approach *is suitable for small-scale power systems obtaining strongly accurate equivalents.* Further, its high accuracy is mainly independent of the number of equivalents and disturbance severity, form, location and duration.
- A drawback of this method is the accumulation of error when it is applied to large number of external machines, such as in the interconnected European power system.
- From practical viewpoint, this approach is appropriate, when
  - Electromechanical external machine parameters are available.
  - The fictional splitting of external machines enables the implementation of mathematical reduction techniques in dynamic equivalencing.
- However, the splitting-based dynamic equivalents are operating point dependent.

## Dynamic ANN-based dynamic equivalencing

- *The ANN-based dynamic equivalents can be applied without restriction to strongly meshed, small-scaled power systems independent of the operating point and the disturbance in terms of time duration, location, and fault sequence.*
- Some restrictions arise when applying this approach to large number of external machines, such as in the interconnected European power system and also the non-linear system dimension can cause some limitations in the computational resources.

- In comparison to others approaches, the ANN-based equivalent is valid for diverse operating points far away (caused by *disconnections of transmission lines, loss of generators and changes in the load-generation balance*) from the derived one.
- This *intelligent robust model of the external area captures the complete dynamic of an external area of a power system on the basis of an extremely reduced MIMO data set.*
- From practical viewpoint, the network operator needs only limited boundary magnitudes of the neighborhood areas to generate the ANN-based dynamic equivalent.
- This approach is more accurate as the results obtained by electromechanical-based identity recognition and splitting-based aggregation in a small-scaled power system, such as the 16 multi-machine system.

### 6.3 Suggestions for future work

This research represents a new way for implementing intelligent systems, such as pattern recognition algorithms, Fuzzy theory, and ANN in dynamic equivalencing for power systems.

In the future, this study can be extended to the following aspects:

#### **Electromechanical-based identity recognition**

- Using the reformulated conditions of the proposed electromechanical-based identity recognition, it would be interesting to generate dynamic equivalents for small stability studies in terms of damping and modal analysis.
- Future prospects should focus on the implementation of this approach in damping analysis of the interconnected European power system UCTE/CENTREL.

#### **Splitting-based aggregation**

- Different mathematical reduction techniques (based upon system decomposition) can be implemented in this approach to form the splitting of the external area machines.
- The impact that splitting of generators in virtual machines would have on the dynamic performance of the reduced power system, should be studied to determine the inaccuracy in large-scale power systems. From such a study, more insights about the role of virtual generators in providing additional electromechanical properties could be gained.

## Dynamic ANN-based dynamic equivalencing

With the increasing concurrence between energy utilities, dynamic ANN as non-linear dynamic equivalents could be employed widely in online transient stability studies of real complex power systems. Thus, this approach as proposed ANN-based equivalent with locally distributed dynamics, could be applied on the homogenous sub areas derived from the interconnected European power system UCTE/CENTREL, taking into account sufficient computational resources.

### 6.4 List of publications

The work in this doctoral project resulted in a number of publications, which are listed below:

- [1] O. Yucra Lino, "Recurrent Neural Network-based Dynamic Equivalencing in Power Systems", IEEE Trans., PSCE Power Systems Conference & Exposition 2004, New York, 10-13 Oct. 2004.
- [2] O. Yucra Lino, Michael Fette, "Electromechanical Identity Recognition in Dynamic Equivalencing", 39th Universities Power Engineering Conference 2004, pp. 1078-1085, Vol.3, Bristol-England, 6-8 Sep. 2004.
- [3] O. Yucra Lino, Michael Fette, Zhao Dong, "Splitting-based Aggregation in Dynamic Equivalencing", PES Power Tech 2005, St. Petersburg-Russia, 27-30 Jun. 2005.
- [4] O. Yucra Lino, Michael Fette, Juan Manuel Ramírez, "Electromechanical Distance and Identity Recognition in Dynamic Equivalencing", PES Power Tech 2005, St. Petersburg-Russia, 27-30 Jun. 2005.
- [5] O. Yucra Lino, Michael Fette, Zhao Dong, Juan Manuel Ramírez, "Non-linear Approaches for Dynamic Equivalencing in Power Systems", accepted for Publication in the IEEE Trans., Power Systems Conference & Exposition 2006, Atlanta-Georgia, Oct. 29-Nov. 1, 2006.

# Bibliography

- [1] H.E. Brown, R.B. Shipley, D. Coleman and R. Neid Jr., "A Study of Stability Equivalents", IEEE Trans. Vol. PAS-88, Nr. 3, pp. 200-207, 1969.
- [2] J.M. Undrill, J. Casazza, L.K. Kirchmayer, "Electromechanical Equivalents for Use in Power System Studies", IEEE Trans. Vol. PAS-90, pp. 2060-2071, 1971.
- [3] P. Kundur, Power System Stability and Control, McGraw-Hill, New York, 1994.
- [4] P. Kundur; L. Wang; S. Yirga, "Dynamic Equivalents for Power System Stability Studies", Fifth Symposium of Specialists in Electric Operational and Expansion Planning, Recife, Brazil, May 1996.
- [5] T. M. McCauley, "Disturbance dependent electromechanical equivalents for transient stability studies", IEEE Winter Power Meeting, New York, January, 1975.
- [6] L. Wang, M. Klein, S. Yirga and P. Kundur, "Dynamic reduction of large power systems for stability studies", Power Systems, IEEE Transactions on Power Systems, Vol. 12, No. 2, pp. 889-895, May 1997.
- [7] W. Price, J. Choe, A. Hargrave, B. Hurysz, P. Hirsch, "Large-scale system testing of a power system dynamic equivalencing program", IEEE Transactions on Power Systems, Vol. 13, No. 3, pp. 768- 773, August 1998.
- [8] W. W. Price, B. A. Roth, "Large-scale implementation for dynamic equivalents", IEEE Trans., Vol. PAS-100, pp. 3811-3817, 1981.
- [9] R. Nath, S. S. Lamba, K. S. Prakasa, "Coherency based system decomposition into study and external areas using weak coupling", IEEE Trans., Vol. PAS-104, pp. 1443-1449, June, 1985.
- [10] J. R. Winkelman, J. H. Chow, B. C. Bowler, B. Avramovic, P. V. Kotokovic, "An Analysis of interarea dynamics of multi-machine systems", IEEE Trans., Vol. PAS-100, pp. 754-763, February, 1981.
- [11] J. H. Chow, "A toolbox for power system dynamics and control engineering education and research", IEEE Transaction on Power Systems, Vol. 7, No. 4, pp. 1559-1564, November, 1992.
- [12] J. H. Chow, "Time-scale modeling of dynamic networks with application to power systems", Lecture Notes in Control and Information Sciences, Vol. 46, Springer-Verlag, 1982.

- 
- [13] S. B. Yusof, G. J. Rogers, "Slow coherency based network partitioning including load buses", IEEE Trans. On Power Systems, Vol. 8, pp. 1375-1382, 1993.
- [14] J. H. Chow, J. Cullum, R. A. Willoughby, "A sparsity-based technique for identifying slow-coherent areas in large power systems", IEEE Trans. PAS-103, No. 3, pp. 463-473, march 1984.
- [15] J. H. Chow "New algorithms for slow coherency aggregation of large power systems", Systems and Control Theory for Power Systems, IMA Volumens in Mathematics and its Applications, Vol. 64, pp. 95-115, Springer-Verlag, 1995.
- [16] L. Wang, A. Semlyem, "Application of sparse eigenvalue techniques to the small signal analysis of large power systems", IEEE Trans. On Power Systems, Vol. 5, pp. 635-642, 1990.
- [17] R. Podmore, "Identification of coherent generators of dynamic equivalents", IEEE Trans., Vol. PAS-97, pp. 1344-1354, 1978.
- [18] U. DiCaprio, "Condition for theoretical coherency in multimachine power system", Automatica, Vol. 17, pp. 687-701, 1981.
- [19] Sung-Kwan Joo, Ch. Liu, J. Choe, "Enhancement of Coherency Identification Techniques for Power System Dynamic Equivalents", Power Engineering Society Summer Meeting 2001, IEEE, Vancouver, Canada, Vol. 3 ,15-19, pp. 1811-1816, July 2001.
- [20] S.T.Lee, F.C. Schweepe, "Distance measures and Coherency Recognition", IEEE Trans., Vol. PAS-82, pp. 1550-1557, Sept/Oct. 1973.
- [21] B. Avramovic, P. V. Kokotovic, J.R. Winkelman, J. H. Chow, "Area decomposition for electromechanical models of power systems", Automatica, Vol. 16, pp. 637-648, 1980.
- [22] P. V. Kokotovic, B. Avramovic, J. H. Chow, J. R. Winkelman, "Coherency based decomposition and aggregation", Automatica, Vol. 18, pp. 47-56, 1982.
- [23] R. Baiasubramanian, S. C. Tripathy and Shivanna, "A Fast Algorithm for Coherency Identification and Dynamic Equivalencing", ACE'90 Proceedings of IEEE India, pp.71-75, Jan. 22-25, 1990.
- [24] A. M. Miah, "Simple dynamic equivalent for fast online transient stability assessment", IEE Proceeding, Generation, Transmission and Distribution, Vol. 145, No. 1, pp. 49-55, January, 1998.
- [25] Byung Chang, Jin Choo, Sae Kwon, "A reduced order equivalent model of large power systems for the stability analysis", IEEE, 2000.
- [26] G. Jang, B. Lee, S. Kwon, H. Kim, Y. Yoon, J. Choo, "Development of KEPCO equivalent systems for the KEPCO enhanced power system simulator", Electrical Power and Energy Systems Vol. 23, pp. 577-583, 2001.
- [27] S. K. Joo, C. C. Liu, L. Jones and J. W. Choe, "Coherency techniques for dynamic equivalents incorporating rotor and voltage dynamics" Bulk Power Systems Dynamics and Control-V, Security and Reliability in a Changing Environment, Hiroshima, Japan, Aug. 2001.

- [28] T. Krishnaparandhama, S. Elangovan, A. Kuppurajulu, "Method for identifying coherent generators", *Electrical Power and Energy Systems*, Vol. 3, No. 2, pp. 85-90, 1981.
- [29] V. Sankaranarayanan, M. Venugopal, S. Elangovan, N. Dahrma, "Coherency identification and equivalents for transient stability studies", *Electric Power Systems Research*, Vol. 6, pp. 51-60, 1983.
- [30] J. H. Chow, R. Galarza, P. Accaci, W. Price, "Inertial and Slow Coherency Aggregation Algorithms for Power System Dynamic Model Reduction", *IEEE Trans.*, Vol. 10, pp. 680-685, 1995.
- [31] J. H. Chow, "Singular Perturbation, Coherency and Aggregation of Dynamic Systems", *IEEE Trans.*, pp. 6-42, July 19981.
- [32] Pierre Accari, Joh H., "Dynamic Aggregation Algorithms for Power System Model Reduction", *IEEE Trans.*, Vol. 10, No. 3, May 1994.
- [33] Lj. B. Jovic, M. Ribbens-Pavella and D. Siljak, "Multimachine Power Systems: Stability, Decomposition and Aggregation", *IEEE Trans.*, Vol. AC-23, pp. 325-332, 1978.
- [34] A. J. Germond, R. Podmore, "Dynamic Aggregation of Generating Unit Models", *IEEE Trans.* Vol. PAS-97, Nr. 4, pp. 1060-1069, 1978.
- [35] M. Hussain, V. Rau, "An efficient and simple method of dynamic equivalent construction for large multi-machine power system", *IEEE International Conference on Advances in Power System Control, Operation and Management*, pp. 90-94, Hong Kong, November 1991.
- [36] A. Ghafurian, G. J. Berg, "Coherency-based multi-machine stability study", *Proc. IEE*, Vol. 129, Part-C, pp. 153-160, 1982.
- [37] G. J. Berg, A. Ghafurian, "Representation of coherency-based equivalents in transient stability studies", *Electric Power Systems, Research*, Vol. 6, pp. 235-241, 1983.
- [38] R. J. Galarza, J. H. Chow, W. W. Price, A. W. Hargrave, P. M. Hirsch, "Aggregation of exciter models for constructing power system dynamic equivalents", *IEEE Transaction on Power Systems*, Vol. 13, No. 3, pp. 782-788, August 1998.
- [39] R. A. Date, J. H. Chow, "Aggregation properties of linearized two-time-scale power networks", *IEEE Trans. On Circuits and Systems*, Vol. 38, No.7, pp. 720-730, July, 1991.
- [40] J. D. McCalley, J. F. Dorsey, J. F. Luini, R. Peter Mackin, G. H. Molina, "Subtransmission reduction for voltage instability analysis", *IEEE Transaction on Applied Superconductivity*, Vol. 3, No. 1, pp. 349-356, March 1993.
- [41] W. F. Tinney, J. M. Bright, "Adaptive reductions for power flow equivalents", *IEEE Trans.*, Vol. PWRS-2, pp. 351-360, May, 1987.
- [42] R. J. Newell, M. D. Risan, L. Allen, K. S. Rao, D. L. Stuehm, "Utility experience with coherency-based dynamic equivalents of very large systems", *IEEE Transaction on Power Apparatus and Systems*, Vol. PAS-104, No. 11, pp. 3056-3063, November 1985.
- [43] K.Tanaka, M Takemura, "Development of Reduction Program for Bulk Power System Stability Study," *IEEE trans.*, pp. 47-54, April 1998.

- [44] A. A. Fouad, S. E. Staton, "Transient stability of a multi-machine power system", IEEE Trans., 1981, PAS-100, pp. 3408-3424, 1981.
- [45] A. A. Fouad, V. Vittal, T. Kyoo, "Critical energy for direct transient stability assessment of a multi-machine power system", IEEE Trans., PAS-103, pp. 2199-2206, 1984.
- [46] Y. Xue, TH. Cutsem, M. Ribbens-Pavella, "A simple direct method for a fast transient stability assessment of large power systems", IEEE Trans., PWSR-3, pp. 400-412, 1988.
- [47] Y. Xue, TH. Cutsem, M. Rubbens-Pavella, "Extended equal area criterion: justifications, generations, applications", IEEE Trans., PWSR-4, pp. 44-52, 1989.
- [48] W. Brown, W. J. Cloues, "Combination load-flow stability equivalents for power system representation on a.c. analyzers", AIEE Transactions, Vol. 74, pp. 782-785, 1985.
- [49] H. E. Brown, R. B. Shipley, O. Coleman, R. E., Nied, "A study of stability equivalents", IEEE Trans. On PAS, Vol. 88, pp. 200-207, March, 1969.
- [50] F. F. Wu, A. Monticelli, "Critical review of external network modeling for online security analysis", Electric Power and Energy Systems, Vol. 5, No. 4, pp. 222-235, October, 1983.
- [51] J. Machowski, A. Cichy, "External subsystem equivalent model for steady-state and dynamic security assessment", IEEE Transactions on Power Systems, Vol. 3, No.4, pp. 1456-1463, November 1988.
- [52] S. Deckmann, A. Pizzolanze, A. Monticelli, B. Stott, "Numerical testing of power system load-flow equivalencing", IEEE Trans. On PAS, PAS-99, pp. 2292-2300, November, 1980.
- [53] Thomas Baldwin, Lamine Mili, Arun Phadke, "Dynamic ward equivalent for transient stability analysis", IEEE Transactions on Power Systems, Vol. 9, No.1, pp. 59-67, February 1994.
- [54] A. Bergen, D. Hill, "A structure preserving model for power system stability analysis", IEEE Transactions on Power Apparatus and Systems, Vol. 100, No. 1, pp. 25-35, January, 1981.
- [55] M. A. Pai, K. R. Padiyar, C. Radhakrishna, "Transient stability analysis of multimachine AC/DC power system via energy function method", IEEE Transactions on Power Apparatus and Systems, Vol. 100, No.12, pp. 5027-5035, December 1981.
- [56] V. Vital, N. Bhatia, A. A. Fouad, G. A. Maria, H. M. Zein El-Din, "Incorporating of non-linear load models in the transient energy function method", IEEE Transaction on Power Systems, Vol. 4, No. 3, pp. 1031-1036, August, 1989.
- [57] T. L. Baldwin, L. Mili, A. G. Phadke, "Ward-type equivalents for transient stability analysis", Proceeding of the IFAC International Symposium on Control of Power Plants and Power Systems, March 9-11, Munich, Germany, pp.251-255, 1992.
- [58] J.M. Undrill, A. Tuner "Construction of Equivalents by Modal Analysis", IEEE Trans. Vol. PAS-90, pp. 2049-2059, 1971.
- [59] W. Price, E. Gulashenski, P. Kundur, G. Loehr, B. Roth, R, Silva, "Testing of the modal dynamic equivalents techniques", IEEE Tras. on PAS, Vol. 97, pp. 1366-1372, July 1978.
- [60] S. D. Spalding, D. B. Goudi, H. Yee, "Use of equivalents and reduction techniques in power system transient stability computation", PSCC Proceeding, Vol. 2, 1975

- [61] S. E. M. de Oliveira, J. F. de Queiroz, "Modal dynamic equivalent for electric power systems", IEEE Transaction on Power Systems, Vol. 3, No. 4, pp. 1723-1730, November 1998.
- [62] S. Takeda, S. Nishida, T. Yamaguchi, "Derivation of dynamic equivalents for stability analysis", Electrical Power and Energy Systems, Vol. 2, pp. 96-102, April, 1980.
- [63] S. Nishida, S. Takeda, "Derivation of equivalents for dynamic security assessment", Electrical Power and Energy Systems, Vol. 6, No. 1, January, 1984.
- [64] W. Price, "Testing of Modal Dynamic equivalents Technique", IEEE Trans. Vol. PAS-97, Nr. 4, pp. 1366-1372, 1978.
- [65] I. J. Perez-Arriaga, C. G. Verghese, F. C. Schwepe, "Selective modal analysis with applications to electric power systems", IEEE Trans. On Power Systems, Vol. 101, No. 9, September 1982.
- [66] S. Geeves, "A modal-coherency technique for deriving dynamic equivalents", IEEE Trans. On Power Systems, Vol. 3, No. 1, February 1988.
- [67] P. M. van Oirsouw, "A dynamic equivalent using modal coherency and frequency response", IEEE Transaction on Power Systems, Vol. 5, No. 1, pp. 289-295, February 1990.
- [68] T. Hiyama, "Identification of coherent generators using frequency response", IEEE Proceeding, C 128, pp. 262-268, 1981.
- [69] G. Ramaswamy, P. Panciatici, L. Rouco, B. Lesieutre, O. Filatre, D. Peltiers, G. Verghese, "Synchronic modal equivalencing for structure-preserving dynamic equivalents", IEEE Transaction on Power Systems, Vol. 11, No. 1, pp. 19-29, February 1996.
- [70] I. J. Perez, G. Verghese, F. L. Pagola, J. Sancha, F. C. Schwepe, "Developments in selective modal analysis of small signal stability in electric power systems", Automatica, Vol. 26, No.2, pp. 215-231, 1990.
- [71] L. Rouco, I. J. Perez, "Multi-area analysis of small signal stability in large electric power systems by SMA", IEEE Transaction on Power Systems, Vol. 8, No.3, pp. 1257-1265, August, 1993.
- [72] A. Chang, M. M. Adibi, "Power system dynamic equivalents", IEEE Trans. On PAS, Vol. 89, pp. 173-175, November, 1970.
- [73] R. W. de Mello, R. Podmore, K. N. Stanton, "Coherency based dynamic equivalents: application for stability studies", PICA Conference Proceedings, pp. 21-23, 1075.
- [74] Y. Ohsaya, M. Hayashi, "Coherency recognition for transient stability equivalents using Liapunov function", 6 th Power System Computation Conference, Vol.2, pp. 815-818, 1978.
- [75] M. A. Pai, C. L. Narayama, "Dynamic equivalents using energy functions", IEEE PES Summer Meeting, July 1977.
- [76] G. Troullinos, J. Dorsdey, H. Wong, J. Myers, "Reducing the order of very large power system models", IEEE Trans. on Power Systems, Vol. 3, No. 1, pp. 127-133, Feb. 1988.

- [77] O. Wasynczuk, Y-M. Diao, P.C. Krause, 'Theory and comparison of reduced order models of induction machines', *IEEE Transactions on Power Apparatus and Systems*, Vol. 24, No.3, pp. 598-606, March 1985.
- [78] F.D. Rodriguez, O. Wasynczuk, 'A refined method of deriving reduced order models of induction machines', *IEEE Transactions on Energy Conversion*, Vol. 2, No.1, pp. 31-37, March 1987.
- [79] T. Noda, M. Takasaki, Okamoto, Fujibayashi, H. Nishigaito, T. Okada, "Low-Order Linear Model Identification Method of Power System", *IEE Transactions of the Institute of Electrical Engineers of Japan*, Vol. 121-B, No.1, pp. 52-57, January 2001.
- [80] A. H. Whitfield, "Transfer Function Synthesis Using Frequency Response Data," *Int. J. Control*, Vol. 43, No. 5, pp. 1413–1426, 1986.
- [81] A. Soysal, A. Semlyen, "Practical Transfer Function Estimation and its Application to Wide Frequency Range Representation of Transformers," *IEEE Trans. on Power Delivery*, Vol. 8, No. 3, pp. 1627–1637, January, 1993.
- [82] J. M. Ramírez, R. Garcia, "A technique to reduce power systems electromechanical models", *Conference Proceeding of the IEEE Transmission and Distribution 2002*, Sao Paulo-Brazil, pp. 51-57, March 2002.
- [83] J. M. Ramirez Arredondo, "Obtaining dynamic equivalents through the minimization of a line flows function", *Electrical Power and Energy Systems*, Vol. 21, pp. 365-373, 1999.
- [84] P. Ganapati, M. Sanjay Kumar, M. Rasmi Rekha, "Adaptive Identification of the Parameters of Nonlinear Systems Using Higher Order Statistics", *Conference Proceeding of the ICSPAT-96*, Boston, MA, pp. 200-204, 1996.
- [85] C. K. Sanathanan, J.Koerner, "Transfer Function Synthesis as a Ratio of Two Complex Polynomials," *IEEE Trans. on Automatic Control*, Vol. 8, pp. 56–58 , 1963.
- [86] M. Burth, G. C. Verghese and M. Vélez-Reyes, "Subset selection for improved parameter estimation in on-line identification of a synchronous generator", *IEEE Trans. on Power Systems*, vol. 14, pp. 218 225, Feb. 1999.
- [87] I. Erlich, H. Pundt, "Digital program for the simulation of electromechanic transients in the medium", *PSCC Helsinki*, pp. 19-24, August 1994.
- [88] B. Kulicke, I. Erlich, S. Demmig, U. Bachmann, W. Glaunsinger, U. Zimmermann, "Netzaequivalentierung für Stabilitätsberechnungen basierend auf der Analyse kohärenter Generatorgruppen", *Elektrizitätswirtschaft Jg. 99, Heft 7*, 37-43, 2000.
- [89] R. Isermann. *Identifikation dynamischer Systeme*, Bd. I, II., Berlin Heidelberg New York: Springer 1992.
- [90] I. A. Hiskens, "Nonlinear dynamic model evaluation from disturbance measurements", *IEEE Trans. on Power Systems*, vol. 16, pp. 702-710, Nov. 2001.
- [91] P.Michaud, "Pattern recognition techniques", *Future generation computer systems*, pp.145-147, 1997.
- [92] D. L. Massart and L. Kaufman, *Cluster Analysis*, Wiley, New York, 1983.

- [93] H. J. Mucha, Clusteranalyse mit Microcomputern, Akademie Verlag, Berlin, 1992.
- [94] B. Mirkin, Mathematical Classification and Clustering, Kluwer Academic Publishers, Dordrecht, Boston, London, 1996.
- [95] R. Dubes, A.K. Jain, Algorithms for Clustering Data, Prentice Hall, Englewood Cliffs, New Jersey, 1998.
- [96] A. Hartigan, Cluster Analysis, Wiley, New York, 1969.
- [97] Y. Lu, "Pattern recognition and Classification", Proc. Int. Joint Conf. On Neural Networks, Vol 1, pp. 471-476, 1990.
- [98] A. Jain, Clustering Algorithms, Prentice Hall, New York, 1991.
- [99] H. P. Kriegel, Report Knowledge Discovery in Databases, Ludwig-Maximilian-University, Munich, 2002.
- [100] R. Dave, "Characterization of noise in clustering", Pattern Recognition Letters, 12, pp. 657-664, 1991.
- [101] Visual Numerics: IMSL Fortran 90 MP Library Help, Stat/Library, Volume 2, Chapter 11: Cluster Analysis.
- [102] J. C. Bezdek, Pattern Recognition with Fuzzy Objective Function Algorithms, Plenum Press, New York, 1981.
- [103] F. Höppner, Obtaining Interpretable Fuzzy Models from Fuzzy Clustering, <http://www.et-inf.fho-emden.de/~dmlab/fc>, Emden, 2002.
- [104] J. Keller, R. Krishnaparum, "A Possibilistic Approach to Clustering", IEEE Tran. On Fuzzy Systems, 1(2), pp. 98-110, 1993.
- [105] J. Bezdek, "On Cluster Validity for the Fuzzy Model", IEEE Trans. On Fuzzy Systems, Vol 3, pp. 3-5, 1995.
- [106] T. Kohonen, Self Organizing and Memories, Springer Verlag, Berlin, 1995.
- [107] S. Mitra, "Self Organizing Maps as a fuzzy Classifier", IEEE Transactions on Fuzzy Systems, 24, pp. 101-123, 1994.
- [108] G. Carpenter, S. Grossberg, "ART2: Self-organization of stable category recognition category of analog input patterns," *Applied Optics* 26, 4919-4949, 1987.
- [109] D. Niebur, A. J. Germond, "Power system static security assessment using the Kohonen neural network classifier," *Procs. of the 7th Power Industry Computer Applications Conference*, Baltimore, May 1991, *IEEE Transaction on Power Systems*, vol. PWRS-7, No. 2, 865-872, May 1992.
- [110] D. Niebur, "Neural network applications in power systems," *Int. Journal of Engineering Intelligent Systems*, Vol. 1, No. 3, 133-158, December 1993.
- [111] Y. H. Pao, Adaptive Pattern Recognition and Neural Networks, Addison-Wesley, Reading, MA, 1989.
- [112] I. T. Jolliffe, Principal Component Analysis, Springer Verlag, New York, 1986.
- [113] O. Alter, P. O. Brown, "Singular value decomposition for genome-wide expression data processing and modeling", Proc. Nat. Acad. Sc. USA, No. 97, pp. 10101-10106, 2000.

- [114] M. W. Berry, "Large scale sparse singular value computations", *Int. Journal of Supercomputer Applications*, Vol. 6, pp. 13-49, 1992.
- [115] F. Deprettere, "SVD and Signal Processing: Algorithms, Analysis and Application", Amsterdam: Elsevier Science Publishers, 1998.
- [116] G. Crapanzano, *Dynamische modellierung von generatoren und generatorgruppen mit künstlichen neuronalen netzen (PhD Thesis)*, Shaker Verlag, Kaiserslautern, 2004.
- [117] R. Rivera-Sampayo and M. Vélez-Reyes, "Gray-box modeling of electric drive systems using neural networks", *Proceedings of the 2001 IEEE International Conference on Control Applications*, pp. 146-151, Sep. 2001.
- [118] K. Narendra, K. Parthasarathy, "Identification and Control of dynamical systems using neural networks", *IEEE Transactions on Neural Networks*, Vol.1, pp 4-27, 1990.
- [119] Z. Zhao, A. M. Stankovic and G. Tadmor, "A study of power system dissipativity using artificial neural networks", in *Proceedings of the 1998 North American Power Symposium*, pp. 241-246, Oct. 1998.
- [120] R. Rico-Martinez and I. G. Kevrekidis, "Nonlinear system identification using neural networks: dynamics and instabilities", *Neural Networks for Chemical Engineers*, pp. 409-442, Elsevier, 1995.
- [121] M. A. Kramer, "Nonlinear principal component analysis using auto-associative neural networks", *AIChE Journal*, vol. 37, pp. 233-243, Feb. 1991.
- [122] M. Kirby and R. Miranda, "Nonlinear reduction of high-dimensional dynamical systems via neural networks", *Physical Review Letters*, vol. 72, pp. 1822-1825, Mar. 1994.
- [123] J. S. Anderson, I. G. Kevrekidis and R. Rico-Martinez, "A comparison of recurrent training algorithms for time series analysis and system identification", *Computers Chem. Eng.*, vol. 20, pp. S751-S756, 1996.
- [124] F. J. Pineda, "Generalization of back-propagation to recurrent neural networks", *Physical Review Letters*, vol. 59, pp. 2229-2232, Nov. 1987.
- [125] C. W. Liu and J. S. Thorp, "New methods for computing power system dynamic response for real-time transient stability prediction", *IEEE Trans. on Circuit and Systems – I: Fundamental Theory and Applications*, vol. 47, pp. 324-337, Mar. 2000.
- [126] R. Rico-Martinez, I. G. Kevrekidis, M. C. Kube and J. L. Hudson, "Discrete- vs. continuous-time nonlinear signal processing: attractors, transitions and parallel implementation issues", in *Proceedings of the 1993 American Control Conference*, vol. 2, pp. 1475-1479, Jun. 1993.
- [127] R. Rico-Martinez and I. G. Kevrekidis, "Continuous time modeling of nonlinear systems: a neural network-based approach", in *Proceedings of the 1993 IEEE International Conference on Neural Networks*, vol. III, pp. 1522-1525, 1993.
- [128] Y. J. Wang and C. T. Lin, "Runge-Kutta neural network for identification of dynamical systems in high accuracy", *IEEE Trans. on Neural Networks*, vol. 9, pp. 294-307, Mar. 1998.

- [129] A. Juditsky, H. Hjalmarsson, A. Benveniste, B. Delyon, L. Ljung, J. Sjöberg, Q. Zhang, "Nonlinear black-box modeling in system identification: Mathematical foundations." *Automatica* 31(12), pp. 1691-1742, 1995.
- [130] I. J. Leontaritis, S. A. Billings, "Input-output parametric models for nonlinear systems. Part 1: Deterministic nonlinear systems", *Int. J. Control* 41, pp. 303-344, 1985.
- [131] H. Tolle, E. Ersü, "Neurocontrol-Learning control systems inspired by neuronal architectures and human problem solving strategies", *Lecture Notes in Control and Information Science* No. 172, Berlin Heidelberg New York: Springer, 1992.
- [132] R. J. Williams, D. Zipser, "A learning algorithm for continually running fully recurrent neural networks.", *Neural Comput.* 1, 1989.
- [133] G. Rogers. "*Power system oscillations*", the Kluwer international series in engineering and computer science, Kluwer Academic Publishers, 2000.
- [134] Yaonan Yu. *Electric Power System Dynamics*. Academic Press, New York, 1983.
- [135] Fette, Michael. *Strukturelle Analyse elektrischer Energieversorgungssysteme (strukturelle Analysis of electric Power Systems)*, Reihe 21: Elektrotechnik, Nr. 140, VDI Verlag, 1993.
- [136] P. W. Sauer and M. A. Pai. *Power system dynamics and stability*, Prentice Hall, 1998.
- [137] T. Van Cutsem and C. Vournas. *Voltage Stability of Electric Power Systems*. Kluwer Academic Publishers, 1998.
- [138] J. C. Das and J. Casey. Effects of excitation controls on operation of synchronous motors. *Industrial & Commercial Power Systems Technical Conference*, 1999.
- [139] R. Kalman. Discovery and invention: The newtonian revolution in systems technology. *Journal of Guidance and Control*, 26(6), pp.833–837, October 2003.
- [140] James Allen. *As You Thinketh*. Putnam Publishing Group, 1959.
- [141] O. Yucra Lino. Software handbook to PSD and development of intelligent, robust and non-linear models in dynamic equivalencing for interconnected power systems. Report of department of electrical and information systems, sustainable energy concepts. University of Paderborn, October 2005.
- [142] U. Bachmann, H. Breulmann, W. Glaunsinger, P. Hoiss, M. Loesing, A. Menze, S. Roemelt, U. Zimmermann, "Verbundstabilität nach dem Synchronanschluss der Netze der Elektrizitätsunternehmen von Bulgarien und Rumänien an UCTE/CENTREL-Verbund", Munich, ETG Tage 1999, ETG-Fachbericht 79, ISBN 3-8007-2502-9, pp. 251-257, 1999.
- [143] Aleksander M. Stankovic, Andrija T. Saric and Mirjana Milosevic, "Identification of non-parametric dynamic power system equivalents with artificial neural network" *Power Systems*, IEEE Transactions on, Vol. 18, Issue: 4, pp. 1478-1486, Nov. 2003.
- [144] J. R. Smith, C. S. Woods, F. Fatehi, G. L. Keenan and J. F. Hauer, "A low order power system model with dynamic characteristics of the Western North American System", in *Proceedings of the 1994 North American Power Symposium*, Part II, pp. 533-539, 1994.

# APPENDIX A Classical dynamic equivalencing approaches

## A.1. Ward equivalent

The *Ward* method consists in eliminating selected nodes of the network [50], which are denoted by index 'l' and generator nodes by 'g', as can be seen in Fig. A.1.

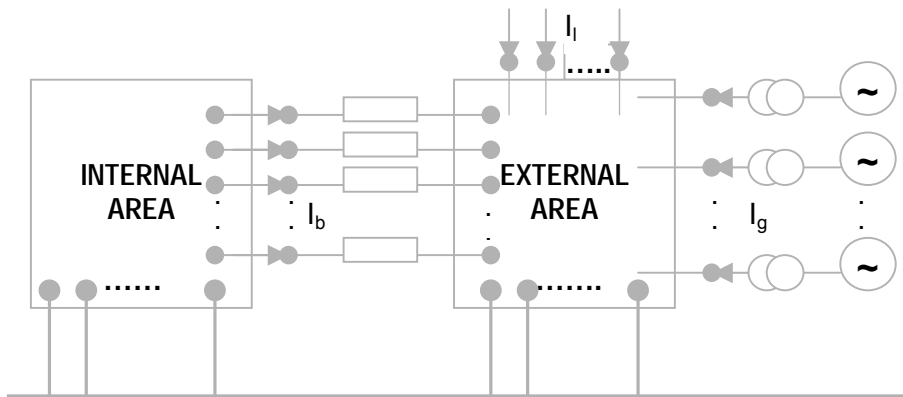


Fig. A.1.- Ward static equivalent by eliminating {L} load and {G} generators nodes.

According to Fig.A.1, the bus current is related to the bus voltage through:

$$\begin{bmatrix} I_g \\ I_l \end{bmatrix} = \begin{bmatrix} Y_{gg} & Y_{gl} \\ Y_{lg} & Y_{ll} \end{bmatrix} \begin{bmatrix} U_g \\ U_l \end{bmatrix} \quad (\text{A.1})$$

The current-voltage relationships are reduced to:

$$I_g^{eq} = Y_{eq} E_{eq} \quad (\text{A.2})$$

where

$$I_g^{eq} = I_g - Y_{gl} Y_{ll}^{-1} I_l \quad (\text{A.3})$$

It denotes the equivalent current injection vector and

$$\underline{Y}_{gg}^{eq} = \underline{Y}_{gg} - \underline{Y}_{gl} \underline{Y}_{ll}^{-1} \underline{Y}_{lg} \quad (\text{A.4})$$

denotes the equivalent bus admittance matrix [50].

- The alternative way to improve accuracy of the Ward-type is to retain selected generator nodes yielding '*the Ward-PV equivalent*' [52-50].
- Replacing, by '*grouping and aggregation of generator nodes*' [51], each selected group by one equivalent generator node, '*the reduced Ward-PV equivalent*' can be obtained.

Fig. A.2 shows schematically the reduced Ward PV-equivalencing.

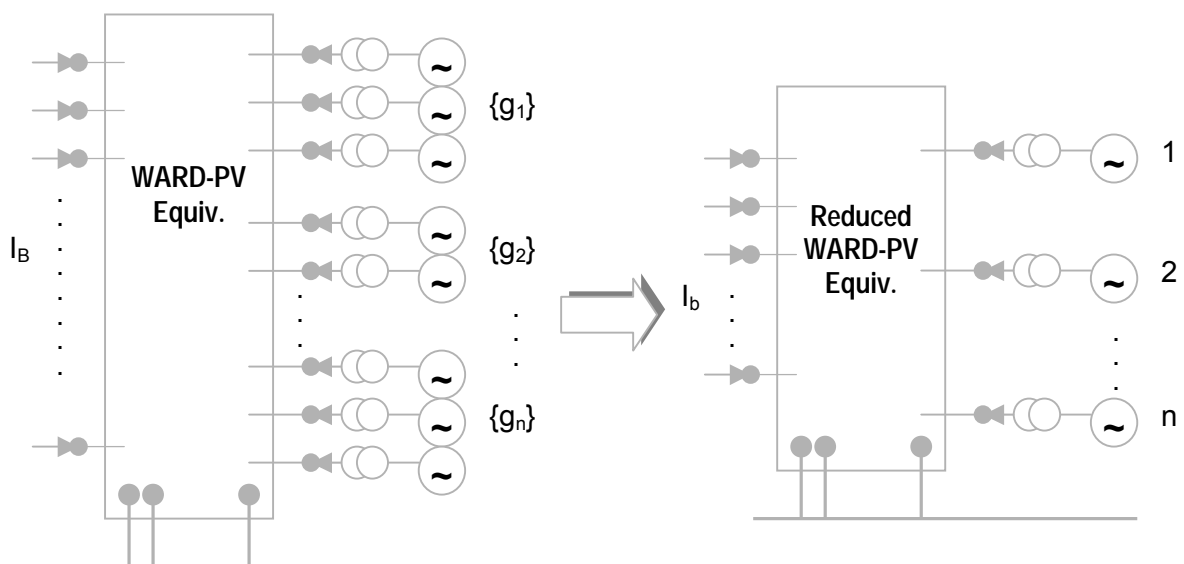


**Fig. A.2.-** Reduction of the Ward-PV equivalent with n number of equivalent generator nodes.

#### Disadvantages:

- This approach is based upon the linearized differential equations of the generator rotor movement. Hence, such equivalents do not retain the dynamic properties of the system.
- A major drawback of all these approaches is the unreliability of the analysis due to the oversimplification of the load nodes [53, 57].

In order to overcome this weakness,

- Bergen [54], Podmore and Germond considered non-linear loads.
- Pai [55] initiated a method based on the assumption that the complex ratios of the voltage phasors at the generator buses to those at the load buses are constant.

### Dynamic Ward equivalent

The main property of this method is a correction formula that allows to update the equivalent current injections at the retained buses as follows:

$$\underline{I}_g^{eq} = \underline{I}_{g0}^{eq} + \Delta \underline{I}_g^{eq} \quad (\text{A.5})$$

Here the subscript '0' refers to the current in the base case operating point. The equivalent current increments can be considered into the generator electric power formulation by:

$$M_i \ddot{\delta}_{gi} + D_i \dot{\delta}_{gi} = P_{m_i} - P_{e_i} \quad (\text{A.6})$$

where  $P_{e_i}$  is the generator electric power obtained from a load flow solution.

When the system is reduced to the internal generator nodes, the equivalent electric powers and their increments are found through:

$$P_{e_{o_i}}^{eq} = E_{g_{o_i}} \sum_{j=1}^n E_{g_{o_j}} Y_{ij}^{eq} \cos(\delta_{g_{o_i}} - \delta_{g_{o_j}} - \vartheta_{ij}^{eq}) \quad (\text{A.7})$$

$$\Delta P_{e_i}^{eq} = E_{g_{o_i}} \Delta I_{g_i}^{eq} \cos(\delta_{g_{o_i}} - \Delta \psi_{g_i}^{eq}) \quad (\text{A.8})$$

$$P_{e_i}^{eq} = P_{e_{o_i}}^{eq} + \Delta P_{e_i}^{eq} \quad (\text{A.9})$$

where

- $Y_{ij}^{eq} \angle \vartheta_{ij}^{eq}$  are the entries of the equivalent bus admittance matrix from (A.4).
- $\Delta I_{g_i}^{eq} \angle \Delta \psi_{g_i}^{eq}$  are updated by the sensitivity matrix.

### Disadvantages:

- The sensitivity matrix is based upon the linearized differential equations of the generator rotor movement.
- The correction formula is performed on linear load models and power flow solutions.

## A.2. Modal-based equivalencing

The external area dynamic, linearized at the operating point, is expressed by [67]:

$$\begin{aligned}\Delta \dot{\mathbf{X}} &= \mathbf{A} \Delta \mathbf{X} + \mathbf{B} \Delta \mathbf{U}_T \\ \Delta \mathbf{I}_T &= \mathbf{C} \Delta \mathbf{X} + \mathbf{D} \Delta \mathbf{U}_T\end{aligned}\quad (\text{A.10})$$

where

- $\mathbf{X}$  is the original state variables
- $\mathbf{U}_T$  is the node terminal bus voltage at interconnected points
- $\mathbf{I}_T$  is the node injection current at interconnected points
- $\mathbf{A}$ ,  $\mathbf{B}$ ,  $\mathbf{C}$ ,  $\mathbf{D}$  are the coefficient matrices composed of generator equations, coordinate transformation equations, algebraic equations of transmission network, etc.
- $\Delta$  is the small deviation from initial value.

The Laplace transformed frequency response formula can be written as:

$$\Delta \underline{\mathbf{X}} = (j\omega \mathbf{I} - \mathbf{A})^{-1} \mathbf{B} \Delta \underline{\mathbf{U}}_T \quad (\text{A.11})$$

The frequency response can be simplified by diagonalizing the system using eigenvalues and eigenvectors as follows:

$$\begin{aligned}\mathbf{T}^{-1} \mathbf{A} \mathbf{T} &= \mathbf{\Lambda} \\ \underline{\mathbf{X}} &= \mathbf{T} \underline{\mathbf{Y}}\end{aligned}\quad (\text{A.12})$$

with:

$$\mathbf{\Lambda} = \text{diag} \{ \mathbf{e}_1, \dots, \mathbf{e}_N \} \quad (\text{A.13})$$

$$\mathbf{T} = \{ \mathbf{v}_1, \dots, \mathbf{v}_N \} \quad (\text{A.14})$$

Using this transformation, the Laplace transformed linearized system can be diagonalized:

$$\Delta \underline{\mathbf{Y}} = (j\omega \mathbf{I} - \mathbf{\Lambda})^{-1} \mathbf{T}^{-1} \mathbf{B} \Delta \underline{\mathbf{U}}_T \quad (\text{A.15})$$

where

- $\Lambda$ ,  $T$  is the diagonal matrix of eigenvalues and the matrix containing eigenvectors, respectively.
- $\underline{Y}$  represents the transformed state variables or state vector in frequency domain on eigenvector basis.

After the transformation, it is easy to calculate the frequency responses for all input frequencies. In general, these equations cannot be interpreted as models of physical devices. Furthermore, model reduction based on modal analysis requires computation of eigenanalysis. Basic concepts of reduction by modal are the reduction by aggregation of similar nodes and elimination of modes, which have large eigenvalues and not included in a similar mode group. This reduction is executed until the number of modes is reduced to a specific number [58-63].

#### **Disadvantages:**

- The modal dynamic equivalent, however, has a limited application. it doesn't have a structural and physical identity. It is a purely mathematical representation the external area and cannot retain its non-linear characteristics.
- The modal technique deals with the modes of the linearized system, in order to eliminate the less significant ones for the disturbance of concern [64].

### **A.3. Coherency-based equivalencing**

- The coherency was proposed by Podmore [17]. In this context, simplified and linearized equations were defined to express the accelerating power deviations of each generator.
- The swing curves obtained are processed to determine the coherent groups of generators. Thus, two generators buses are *defined as coherent if their phase angular difference is constant within a certain tolerance over a certain time interval*.

#### **Disadvantages:**

- *The determined coherent groups are independent of the amount of detail in the machine model, i.e. the real modeling parameters and physical properties of the generators.*
- *Coherent groups are dependent of the size and art of the disturbances. Therefore, the determined equivalents are not exact enough.*

**Remarks:**

- Methods proposed by Di Caprio [18], Avramovic [21], Kokotovic [22] and Balasubramanian [23] are based on the coherency concept.
- The coherency is determined using different magnitudes of the generator, such as moment inertia [23], rotor angle [17], relative rotor angle [67], modes of the eigenvalues [66], and similarity of eigenvectors, amongst others.
- With the coherency-based procedure, which is presented in [23, 24], direct methods, such as the transient energy function methods [44, 45] and extended equal area criterion [46, 47] can be made even faster and optimized.
- The property of coherency of Chang and Abibi [72], Ohsawa and Hayashi [74], Pai and Narayama [75], De Mello [73], Podmore [17], Germond and Podmore [34] are taken from stability simulation cases of the original system, or from inspection of the contribution for the system potential energy associated with the relative motion between each pair of external area generators.

**Coherency in frequency domain**

- Coherency of linear system swings depends on the frequency and damping of a particular swing may be detected. For one selected mode the frequency and damping are evaluated. Thus, coherency is described by the corresponding right eigenvector.
- Considering only that the generator are characterized by the reduced right eigenvector, which describes the so-called *rotor mode shape*, coherent generator groups can be identified based on the small angles between the elements of this reduced eigenvector.
- It is shown in Figure A.4. The magnitudes of the vectors are not significant.

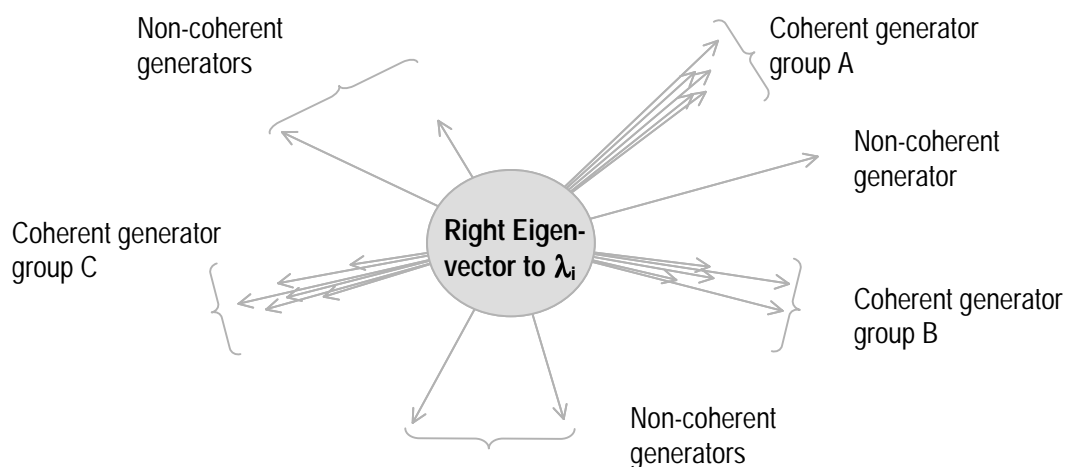


**Fig.A.4.-** Recognition of coherent generators based on generators electromechanical eigenvector

#### A.4. Hybrid modal procedures

Based on ‘*modal analysis*’ and ‘*coherency identification*’, following hybrid procedures show important alternatives to develop dynamic equivalents:

- (i) Modal coherency using frequency response and
- (ii) Synchronic modal equivalencing.

##### (i) Modal coherency using frequency response [65-68]

- After the linearization, diagonalization and transformation of (A.10), the frequency response for all input frequencies is calculated, since the matrix to be inverted for each frequency now is a complex diagonal matrix, as can be seen in Fig. A.3:

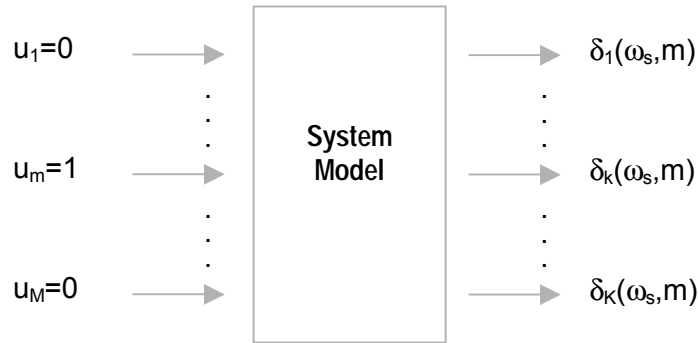


**Fig. A.3.-** Frequency response for input m.

In Fig. A.3 all inputs  $u_i$  are zero, except input  $m$ . The excitation frequency is  $\omega_s$ . The output vector element  $\delta_k(\omega_s, m)$  represents the relative rotor angle in frequency domain of generator  $k$  for a perturbation with frequency  $\omega_s$ , applied at input  $m$ .

According to the frequency analysis, an index  $C_{i,j}$  is calculated and compared between the external generators  $i$  and  $j$  for a sine shaped perturbation of frequency  $\omega_s$ , applied at a single input  $m$  as follows.

$$C_{i,j} = \sum_{m=1}^M \sum_{s=1}^S \left( \frac{|\delta_i(\omega_s, m) - \delta_j(\omega_s, m)|}{|\delta_i(\omega_1, m) - \delta_j(\omega_1, m)|} \right)^2 \quad (\text{A.16})$$

Two generators  $i$  and  $j$  are coherent with respect to the perturbation in the internal area if their index is less than a certain tolerance. Thus, a grouping process according to this index is realized.

**(ii) Synchronic modal equivalencing [69]**

It generates equivalents using *both a linear multiport admittance, replaced by voltage controlled injected currents at the replaced generator buses and external reference generators, one for each external synchronic group.*

- The decomposition into synchronic areas *is defined with respect to a selected subset of modes  $\nu$  of a linearized model.*
- *Two generators are synchronic, if their angular variations are exactly or approximately in constant proportion for any transient, in which only the modes in  $\nu$  are excited.*
- The injected current as multiport admittance is a linear function of the voltages of the buses of the equivalenced generators. This approach grows out of multi-area ‘*Selective Modal Analysis*’ [70, 71] and ‘*slow-coherency*’[12].

**A.5. Linear model reduction**

This *analytical method reduces the order of a full linear system (A.10) [76-78].* The transfer function matrix between outputs  $\mathbf{Y}$  and inputs  $\mathbf{U}$  in (A.10) is given by:

$$\mathbf{G}(j\omega) = \mathbf{C}(j\omega\mathbf{I} - \mathbf{A})^{-1}\mathbf{B} + \mathbf{D} \quad (\text{A.17})$$

One of the main reasons for model reduction bases on the fact, that many poles of the transfer function are compensated by zeros. The positions of the zeros depend on the chosen inputs and outputs, whereas the poles are the same for the whole model.

The task of model reduction, in terms of system theory, can be formulated for a asymptotically stable system, i.e.  $\text{Re}\{\lambda_i(\mathbf{A})\} < 0$  as follows:

$$\dot{\hat{\mathbf{x}}}_R = \hat{\mathbf{A}}_R \hat{\mathbf{x}}_R + \hat{\mathbf{B}}_R \mathbf{u} \quad (\text{A.18})$$

$$\mathbf{y} = \hat{\mathbf{C}}_R \hat{\mathbf{x}}_R + \mathbf{D} \mathbf{u} \quad (\text{A.19})$$

with  $\hat{\mathbf{x}}_R$  as state-vector of the reduced system with  $n_R < n$  and  $\text{Re}\{\lambda_i(\hat{\mathbf{A}}_R)\} < 0$ .

For the approximation error can be used:

- (i) the  $H_\infty$ - Norm or
- (ii) an optimization procedure.

(i) The  $H_\infty$ -Norm of the difference between the frequency response matrices of the non-reduced and reduced system is:

$$\left\| \mathbf{G}(j\omega) - \hat{\mathbf{G}}_R(j\omega) \right\|_\infty = \sup_{\omega} \bar{\sigma} \{ \mathbf{G}(j\omega) - \hat{\mathbf{G}}_R(j\omega) \} \quad (\text{A.20})$$

where

- $\bar{\sigma} = \bar{\sigma}(\omega)$  is greatest singular value.
- $\mathbf{G}(j\omega)$  is the transfer function matrix of the system.
- $\hat{\mathbf{G}}_R(j\omega)$  is the transfer function matrix of the reduced one in frequency domain.

The greater the dimension  $n_R$  the smaller is the approximation error.

(ii) The dynamic equivalent can be calculated solving the following minimization problem as optimization procedure using e.g. genetic algorithms,

$$\min \sum_{k \in K} \{ \lambda(\mathbf{A}_k) - \lambda(\hat{\mathbf{A}}_{R\_k}) \} \quad (\text{A.21})$$

where

- $K$  is the set of operating conditions under study;
- $\lambda(\mathbf{A}_k)$  is the set of electromechanical modes with relevant contributions of generators of the studied system;
- $\lambda(\hat{\mathbf{A}}_{R\_k})$  is the associated set of electromechanical modes of the reduced system.

A multi-machine power system model linearized around a equilibrium point is represented by  $\mathbf{A}_k$  and defining  $\hat{\mathbf{A}}_{R\_k}$  as the state matrix of the corresponding linearized reduced model in (A.17) around the  $k$ th equilibrium point, when just generators of the internal area and some fictitious generators representing the external area are retained [79-83].

On this base, least-squares methods [79-81], genetic algorithms in [82] according to balance realizations and statistical approaches [83] can be used too.

#### Disadvantages:

- The significant drawback of this method is principally that *the resulting equivalent system is not composed of physical components.*
- The estimation of a set of state variable parameters is *based upon the linear state space system* that is assumed to describe *only linear parts of the reduced power system.*

## A.6. Model identification methods

The relationship between inputs, outputs, and unmeasured inputs can be described by the state-space representation described in (A.10) and illustrated as follows:

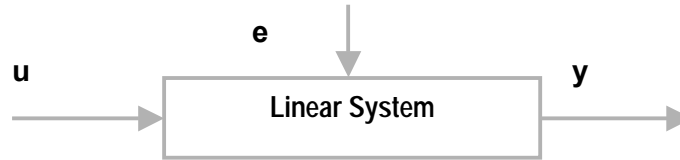


Fig. A.5.- Input Signals  $u$ , Output Signals  $y$ , and Disturbances  $e$

The *identification of the model parameters from (A.10), i.e.  $A$ ,  $B$ ,  $C$  and  $D$  should be realized by several modeling methods in parametric form.*

Assuming the discretized signals are related by a linear system, the relationship of general linear models can be written as.

$$\mathbf{y}(t) = G(q)\mathbf{u}(t) + H(q)\mathbf{e}(t) \quad (\text{A.23})$$

where

- $q$  is the shift operator.
- $G(q)$  is the transfer function of the system.
- $H(q)$  represents the disturbance filter.

The estimation of the transfer functions  $G(q)$  and  $H(q)$  of a model can be realized with different *parametric or nonparametric models* [89, 90].

The identification of dynamic equivalents can be solved using the parametric ARX model with

$$G(q) = q^{-nk} \frac{B(q)}{A(q)} \quad H(q) = \frac{1}{A(q)} \quad (\text{A.24})$$

where  $nk$  corresponds to the number of delays from input to output and  $A$  and  $B$  are polynomials in the delay operator  $q^{-1}$  described as follows:

$$\begin{aligned} A(q) &= 1 + a_1 q^{-1} + \dots + a_{na} q^{-na} \\ B(q) &= b_1 + b_2 q^{-1} + \dots + b_{nb} q^{-nb+1} \end{aligned} \quad (\text{A.25})$$

The model is usually written as:

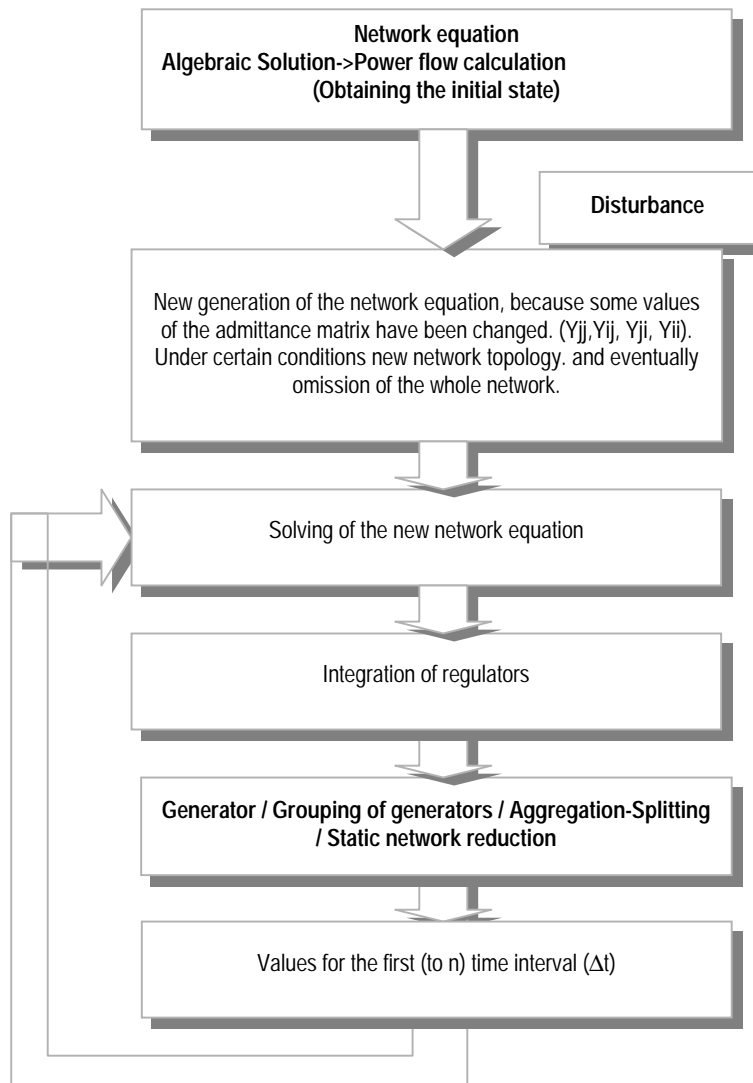
$$A(q)y(t) = B(q)u(t - nk) + e(t) \quad (\text{A.26})$$

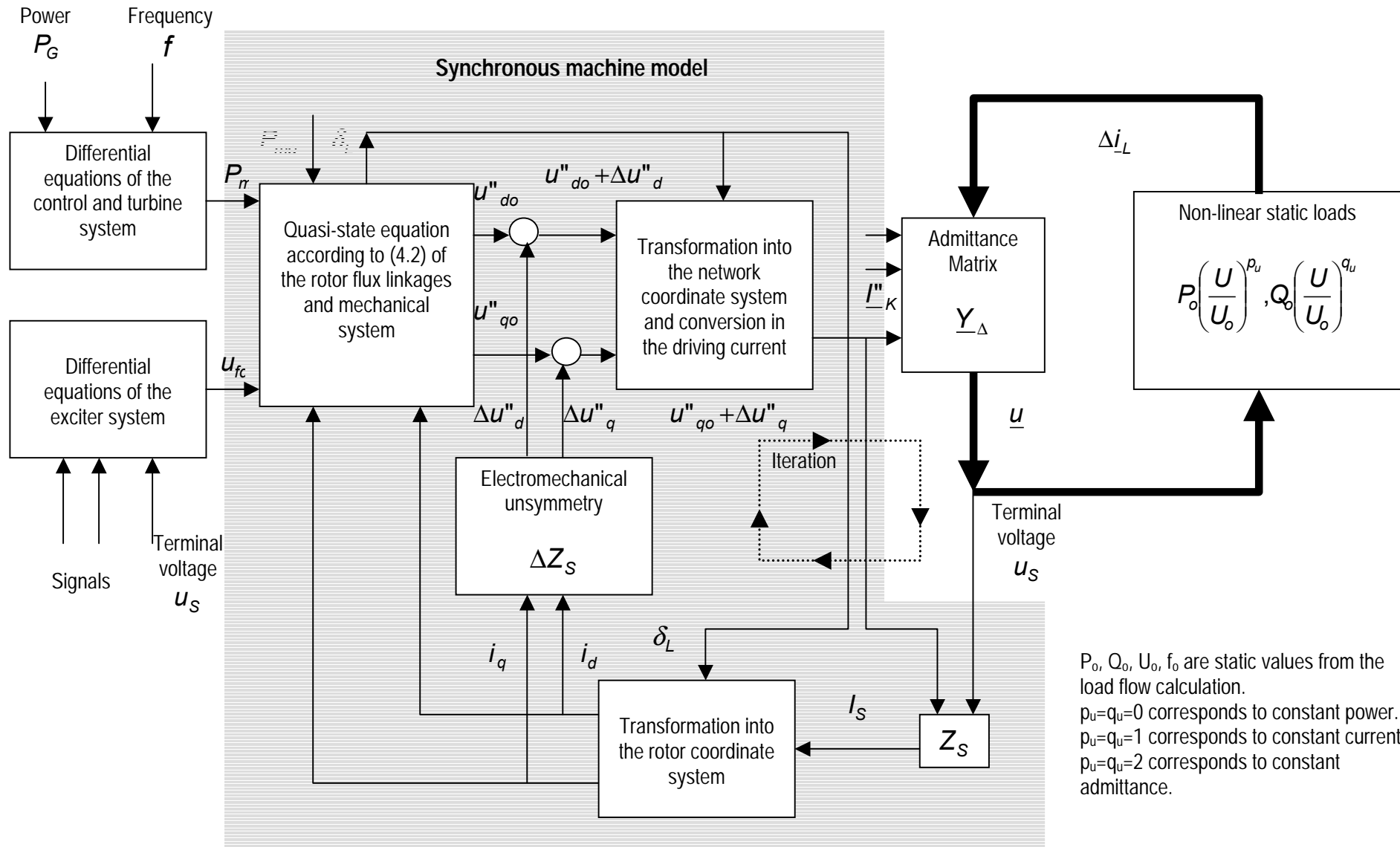
The identification of the ARX-model parameters  $a_i$  and  $b_i$  is based on the least squares estimation method.

### Disadvantages:

- Linearization around the equilibrium yields *mathematically tractable linear models* but according to the power system components *not completely non-linear compatible*.
- Non-linear systems could be *approximated partly in their normal ranges of operation*.
- The disadvantage of this method is principally that *the resulting dynamic equivalent model is not composed of physical components*.

### A.7. Flow chart of the power system simulation tool PSD





$P_o, Q_o, U_o, f_o$  are static values from the load flow calculation.  
 $p_u=q_u=0$  corresponds to constant power.  
 $p_u=q_u=1$  corresponds to constant current.  
 $p_u=q_u=2$  corresponds to constant admittance.

A.8. Flow chart of the coupling of the machine model to the analysis algorithm PSD

## APPENDIX B Identity recognition algorithms

### B.1. Hierarchical clustering

Hierarchical clustering starts with the calculation of all distances  $d_{ij}$  between all the objects in the multidimensional space. Thus, the number of cluster  $c$  initially corresponds to the number of objects of generatorts  $N$ . In total,  $N(N+1)/2$  distances are computed hierarchically. If at a certain step during the clustering process two clusters  $P$  and  $Q$  are agglomerated into a new cluster  $K$ , then the distance between cluster  $K$  and any other cluster  $R$  can be computed according to the following general hierarchical distance form:

$$d_{(K,R)} = \delta_1 d_{(P,R)} + \delta_2 d_{(Q,R)} + \delta_3 d_{(P,Q)} + \delta_4 |d_{(P,R)} - d_{(Q,R)}| \quad (\text{B.1})$$

Where the coefficients are different for different strategies, such as *the single-, complete-, simple average-, average linkage, centroid, median and Ward's method* after table B.1.

**Table B.1.-** Computation of distances [101]

Name	$\delta_1$	$\delta_2$	$\delta_3$	$\delta_4$
Single linkage	1/2	1/2	0	-1/2
Complete linkage	1/2	1/2	0	1/2
Simple Average linkage	1/2	1/2	0	0
Average linkage	$\frac{n_P}{n_P + n_Q}$	$\frac{n_Q}{n_P + n_Q}$	0	0
Centroid	$\frac{n_P}{n_P + n_Q}$	$\frac{n_Q}{n_P + n_Q}$	$\frac{n_P n_Q}{(n_P + n_Q)^2}$	0
Median	1/2	1/2	-1/4	0
Ward	$\frac{n_R + n_P}{n_R + n_P + n_Q}$	$\frac{n_R + n_Q}{n_R + n_P + n_Q}$	$\frac{-n_R}{n_R + n_P + n_Q}$	0

## B.2. Partitioning clustering: K-means

This clustering permits objects to *change group membership through a cluster formation process* [99]. The reallocation occurs according to the following optimality criterion [101]:

$$S_{\text{squared}} E_{\text{error}}(K)_{\text{in}} = \sum_{j=1}^N \sum_{i=1}^K \sum_{l=1}^M (x_{j,l} - c_{i,l})^2 \rightarrow \min \quad (\text{B.2})$$

where  $x_j$  is a data vector,  $c_i$  is a centroid vector of a group,  $M$  denotes the number of variables,  $N$  the number of objects and  $K$  the number of cluster groups.

The total squared error of the procedure is constant; the minimum of squared error in the clusters corresponds to a maximization of the squared error between the clusters, as follows:

$$S_{\text{squared}} E_{\text{error}}(K)_{\text{between}} = SE_{\text{Total}} - S_{\text{squared}} E_{\text{error}}(K)_{\text{in}} \quad (\text{B.3})$$

The flow chat of K-means algorithm is described schematically as:

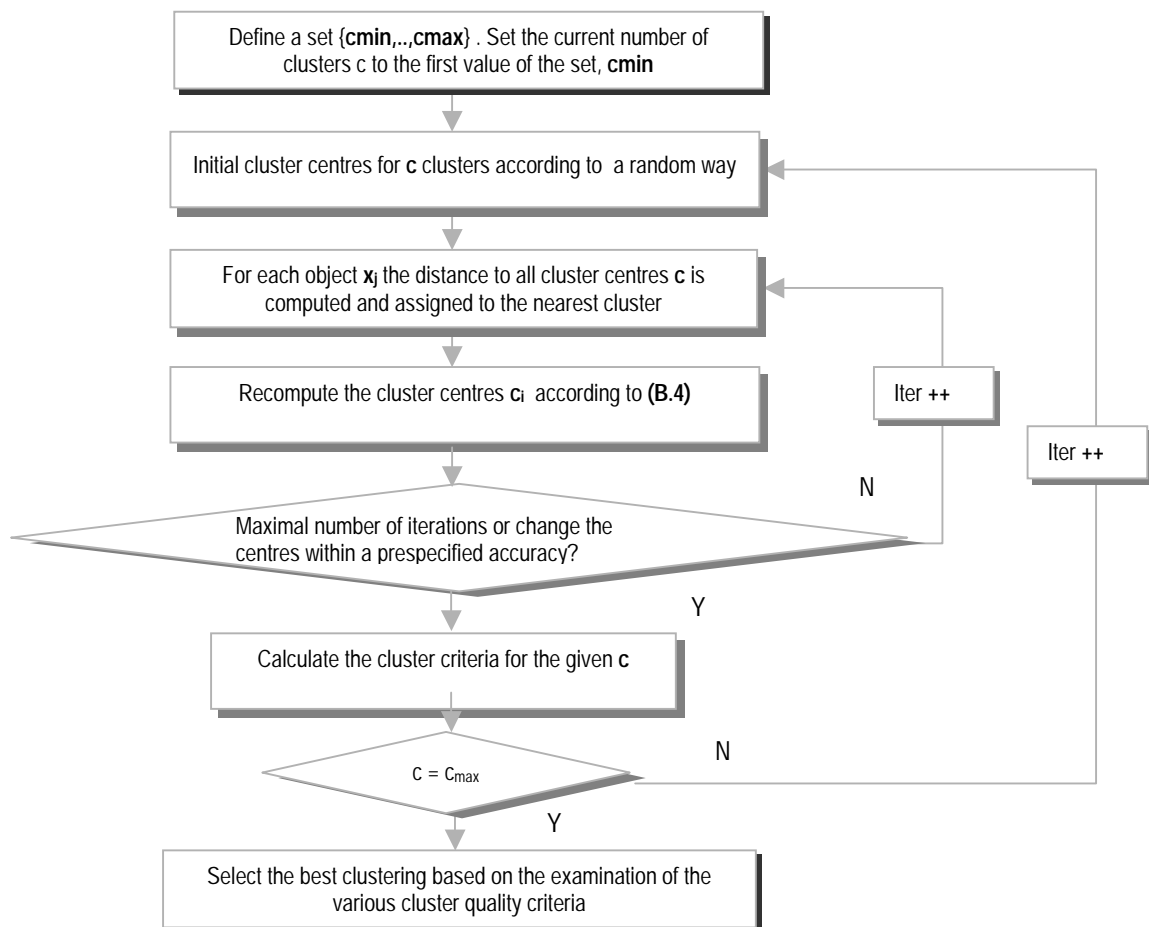


Fig. B.1.- Flow chart of the concept of K-means for a set of clusters

The algorithm for this method can be modified to realize this procedure automatically not only for one specified number of cluster, but rather for a set of clusters between  $c_{min}$  and  $c_{max}$ . The iterative partitioning of reassignment in the cluster centers is calculated by:

$$c_i = \frac{1}{N_i} \sum_{j=1}^{N_i} x_j \quad \therefore i = 1, \dots, K \quad (\text{B.4})$$

### B.3. Fuzzy clustering

The key idea of this clustering is to extend the classical within groups sum of squared error objective function to a Fuzzy version by minimizing an objective function [102-105]. The Fuzzy clustering conditions can be derived as the following way.

In classical variational theory, a fundamental continuous-time continuous-state functional optimisation problem (minimizing) in its simplest form is defined as:

$$J_y = \int_{t_0}^{t_1} F(t, y(t), \dot{y}(t)) dt \rightarrow \min \quad (\text{B.5})$$

If bundle  $y$  is a weak relative minimum to (B.5), and if  $t$  is any point in  $[t_0, t_1]$  where derivative  $\dot{y}(t)$  exists, then the Euler-Lagrange equation in its differentiated form holds:

$$\frac{\partial F}{\partial y} - \frac{d}{dt} \frac{\partial F}{\partial \dot{y}} = 0 \quad (\text{B.6})$$

A functional optimisation problem in discrete time can be defined as:

$$J_y = \sum_{t=0}^N F(t, y(t), y(t+1)) \rightarrow \min \quad (\text{B.7})$$

Such a functional is solved by discrete-time Euler-Lagrange equations. Although these results do not consider constraints, side constraints, including Lagrange constraints and isoperimetric constraints, can be included. Constraints are typically handled by using Lagrange multipliers to transform a constrained problem into an unconstrained one, and by applying the Euler-Lagrange condition on the Lagrangian function to get the Euler Lagrange equations, as follows:

Thus, a *generalized Lagrangian function (constrained functional)*:

$$\hat{J}_y = \int_{t_0}^{t_1} L(t, y(t), \dot{y}(t), \lambda) dt \rightarrow \min \quad (\text{B.8})$$

subject to 
$$g(t, y(t), \dot{y}(t)) = 0 \quad (\text{B.9})$$

with

$$L(t, y(t), \dot{y}(t), \lambda) = F(t, y(t), \dot{y}(t)) + \lambda^T g(t, y(t), \dot{y}(t)) \quad (\text{B.10})$$

may be solved by the Euler-Lagrange equation, too:

$$\frac{\partial L}{\partial y} - \frac{d}{dt} \frac{\partial L}{\partial \dot{y}} = 0 \quad (\text{B.11a})$$

$$\frac{\partial L}{\partial \lambda} - \frac{d}{dt} \frac{\partial L}{\partial \dot{\lambda}} = 0 \quad (\text{B.11b})$$

This concept can be extended to consider a discrete constrained optimisation problem of Fuzzy clustering. The objective function is:

$$J_m(X, C, \mu) = \sum_{j=1}^N \sum_{i=1}^K \mu_{i,j}^m d_{i,j}^2 = \sum_{j=1}^N \sum_{i=1}^K \mu_{i,j}^m \|x_j - c_i\|^2 \rightarrow \min \quad (\text{B.12})$$

where

- N corresponds to the number of objects and K to the number of clusters.
- $d_{ij}$  is the distance between the datum vector and cluster centers.
- $\mu_{ij}$  is the membership degree of datum  $x_j$  to cluster  $c_i$ .
- $m > 1$  is the fuzziness index and influences the “fuzziness” of the obtained partition.

The objective function is subjected to the following discrete variable constraints of  $\mu_{ij}$ :

$$\forall 1 < j \leq K: \sum_{i=1}^N \mu_{i,j} > 0, \quad \forall 1 < j \leq N: \sum_{i=1}^K \mu_{i,j} = 1 \quad (\text{B.13})$$

(B.12) can be minimized, while too for all  $\mu$  the sum  $\sum_{c \in C} \mu_c^m d^2(x, c)$  will be minimized. A *generalized discrete Lagrangian function* of (B.12) is:

$$L(\mu, \lambda) = \sum_{c \in C} \mu_c^m d^2(x, c) + \lambda \left( \sum_{c \in C} \mu_c - 1 \right) \quad (\text{B.14})$$

This applicability doesn't pose problems here because it doesn't require the differentiability. Applying the Euler-Lagrange equation following equations are obtained:

$$\frac{\partial}{\partial \lambda} L(\mu, \lambda) = \left( \sum_{c \in C} \mu_c \right) - 1 = 0 \quad (\text{B.15})$$

$$\frac{\partial}{\partial \mu_c} L(\mu, \lambda) = m * \mu_c^{m-1} * d^2(x, c) + \lambda = 0 \quad (\text{B.16})$$

Dissolving the membership degree in (B.16) and replacing in (B.15) results:

$$\mu_c = \left( -\frac{\lambda}{m * d^2(x, c)} \right)^{\frac{1}{m-1}} \quad (\text{B.17})$$

$$1 = \sum_{i \in C} \mu_i = \left( -\frac{\lambda}{m} \right)^{\frac{1}{m-1}} \sum_{i \in C} \left( \frac{1}{d^2(x, i)} \right)^{\frac{1}{m-1}} \quad (\text{B.18})$$

The resulting constant:

$$\left( -\frac{\lambda}{m} \right)^{\frac{1}{m-1}} = \frac{1}{\sum_{i \in C} \left( \frac{1}{d^2(x, i)} \right)^{\frac{1}{m-1}}}$$

together with (B.17) forms the membership degree condition as:

$$\mu_c = \frac{1}{\sum_{i \in C} \left( \frac{1}{d^2(x, i)} \right)^{\frac{1}{m-1}}} * \left( \frac{1}{d^2(x, c)} \right)^{\frac{1}{m-1}} \Rightarrow \mu_c = \left( \sum_{i \in C} \left( \frac{d(x, c)}{d(x, i)} \right)^{\frac{2}{m-1}} \right)^{-1}$$

$$\mu_{i,j} = \left( \sum_{r=1}^M \left( \frac{d_{i,j}}{d_{i,r}} \right)^{\frac{2}{m-1}} \right)^{-1} \quad i=1..K; j=1..N \quad (\text{B.19})$$

For the initial values of the membership degree, the following formulation can be used:

$$u_{ij} = \frac{d_{ij}^{-1}}{\sum_{i=1}^K d_{ij}^{-1}} \quad (\text{B.20})$$

Another condition for local extreme is based upon the differentiation of  $J_m$  to  $c_i$  using the residue principle as:

$$\begin{aligned} 0 &= \frac{\partial}{\partial c_i} \sum_{j=1}^N \sum_{i=1}^K \mu_{i,j}^m \|x_j - c_i\|^2 = \sum_{j=1}^N \mu_{i,j}^m \frac{\partial}{\partial c_i} \|x_j - c_i\|^2 \quad (\text{B.21}) \\ 0 &= \sum_{j=1}^N \mu_{i,j}^m \lim_{t \rightarrow 0} \frac{\|(x_j - c_i) + t\xi\|^2 - \|x_j - c_i\|^2}{t} \\ 0 &= \sum_{j=1}^N \mu_{i,j}^m \lim_{t \rightarrow 0} \frac{1}{t} ((x_j - c_i) - t\xi)^T ((x_j - c_i) - t\xi) - (x_j - c_i)^T (x_j - c_i) \\ 0 &= \sum_{j=1}^N \mu_{i,j}^m \lim_{t \rightarrow 0} \frac{-2t(x_j - c_i)^T \xi + t^2 \xi^T \xi}{t} = -2 \sum_{j=1}^N \mu_{i,j}^m (x_j - c_i)^T \xi \end{aligned}$$

According with the condition for local extreme:

$$\frac{\partial}{\partial c_i} J = 0 \Rightarrow \sum_{j=1}^N \mu_{i,j}^m (x_j - c_i) = 0 \quad (\text{B.22})$$

following condition can be reached:

$$\Rightarrow c_i = \frac{\sum_{j=1}^N \mu_{i,j}^m x_j}{\sum_{j=1}^N \mu_{i,j}^m} \quad \therefore 1 \leq i \leq K \quad (\text{B.23})$$

Conditions (B.19), (B.20) and (B.23) are first-order necessary conditions for local extreme of  $J_m$ . Thus, all Fuzzy algorithms used to solve (B.12) should satisfy (B.19), (B.20) and (B.23).

The algorithm realized for Fuzzy clustering is described schematically as follows:

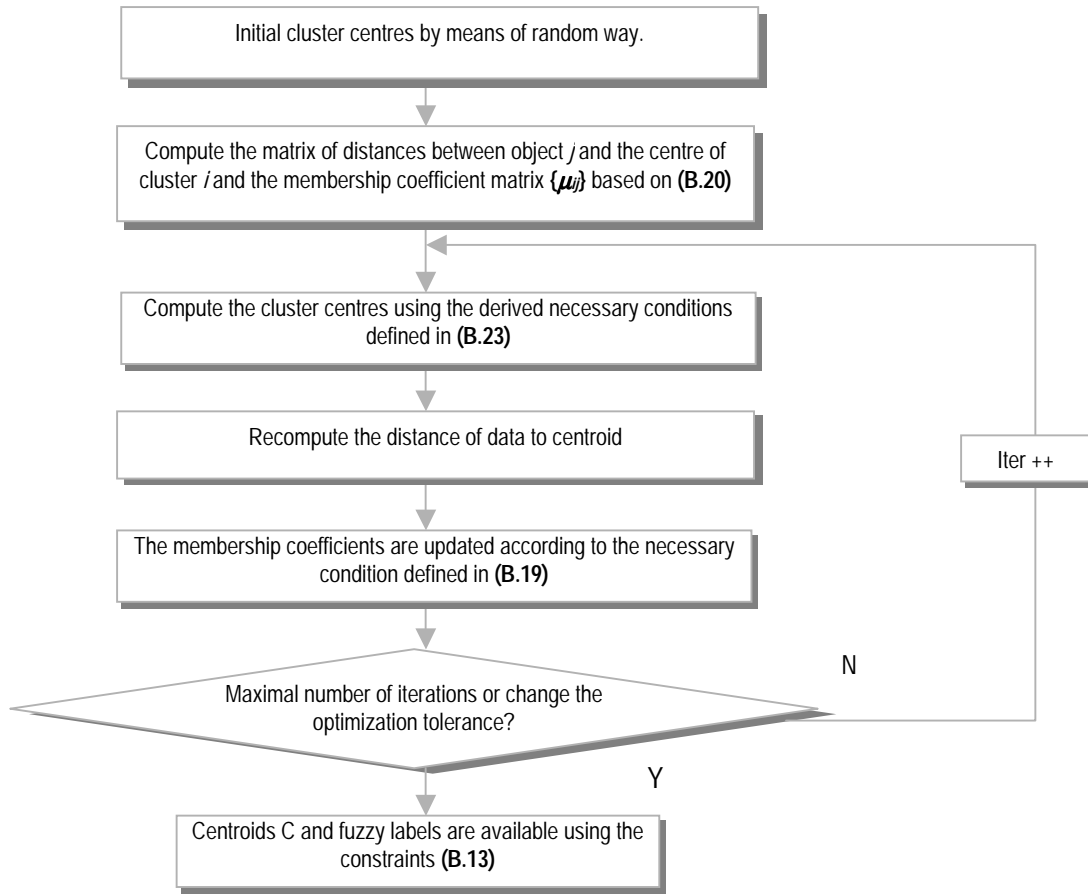


**Fig. B.2.-** Flow chart of the concept of fuzzy c-means clustering.

#### B.4. Relationship between K-means (hard clustering) and Fuzzy clustering

The difference between K-means and Fuzzy clustering can be described mathematically according to the conditions (B.19) and (B.23) as follows:

- Considering the convergence  $m \rightarrow 1$ , following equations can be obtained:

$$\lim_{m \rightarrow 1} \{\mu_k\} = \lim_{m \rightarrow 1} \left( \frac{1}{\sum_{i \in C} \left( \frac{d(x, c)}{d(x, i)} \right)^{\frac{2}{m-1}}} \right) = \begin{cases} 1; d(x, c) < d(x, i) \quad \forall i \neq c \\ 0; \text{sonst} \end{cases} \quad (\text{B.24})$$

$$\lim_{m \rightarrow 1} \{c_i\} = \lim_{m \rightarrow 1} \left( \frac{\sum_{j=1}^N \mu_{ij}^m x_j}{\sum_{j=1}^N \mu_{ij}^m} \right) = \frac{\sum_{x_k \in X_i} x_k}{N_i}, \quad 1 \leq i \leq K \quad (\text{B.25})$$

This convergence corresponds to the K-means partition and represents the classical within-groups sum of squared errors. The cluster centers are defined as the average sum of objects assigned to the corresponding clusters.

- Considering the convergence  $m \rightarrow \infty$ , i.e. in this case, the clusters are nearly undistinguishable. The following equations can be obtained:

$$\lim_{m \rightarrow \infty} \{\mu_k\} = \lim_{m \rightarrow \infty} \left( \frac{1}{\sum_{i \in C} \left( \frac{d(x, c)}{d(x, i)} \right)^{\frac{2}{m-1}}} \right) = \frac{1}{K} \quad (\text{B.26})$$

$$\lim_{m \rightarrow \infty} \{c_i\} = \lim_{m \rightarrow \infty} \left( \frac{\sum_{j=1}^N \mu_{ij}^m x_j}{\sum_{j=1}^N \mu_{ij}^m} \right) = \frac{\frac{1}{K} x_1 + \dots + \frac{1}{K} x_n}{\frac{1}{K} + \dots + \frac{1}{K}} = \frac{\sum_{k=1}^N x_k}{N} = \bar{C} \quad \therefore 1 \leq i \leq K \quad (\text{B.27})$$

Where  $u_k$  and  $c_i$  represent a single large cluster group, in which is included all data vectors. All those objects show same membership degree [105].

### B.5. Self organizing features maps (SOFM)

The unsupervised ANN learn to recognize groups of similar input vectors in such a way that neurons physically close together in the neuron layer respond to identical objects [110].

The following graphic shows the schematic representation of a SOFM.

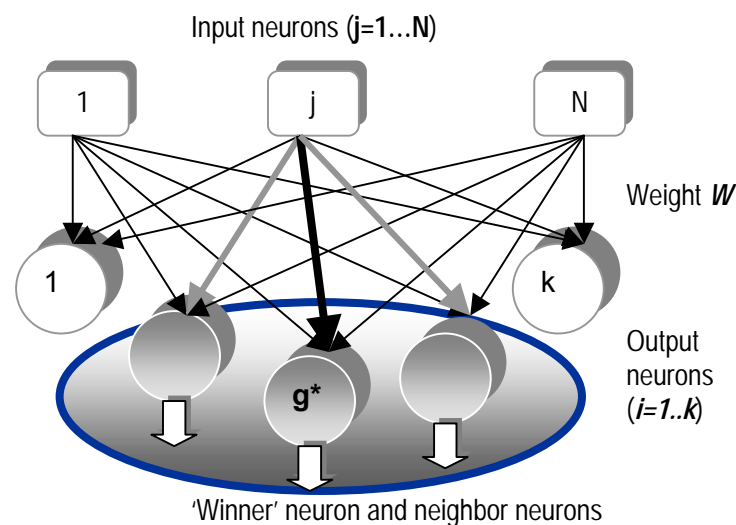


Fig. B.3.- Schematic representation of SOFM

Thus, the weights of the winning neuron has to be adjusted so as to move it closer to the input vector by the following learning rule (Kohonen learning rule):

$$W_g(t) = W_g(t - 1) + \alpha(t)N_g(t, d)[x_j(t) - W_g(t - 1)] \tag{B.28}$$

Hereby, the corresponding vector of the input weight matrix  $W_g$  of the neurons has to be adjusted and updated according to a *learning* function  $\alpha(t)$  and neighborhood function  $N(t)$ .

**The ‘winner’ neuron** can be determined by the following *Euclidean distance* criterion that for the  $g^{th}$  neuron obtains minimum value.

$$D(g) = \sum_{l=1}^M (x_{jl} - w_{gl})^2 \rightarrow min \tag{B.29}$$

In this expression  $x_{jl}$  is the pattern of the time response of matrix  $X(M,N)$  and  $w_{gl}$  is the weight vectors of  $W$  matrix of order  $(k,M)$  with  $k$  corresponding to number of clusters.

**B.6. Clustering quality**

A problem in clustering is the choice of the correct number of clusters and its quality. Clustering criteria can help to suggest these aspects. The Fig. B.4 shows these aspects:

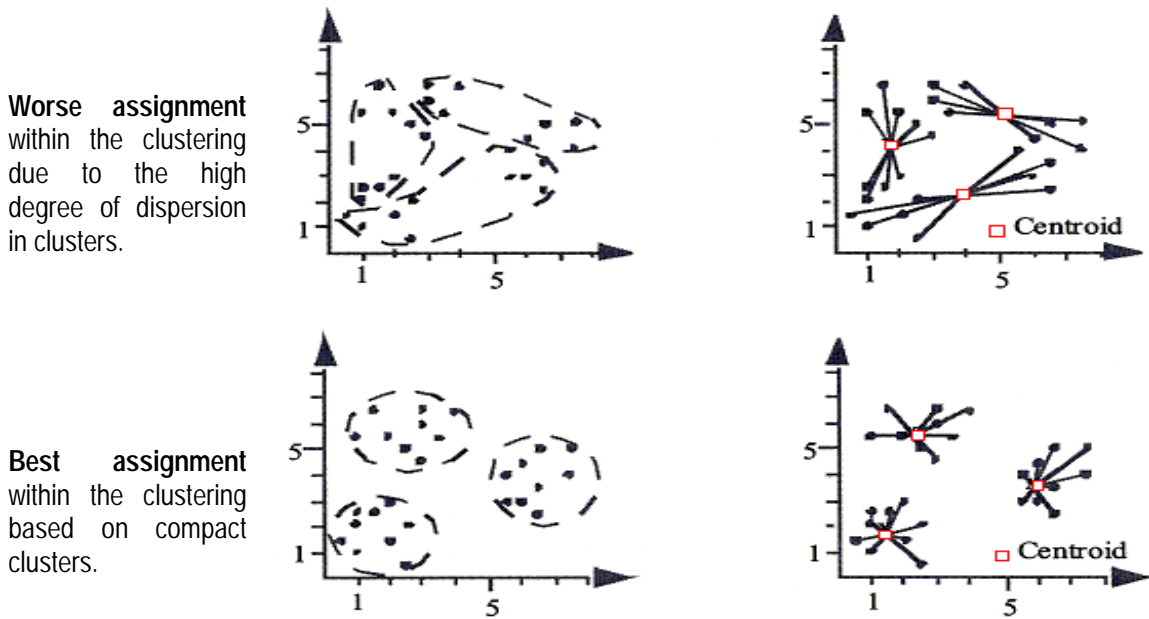


Fig. B.4.- Schematic representation of the clustering quality

The problem has been discussed extensively in the literature in [93-98]. The question, "*which clustering criterion gives the best results?*" remains. It is suitable that a fruitful approach implies the application of several criteria because each has strong and weak points. The criteria implemented are the total error sum of squares, Davies-Bouldin index and the Silhoutten coefficient discussed extensively in [93-99], whose criteria principally are based on the within-cluster variation.

### **B.7. Practical comparison of identity recognition algorithms**

The strengths and weaknesses of each algorithm implemented in [141] are:

- **Accuracy.-** The electromechanical K-means and Fuzzy show a similar high accuracy in the forming of identical groups of generators with a non-significant computational requirement. In contrast to this, Kohonen SOFM shows the worst accuracy.
- **Complexity and processing time.-** The resource consumption varies considerably between the K-means and SOFM. SOFM are impractical for large power system. SOFM inefficiency, resulting from search of the winner neuron, increases the time cost and it shows a slower convergence rate. The simplicity of the K-means and its speed of convergence are obvious advantages for the applicability in large power systems. Fuzzy has own computational advantages due to its optimization nature, but its processing time due to the iterative operation of the objective function, is computing resource-based.
- **Efficiency.-** K-means, hierarchical and Fuzzy efficiency depends largely on the inputs patterns. The efficiency of SOFM depends on how accurately the learning and neighborhood function represent the input patterns in the weight vectors. Electromechanical Fuzzy and K-means are numerically stable as well consistent, and it is applicable to power systems with larger amounts of generators.

# APPENDIX C DANN-based dynamic equivalencing

## C.1. ANN preliminaries

### Architecture and topology

A non-linear system can be captured by the following ANN structure:

- The feedforward ANN mathematical description is given by:

$$y = h(\boldsymbol{\varphi}, \boldsymbol{\theta}) = \mathbf{W}_2 \kappa(\boldsymbol{\varphi}^T \mathbf{W}_1 + \mathbf{B}_1) + \mathbf{B}_2 \quad (\text{C.1})$$

where  $\boldsymbol{\varphi}$  are neuron inputs,  $\mathbf{W}_i$  is the weight matrix and  $\mathbf{B}_i$  denotes the bias that is considered, for simplicity, a weight associated with a unitary input.

- The activation function  $\kappa(\cdot)$  representing the non-linearity property of the ANN, may be:

The tangent hyperbolic:  $\kappa(x) = \tanh(x) = \frac{e^x - e^{-x}}{e^x + e^{-x}} \quad (\text{C.2})$

Sigmoidal type:  $\kappa(x) = \sigma(x) = \frac{1}{1 + e^{-x}} \quad (\text{C.3})$

Gaussian:  $\kappa(x) = \frac{1}{\sqrt{2\pi}} e^{-\frac{x^2}{2}} \quad (\text{C.4})$

- The ANN weights are updated by the back-propagation according to:

$$\Delta \theta_{ij}(t) = -\eta \frac{\partial E(t)}{\partial \theta_{ij}(t)} + \alpha \Delta \theta_{ij}(t-1) \quad (\text{C.5})$$

where  $\eta$  is the learning rate, which controls the rate at which the ANN learns,  $\frac{\partial E(t)}{\partial \theta(t)}$  is

the derivative of the error with respect to the weight and  $\alpha$  is the momentum.

- The output layer is a linear type function.

## C.2. Learning strategies

The learning strategy used is to minimize the difference between the desired and the actual output of the network, using following optimization strategies [124-128]:

- **The Back-propagation** is based on the propagation of the output errors until it reaches the first layer of the neural network. The ANN weights in (C.5) can be updated by the back-propagation according to the sensitivity of the error with respect to the weighting.
- **The Levenberg-Marquardt optimization** uses this approximation to the Hessian matrix in the following Newton-like update:

$$\boldsymbol{\theta}(t+1) = \boldsymbol{\theta}(t) - [\mathbf{J}^T \mathbf{J} + \mu \mathbf{I}]^{-1} \mathbf{J}^T \mathbf{E}(t) \quad (\text{C.6})$$

$$\mathbf{H} = \mathbf{J}^T \mathbf{J} \quad (\text{C.7})$$

$$\mathbf{g} = \mathbf{J}^T \mathbf{E}(t) \quad (\text{C.8})$$

where  $x_k$  is a vector of current weights and biases. When the scalar  $\mu$  is zero, this is just Newton's method, using the approximate Hessian matrix. When  $\mu$  is large, this becomes gradient descent with a small step size. The Hessian matrix and the gradient can be approximated in (C.7) and (C.8).  $\mathbf{J}$  is the Jacobian matrix that contains first derivatives of the network errors with respect to the weights and biases, and  $\mathbf{E}$  is a vector of errors.

## C.3. Modeling

The modeling may be divided into the following basic functions:

- **Regression vector.**- It may be implemented in form of a delay space embedding of input and output variables and represents the long-term prediction capability of a model providing sufficient information to reconstruct the states of the system.

A collection of time lags in a regressor vector space of  $d$  dimensions can be:

$$\boldsymbol{\varphi}(t) = \boldsymbol{\varphi}(u(t), u(t-T), \dots, u(t-(d-1)T), y(t-T), y(t-2T), \dots, y(t-(d-1)T)..) \quad (\text{C.9})$$

- **Non-linear mapping.**- The non-linear mapping is described by the modeling capability of the ANN. The most difficult part of the system modeling is not the parameter estimation but the selection of the suitable model structure and the feature extraction for the nonlinear mapping

#### C.4. Non-linear models

The following non-linear models may be considered [117, 118]:

- **Non-linear Output Error (NOE structure):**

$$\hat{y}(t+1) = \hat{h} \left( \hat{y}(t), \dots, \hat{y}(t-n_y+1), u(t), \dots, u(t-n_u+1) \right) \quad (\text{C.10})$$

- **Non-linear AutoRegressive models with eXogenous inputs (NARX structure):**

$$\hat{y}(t+1) = \hat{h} \left( y(t), \dots, y(t-n_y+1), u(t), \dots, u(t-n_u+1) \right) \quad (\text{C.11})$$

- **Non-linear AutoRegressive Moving Average with eXogenous inputs (NARMAX):**

$$\hat{y}(t+1) = \hat{h} \left( \hat{y}(t), \dots, \hat{y}(t-n_y+1), u(t), \dots, u(t-n_u+1) \right) + e(t) \quad (\text{C.12})$$

where  $\hat{y}$  is the output of the identification model  $\hat{h}$ ,  $y$  of the non-linear system.

#### C.5. Power system model

##### Modeling of the excitation system

The excitation system including PSS, whose basic function is to add damping to the generator rotor oscillations by controlling its excitation, may be represented by the equations:

$$\dot{\mathbf{x}}_E = \mathbf{A}_E \mathbf{x}_E + \mathbf{B}_{E1} \mathbf{u}_{PSS} + \mathbf{B}_{E2} \mathbf{u}_t \quad (\text{C.13})$$

$$E_{fd} = E_{fd}(\mathbf{x}_E) \quad (\text{C.14})$$

where  $u_{pss}$  is the input signal to the PSS or the exciter input voltage.

If it is derived from the rotor velocity then  $u_{pss} = \omega \cdot U_t$  corresponds to the terminal voltage magnitude. In general,  $E_{fd}$  is a linear function of  $x_E$  except when limits of  $E_{fd}$  are to be considered.

Control of the excitation system of a synchronous machine has a very strong influence on its performance, voltage regulation, and stability [135, 137, and 138].

### Modeling of the turbine and governor

The turbine-governor system can be expressed generally by the equations [136]:

$$\dot{\mathbf{x}}_T = \mathbf{A}_T \mathbf{x}_T + \mathbf{B}_{T1} \omega + \mathbf{B}_{T2} P_m^{ref} \quad (\text{C.15})$$

$$T_m = T_m(\mathbf{x}_T) \quad (\text{C.16})$$

where  $P_m^{ref}$  is the reference power set by Load Frequency Control (LFC) or Automatic Generation Control (AGC).

The variables and parameters of equations (C.13–C.16) are given in [136]. They are important pieces of power system equipment.

The dynamics of the turbine and governor are normally much slower than that of the exciter. Hence, the dynamics of these devices can be neglected.

### Remarks:

Thus, the generator equations comprise following important parts [136]:

- *Rotor electrical,*
- *Mechanical,*
- *Excitation and*
- *Turbine-governor equations* according to the basic components of power systems.

The interconnections among the various subsystems of the generator are shown schematically as follows:

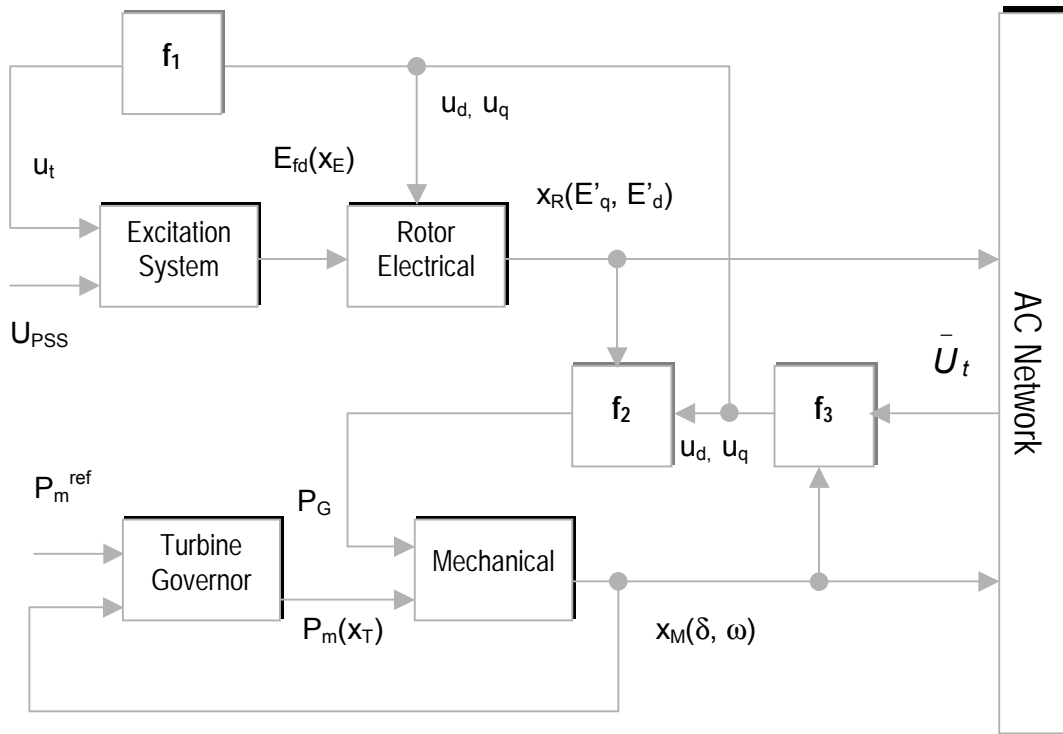


Fig. C.1.- Interconnections among subsystems

Hereby  $f_1$ ,  $f_2$  and  $f_3$  are non-linear functions of the input variables obtained from equations given above,  $u_q$  and  $u_d$  are derived from the knowledge of the phasor  $\bar{U}_t$  expressed with reference to a common reference frame and the generator rotor angle  $\delta$ , as given below according to  $f_3$  depicted in Fig. C.1.

$$(u_q + ju_d) = \bar{U}_t e^{-j\delta} = U_t e^{j(\theta-\delta)} \quad (C.17)$$

$\bar{U}_t$  and  $\bar{I}_t$  are the terminal voltage and terminal current phasors of the generator.

From this expression, the following relationship can be obtained:

$$\begin{aligned} u_q &= U_t \cos(\theta - \delta) \\ u_d &= U_t \sin(\theta - \delta) \end{aligned} \quad (C.18)$$

and  $U_t$  based on function  $f_1$  in Fig. C.1 can be expressed as:

$$U_t = \sqrt{u_d^2 + u_q^2} \quad (C.19)$$

where  $\theta$  is the bus angle at the generator terminals obtained from the network solution.

## APPENDIX D Data sets of 16 Multi-machine system

**Table D.1.-** Data sets of investigated multi-machine systems

	16-machine system	12-machine system	European Interconnected Power System UCTE/CENTRAL
Number of generating units	16	12	496
Number of transmission lines	54	60	2098
Number of Nodes	66	58	2016
Number of two winding transformer units	16	12	1032
Number of three winding transformer units	12	0	0

**Table D.2.-** Generator data set of 16 multi-machine system

Name	Mod. Order	SN [MVA]	T <sub>m</sub>	UN[kV]	r <sub>a</sub> [p.u.]	x <sub>s</sub> [p.u.]	x <sub>d</sub> ' [p.u.]	x <sub>d</sub> '' [p.u.]
A01aG	5	220	1518	15,75	0,001	0,195	0,43	0,225
A01bG	5	220	1518	15,75	0,001	0,195	0,43	0,225
A02aG	5	220	1518	15,75	0,001	0,195	0,43	0,225
A02bG	5	220	1518	15,75	0,001	0,195	0,43	0,225
A03_G	5	220	1518	15,75	0,001	0,195	0,43	0,225
A06_G	5	247	1729	15,75	0,002	0,19	0,36	0,24
B02aG	5	259	2719,5	15,75	0,001	0,156	0,29	0,2
B02bG	5	259	2719,5	15,75	0,001	0,156	0,29	0,2
B03_G	5	259	2719,5	15,75	0,001	0,156	0,29	0,2
B08_G	5	247	1729	15,75	0,002	0,19	0,36	0,24
B10_G	5	259	2719,5	15,75	0,001	0,156	0,29	0,2
C02_G	5	247	1729	15,75	0,002	0,19	0,36	0,24
C07_G	5	247	1729	15,75	0,002	0,19	0,36	0,24
C10_G	5	247	1729	15,75	0,002	0,19	0,36	0,24
C12_G	5	247	1729	15,75	0,002	0,19	0,36	0,24
C14_G	5	247	1729	15,75	0,002	0,19	0,36	0,24

**Table D.3.-** Transmission line data set of 16- machine system

From bus	To bus	Long	r [p.u.]	x [p.u.]	b [p.u.]
A01_L380	A04_L380	50	0,0155	0,1358	0,0267
A01_L380	A02_L380	100	0,0155	0,1358	0,0267
A04_L380	A05aL380	100	0,0155	0,1358	0,0267
A02_L380	A05aL380	100	0,0309	0,266	0,0136
A02_L380	A05bL380	100	0,0309	0,266	0,0136
A02_L380	A03_L380	100	0,0309	0,266	0,0136
A05aL380	A07_L380	50	0,0309	0,266	0,0136
A05aL380	C01_L380	200	0,0309	0,266	0,0136
A05aL380	C01_L380	200	0,0309	0,266	0,0136
A05aL380	A05bL380	0,1	0,01	0,01	0,01
A05bL380	A07_L380	50	0,0309	0,266	0,0136
A05bL380	B01_L380	220	0,0309	0,266	0,0136
A05bL380	B01_L380	220	0,0309	0,266	0,0136
A06_L220	A07_L220	50	0,0792	0,2901	0,0126
B01_L380	B02_L380	100	0,0309	0,266	0,0136
B02_L380	B03_L380	100	0,0309	0,266	0,0136
B01_L220	B04_L220	40	0,0792	0,2901	0,0126
B01_L220	B07_L220	40	0,0792	0,2901	0,0126
B02_L220	B04_L220	40	0,0792	0,2901	0,0126
B02_L220	B05_L220	50	0,0395	0,1474	0,0248
B02_L220	B06_L220	50	0,0792	0,2901	0,0126
B02_L220	C08_L220	180	0,0395	0,1474	0,0248
B03_L220	B06_L220	40	0,0792	0,2901	0,0126
B03_L220	B11_L220	70	0,0395	0,1474	0,0248
B05_L220	B09_L220	40	0,0395	0,1474	0,0248
B07_L220	B08_L220	50	0,0792	0,2901	0,0126
B08_L220	B09_L220	60	0,0792	0,2901	0,0126
B09_L220	B10_L220	50	0,0792	0,2901	0,0126
B10_L220	B11_L220	40	0,0792	0,2901	0,0126
C01_L380	C02_L380	50	0,0309	0,266	0,0136
C01_L380	C07_L380	80	0,0309	0,266	0,0136
C02_L380	C03_L380	50	0,0155	0,1358	0,0267
C03_L380	C04_L380	90	0,0309	0,266	0,0136
C03_L380	C05_L380	70	0,0309	0,266	0,0136
C04_L380	C06_L380	70	0,0155	0,1358	0,0267
C04_L380	C07_L380	70	0,0155	0,1358	0,0267
C05_L380	C06_L380	80	0,0309	0,266	0,0136
C05_L110	C16_L110	30	0,192	0,4	0,0085

C05_L110	C19_L110	20	0,096	0,2	0,017
C06_L220	C08_L220	40	0,0792	0,2901	0,0126
C06_L220	C15_L220	40	0,0792	0,2901	0,0126
C07_L380	C08_L380	80	0,0155	0,1358	0,0267
C08_L220	C09_L220	40	0,0792	0,2901	0,0126
C09_L220	C10_L220	50	0,0792	0,2901	0,0126
C10_L220	C11_L220	30	0,0792	0,2901	0,0126
C11_L220	C12_L220	30	0,0792	0,2901	0,0126
C12_L220	C13_L220	40	0,0395	0,1474	0,0248
C13_L220	C14_L220	40	0,0792	0,2901	0,0126
C14_L220	C15_L220	40	0,0395	0,1474	0,0248
C14_L110	C16_L110	20	0,192	0,4	0,0085
C14_L110	C17_L110	20	0,192	0,4	0,0085
C17_L110	C18_L110	20	0,192	0,4	0,0085
C18_L110	C19_L110	20	0,192	0,4	0,0085

**Table D.4.-** Comparison of aggregation algorithms considering the classical inertial aggregation and the proposed splitting-based aggregation by the mean value of  $J$  of the intern machines for a fault located at the internal node with different number of external equivalents.

Number of Dynamic equivalents	3	6
Splitting with Fuzzy	0,9925	0,9935
Classical Aggregation with Fuzzy	0,989	0,9926
Classical Aggregation with K-means	0,992	0,9938

**Table D.5.-** Evaluation of the prediction capability of ANN considering different operating conditions and points calculating  $\overline{E}_s(j)$

Internal Area	Changed operating point	Training operating point
A	0,972	0,991
B	0,9845	0,994
C	0,959	0,968

**Table D.6.-** Sum squared distance error and average error of the predicted boundary behavior following disturbances at all non-trained nodes of internal area A considering different operating points

Internal Area A part 380 kV							
Nodes	A1	A2	A3	A4	A5a	A5b	A7
Training operating point	0,034	$1,4 \cdot 10^{-3}$	$4,2 \cdot 10^{-3}$	$3,9 \cdot 10^{-3}$	0,054	$1,4 \cdot 10^{-3}$	0,003
Changed operating point	0,031	$5,2 \cdot 10^{-3}$	$4,1 \cdot 10^{-3}$	$3,9 \cdot 10^{-3}$	0,147	$4,4 \cdot 10^{-3}$	$3,2 \cdot 10^{-3}$

Internal Area A part 220 kV		Internal Area A part 110 kV		Sum squared error $E_N(j)$	Average standardized error function $\overline{E_S(j)}$
A6	A7	A4	A6		
$2,2 \cdot 10^{-4}$	$7,1 \cdot 10^{-4}$	$1,1 \cdot 10^{-4}$	$1,6 \cdot 10^{-4}$	0,099	0,991
$2,3 \cdot 10^{-4}$	$6,3 \cdot 10^{-3}$	$1,2 \cdot 10^{-3}$	0,0101	0,308	0,972

**Table D.7.-** Sum squared distance error and average error of the predicted boundary behaviour following disturbances at all non-trained nodes of internal area B considering different operating points

Internal Area B part 220 kV											
Nodes	B1	B2	B3	B4	B5	B6	B7	B8	B9	B10	B11
Training operating point	$3,02 \cdot 10^{-4}$	0,0454	$8,52 \cdot 10^{-4}$	$4,65 \cdot 10^{-4}$	$2,29 \cdot 10^{-4}$	$1,57 \cdot 10^{-4}$	$2,67 \cdot 10^{-4}$	$2,69 \cdot 10^{-4}$	$2,37 \cdot 10^{-4}$	$3,68 \cdot 10^{-4}$	$3,65 \cdot 10^{-4}$
Changed operating point	$3,87 \cdot 10^{-4}$	0,0247	0,0016	$5,13 \cdot 10^{-4}$	$7,18 \cdot 10^{-4}$	$1,65 \cdot 10^{-4}$	$3,52 \cdot 10^{-4}$	$7,39 \cdot 10^{-4}$	$9,37 \cdot 10^{-4}$	$8,46 \cdot 10^{-4}$	$6,0 \cdot 10^{-4}$

Internal Area B part 380 kV			Sum squared error $E_N(j)$	Average standardized error function $\overline{E_S(j)}$
B1	B2	B3		
0,026	$1,3 \cdot 10^{-3}$	$2,1 \cdot 10^{-3}$	0,0784	0,9944
0,072	0,052	0,0276	0,217	0,9845

**Table D.8.-** Sum squared distance error and average error of the predicted boundary behaviour following disturbances at all non-trained nodes of internal area C considering different operating points

Internal Area C part 380 kV								
Disturbance applied at nodes	C1	C2	C3	C4	C5	C6	C7	C8
Training operating point	0,04	0,0156	$2,6 \cdot 10^{-3}$	$4,6 \cdot 10^{-3}$	$6,0 \cdot 10^{-3}$	$2,7 \cdot 10^{-3}$	0,16	$5,4 \cdot 10^{-3}$
Changed operating point	0,2	0,12	0,05	0,09	0,043	0,09	0,3	0,1

Internal Area C part 220 kV								
C6	C8	C9	C10	C11	C12	C13	C14	C15
$3,1 \cdot 10^{-3}$	0,0185	$1,7 \cdot 10^{-3}$	0,40	$4,1 \cdot 10^{-3}$	0,027	$1,9 \cdot 10^{-3}$	0,06	$5,4 \cdot 10^{-4}$
0,067	0,091	0,025	0,237	0,268	0,018	0,07	0,016	0,05

Internal Area C part 110 kV						Sum squared error $E_N(j)$	Average standardized error function $\overline{E}_s(j)$
C5	C14	C16	C17	C18	C19		
$3,4 \cdot 10^{-5}$	$1,76 \cdot 10^{-4}$	$4,8 \cdot 10^{-5}$	$1,04 \cdot 10^{-4}$	$8,7 \cdot 10^{-5}$	$6,4 \cdot 10^{-5}$	0,672	0,968
$3,6 \cdot 10^{-3}$	$7,8 \cdot 10^{-3}$	$2,2 \cdot 10^{-3}$	$2,1 \cdot 10^{-3}$	$1,4 \cdot 10^{-5}$	$1,8 \cdot 10^{-3}$	0,943	0,959

## APPENDIX E Data sets of 12 Multi-machine system

**Table E.1.-** Generator data set of 12-machine system

Name	Mod. Order	SN [MVA]	Tm	UN[kV]	$r_a$ [p.u.]	$x_s$ [p.u.]	$x_d'$ [p.u.]	$x_d''$ [p.u.]
A2_G	5	225	690	15,75	0,001	0,195	0,43	0,25
A3_G	5	275	1518	15,75	0,001	0,195	0,43	0,225
A8_G	5	575	1518	15,75	0,002	0,195	0,43	0,25
A5_G	5	225	1729	15,75	0,002	0,195	0,43	0,225
A12_G	5	225	2719,5	15,75	0	0,195	0,29	0,225
A13_G	5	225	690	15,75	0,002	0,195	0,36	0,225
A14_G	5	225	690	15,75	0,001	0,195	0,29	0,225
A15_G	5	225	690	15,75	0,001	0,19	0,43	0,225
A20_G	5	225	1200	15,75	0	0,156	0,43	0,225
A25_G	5	275	1200	15,75	0	0,156	0,43	0,24
A29_G	5	175	1200	15,75	0	0,195	0,29	0,24
A45_G	5	225	690	15,75	0	0,195	0,43	0,225

**Table E.2.-** Transmission line data set of the 12-machine system

From bus	To bus	Long	$r$ [p.u.]	$x$ [p.u.]	$b$ [p.u.]
A16	A4	50	0,0309	0,266	0,0136
A4	A3	50	0,0309	0,266	0,0136
A3	A7	50	0,0309	0,266	0,0136
A31	A6	50	0,0309	0,266	0,0136
A5	A6	50	0,0309	0,266	0,0136
A9	A21	50	0,0792	0,2901	0,0126
A8	A9	50	0,0309	0,266	0,0136
A8	A39	50	0,0309	0,266	0,0136
A39	A12	50	0,0309	0,266	0,0136
A8	A18	50	0,0309	0,266	0,0136
A12	A18	50	0,0792	0,2901	0,0126
A18	A19	50	0,0309	0,266	0,0136
A19	A22	50	0,0309	0,266	0,0136

A12	A13	50	0,0155	0,1358	0,0267
A12	A17	50	0,0309	0,266	0,0136
A13	A38	20	0,0309	0,266	0,0136
A38	A1	20	0,0309	0,266	0,0136
A1	A14	50	0,0309	0,266	0,0136
A17	A37	20	0,0309	0,266	0,0136
A37	A1	20	0,0309	0,266	0,0136
A14	A15	50	0,0309	0,266	0,0136
A15	A36	50	0,0309	0,266	0,0136
A36	A35	50	0,0309	0,266	0,0136
A35	A34	50	0,0155	0,1358	0,0267
A34	A5	20	0,0395	0,1474	0,0248
A13	A10	50	0,0792	0,2901	0,0126
A10	A16	50	0,0395	0,1474	0,0248
A30	A11	50	0,0792	0,2901	0,0126
A14	A11	50	0,0395	0,1474	0,0248
A20	A21	50	0,0309	0,266	0,0136
A21	A23	50	0,0309	0,266	0,0136
A21	A22	50	0,0309	0,266	0,0136
A22	A3	50	0,0792	0,2901	0,0126
A23	A24	50	0,0792	0,2901	0,0126
A24	A25	50	0,0792	0,2901	0,0126
A25	A26	50	0,0309	0,266	0,0136
A26	A3	50	0,0309	0,266	0,0136
A26	A27	50	0,0395	0,1474	0,0248
A27	A28	50	0,0395	0,1474	0,0248
A28	A29	80	0,0309	0,266	0,0136
A29	A47	80	0,0309	0,266	0,0136
A31	A47	80	0,0309	0,266	0,0136
A31	A30	50	0,0155	0,1358	0,0267
A30	A3	50	0,0155	0,1358	0,0267
A28	A32	50	0,0155	0,1358	0,0267
A29	A32	50	0,0155	0,1358	0,0267
A32	A33	50	0,0309	0,266	0,0136
A34	A33	50	0,0309	0,266	0,0136
A25	A40	80	0,0309	0,266	0,0136
A24	A40	80	0,0309	0,266	0,0136
A39	A41	50	0,0309	0,266	0,0136
A41	A40	80	0,0395	0,1474	0,0248
A14	A42	50	0,0395	0,1474	0,0248

**Table E.3.-** Evaluation of the standardized prediction error of recurrent ANN considering different disturbance duration ( $t_{min}=100$  ms,  $t_{max}=150$  ms) and two sequential disturbances ( $t_1=100$ ms after 1s,  $t_2=120$  ms after 2s)

Number of Boundary Nodes	Minimal disturbance duration $T_{min}$	Maximal disturbance duration $T_{max}$	Sequential disturbances $T_1 - T_2$
3	0,9994	0,9991	0,9981
5	0,9956	0,9952	0,9948
6	0,9874	0,9844	0,9838
7	0,9832	0,981	0,9781
8	0,9816	0,9798	0,978

**Table E.4.-** Evaluation of the robustness of the recurrent ANN depending on the cases explained in table 5.2 and networks based on the 12-multi-machine system with different boundary nodes

Cases of changed operating points after table 5.2	Number of boundary nodes			
	3	4	6	8
1 (Initial o.p. or trained o.p.)	0,9994	0,9974	0,9874	0,9853
2 (Gen. disconnection)	0,9993	0,9973	0,9865	0,9820
3 (Lines disconnection)	0,9992	0,9975	0,9848	0,9758
4 (Gen., Line disconnection and Load reduction)	0,9985	0,9943	0,9830	0,9745
5 (Load reduction to half)	0,9974	0,9931	0,9811	0,9752

**Table E.5.-** Scenarios to power-flow changes and losses considering 12-machine system with 3 boundary nodes after Fig.B.1

Cases	Load Conditions	Location in network	Network power flow loss (MVA)
1	Initial Loading Condition (Training operating point)		291,61+j1720,88
2	Generator Disconnection	G1	312,93+j1942,50
3	Transmission Line Disconnection	L1, L2	295,42+j1791,61
4	Generator, Line Disconnection and Load Reduction	G1, L1, L2 and load reduction on all nodes of internal area	174,05+j666,69
5	Load Reduction to half	On almost all load nodes in internal area	159,72+j488,42

**Table E.6.-** Scenarios to power-flow changes and losses considering 12-machine system with 4 boundary nodes after Fig.B.2

<b>Cases</b>	<b>Load Conditions</b>	<b>Location in network</b>	<b>Network power flow loss (MVA)</b>
<b>1</b>	Initial Loading Condition (Training operating point)		218,08+j980,68
<b>2</b>	Generator Disconnection	G1	232,93+j1135,52
<b>3</b>	Transmission Line Disconnection	L1, L2	218,93+j1020,40
<b>4</b>	Generator, Line Disconnection and Load Reduction	G1, L1, L2 and load reduction on all nodes of internal area	128,67+j183,49
<b>5</b>	Load Reduction to half	On almost all load nodes in internal area	119,32+j56,2

**Table E.7.-** Scenarios to power-flow changes and losses considering 12-machine system with 6 boundary nodes after Fig.E.4

<b>Cases</b>	<b>Load Conditions</b>	<b>Location in network</b>	<b>Network power flow loss (MVA)</b>
<b>1</b>	Initial Loading Condition (Training operating point)		244,48+j927,08
<b>2</b>	Generator Disconnection	G1	256,43+j1058,50
<b>3</b>	Transmission Line Disconnection	L1, L2	245,6+j975,31
<b>4</b>	Generator, Line Disconnection and Load Reduction	G1, L1, L2 and load reduction on all nodes of internal area	236,82+j895,43
<b>5</b>	Load Reduction to half	On almost all load nodes in internal area	225,08+j733,52

**Table E.8.-** Scenarios to power-flow changes and losses considering 12-machine system with 7 boundary nodes after Fig. E.5

Cases	Load Conditions	Location in network	Network power flow loss (MVA)
1	Initial Loading Condition (Training operating point)		262,62+j815,51
2	Generator Disconnection	G1	275,46+j962,46
3	Transmission Line Disconnection	L1, L2	263,03+j859,40
4	Generator, Line Disconnection and Load Reduction	G1, L1, L2 and load reduction on all nodes of internal area	216,36+j426,08
5	Load Reduction to half	On almost all load nodes in internal area	178,39+j14,99

**Table E.9.-** Scenarios to power-flow changes and losses considering 12-machine system with 8 boundary nodes after Fig. 5.18

Cases	Load Conditions	Location in network	Network power flow loss (MVA)
1	Initial Loading Condition (Training operating point)		312,65+j1015,60
2	Generator Disconnection	G1	325,89+j1164,65
3	Transmission Line Disconnection	L1, L2	316,74+j1094,22
4	Generator, Line Disconnection and Load Reduction	G1, L1, L2 and load reduction on all nodes of internal area	272,31+j680,40
5	Load Reduction to half	On almost all load nodes in internal area	239,04+j291,85

**12 Multi-machine systems topologically adapted from 3 to 8 boundary nodes and illustrated in Fig. E.1 to Fig. E.5**

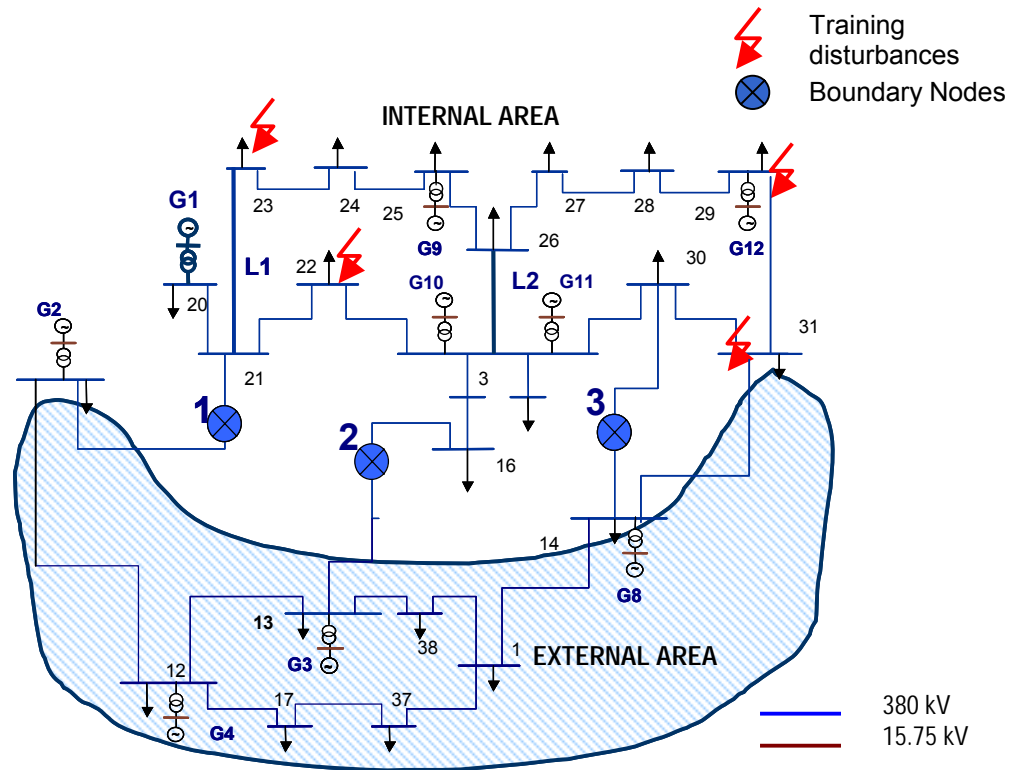


**Fig. E.1.- 12-machine system with three boundary nodes**

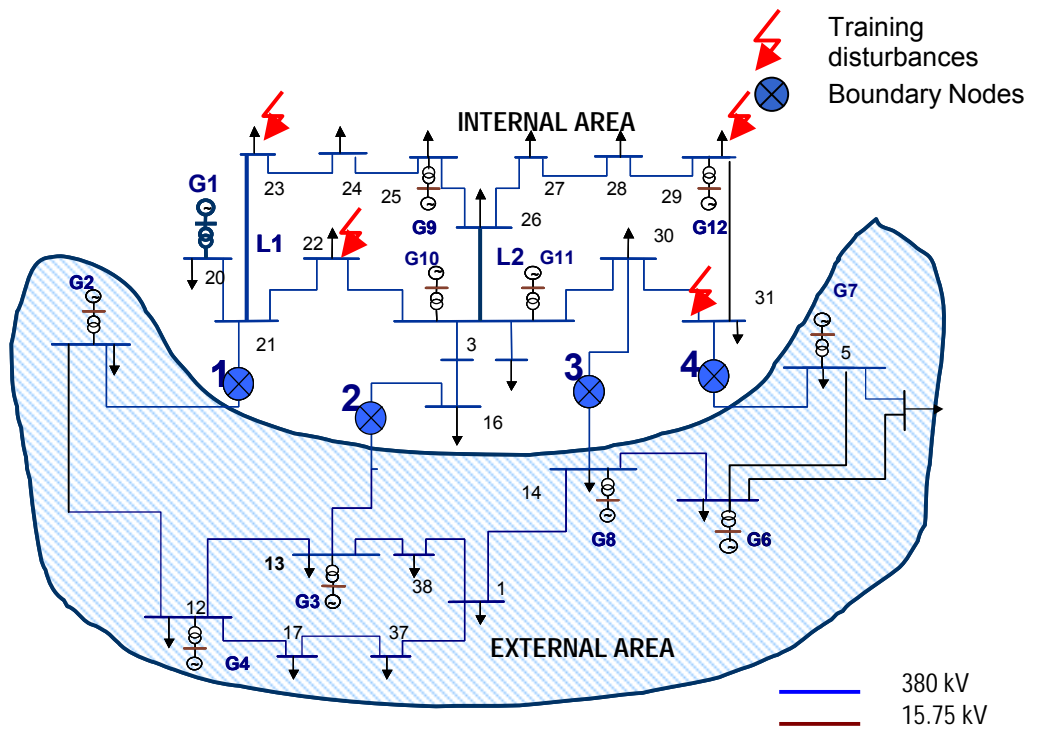


**Fig. E.2.- 12-machine system with four boundary nodes**

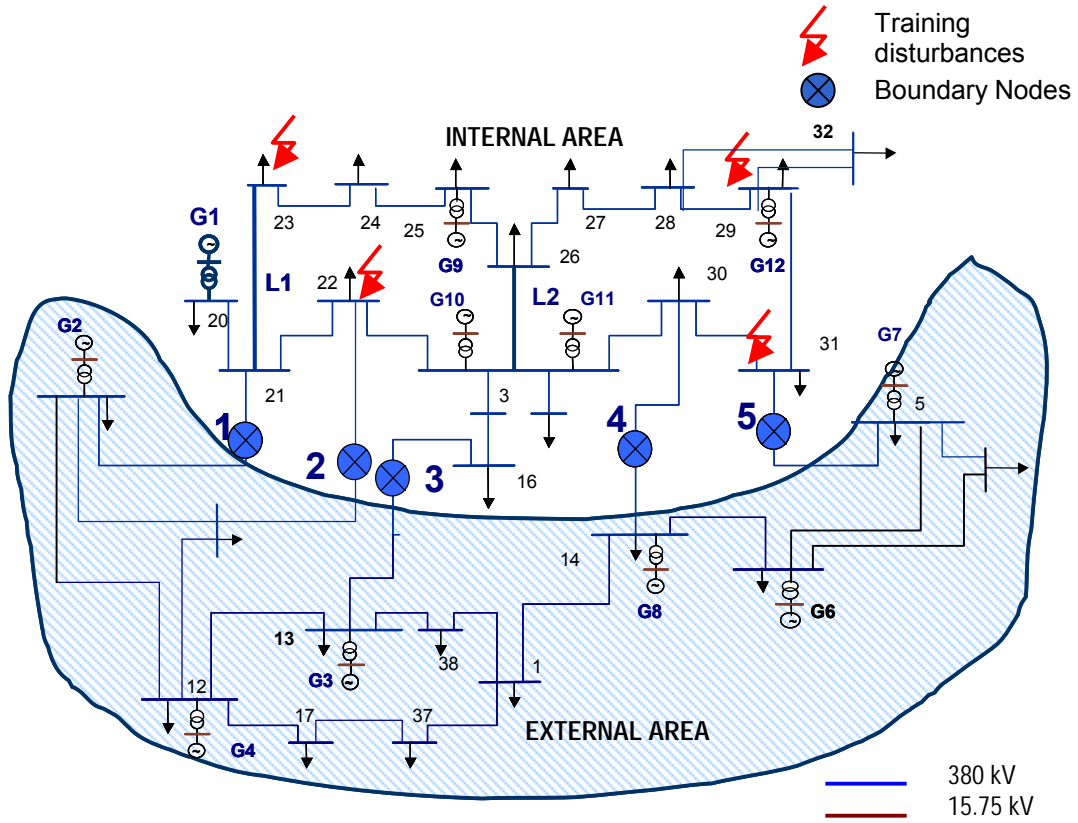


Fig. E.3.- 12 multi-machine system with five boundary nodes

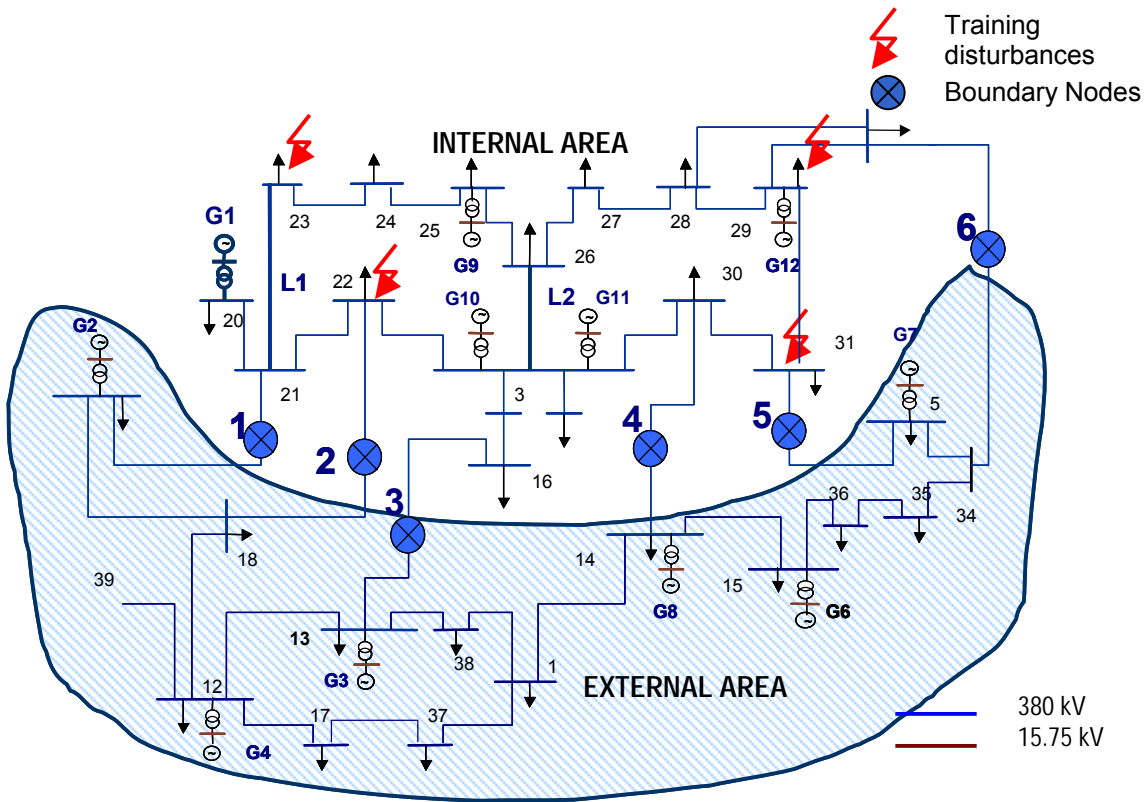


Fig. E.4.- 12 multi-machine system with six boundary nodes

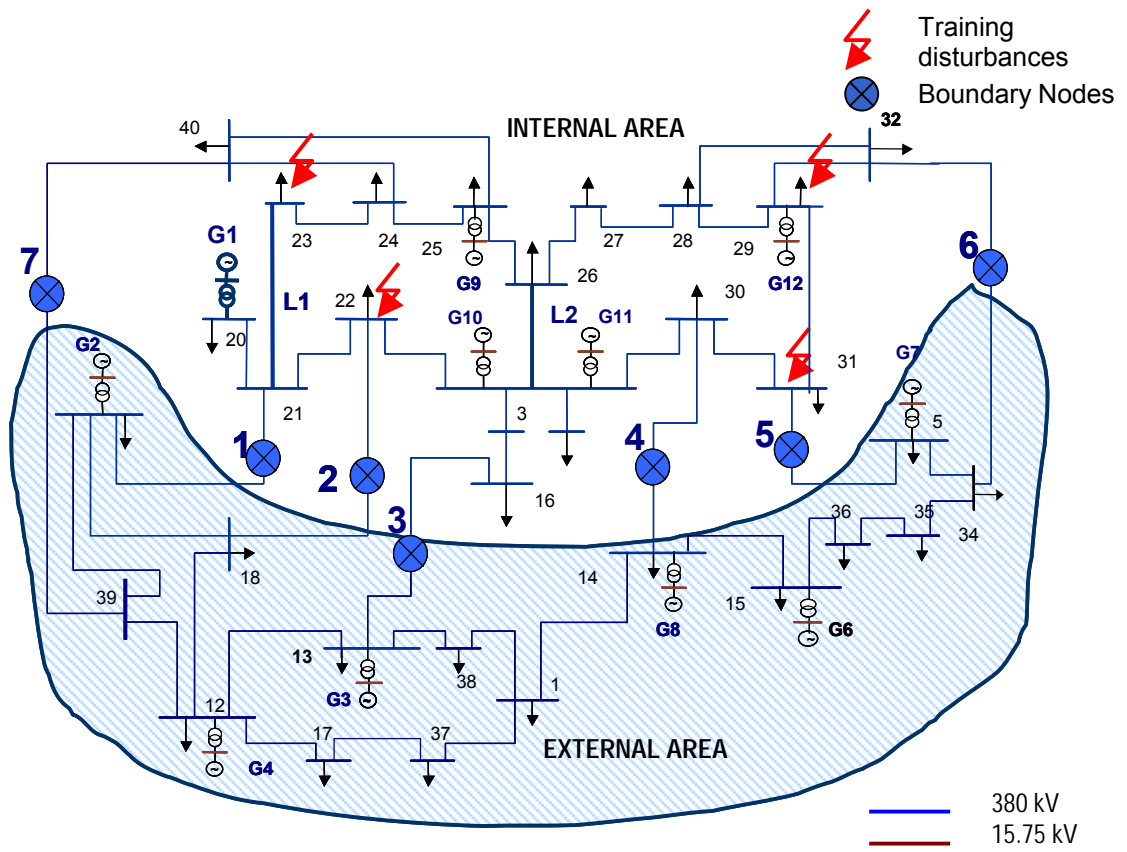


Fig. E.5.- 12 multi-machine system with eight boundary nodes

# APPENDIX F Data sets of the interconnected European power system UCTE / CENTREL

**Table F.1.-** Part of the generator data set of the European Interconnected Power System [142]

Name	Mod. Order	SN [MVA]	Tm	UN[kV]	$r_a$ [p.u.]	$x_s$ [p.u.]	$x_d'$ [p.u.]	$x_d''$ [p.u.]
ALMARAUS	G5	3600	5,6	21		0,16	0,326	0,255
ASCO US	G5	2100	7	21		0,27	0,45	0,33
FRLEC S-	G5	18000	11,2	21	0,005	0,255	0,51	0,34
FRBLA S-	G5	7000	12,6	24	0,004	0,22	0,4	0,3
FRTAV S-	G5	13300	8	21		0,25	0,45	0,33
FRVIG S-	G5	5650	11,2	20	0,005	0,255	0,509	0,344
RWBUETA-	G5	1500	9,4	27		0,29	0,5	0,36
RWBUETB-	G5	1530	9,2	27		0,295	0,51	0,37
RWGUNLA-	G5	1530	6,8	27		0,295	0,51	0,37
RWGUNLB-	G5	1530	6,8	27		0,295	0,51	0,37
RWWTHMS-	G5	1635	8,55	27	1,759	1,709	0,153	0,00025
BWDAXNS-	G5	622	11,6	21		0,2	0,33	0,231
BWKUESS-	G5	870	7,1	21		0,2	0,34	0,23
NLDIEMN-	G5	2400	8	21		0,25	0,41	0,33
NLDODEA-	G5	4050	7	21		0,24	0,42	0,33
ITBENE4-	G5	370	8,2	20		0,24	0,4	0,32
ITBRIS4-	G5	2300	5,7	20		0,12	0,3	0,15
62-ELSAM	G5	4800	15	21	2,41	2,11	0,10129	0,03039
63-SHEG8	G5	825	7,2	21	0,00143	0,233	0,347	0,274
KIEL 1 1	G5	400	6,6	21	2,14	1,84	0,13644	0,04093
BDOR 1 1	G5	1640	8,6	27	1,91	1,81	0,1947	0,05842
BRUH 1 1	G5	1006	9,7	27	1,6	1,5	0,18655	0,05597
KRUH 1 1	G5	1530	9,2	27	1,83	1,73	0,18565	0,05569
68-SIEMS	G5	537,5	8,8	21		0,221	0,321	0,284
STDE 1 1	G5	780	12	21	1,89	1,72	0,24577	0,07373
UWES 1 1	G5	1530	9,2	27	1,8462	1,744	0,17427	0,05228
FARG 1 1	G5	400	6,3	21	2,16	1,89	0,09624	0,02887
G4LIP1	G5	1167	8	27	0,001	0,101	0,291	0,196

G4LIP2	G5	1167	8	27	0,001	0,101	0,291	0,196
G4SWPA	G5	1000	9,03	27	0,0012	0,235	0,34	0,275
G4SWPB	G5	1000	9,03	27	0,0012	0,235	0,34	0,275
P4WIE-G1	G5	470	7	15,75		0,11	0,275	0,191
P4ROG-G3	G5	1278	6,45	22		0,199	0,319	0,235
P4PEL-G1	G5	705	7	15,75		0,11	0,275	0,191
EBOV23	G5	518	9,89	15,75	0,0017	0,166	0,267	0,199
EBOV24	G5	518	9,89	15,75	0,0017	0,166	0,267	0,199
EMO1	G5	518	9,89	15,75	0,0017	0,166	0,267	0,199
EMO2	G5	518	9,89	15,75	0,0017	0,166	0,267	0,199
COFRENUS	G5	1200	7	21		0,27	0,38	0,33
GUENESUS	G5	1800	8	21		0,27	0,45	0,33
MEQUINUS	G5	1800	7,8	21		0,27	0,45	0,33
MONTEAUS	G5	1800	8,5	21		0,27	0,4	0,33
PLANA US	G5	1800	7	21		0,27	0,45	0,33
ROBLA US	G5	750	7,5	21		0,27	0,4	0,33
SANTURUS	G5	700	7	21		0,27	0,4	0,33
TERUELUS	G5	1250	7	21		0,27	0,45	0,33
TRILLOUS	G5	1300	7,41	21		0,127	0,3415	0,2426
VALDECUS	G5	3500	8	21		0,27	0,4	0,33
VANDELUS	G5	1300	7,8	21		0,27	0,45	0,33
KREMS	G5	330	8	21		0,2	0,3	0,27
LAVRI.1	G5	350	8	21		0,2	0,3	0,27
LAVRI.2	G5	200	8	21		0,2	0,3	0,27
PTOLE.1	G5	82	10	15,8	0,00186	0,08	0,21	0,135
PTOLE.4	G5	375	8,9	21	0,00144	0,13	0,3	0,18
MEGAL.1	G5	370	8	21		0,2	0,3	0,27
MEGAL.2	G5	280	8	21		0,2	0,3	0,27
WGACKO	G5	353	3,53	22	0,0035	0,16	0,39	0,23
WJABLA	G5	113	7	13,8	0,0045	0,22	0,48	0,29
WKAKAN	G5	287	5,72	15,75	0,0016	0,15	0,24	0,18
WMOSTA	G5	240	10	22	0,0035	0,16	0,39	0,23
WSALAK	G5	62	6,33	15	0,0049	0,16	0,23	0,19
WTREBI	G5	140	6,11	15	0,0049	0,16	0,23	0,19

**Table F.2.-** Part of the transmission line data set of the European Interconnected Power System

From bus	To bus	r [p.u.]	x [p.u.]	b [p.u.]
ITGORL41	CHROBB41	2,32	31,63	1,542
ITBULC41	CHSOZZ41	2,71	32,21	1,004
ITMUSI41	CHLAVOG4	1,18	19,77	0,749
BGAUB SA	FRMOU SA	0,21	2,41	0
BGAVELE4	FRAVE SA	1,32	14,26	0
BGGRAESA	FRLON SA	2,8685	34,016	0
BGDOELA4	NLGEERR4	1,5773	18,965	0
BGHERRAB	NLMAARSA	1,5467	17,32	0
BGCOO_A4	BGGRAESA	1,4146	14,998	0
BGDOELA4	BGDOELB4	1,3359	13,768	0
BGDOELA4	BGGRAESA	7,0571	75,847	0
BGDOELB4	BGGRAESA	3,986	38,13	0
BGGRAESA	BGHERRAB	1,2424	13,901	0
BWLAUFB2	CHLAUBOR	0,01	0,111	0
BWKUESSB	CHLAUBSB	0,293	2,307	0
BWKUESSA	CHLAUBSA	0,2708	2,2122	0
BWKUESSB	CHLAC SA	2,1111	21,212	0
CHLAUBSB	EVPULDSA	8,5708	105,76	0
CHLAUBSB	EVPULDSB	8,5455	105,97	0
CHAIROSA	CHGOEESA	4,26	48	0
EVPULDSB	RWVOEGSA	3,4894	34,889	0
EVOMOOE2	RWDELL 2	2,2939	19,394	0
FRCOR S1	FRZME S1	0,01	367,93	0
FRALB SA	FRAVE SA	0,01	150,83	0
FRALB SA	FRB.T SA	0,0016	40,42	0
FRALB SA	FRLON SA	0,01	389,01	0
FRALB SA	FRMAM SA	0,01	228,36	0
NLMAARSA	RWOBZRSB	1,6871	16,1	0
NLMAARSA	RWROK SA	2,358	22,291	0
RWKW_IB2	VEHANEN2	3,899	24,596	0
RWNSTEM2	RWURB GN	53,83	188	0
RWBUETSA	RWBUETSB	14,288	140,61	0
RWBUETSA	RWUCHFSA	20,438	229,17	0
RWBUETSA	RWURB SA	1,7543	16,228	0
BRUH4201	HAMH4201	1,07	13,95	0,86
DOLL4201	HAMS4201	0,91	7,07	0,4145

DOLL4201	HAMS4201	0,91	7,07	0,4145
HAMH4201	HAMO4201	1,04	7,82	0,4265
HAMH4201	HAMO4201	1,04	7,82	0,4265
HAMO4201	HAMS4201	0,99	7,44	0,447
HAMO4201	HAMS4201	0,99	7,44	0,447
HAMO4201	KRUH4201	0,47	6,26	0,429
HAMO4201	KRUH4201	0,47	6,26	0,429
KRUE4201	KRUH4201	0,006	0,05	0
KRUE4201	KRUH4201	0,006	0,05	0
JKRALJ2	JUPOZE2	5,23	27,64	0,5398
JPLJEV2	JUPOZE2	7,37	40,14	0,7633
JPANCE2	JZRENJ2	5,87	32,23	0,6006
ABURRE21	AELBAS21	6,59	25,7	0,6525
ABURRE21	AFIERZ21	7,54	38,87	0,9899
AELBAS21	AELBAS22	0,26	1,62	0,0413
ASHKOP52	AULZA 51	2,15	2,7	0,0477
ASLT4 51	ATIRAN51	3,64	5,69	0,0986
ATIRAN51	AUTR4 51	1,89	3,03	0,0509
WGACKO11	WTREBI11	1,92	21,12	0,7171
WGACKO11	WMOSTA11	1,8	20,92	0,6815
WMOSTA11	WSARAJ11	2,76	32	1,042
WSARAJ11	WTUZLA11	2,5	28,98	0,9441
WTUZLA11	WUGLJE11	1,26	13,86	0,5357
WMOSTA2B	WTREBI21	6,74	35,72	0,7174
WMOSTA2B	WTREBI21	6,74	35,72	0,7174
WGRADA21	WTUZLA21	4,22	21,8	0,4548
WJABLA21	WJAJCE21	7,46	39,55	0,7945
WJABLA21	WKAKAN21	4,83	25,62	0,5147
WJABLA21	WMOSTA2B	3,64	19,3	0,3877
WKAKAN21	WPRIJE21	10,61	55,06	2,02
WKAKAN21	WSALAK21	6,94	37,31	0,7496
WKAKAN21	WTUZLA21	5,68	30,11	0,6047
WKAKAN21	WZENIC21	1,81	9,59	0,1925

**Table F.3.-** Comparison of identity recognition algorithms considering electromechanical weighted distances by the mean value of  $J$  of the 67 German intern machines for a fault located at the boundary node **VEGROUSB(VEW)** with different number of external equivalents.

Identity techniques (K=K-means, H=Hierarchical, P=Preclustering, E=Electromechanical distance, F=Fuzzy)	Number of reduced equivalent machines and their reduction degree (Reduction degree in percentage)					
	5,04%	8,82%	16,37%	22,67%	36,52%	45,34%
	20	35	65	90	145	180
<b>K-means</b>	0,99247	0,99506	0,99594	0,9956	0,99603	0,99752
<b>Electrom. K-means</b>	0,99425	0,99538	0,9976	0,99789	0,9984	0,99826
<b>K-means with Preclustering</b>	0,9893	0,9951	0,9969	0,99695	0,9967	0,9979
<b>Electrom. K-means with Preclust.</b>	0,9923	0,99524	0,9969	0,9971	0,99792	0,9978
<b>Hierarchical</b>	0,9935	0,9954	0,9976	0,99783	0,998	0,9978
<b>Electrom. Hierarchical</b>	0,99296	0,99227	0,9938	0,99694	0,99775	0,9981
<b>Fuzzy</b>	0,9889	0,9927	0,9943	0,99087	0,9932	0,99579
<b>Fuzzy with Preclus.</b>	0,99225	0,99485	0,99745	0,99482	0,9952	0,99647
<b>Electrom. Fuzzy</b>	0,99287	0,9956	0,9976	0,9963	0,9976	0,99798
<b>SOFM</b>	0,99106	0,9943	0,99571	0,993	0,9937	0,992

### German power system operators in the present liberalized power markets

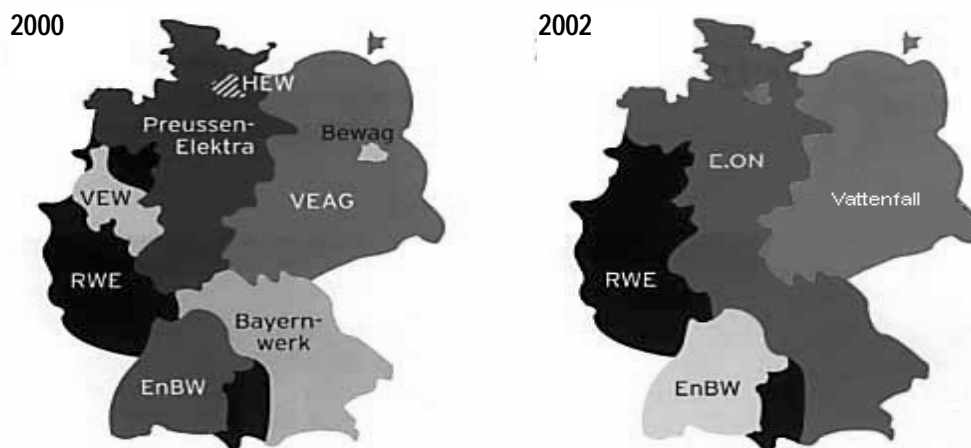


**Fig. F.1.-** As consequence of the fusion of traditional network operators : BAG, BEWAG, EnBW, PE, RWE, VEAG and VEW the number of the current operators has been considerably reduced.